ISSN 0021-9673

VOL. 194 NO. 2 JUNE 20, 1980

JOURNAL OF CHROMATOGRAPHY

INTERNATIONAL JOURNAL ON CHROMATOGRAPHY, ELECTROPHORESIS AND RELATED METHODS

ELSEVIER SCIENTIFIC PUBLISHING COMPANY
AMSTERDAM

JOURNAL OF CHROMATOGRAPHY

Scope. The *Journal of Chromatography* publishes papers on all aspects of chromatography, electrophoresis and related methods. Contributions consist mainly of research papers dealing with chromatographic theory, instrumental development and their applications. The section *Biomedical Applications*, which is under separate editorship, deals with the following aspects: developments in and applications of chromatographic and electrophoretic techniques related to clinical diagnosis (including the publication of normal values); screening and profiling procedures with special reference to metabolic disorders; results from basic medical research with direct consequences in clinical practice; combinations of chromatographic and electrophoretic methods with other physicochemical techniques such as mass spectrometry. In *Chromatographic Reviews*, reviews on all aspects of chromatography, electrophoresis and related methods are published.

Submission of Papers. Papers in English, French and German may be submitted, if possible in three copies. Manuscripts should be submitted to: The Editor of *Journal of Chromatography*, P.O. Box 681, 1000 AR Amsterdam, The Netherlands, or to: The Editor of *Journal of Chromatography, Biomedical Applications*, P.O. Box 681, 1000 AR Amsterdam, The Netherlands. Reviews are invited or proposed by letter to the Editors and will appear in *Chromatographic Reviews* or *Biomedical Applications*. An outline of the proposed review should first be forwarded to the Editors for preliminary discussion prior to preparation. Submission of an article is understood to imply that the article is original and unpublished and is not being considered for publication elsewhere. Upon acceptance of an article by the journal, the author(s) resident in the U.S.A. will be asked to transfer the copyright of the article to the publisher. This transfer will ensure the widest possible dissemination of information under the U.S. Copyright Law.

Subscription Orders. Subscription orders should be sent to: Elsevier Scientific Publishing Company, P.O. Box 211, 1000 AE Amsterdam, The Netherlands. The *Journal of Chromatography, Biomedical Applications* can be subscribed to separately.

Publication. The *Journal of Chromatography* (including *Biomedical Applications* and *Chromatographic Reviews*) has 22 volumes in 1980. The subscription price for 1980 (Vols. 181–202) is Dfl. 2838.00 plus Dfl. 352.00 (postage) (total *ca.* US$ 1636.00). The subscription price for the *Biomedical Applications* section only (Vols. 181–183) is Dfl. 399.00 plus Dfl. 48.00 (postage) (total *ca.* US$ 229.25). Journals are automatically sent by air mail to the U.S.A. and Canada at no extra costs, and to Japan, Australia and New Zealand with a small additional postal charge. Back volumes of the *Journal of Chromatography* (Vols. 1 through 180) are available at Dfl. 140.00 (plus postage). Claims for issues not received should be made within three months of publication of the issue. If not, they cannot be honoured free of charge. For customers in the U.S.A. and Canada wishing additional bibliographic information on this and other Elsevier journals, please contact Elsevier/North-Holland Inc., Journal Information Centre, 52 Vanderbilt Avenue, New York, NY 10164. Tel: (212) 867-9040.

Abstracts/Contents Lists published in Biochemical Abstracts, Biological Abstracts, Chemical Abstracts, Chemical Titles, Current Contents/Physical, Chemical & Earth Sciences, Current Contents/Life Sciences, Index Medicus, and Science Citation Index.

See page 3 of cover for Publication Schedule, Information for Authors, and information on the News Section and Advertisements.

Printed in The Netherlands

CONTENTS

(Continued overleaf)

Contents (continued)

Notes

Book Reviews

H.P.L.C.?

Du Pont has got what you're looking for.

We've got the experience.

Since introducing the first commercial High Performance Liquid Chromatograph in 1969, Du Pont has continued to lead the field in this important separation technique.

Today, Du Pont offers the most versatile range of HPLC and HP Preparative LC systems available anywhere.

We've got the performance.

Some of the recent advances you'll find in our HPLC systems include microprocessor control, precision gradient programming, state-of-the-art detectors, automatic samplers, built-in diagnostics and self-contained "memory" for ready recall of up to 8 stored analytical programmes.

It all adds up to unbeatable high performance. Speed. Reliability. Superb reproducibility. Excellent resolution of peaks. And of course, ease of operation.

And Du Pont "Zorbax" columns ensure highest performance throughout the analysis.

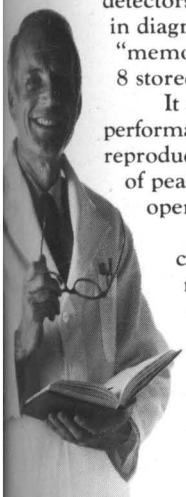

We've got the versatility.

Because Du Pont HPLC systems are designed and built on a modular basis, you can start with a basic system and add on at a later date according to your needs, and your budget.

Modules currently available include gradient, autosampler, SEC data analyser, automated sample processor plus several detectors and accessories. A wide range of "Zorbax" columns is also available.

We've got the reputation.

As one of the world's leading manufacturers of precision analytical instruments, Du Pont enjoys an outstanding reputation for product quality and service support.

Ask any of our customers. Or better still, contact Du Pont now and get the facts first hand.

Free book.

If you're seriously considering the purchase of a new HPLC system within the next 6-9 months, a fascinating book on Liquid Chromatography written by a leading Du Pont authority could be yours free, just by inviting our representative to call. Simply complete and return the coupon before December 31 to qualify.

Du Pont de Nemours International S.A.
Room N102/P.O. BOX
CH-1211 Geneva 24, Switzerland-Tel. (022) 27 81 11

DuPont Instruments DUPONT

I intend to buy a new HPLC system within the next 6-9 months. Please ask your representative to phone for an appointment.

NAME: _____

POSITION: _____

COMPANY/INSTITUTION: _____

ADDRESS: _____

TEL.: _____ JC

Post to: Du Pont de Nemours International S.A., **"Dept. F.R"**, Room N102 - P.O. BOX - CH - 1211 Geneva 24, Switzerland.

ref no 179

Euroanalysis III

edited by **D. M. CARROLL,** *Institute for Industrial Research and Standards, Dublin, Ireland*

6 × 9″ (15·5 × 23 cm). xvi + 428 pages. 137 illus. 1979.

This book contains the plenary and keynote lectures presented at the Third European Conference on Analytical Chemistry, Euroanalysis III, held in Dublin in August 1978, organised by the Institute of Chemistry of Ireland on behalf of the Working Party on Analytical Chemistry of the European Federation of Chemical Societies.

It provides a comprehensive review of the present situation and future prospects in chemical, pharmaceutical and environmental analysis as well as the role of analytical chemistry in the earth sciences and the analysis of solid surfaces.

CONTENTS: 1. Irish contributions to European analytical chemistry. 2. Stable free radicals—electron spin resonance—analytical chemistry. 3. Are you still eating? Chemical food analysis—fact and fiction. 4. Clinical laboratory reference materials and methods—present status and future prospects. 5. Atomic spectrochemical analysis in soil science research. 6. *In-situ* microanalysis and surface analysis by electron probe techniques. 7. Computers in spectroscopy. 8. Reference materials: Their production, certification and use in compatible measurement networks. 9. Ion-selective electrodes—application in flowing systems. 10. Modern polarographic and voltammetric techniques. 11. Recent developments in high performance liquid chromatography. 12. Infrared spectroscopy of biocontact surfaces. 13. Analytical chemistry in the dairy industry. 14. Electron spectroscopy for chemical analysis. 15. Analytical chemistry in the earth sciences. 16. Conformational analysis: An account of experimental and theoretical methods applied to the analysis of mixtures and of constituent structures. 17. Hydrocarbon analysis. 18. Environmental analysis—air quality evaluation. 19. Pharmaceutical analysis. 20. Clinical biochemical analysis. Index.

APPLIED SCIENCE PUBLISHERS Ltd
Ripple Road, Barking, Essex, England

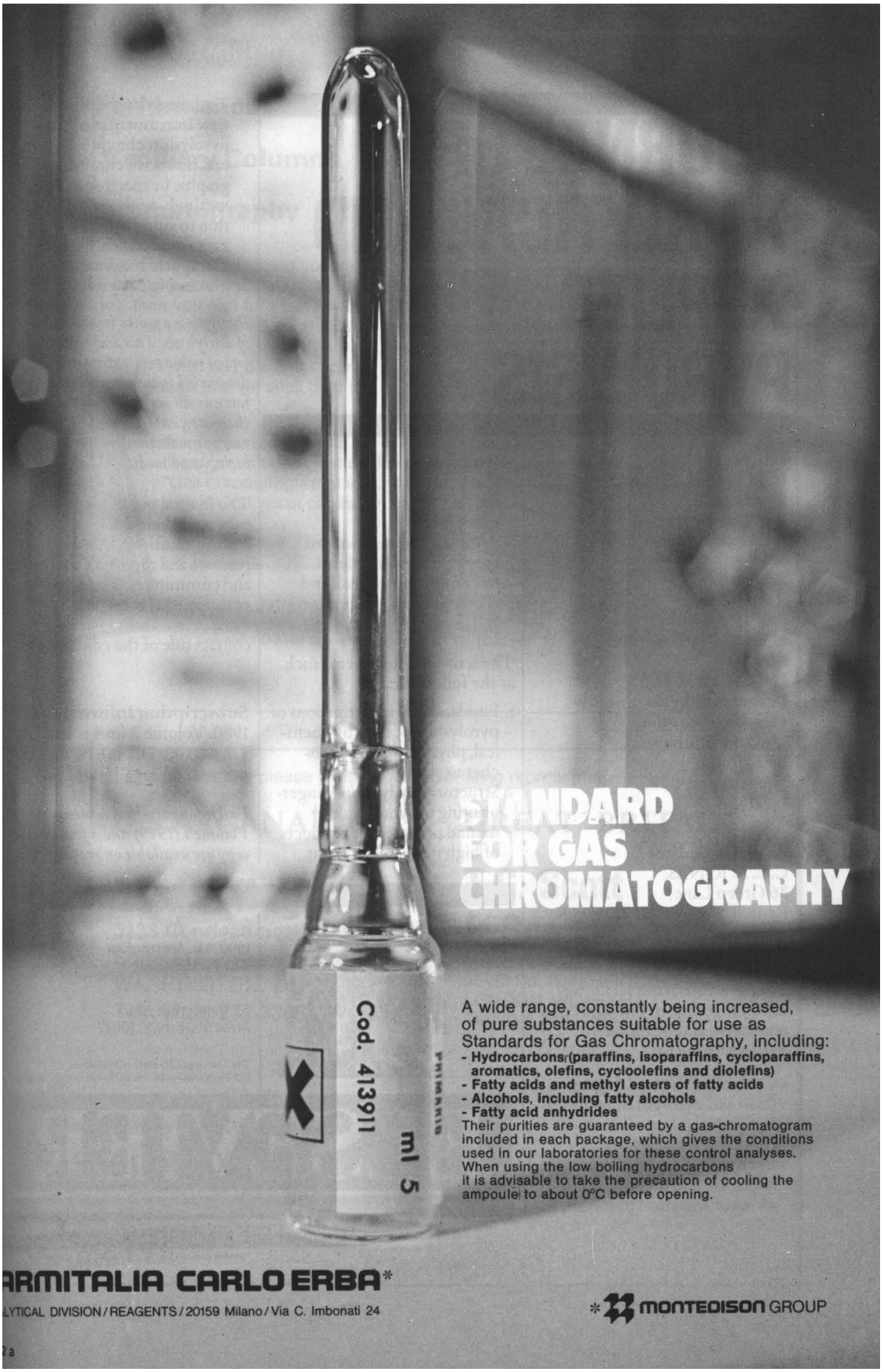

A wide range, constantly being increased, of pure substances suitable for use as Standards for Gas Chromatography, including:

- **Hydrocarbons (paraffins, isoparaffins, cycloparaffins, aromatics, olefins, cycloolefins and diolefins)**
- **Fatty acids and methyl esters of fatty acids**
- **Alcohols, including fatty alcohols**
- **Fatty acid anhydrides**

Their purities are guaranteed by a gas-chromatogram included in each package, which gives the conditions used in our laboratories for these control analyses. When using the low boiling hydrocarbons it is advisable to take the precaution of cooling the ampoule to about 0°C before opening.

ARMITALIA CARLO ERBA*

LYTICAL DIVISION / REAGENTS / 20159 Milano / Via C. Imbonati 24

*MONTEDISON GROUP

2a

JOURNAL OF ANALYTICAL AND APPLIED PYROLYSIS

Editors:
H. L. C. MEUZELAAR
Biomaterials
Profiling Center,
University of Utah,
391 South Chipeta
Way,
Research Park,
Salt Lake City,
UT 84108, U.S.A.

H.-R. SCHULTEN
Institut für Physikalische Chemie der
Universität Bonn,
5300 Bonn,
Wegelerstrasse 12,
G.F.R.

Associate Editor:
C. E. R. JONES,
36 Green Lane,
Redhill, Surrey RH1 2DF, U.K.

This new international journal brings together, in one source, qualitative and quantitative results relating to:

- Controlled thermal degradation and pyrolysis of technical and biological macromolecules;
- Environmental, geochemical, biological and medical applications of analytical pyrolysis;
- Basic studies in high temperature chemistry, reaction kinetics and pyrolysis mechanisms;
- Pyrolysis investigations of energy related problems, fingerprinting of fossil and synthetic fuels, coal extraction and liquefaction products.

The scope includes items such as the following:

1. Fundamental investigations of pyrolysis processes by chemical, physical and physicochemical methods.
2. Structural analysis and fingerprinting of synthetic and natural polymers or products of high molecular weight.
3. Technical developments and new instrumentation for pyrolysis techniques in combination with chromatographic or spectrometric methods, with special attention to automation, optimization and standardization.
4. Computer handling and processing of pyrolysis data.

Pyrolysis is applied in a wide range of disciplines. This journal is therefore of value to scientists in such diverse fields as polymer science, forensic science, soil science, geochemistry, environmental analysis, energy production, biochemistry, biology and medicine.

The journal publishes original papers, technical reviews, short communications, letters, book reviews and reports of meetings and committees. The language of the journal is English. Prospective authors should contact one of the editors.

Subscription Information:
1980: Volume 2 (in 4 issues),
US $ 80.00/Dfl. 156.00 including postage.

Full information on contents of Volume 1 (1979) and a free sample copy are available on request.

P.O. Box 211,
1000 AE Amsterdam
The Netherlands

52 Vanderbilt Ave
New York, N.Y. 10017

The Dutch guilder price is definitive.
US $ prices are subject to exchange rate fluctuations.

ELSEVIER

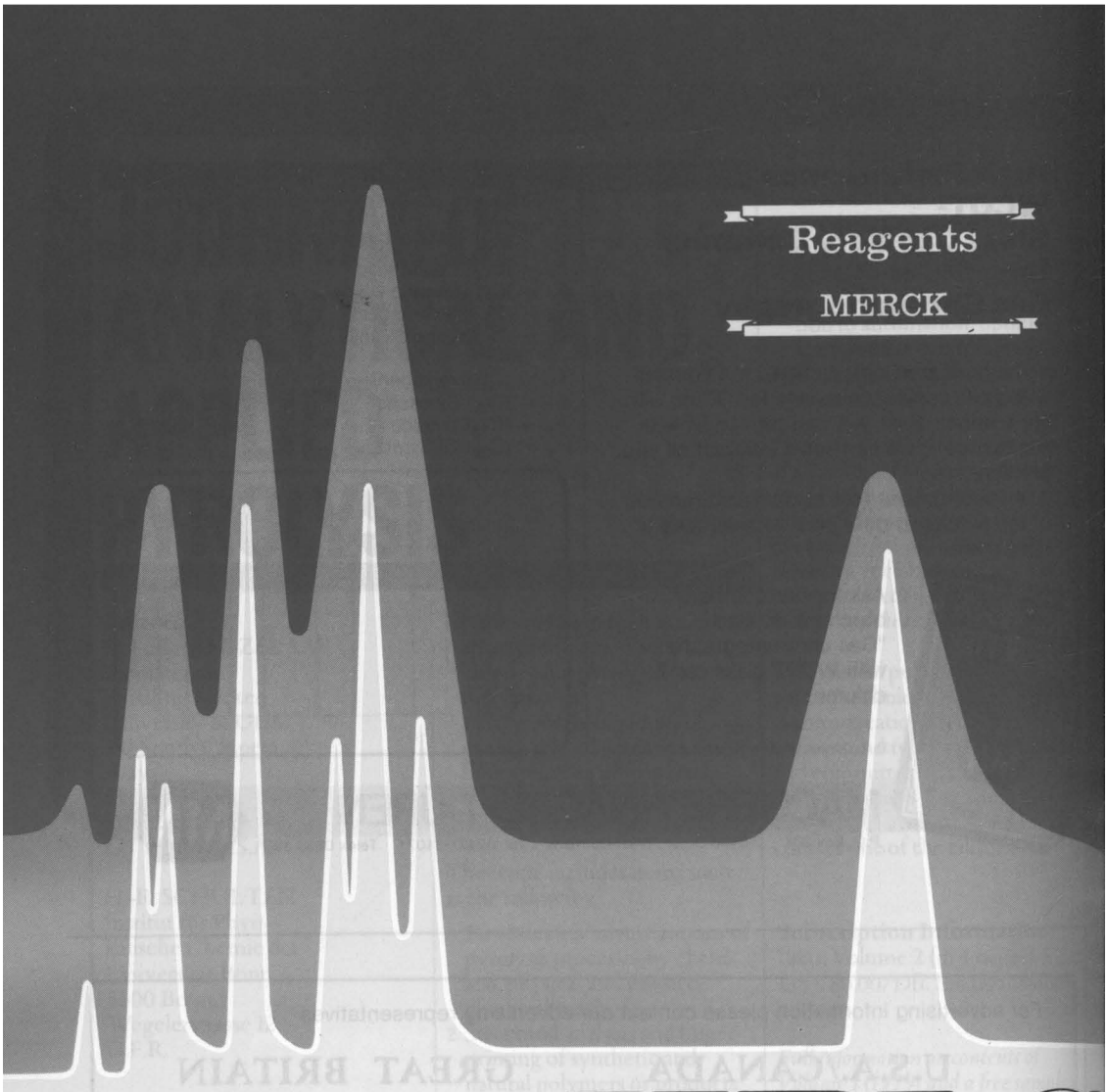

Preparations for HPLC

High Performance Liquid Chromatography

Our up-to-date product line for analytical and preparative HPLC enables you to solve every separation problem.
Our packing materials are systematically classified according to
- particle size
- pore structure
- chemical surface modification

resulting in
- extremely high separation efficiency and capacity
- graduated selectivity
- reproducibility

LiChrosorb® – LiChrospher® – Perisorb® – LiChroprep®

NEW: Hibar® Pre-packed Columns RT and EC / 250 mm and 125 mm length, 4 mm ∅
available with our well established packing materials LiChrosorb® and LiChrospher®.

For prep scale use our
Lobar® Pre-packed Columns LiChroprep® Si 60 and LiChroprep® RP-8, available in various lengths and diameters.

Ask for our special brochures.

E. Merck, Darmstadt, Federal Republic of Germany

Eu

Journal of Chromatography, 194 (1980) 105–119
Elsevier Scientific Publishing Company, Amsterdam — Printed in The Netherlands

CHROM. 12,734

FUNDAMENTAL, PREDICTIVE APPROACH TO DIPOLE–DIPOLE INTERACTIONS BASED ON THE DIPOLE MOMENT OF THE SOLUTE AND THE DIELECTRIC CONSTANT OF THE SOLVENT

PETER W. CARR
Department of Chemistry, University of Minnesota, Minneapolis, MN 55455 (U.S.A.)
(First received October 22nd, 1979; revised manuscript received January 31st, 1980)

SUMMARY

A new solvent polarity scale, the Taft π^* scale, is explored for its utility in predicting partition coefficients and solubility parameters of non-hydrogen-bonding, non-aromatic solvents. A function of the dielectric constant of the solvent and the dipole moment and molar volume of the solute is used to obtain *a priori* estimates of orientation (permanent dipole–permanent dipole) solubility parameters. The correlation coefficient between measured and predicted orientation solubility parameters is 0.97; the slope is close to unity.

INTRODUCTION

Although great progress has been made in understanding the many factors which influence the efficiency of chromatographic systems[1], one of the chief remaining problems in separation science is the primitive level of understanding of the intermolecular processes which are the driving force for the separation. A complete theoretical understanding of intermolecular interactions would permit the *a priori* estimation of the equilibrium constant (defined below) for the transfer of solute from the mobile to the stationary phase:

$$A_{(\text{mobile})} \rightleftharpoons A_{(\text{stationary})} \tag{1}$$

$$K_{eq} = \frac{[A]_s}{[A]_m} \tag{2}$$

If such partition coefficients (K_{eq}) could be predicted, then one could rationally choose the most appropriate mobile and stationary phases for a particular separation.

There are many approaches to the prediction of solute retention. Most methods rely upon a combination of theory and experiment. These approaches include: factor analysis, which attempts to identify chromatographically significant molecular parameters[2] (*e.g.* refractive index and dipole moment); Snyder's empirical

0021-9673/80/0000–0000/$02.25

solvent strength scale (ε^0) for adsorption chromatography[3]; the use of functional group parameters[4] and linear free energy relationships[5]; and the Rohrschneider–McReynolds multiple test solute retention scheme[6,7], which has been used as the basis for both gas chromatographic (GC) and liquid chromatographic (LC) solvent polarity scales, and selectivity classifications[8–10].

One of the most important and fundamental approaches to quantifying intermolecular interactions is the solubility parameter concept developed by Hildebrand *et al.*[11]. Chromatographic applications of this concept have been widespread[12,13]. In its original form, the solubility parameter was thought to be strictly applicable only to interactions which obey a geometric mean relationship, *e.g.*, London dispersion interactions. The approach has been used, even by Hildebrand *et al.*[11], to estimate the strength of polar interactions which may not follow a geometric mean interaction. In recent work, the solubility parameter has been treated as a multi-dimensional quantity which represents the totality of dispersion (δ_d), orientation (δ_o), induction (δ_{in}), and hydrogen-bonding donor (δ_a) and acceptor (δ_b) contributions. In accord with common usage, orientation processes, represented by δ_o, refer to the interaction between two permanent dipoles. Induction processes (δ_{in}) refer to the interaction which occurs when a permanent dipole induces a dipole in a normally non-polar but polarizable molecule. As will develop, our main interest here is in the interaction of two permanent bond dipoles. Keller *et al.*[14] and Karger *et al.*[15] have presented a systematic approach to evaluating all of these individual solubility parameters and have done so for a series of common solvents. They have also derived relationships between individual solubility parameters and important chromatographic measures of retention, such as partition coefficients for gas–liquid, liquid–liquid, and adsorption chromatography, and they have related solubility parameters to Kováts' retention index, adsorbent solvent polarity, and functional group adsorption energies[16].

From a chromatographic viewpoint, intermolecular interactions fall into three broad classes: dispersion interactions, which are general and relatively non-selective; simple polar interactions, *i.e.* those due to permanent dipole and induced dipole moments, which are somewhat selective; and a number of very selective interactions which may be described as various hard–soft acid–base processes such as hydrogen bonding. Of these various forces, only dispersion interactions have been successfully predicted from fundamental molecular properties. Keller *et al.*[14] and Karger *et al.*[15] were able to correlate the solubility parameters (within $\pm$ 0.2 $(cal/ml)^{1/2}$) of nearly 100 hydrocarbons with a simple function of the refractive indices of these compounds. They used this correlation to dissect the total solubility parameter of polar compounds into dispersion and net polar contributions. The homomorph approach[11] to the estimation of the dispersion contribu ion to the total solubility parameter is useful to within $\pm$ 0.7 $(cal/ml)^{1/2}$ for the same set of compounds[15].

In addition to the polarity indices mentioned above, physical chemists have described a variety of solvent polarity scales which have been rather neglected by chromatographers. These scales (see Table I) include: Dimroth's[17] E_T, Brooker's[18] χ_R, Lassau and Jungers'[19] log k (Pr_3N + MeI), Walther's[20] E_K, Knauer and Napier's[21] A_N, Allerhand and Schleyer's[22] G, Taft's[23] P, and Braunstein's[24] S. These scales are based on the dependence of some characteristic of either a test molecule or reaction on the nature of the solvent. Generally, this includes the effect of solvent on a reaction rate or equilibrium constant, or the effect of solvent on some spectroscopic property, such

TABLE I

TAFT CORRELATION OF EMPIRICAL SOLVENT POLARITY SCALES[§]

n = Number of solvents included in the linear regression; ϱ = linear regression correlation coefficient.

Scales correlated[§§]	n	ϱ
μ *vs.* π^*	23	0.985
E_T *vs.* π^*	12	0.987
χ_R *vs.* π^*	16	0.987
log k *vs.* π^*	13	0.985
E_K *vs.* π^*	9	0.977
A_N *vs.* π^*	6	0.993
G *vs.* π^*	8	0.993
P *vs.* π^*	12	0.989
S *vs.* π^*	10	0.981

[§] Data from ref. 26. The solvents employed are listed therein.
[§§] See text for references to the scales employed.

as the nuclear magnetic resonance, infrared or ultraviolet absorption energy of a solvent-sensitive transition.

The most recent and perhaps the most extensive such scale is the Taft system, which is based on the effect of solvent on the frequency of maximum absorption of the $\pi \rightarrow \pi^*$ or p $\rightarrow \pi^*$ transition of a judiciously chosen set of test solutes[25–27]. In the absence of specific interactions such as hydrogen bonding, Taft and coworkers have shown that certain properties (denoted $(XYZ)_o$), which are linear with respect to free energy, are related to their solvent scale as follows:

$$(XYZ)_o = (XYZ)_c + s(\pi^* + d\triangle) \tag{3}$$

$(XYZ)_c$ denotes the value of the measured variable in cyclohexane, which is taken as the reference solvent in their system ($\pi^* = 0$). π^* is the solvent polarity parameter, s is the susceptibility of the variable $(XYZ)_0$ towards solvent polarity changes. The term $d\triangle$ accounts for the enhanced polarizability and other effects involved in aromatic and halogenated solvents.

They have observed that for a class of solvents, which is termed "select", namely aprotic, aliphatic solvents with a dominant bond dipole, all of the empirical solvent polarity scales listed in Table I give equivalent results[26]. This is a very significant finding since the parameters correlated encompass a wide range of observables. Obviously, there must be a single physical process characteristic of the effect of the solvent on all of these variables. In a subsequent paper, Abboud and Taft[27] showed an excellent linear correlation between the empirical π^* values and a simple function of solvent dielectric constant (D). The relationship between π^* and D was obtained from Block and Walker's[28] modification of Kirkwood's equation for the interaction of permanent dipoles in solution[29]. Their work is unique in that it allows the *a priori* calculation of the free energy of interaction based on the knowledge of the solute dipole moment (μ) and radius (a) and the solvent's dielectric constant. It is significant that Taft's definition of a "select" solvent is close to the concept of a non-

hydrogen-bonding polar solvent elaborated by Keller *et al.*[14]. Taft's definition, however, excludes aromatic and halogenated solvents.

The objective of this work was to investigate whether Taft's π^* polarity scale is correlated with commonly used chromatographic measures of retention such as Snyder's ε^0 scale for adsorption on alumina, and estimates of orientation solubility parameters. Although purely dipolar interactions are reasonably selective and therefore chromatographically more interesting than dispersion interactions, it is perhaps even more important to be able to estimate the strength of dipole forces to be better able to discern the contribution of very selective forces to the net intermolecular interaction. The present approach is evidently of little utility in reversed-phase liquid chromatography since these methods rely upon the use of mixed solvents which invariably contain water. It should find its greatest utility in gas–liquid chromatography (GLC).

RESULTS AND DISCUSSION

As stated above, Taft has pointed out the existence of a linear relationship between the π^* polarity value of "select" solvents and a function, termed Θ, of the solvent's dielectric constant. This relationship is obtained from a model which allows the calculation of the electrostatic contribution to the chemical potential of a dipole. Basically, the dipole is assumed to exist in a spherical cavity of radius a, defined by the solute size. The dielectric constant within the cavity is taken as exactly unity. Outside the cavity the dielectric constant is allowed to asymptotically approach the bulk dielectric constant D according to a specific but herein irrelevant relationship given by Block and Walker[28].

By Kirkwood's approach, the work (W) and thus the assumed free energy of charging of a point dipole is given by the equation:

$$W = \frac{-1}{2}\frac{\mu^2}{a^3}\Theta(D) \tag{4}$$

where μ is the dipole moment of the solute (A). The function $\Theta(D)$ is given below and plotted in Fig. 1.

$$\Theta(D) = \frac{3D \ln D}{D \ln D - D + 1} - \frac{6}{\ln D} - 2 \tag{5}$$

Θ varies from 0 at D equal to 1.00, which pertains to a vacuum, to a value of 1.000 at very high dielectric constant. Note that even for a solvent as polar as water, Θ is equal to only 0.504.

A final important point is the assumption of a non-polarizable solute. Estimates indicate that this is unlikely to cause errors of greater than 20%[27]. Implicit in the above discussion is the idea that the solute cavity size is solely established by the solute. Taft points out that this is not necessarily true, particularly if the solvent has a large non-polar end[27]. It is also important to recognize at the outset that the $\Theta(D)$ is also found to be linearly related to the solvent's dipole moment[27].

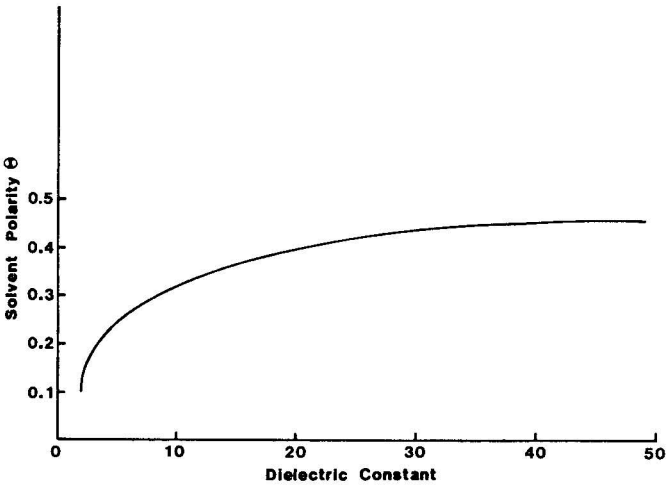

Fig. 1. Solvent polarity function plotted against solvent dielectric constant; computed according to eqn. 5.

The partition coefficient corresponding to transfer of solute from the mobile phase to the stationary phase may be obtained directly from Taft's work as follows:

$$\ln K_{eq} = \frac{1}{2}\frac{\mu_A^2}{RT\,a^3}\left(\Theta(D_s) - \Theta(D_m)\right) \tag{6}$$

This equation can be put in terms of macroscopic properties by assuming a spherical solute molecule and a value for the voidage between molecules in the condensed state (taken here as 0.40[30]). When the dipole moment is assigned units of Debyes, eqn. 6 (at 25 °C) numerically evaluates as:

$$\ln K_{eq} = 50.5\,\frac{\mu_A^2}{\bar{V}_A}\left(\Theta(D_s) - \Theta(D_m)\right) \tag{7}$$

where $\bar{V}_A$ is the molar volume of the solute. This equation is obviously of great chromatographic significance. In essence, it predicts the part of the partition coefficient that is due to the interaction of the solute's permanent dipole with the general polarity function (Θ) of the solvent. It clearly does not include dispersion interactions or acid–base interactions, nor does it encompass induction forces. Physically it corresponds to the dipole orientation solubility parameter (δ_o) as described by Karger *et al.*[15]. However, eqn. 6 agrees with the observation of Karger *et al.*[15] that the strength of a solute's dipole–dipole interaction is proportional to its dipole moment. We believe that eqn. 6 and its roots in Block and Walker's work is the fundamental explanation for their observation. As will be seen later, eqn. 6 can be used to predict the slope of the relationship between free energy of transfer and solvent–solute properties, whereas a numerical value of the slope is not predicted by Karger's[15] entirely empirical correlation of δ_o against μ but is obtainable *a posteriori*. The physical and mathematical formalism used to obtain eqn. 6 is very different from that

which is used in solubility parameter theory. It is very important to note that the interaction is not of the geometric mean type. The function Θ is not proportional to the square of the solvent's dipole moment but rather, as shown by Taft[27], Θ and π^* correlate closely with a linear function of the solvent's dipole moment. If the physical reality behind eqns. 4 and 5 is correct, then permanent dipoles do not interact by geometric mean processes; consequently, the mathematical approach and the experimental values of δ_0, which are estimated by use of mathematics based on the geometric mean, are, strictly speaking, not exact. Thus, one will not be able to demonstrate complete consistency between experimental values of δ_0 and the function $\Theta(D)$. It should further be noted that in the approach taken by Keller *et al.*[14] and Karger *et al.*[15,16] the orientation interaction was treated as being first-order in both the solute and solvent dipole moment. This is clearly not the case for eqns. 4 and 6, *i.e.*, the solute dependence is the same as that predicted in their work but the solvent dependence on dipole moment is weaker.

Eqn. 4 has direct applicability to the estimation of partition coefficients for liquid–liquid chromatography. It should also be useful for comparing the relative GLC retention of two solutes of equal vapor pressure or the effect of change in stationary phase on the retention of a single solute. Although the equation is inapplicable to adsorption processes, it is interesting to compare the function Θ to Snyder's ε^0 values for adsorption on alumina.

Correlation with Rohrschneider's data for GLC

Recently, Rohrschneider reported the gas-phase partition coefficient of a set of solutes, including nitromethane, in common solvents, many of which are "select"[8]. Since nitromethane is a quintessential select solvent, we attempted to see if Rohrschneider's data would correlate with eqn. 7. The relevant data from Rohrschneider, corrected for the molar volume of the solvents as described by Snyder[9] and employed by Karger *et al.*[16] are given in Table II and plotted *vs.* Θ in Fig. 2. A correlation coefficient of 0.936 was obtained. (See Table III, line 2, for statistical results.) When Rohrschneider's data are plotted *vs.* π^* (see Table II), a correlation coefficient of 0.955 is obtained. Thus the experimental π^* value is only slightly superior to the theoretical Θ value. To see how good a correlation coefficient this actually is, the same set of select solvents have a correlation coefficient of 0.971 when π^* is regressed against Θ (Table III, line 1). Obviously, neither is perfect but, in the first case, recalling the definition of the correlation coefficient, over 93% of the variation in ln K_{eq} is due to changes in Θ. It should be noted that we have used data for solvents which are common to both Taft's and Rohrschneider's work, excluding the non-select solvents. Values of Θ were those reported by Taft; no attempt was made to estimate Θ values for other solvents. It is evident that a linear relationship exists between ln K_{eq} (nitromethane) and Θ as well as π^*. For nitromethane ($\overline{V} = 54$ ml/mol, $\mu = 3.9$ Debye) the slope of a plot of ln K_{eq} *vs.* $\Theta(D)$, as indicated by eqn. 7, should be 14.2. The slope of the least squares best line is 4.5 ± 0.42. The discrepancy between the good correlation coefficient yet poor agreement between the theoretical and experimental slopes is discussed later.

We also correlated Rohrschneider's data for the partitioning of methyl ethyl ketone in a series of 17 select solvents with Θ. The correlation coefficient was only 0.634, which is much poorer than that for nitromethane. In fact, the correlation

coefficient of the partition coefficient of nitromethane *vs.* methyl ethyl ketone for these 17 solvents was only 0.666. It should be noted that the slope of a plot of ln K_{eq} (methyl ethyl ketone) *vs.* Θ was 1.55 $\pm$ 0.48 (see Table III, line 3). The theoretical slope should be 4.09. Neither methyl ethyl ketone nor nitromethane is a hydrogen-bond donor, and the solvents tested all conformed to the "select" definition. It is evident that other factors, *e.g.* dispersion (see below), must have a greater relative influence on the ketone data than on the nitromethane data. This is possible since the total change in free energy of transfer of the ketone is considerably less than that of the nitromethane.

Abboud and Taft[27] have examined the free energy of transferring the extremely polar tetramethylammonium chloride ion pair from dimethylformamide to a series of nine solvents ranging from hexane to dimethyl sulphoxide. An excellent correlation coefficient (0.999) was obtained. It is reasonable to expect a good correlation in this case since the dipole moment of the solute is extraordinarily large, thus permanent dipole interactions would overwhelm dispersion processes. The total change in transfer free energy is nearly 18 kcal/mol in this case but only 1100 and 830 cal/mol for nitromethane (Table II) and methyl ethyl ketone, respectively. However, no comparison of the experimental and the theoretical slope was made.

The molar volume of tetramethylammonium chloride has been reported[31] as 107 ml. Using this value and a conservative estimate of the ion pair dipole moments (8.5 D[27], eqn. 7 predicts a slope of 34.1, which should be compared to the value 50.1 observed by Abboud and Taft[27]. The discrepancy between predicted and observed slopes in this case is not as great and may well be due to the error in estimating α from the molar volume since the charges in the dipole are probably closer together than estimated from $\bar{V}_A$. Secondly, the quadrupole contribution to the transfer energy may be as large as 10% in this case[32].

Correlation with orientation solubility parameters

As explained above, the relationship between the Θ polarity function and the orientation solubility parameter (δ_o) cannot be rigorously valid owing to the requirement for a geometric mean interaction. Nonetheless it is interesting to ignore such difficulties and examine the formal relationship between Θ and δ_o. Since Θ represents only interaction between permanent bond dipoles, we will relate it to the *orientation* solubility parameter (δ_o). Let us imagine a perfectly non-polarizable, dipolar molecule. By this definition, the dispersion parameter (δ_o) is exactly zero, thus, by the definition of the solubility parameter, the internal energy which may be taken as the molar energy of vaporization, ΔE^v, will be

$$-\Delta E^v = \bar{V}\,\delta_0^2 \tag{8}$$

where $\bar{V}$ is the molar volume of the pure liquid.

This may be equated with the work needed to transfer 1 mol of A to an ideal gas phase (see eqn. 4) from a solution of pure A, thus

$$\left(\delta_0^A\right)^2 = \frac{1}{2}\frac{\mu_A^2}{\alpha^3\,\bar{V}_A}\Theta(D_A) \tag{9}$$

TABLE II

PROPERTIES OF COMMON SOLVENTS[a]

	Solvent	*Type*[b]	$\bar{V}$[c]	μ[d]	π^*[e]	$\Theta(D)$[f]	$\ln K_{NM}$[g]	$\ln K_{MEK}$[h]	$\delta^{2i}_{o,th}$	$\delta^{2j}_{o,exp}$	δ^{2k}_{p}	δ^{2l}_{p}	ε[m]
1	Hexane	*S*	130	0	−0.081	0.103	4.25	4.67	0	0	0	0	0
2	Heptane	*S*	146	0	0.081	0.104	—	—	0	0	C	0	0
3	Cyclohexane	*S*	108	0	0.000	0.112	4.14	4.59	0	0	0	0	0.4
4	Triethylamine	*S*	140	0.7	0.140	0.138	4.81	4.98	0.10	0	—	—	—
5	Di-*n*-butyl ether	*S*	170		0.239	0.172	4.92	5.00					—
6	Diisopropyl ether	*S*	108	1.1	0.271	0.204	5.01	5.05	0.71	1.0	2.38	—	0.28
7	Diethyl ether	*S*	105	1.2	0.273	0.219	5.09	5.02	0.85	5.76	12.8	1.96	0.38
8	Carbon tetrachloride		97	0	0.294	0.127	—	—	0	0	0	0	—
9	Propanol		75	—	0.534	—	—	—	—	6.76	63.5	—	—
10	Toluene		107		0.535		—	—		0	0	0	—
11	Ethanol		59	—	0.540	—	—	—	—	11.56	18.3	—	—
12	Ethyl acetate	*S*	98	1.9	0.545	0.260	5.71	—	2.91	16	20	6.76	0.58
13	Dioxane		86	—	0.553	—	—	—	—	27.04	42.6	—	—
14	Ethyl bromide	*S*	77	2.0	0.558[n]	0.313	5.20	5.64	6.29	9.61	18.97	2.25	0.37
15	Methyl acetate	*S*			0.56								0.60
16	Tetrahydrofuran	*S*	82	1.8	0.576	0.285	5.64	5.24	4.09	12.25	24.41	7.84	0.58
17	Methanol		41	—	0.586	—	—	—	—	24.01	33.9	—	—
18	Benzene		89	0.0	0.588	0.132	—	—	0	0	0	0	—
19	Methyl ethyl ketone	*S*	90	2.7	0.674	0.383	5.80	—	10.3	22.1	39.13	19.36	0.51
20	Acetone	*S*	74	2.9	0.683	0.394	5.81	5.32	18.0	26.0	46.4	21.0	0.56
21	Chlorobenzne		102	1.6	0.709	0.252	—	—	1.85	3.61	9.1	4.41	—
22	Acetonitrile	*S*	53	3.7	0.713	0.446	5.85	5.19	64.7	70.6	104	77.4	0.71
23	Anisole		109	1.3	0.734	0.219	—	—	0.93	4.45	11.69	—	—
24	Cyclohexanone	*S*	104	3.1	0.755	0.367	5.75	5.26	—	—	—	—	—
25	Chloroform		81	1.3	0.760	0.232	—	—	1.78	9.0	17.1	—	—
26	Bromobenzene		105		0.794		—	—		2.25	4.5	7.3	—

27	1,2-Dichloropropane		79		0.807	—	—	—	—	17.6	25.8	—	—
28	Propionitrile	*S*	71	4.0	0.387[n]	0.419	—	—	41.8	43.6	68.4	49.0	—
29	Nitromethane	*S*	54	3.5	0.848	0.448	—	5.19	55.6	68.9	113	84.6	0.64
30	Nitropropane		88	3.6	0.860[n]	0.408	—	—	—	—	—	—	0.53
31	Nitroethane	*S*	71	3.7	0.860[n]	0.425	5.78	5.32	34.4	36.0	68.1	57.8	—
32	Pyridine		81	2.2	0.867	0.342	—	—	7.51	14.4	32.4	18.5	—
33	Hexamethylphosphoramide	*S*	176	—	0.871	—	—	—	—	11.6	40.1	—	—
34	γ-Butyrolactone	*S*	77		0.873	—	—	—	—	51.8	103	—	—
35	Dimethylformamide	*S*	77	3.8	0.875	0.444	6.03	5.22	32.2	38.4	76.4	44.9	—
36	Dimethylacetamide	*S*	92	3.8	0.882	0.447	6.09	5.27	22.7	22.1	48.3	31.4	—
37	2-Methylpyrolidone	*S*	76	4.1	0.921	0.433	6.09	5.21	37.1	—	—	72.3	—
38	Ethylene glycol		56	—	0.932	—	—	—	—	46.2	65.8	—	—
39	Dimethyl sulfoxide	*S*	71	3.9	1.00	0.467	6.00	4.95	42.0	37.2	72.5	64.0	0.62
40	Nitrobenzene		103	3.9	1.029	0.440	—	—	18.8	13.0	33.9	17.6	—

[a] These solvents are those which are common to Taft's list of π^* values and either Karger *et al.*'s[15] or Barton's[33] list of solubility parameters. Only select solvents were tested in any correlation except where indicated in the text.

[b] The solvents indicated with an *S* in this column are defined as being select by Abboud and Taft[27].

[c] The molar volume of the solvent (ml/mol).

[d] The dipole moment in Debyes from ref. 26, except as indicated.

[e] The Taft π^* value from ref. 25.

[f] The value of the Θ function for the solvent from ref. 27.

[g] The natural logarithm of the mole fraction equilibrium constant for the partitioning of nitromethane between the gas phase and the indicated solvent, from ref. 8.

[h] The natural logarithm of the mole fraction equilibrium constant for the partitioning of methyl ethyl ketone between the gas phase and the indicated solvent, from ref. 8.

[i] The theoretical value of δ_0^2, computed from eqn. 10 (cal/ml).

[j] The experimental orientation solubility parameter (cal/ml), from ref. 15.

[k] The experimental polar solubility parameter computed from eqn. 12 with the data of ref. 14.

[l] The experimental polar solubility parameter, from ref. 33.

[m] The solvent strength for alumina as an adsorbent, from ref. 3.

[n] Estimated from Taft's correlation of dipole moment with π^*.

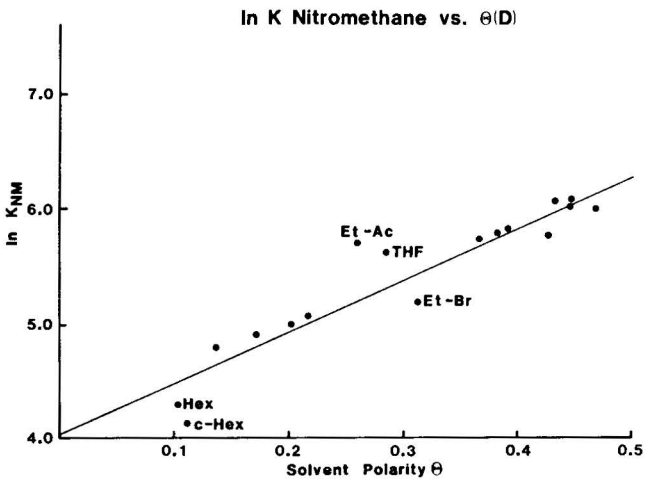

Fig. 2. Plot of logarithm of mole fraction partition coefficient of nitromethane against solvent polarity function (Θ). The number on each point refers to the list of solvents in Table II.

Since eqn. 4 and, therefore, eqn. 9, are inherently based on the assumption of a spherical solute, we proceed, as before, to replace a^3 with the molar volume of the solute. When μ and δ are assigned units of Debyes and $(\text{cal/ml})^{1/2}$ respectively, we obtain

$$\left(\delta^{A}_{0,th}\right)^2 = 2.98 \cdot 10^4 \left(\frac{\mu_A}{\bar{V}_A}\right)^2 \Theta(D_A) \tag{10}$$

This equation may be used to compute a theoretical value of the orientation solubility parameter (designated $\delta_{o,th}$) which can then be compared to experimental values ($\delta_{o,exp}$) such as those compiled by Barton[33] based on the homomorph approach, and those based on the more recent approach of Keller *et al.*[14]. In order not to be misleading, it should be pointed out that Karger *et al.*[15] empirically found that their δ_o values did correlate with the same explicit dependence on the solvent's dipole moment and molar volume. Their approach did not, however, yield any method for the *a priori* prediction of the slope of a plot of δ_o *vs.* $\mu_A/\bar{V}_A$, nor did it encompass the dependence of δ_o on the solvent's dielectric constant.

The results are summarized in Table III and plotted in Fig. 3. It should be noted that the correlation was conducted in terms of the square of the solubility parameter so that the scale would be linear in energy and therefore comparable to the scale used in Fig. 2. This has the consequence that large values of δ_o are weighted very heavily. We consider this to be a fair basis for comparison, particularly since the $\delta_{o,exp}$ values are estimated from differences in large quantities[14] and thus small values tend to be very imprecise. Secondly, when δ_o are small, non-polar processes are dominant.

Hildebrand *et al.*[11] indicate that one can expect an internal consistency amongst solubility parameters which is no better than some fraction of *RT*, *i.e.* of the thermal energies; in their work the value 1/5 is chosen arbitrarily. This amounts to $\pm$ 120 cal/mol at room temperature. For a species with $\bar{V}$ of 75 ml/mol this

TABLE III

RESULTS OF VARIOUS CORRELATIONS

A conventional (slope, intercept) unweighted linear least-squares program was used except where indicated. All solubility parameters are from ref. 14 except where indicated. n = Number of data pairs in the correlation.

	Correlation (y vs. x)	n[§]	*Correlation coefficient*	*Slope ± S.D.*	*Intercept ± S.D.*
1	Θ *vs.* π^*	17	0.970	0.36 ± 0.15	0.12 ± 0.15
2	ln K_{NM} *vs.* Θ	18	0.936	4.5 ± 0.4	4.0 ± 0.14
3	ln K_{MEK} *vs.* Θ	17	0.666	1.55 ± 0.48	3.65 ± 0.4
4	$(\delta_{o,exp})^2$ *vs.* $(\delta_{o,th})^2$[§]	17	0.972	1.02 ± 0.06	3.9 ± 1.8
5	$(\delta_{o,exp})^2$ *vs.* $(\mu/\bar{V})^2$[§]	17	0.979	$(1.4 \pm 0.07) \cdot 10^{+4}$	$(2.5 \pm 1.6) \cdot 10^{-4}$
6	$(\delta_{o,exp})^2$ *vs.* $(\delta_{o,th})^2$[§§§]	17	0.984	1.11 ± 0.05	0[§§§]
7	$(\delta_{o,exp})^2$ *vs.* $(\mu/\bar{V})^2$[§,§§§]	17	0.975	$(1.48 \pm 0.06) \cdot 10^{-4}$	0[§§§]
8	δ_ϱ^2 *vs.* $(\delta_{o,th})^2$[§]	16	0.963	1.60 ± 0.12	11.6 ± 3.5
9	δ_ϱ^2 *vs.* δ_ϱ^2[§§]	15	0.973	0.82 ± 0.05	−7.9 ± 3.2

[§] Data are from ref. 14.

[§§] This is a correlation of $\delta_\varrho(y)$ from ref. 30 with $\delta_\varrho(x)$ computed from the data in ref. 14.

[§§§] A modified unweighted least-squares program which forces a zero intercept was employed.

amounts to an uncertainty of ± 0.8 $(\text{cal/ml})^{1/2}$ at δ equal to 1 and only ± 0.2 at δ equal to 4. Thus there is good reason to rely on the small δ values less heavily than on the larger values.

We note from Table III that the correlations of $(\delta_{o,exp})^2$ *vs.* $(\delta_{o,th})^2$ and against $(\mu/\bar{V})^2$ are both very good. Indeed, the patterns of signs of the residuals for both correlations are identical. One could argue that the term Θ in eqns. 9 and 10 is only responsible for a small part of the correlation and that the dominant effect is due to

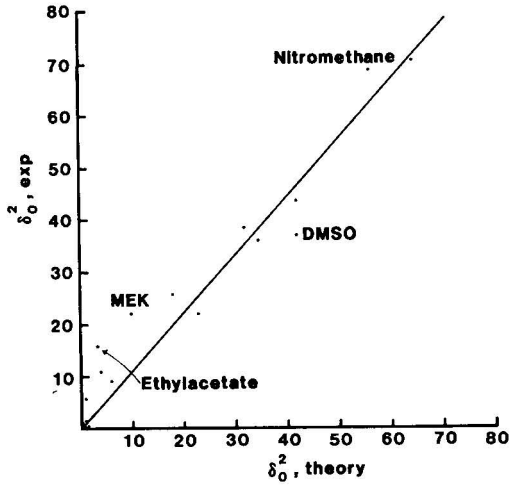

Fig. 3. Comparison of experimental and theoretical orientation solubility parameters. Experimental data are from ref. 14 and theoretical data are computed from the data in Table II. Note that solubility parameters are squared.

the term $\mu/\overline{V}$, and that perhaps the Θ function is really rather trivial. It should also be noted that both correlations yield a significant positive intercept. We felt that the use of a two-parameter (slope, intercept) fit might not be valid in view of the fact that both eqn. 10 and simple proportionality between $(\delta_{o,exp})^2$ and $(\mu/\overline{V})^2$ predict a zero intercept which is supported by all the data for totally non-polar molecules (see Table II). The regression was re-run, using a least squares program that forced a zero intercept. In this case the correlation *vs.* $(\delta_{o,th})^2$ produces a slightly better correlation coefficient than does the correlation $(\mu/\overline{V})^2$. The improvement is statistically insignificant at the 90% confidence level.

It should be noted as stated above that Karger *et al.*[15] observed that δ_o was closely correlated with $\mu/\overline{V}$, thus the correlation is not surprising. Abboud and Taft[27] have shown that Θ strongly correlates with a linear function of dipole moment. Owing to the presence of a large intercept in the correlation of Θ *vs.* μ, eqn. 10 actually predicts a cubic dependence of δ_o at high dipole moment but only a quadratic dependence at low dipole moment. At present, there is too much scatter in the data to disclose any such non-linearity.

We believe that the most important point in this work is not the prediction of the dependence of δ_o on $\mu/\overline{V}$ but the fact that *we are able to predict the correct slope* of the relationship. As indicated by the data of Table III, the slope of $(\delta_{o,exp})^2$ *vs.* $(\mu/\overline{V})^2$ is $1.4\cdot10^{-4}$ (line 5, Table III) whenever the slope of $(\delta_{o,exp})^2$ *vs.* $(\delta_{o,th})^2$ is 1.02 (line 4, Table III). We believe that the ability of eqn. 4, which includes $\Theta(D)$, to successfully predict the correct slope is the strongest argument for its use and the importance of the term $\Theta(D)$.

To a certain extent this excellent agreement is unexpected in view of the factor of 4 discrepancy in the observed and the theoretical slope of the plot of ln K_{eq} *vs.* Θ shown in Fig. 2.

Part of the difficulty may be due to the use of a sphere to represent the shape of all the solutes. Meyers[34] has found that the correlation between boiling temperature and molar volume can be greatly improved by taking molecular shape into account. Nonetheless, it is difficult for this alone to reconcile the error of a factor of 4 in the slope of the data of Fig. 2 with the fact that eqn. 10 underestimates δ_o of nitromethane by only 25%.

The data of Fig. 3 obviously apply only to orientation interactions. In contrast, the data of Fig. 2 necessarily involve other types of interaction, notably dispersion and induction. Karger *et al.*[15] have presented a model for GLC in terms of the interactions of the individual components of the solubility parameters of any two molecules. When their approach is applied to a non-hydrogen-bonding pair of solute (A) and solvent (S) molecules, one obtains:

$$-RT \ln K_{eq} = \overline{V}_A [\delta_S^2 - 2\delta_{d,A} \cdot \delta_{d,S} - 2\delta_{o,A} \cdot \delta_{o,S} - 2\delta_{in,A} \cdot \delta_{d,S} - 2\delta_{d,A} \cdot \delta_{in,S}] \quad (11)$$

One can show that a correlation exists for the available data between the term $\delta_{o,A}\cdot\delta_{o,S}$ and the sum of all other terms in brackets in eqn. 11. In fact, the correlation coefficient (−0.967) indicates an inverse dependence. Obviously, the low slope of the data of Fig. 2 is due to a cancellation of terms. We felt that this might reflect a correlation between δ_d and δ_o for the solvents tested. No significant correlation exists

($\varrho = -0.067$). At this time, we do not know the physical source of the correlation which, nonetheless, is statistically real for this data set.

Clearly, the effect of dispersion and induction shows up in Rohrschneider's partition coefficients but, owing to the way δ_o is defined and its direct physical relationship to eqns. 4 and 10, other factors are excluded. Thus, the error in the predicted slope of the data of Fig. 2 is due to the presence of other factors in the data, and the accuracy of the slope of Fig. 3 is due to their successful exclusion from experimental δ_o values.

Several other correlations were tested for the sake of completeness. The total *polar* solubility parameters for the select solvents were computed from literature data according to the equation:

$$\delta_\varrho^2 = \delta_0^2 + 2\delta_{in} \cdot \delta_d \tag{12}$$

Since the inductive solubility parameter must also depend[16,33] upon $\mu/\overline{V}$, we correlated $(\delta_{o,th})^2$ with the total experimental polar solubility parameters. As Table III (line 8) indicates, the correlation coefficient decreases slightly but the slope increases quite significantly to 1.60 ± 0.12. The polar solubility parameter data of Karger *et al.*[15] are correlated against the polar solubility parameters obtained from Barton[33]. It is evident (Table III) that the correlation between experimental measures of the same parameters are no better than the *a priori* prediction from eqn. 10. In fact, the slope of this regression is 0.82 ± 0.05. The two experimental polar solubility parameter scales are not completely consistent. We should point out that for non-polar hydrocarbons the refractive index method of predicting δ_d was only precise to within ± 0.4 (cal/ml)$^{1/2}$. Obviously it must be assumed that the correlation of δ_d with refractive index holds up even for polar compounds. This may not be entirely valid.

Correlation with Snyder's adsorbent polarity scale

Fig. 4 is a plot of Snyder's solvent strength parameter ε^0 *vs.* Θ for 15 solvents

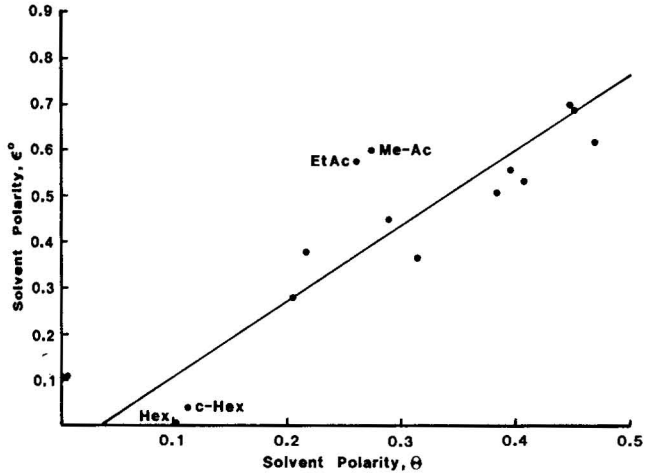

Fig. 4. Plot of adsorption chromatography solvent strengths parameters against solvent polarity function. All data are from Table II.

ranging in polarity from hexane ($\varepsilon^0 = 0$; $\Theta = 0.103$) to acetonitrile ($\varepsilon^0 = 0.50$; $\Theta = = 0.446$). It is obvious that the correlation is not nearly as good as that in Figs. 2 and 3. The correlation coefficient is only 0.930. When the three non-polar hydrocarbons are deleted from the line, the correlation coefficient drops to only 0.69. It is not surprising that the Θ function does not adequately represent the interactions of solvent molecules with the surface of an adsorbent. Obviously there are enormous differences in the geometry of the allowable interactions. Secondly, the Θ polarity function only accounts for orientation interactions. Karger *et al.*[16] have presented convincing data that electron pair acceptor sites on alumina are very important in adsorption chromatography. The chief reason why a correlation coefficient as high as 0.92 is obtained in this case is because dispersion interactions which are associated with non-polar groups are relatively unimportant for adsorption on alumina.

CONCLUSIONS

At this point, we believe that the Θ polarity function described by Taft, and the related π^* polarity scale, have considerable importance in chromatography. It is clear that none of the correlations of the properties of select solvents described in this work is quite as good as those found by Taft (see Table I). This can be attributed to the fact that partition equilibria are governed by the sum of all intermolecular forces on all atoms in a molecule. In contrast, solvent effects on reaction rates, chemical equilibria between two species or photon absorption tend, to a first approximation, to be localized about those groups on the molecule which participate in the chemical reaction or are responsible for photon absorption. In our view the Taft π^* polarity scale is rather sensitive to dipolar interactions and rather insensitive to dispersion interactions. This concept is supported by the linear relationship between π^* and Θ since Θ is not strongly dependent on molecular polarizability but is closely related to the solvent's dipole moment. Chromatographic retention is evidently very sensitive to both dispersive and polar forces. It would seem that net retention in select solvents could be better described by a combination of dispersion interaction via δ_d and Taft's π^* or by the Θ function as a measure of permanent dipole interactions.

ACKNOWLEDGEMENTS

I would like to thank Mr. James Brady and Professor Maurice Kreevoy of this department for many helpful conversations about this work, and the National Institute of Occupational Safety and Health for partial financial support (RO1-OH-00876).

REFERENCES

1 J. C. Giddings, *Dynamics of Chromatography*, Marcel Dekker, New York, 1965.
2 P. H. Weiner, C. J. Dack and D. G. Howery, *J. Chromatogr.*, 59 (1972) 249.
3 L. R. Snyder, *Principles of Adsorption Chromatography*, Marcel Dekker, New York, 1968.
4 I. Molnár and Cs. Horváth, *J. Chromatogr.*, 145 (1978) 371.
5 B. L. Karger, Y. Elmehrik and W. Andrade, *J. Chromatogr.*, 7 (1969) 209.
6 L. Rohrschneider, *J. Chromatogr.*, 22 (1966) 6.

7 W. O. McReynolds, *J. Chromatogr. Sci.*, 8 (1970) 685.
8 L. Rohrschneider, *Anal. Chem.*, 45 (1973) 1241.
9 L. R. Snyder, *J. Chromatogr.*, 92 (1974) 223.
10 L. R. Snyder, *J. Chromatogr. Sci.*, 16 (1978) 223.
11 J. H. Hildebrand, J. M. Prausnitz and R. L. Scott, *Regular and Related Solutions*, Van Nostrand-Reinhold, New York, 1970.
12 B. L. Karger, L. R. Snyder and Cs. Horváth, *An Introduction to Separation Science*, Interscience, New York, 1973.
13 L. R. Snyder and J. J. Kirkland, *Introduction to Modern Liquid Chromatography*, Wiley-Interscience, New York, 2nd ed., 1979, p. 246.
14 R. A. Keller, B. L. Karger and R. L. Snyder, in R. Stark and S. C. Perry (Editors), *Gas Chromatography 1970*, Institute of Petroleum, London, 1971, p. 195.
15 B. L. Karger, L. R. Snyder and C. Eon, *J. Chromatogr.*, 125 (1976) 71.
16 B. L. Karger, L. R. Snyder and C. Eon, *Anal. Chem.*, 50 (1978) 2126.
17 K. Dimroth, C. Reichardt, T. Seipman and F. Bohlmann, *Justus Liebig's Ann. Chem.*, 661 (1963) 1.
18 L. G. S. Brooker, A. C. Craig, P. W. Heseltine, P. W. Jenkins and L. L. Lincoln, *J. Amer. Chem. Soc.*, 87 (1965) 2433.
19 C. Lassau and J. C. Jungers, *Bull. Soc. Chim. Fr.*, (1968) 2678.
20 D. Walther, *J. Prakt. Chem.*, 316 (1974) 604.
21 B. Knauer and J. J. Napier, *J. Amer. Chem. Soc.*, 98 (1976) 4395.
22 A. Allerhand and P. v. R. Schleyer, *J. Amer. Chem. Soc.*, 85 (1963) 374.
23 R. W. Taft, G. B. Klingensmith, E. Price and I. R. Fox, *Prepr. Pa. Symp. LFE Relat.*, (1964) 265.
24 S. Braunstein, *Can. J. Chem.*, 38 (1960) 1590.
25 M. J. Kamlet, J. L. Abboud and R. W. Taft, *J. Amer. Chem. Soc.*, 99 (1977) 6027.
26 J. L. Abboud, M. J. Kamlet and R. W. Taft, *J. Amer. Chem. Soc.*, 99 (1977) 8325.
27 J. L. Abboud and R. W. Taft, *J. Phys. Chem.*, 83 (1979) 412.
28 H. Block and S. M. Walker, *Chem. Phys. Lett.*, 19 (1973) 363.
29 J. G. Kirkwood, *J. Chem. Phys.*, 2 (1934) 251.
30 W. C. Duer, J. R. Greenstein, G. B. Oglesby and F. J. Millero, *J. Chem. Educ.*, 54 (1977) 139.
31 M. H. Abraham and G. F. Johnston, *J. Chem. Soc., A*, (1971) 1610.
32 M. H. Abraham and R. J. Abraham, *J. Chem. Soc., Perkin Trans. II*, (1974) 47.
33 A. F. M. Barton, *Chem. Rev.*, 75 (1975) 731.
34 R. T. Meyers, *J. Phys. Chem.*, 83 (1979) 294.

Journal of Chromatography, 194 (1980) 121–134
Elsevier Scientific Publishing Company, Amsterdam — Printed in The Netherlands

CHROM. 12,739

TOPOLOGICAL ANALYSIS OF THE BEHAVIOUR OF LINEAR ALKENES UP TO TETRADECENES IN GAS–LIQUID CHROMATOGRAPHY ON SQUALANE

JACQUES-EMILE DUBOIS and JACQUES R. CHRÉTIEN*

Institut de Topologie et de Dynamique des Systèmes, Université Paris VII, associé au C.N.R.S., 1 Rue Guy de la Brosse, 75005 Paris (France)

LADISLAV SOJÁK

Chemical Institute of Comenius University, Bratislava (Czechoslovakia)

and

JACK A. RIJKS

Department of Instrumental Analysis, Eindhoven University of Technology, Eindhoven (The Netherlands)

(Received February 4th, 1980)

SUMMARY

DARC topological analysis (DTA) has been applied to Kováts retention indices for a series of 84 linear alkenes up to tetradecenes studied by gas–liquid chromatography on squalane at 100 °C. The topology–information diagram gives information at the skeletal carbon atom level of the alkene molecules. Very small structural effects are detected and discussed on a statistical basis. This set of *n*-alkenes constitutes a good model for testing the interpretative and physico-chemical potentialities of DTA in order to establish a set of precise reference data for higher *n*-olefins of petrochemical interest.

INTRODUCTION

In petrochemistry, much attention has been devoted to the catalytic dehydrogenation of *n*-alkanes in order to make optimal use of all of the crude oil cut[1]. This dehydrogenation gives a mixture of unsaturated hydrocarbons in which *n*-alkenes are the major and the most interesting components. These *n*-alkenes include all possible positional and geometric isomers with a number of carbon atoms corresponding to the respective *n*-alkanes.

The properties of these isomers are very similar and therefore they can only be separated by high-performance capillary gas chromatography. The problem of identifying individual isomers has been solved particularly on squalane[2,3]. Even for lower *n*-alkenes the separation of every isomer may be difficult. When the number of carbon atoms increases the number of possible isomers increases rapidly. The series of *n*-alkenes from 2 to 20 carbon atoms includes 181 compounds. The greater the

0021-9673/80/0000–0000/$02.25

chain length and the more central the position of the carbon–carbon double bond, the more difficult is the separation of these positional isomers. For example, the total separation ($R \neq 1.5$) of *cis*-9- from *cis*-8-octadecene and of *trans*-9- from *trans*-8-octadecene requires high-performance capillary columns which should have about $5 \cdot 10^6$ theoretical effective plates[4]. Such separations are beyond the possibilities of contemporary gas chromatography.

With more polar phases (Carbowax 20M) the separation of these particular positional isomers encounters similar difficulties[4]. Nevertheless, when the polarity of the stationary phase increases, the *cis* isomer is retained more than its corresponding *trans* isomer. Since 1972, the limits of systematic studies of higher *n*-alkenes have been refs. 2, 3, 5, 6 and are still being pushed ahead[4,7]. Thus, the characterization of *n*-hepta- and *n*-octadecenes on apolar and polar phases (hydrocarbon C_{87}, Apiezon L and Carbowax 20M) has recently been carried out[4] and the characterization of *n*-nonadecenes and *n*-docosenes is under way.

Simultaneously, the development and utilization of data banks[8] require interpolation and extrapolation of experimental data with appropriate data processing methods. Topological analysis (DTA) based on the concepts of the DARC topological system (DARC stands for Description, Acquisition, Retrieval and Computer-aided design[9–11]) has been developed for this purpose[12,13]. The precision of gas chromatographic data offers a good model for the physico-chemical interpretation of the behaviour of compounds expressed at the carbon atom level[14,15] to work out specific interactions which represent another exciting and new direction of research for DTA[16].

In this work we have used DTA to analyse and summarize previous experimental data on *n*-alkenes in order to orientate and minimize further experiments with higher unsaturated *n*-alkenes, dienes or branched alkenes of interest in petrochemistry by calculating a set of precise reference data. Further, the *n*-alkene series is one of the simplest from a structural point of view, but corresponding data have been determined with great precision[2] and very small structural effects can be detected[17]. Consequently, this series constitutes a good model for testing the interpretative potentialities of DTA for the physico-chemical exploitation of retention data in gas–liquid chromatography at the skeletal carbon atom level of the alkene molecules.

EXPERIMENTAL

The data used[2] were determined at 100 °C by high-performance capillary gas chromatography on a stainless-steel capillary column (200 m × 0.25 mm I.D.) coated with squalane. The reproducibility of the measurements, calculated as the standard deviation, was 0.18 Kováts index (KI) with C_6–C_{10} *n*-alkenes and 0.10 KI with higher *n*-alkenes. Kováts indices on squalane at 100 °C for lower alkenes (ethene, propene and 1-butene) were taken from Hively and Hinton[18], whereas for *trans*-2-butene, *cis*-2-butene and isomeric pentenes the data were taken from Rijks and Cramers[19].

We used DARC topological analysis, which is particularly adapted for the treatment of chromatographic retention data of linear and branched compounds[12–16], but which can also be used for this simple model. This method agrees with the criteria underlined by Souter[20] to define a good method of data processing, that is, simul-

taneous optimization of the number of parameters, the number of compounds used, the precision of the calculation and potential of prediction[19]. The correlations were set up by the DARC/PELCO (Perturbation of an Environment Limited Concentric and Ordered) procedure[9–11]. The principles of this procedure have already been discussed previously with respect to their applications in chromatography[12]. Only certain terms and salient features will be recalled.

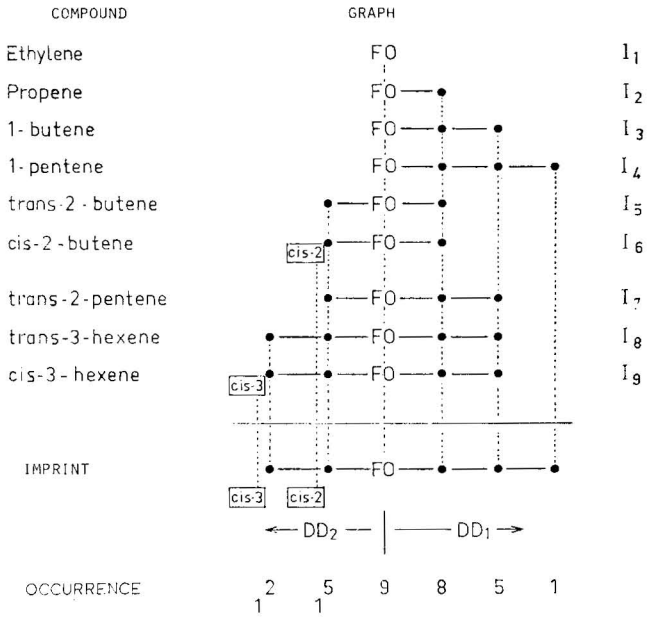

Fig. 1. Principle of superposition of elementary alkene graphs giving an imprint or trace (Tr) characteristic of this set of nine compounds.

Fig. 1 shows how a set of nine *n*-alkenes (CH_2=CH–R, and R′–CH=CH–R) is derived from ethene by progressive and ordered substitution. The pattern C=C is taken as the focus. A graph is associated with each of these linear alkenes. The topological sites correspond to the nodes of the graph. Here these nodes correspond to the skeletal carbon atoms of the alkene molecules. Superposition of these elementary graphs gives the characteristic imprint or trace of this set of compounds.

The two development directions DD_1 and DD_2 are non-equivalent because the graphs are ordered. DD_1 is the priority direction, corresponding to lengthening of the alkyl chain R in 1-alkenes CH_2=CH–R and in R′–CH=CH–R with $R \geqslant R'$. A 180° rotation of the graph of *trans*-2-pentene, in Fig. 1, would be in contradiction with the convention of DD_1 precedence. *Cis* isomers are identified relative to the corresponding *trans* isomers by a supplementary parameter labelled *cis*. In Fig. 1 the occurrence of the focus, topological sites and *cis* parameters is indicated.

Fig. 2a gives the imprint, also called trace (Tr) on generation grounds[10], of the 84 alkenes listed in Table I. The generation order of all sites is expressed by the

concept of an "Environment that is Limited Concentric and Ordered" (ELCO). Each site is localized in the ELCO by a linear order labelling A_i or B_{ij} (Fig. 2b) with $j = i = 1$ in the particular case of n-alkenes. The influence of the site is interpreted as a perturbation term (P). For example, the evaluation of term A_1 in the second environment E_B^2 of the first development direction DD_1 (Fig. 2b) corresponds to the difference between information I_4 and information I_3 in Fig. 1, which are relative to 1-pentene and 1-butene, respectively. Actually, the perturbation term of a site is an average value, and is optimized by using a multiple regression program that takes into account all the members of a given population containing this site. This multiple regression shows the interest of giving the occurrence of every topological site to calculate their contribution on statistical bases. Site A_1 in the above example occurs 75 times in the alkene population studied (Fig. 2c).

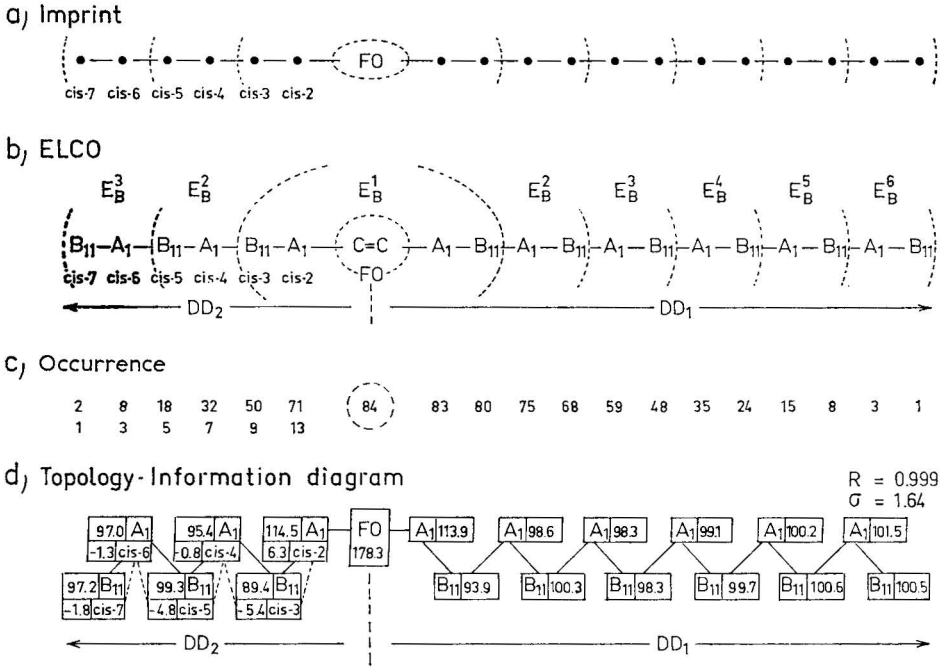

Fig. 2. Organization and distribution of the topological sites. (a) Imprint of the population of 84 n-alkenes obtained by superposition of their corresponding elementary graphs. (b) Organization of molecular environment by the ELCO concept. (c) Occurrence indicates the number of times that each topological site appears when the imprint is determined. (d) Topology–information diagram of the topological analysis of Kováts indices of 84 n-alkenes on squalane at 100°C (this correlation has 25 parameters).

The perturbation terms are the components of vector $\vec{I}(m)$ that characterizes the information for an experimental population made up of m compounds. This vector is defined by the basic topology–information relationship

$$I(\mathscr{E}) = < \vec{T}(\mathscr{E}) \mid \vec{I}(m) >$$

where $I(\mathscr{E})$ is the contribution from the environment to the Kováts index and $\vec{T}(\mathscr{E})$

is the topological vector of the environment $\vec{T}(\mathscr{E}) = (x_1, \ldots, X_n)$ with $X_n = 1$ when the nth site of the environment is occupied, and $X_n = 0$ when it is not. The DARC–PELCO method[9–11] consists in calculating the contribution of the focus FO and of the $I(m)$ vector and in defining thereby a topology–information correlation which can be presented as the topology–information diagram of Fig. 2d. The principle of the utilization of such a diagram is given in Fig. 3.

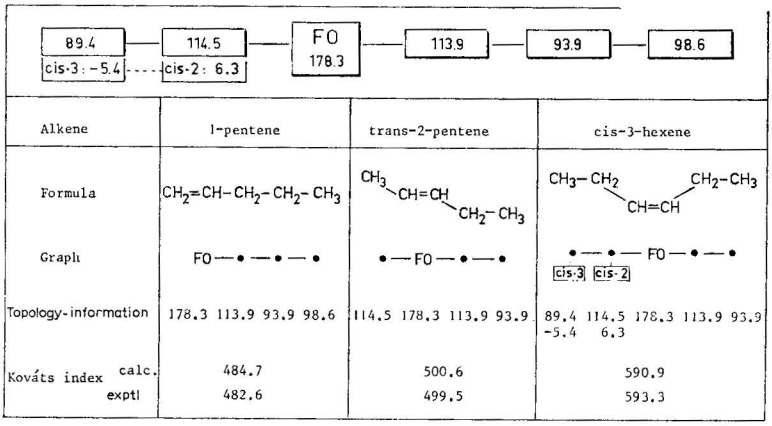

Fig. 3. Application of the diagram in Fig. 2d to some examples from Fig. 1. We have recalled here a portion of the topology–information diagram useful for these examples.

Calculated Kováts indices with this correlation are compared with experimental Kováts indices in Table I. The corresponding correlation has 25 parameters and the statistical tests are very good: the correlation coefficient is $R = 0.9999$ and the standard deviation is $\sigma = 1.64$. In previous studies on linear and branched alkenes[12,13,15] we gave only one parameter to characterize the average behaviour of *cis*-alkenes relative to the *trans*-alkenes. By this procedure the correlation is limited to 20 parameters, the correlation coefficient remains practically the same, but the standard deviation increases ($\sigma = 2.78$). The *cis* parameter equals 1.16 KI. With this 20-parameter correlation, estimated Kováts indices and their differences from experimental values are also given in Table I.

RESULTS AND DISCUSSION

Fig. 2d summarizes the behaviour of the 84 alkenes in terms of the contribution of every topological site. It gives the role played by every carbon atom when the chain length increases for every kind of *n*-alkene, *i.e.*, 1-alkenes, *cis*- and *trans*-2-alkenes, etc., up to *cis*- and *trans*-7-alkenes. Fig. 3 explains how such a diagram is used to calculate the Kováts indices of *n*-alkenes which have a graph included in the imprint of the population studied even if the compound has been studied previously or not.

For homologous series, analysts are accustomed to use a graphical exploitation of retention data in the form of linear relationships of Kováts index *versus* the number of carbon atoms. Such a graph will have here about 14 straight parallel lines

TABLE I

TOPOLOGICAL ANALYSIS OF KOVÁTS INDICES FOR 84 *n*-ALKENES ON SQUALANE AT 100 °C.

Parameters of the topology–information correlations having 25 parameters are given in Fig. 3.

No.	*n-Alkene*	*Kováts index*				
		Exptl. *(a)*	*Calc.* *(b)*	*Difference* *(a) − (b)*	*Calc.* *(c)*	*Difference* *(a) − (c)*
Correlation:						
	Number of compounds used		84		84	
	Number of parameters		25		20	
	Correlation coefficient, R		0.999		0.999	
	Standard deviation, σ		1.64		2.78	
1	Ethene	178.30	178.31	−0.01	178.31	−0.01
2	Propene	288.20	292.19	−3.99	292.33	−4.13
3	1-Butene	385.20	386.09	−0.89	386.23	−1.03
4	*trans*-2-Butene	405.90	406.70	−0.80	409.44	−3.54
5	*cis*-2-Butene	417.80	413.00	4.79	410.15	7.65
6	1-Pentene	482.60	484.71	−2.11	484.84	−2.24
7	*trans*-2-Pentene	499.50	500.60	−1.10	503.34	−3.84
8	*cis*-2-Pentene	505.40	506.91	−1.51	504.06	1.34
9	1-Hexene	583.80	585.02	−1.22	585.16	−1.36
10	*trans*-3-Hexene	591.10	589.96	1.13	590.08	1.02
11	*cis*-3-Hexene	593.30	590.90	2.40	590.80	2.51
12	*trans*-2-Hexene	596.50	599.22	−2.72	601.95	−5.45
13	*cis*-2-Hexene	604.90	605.52	−0.62	602.67	2.23
14	1-Heptene	683.10	683.36	−0.26	683.50	−0.40
15	*trans*-3-Heptene	687.40	688.57	−1.17	688.69	−1.29
16	*cis*-3-Heptene	692.00	689.51	2.49	689.41	2.59
17	*trans*-2-Heptene	698.70	699.53	−0.83	702.27	−3.57
18	*cis*-2-Heptene	704.70	705.83	−1.13	702.98	1.72
19	1-Octene	782.60	781.66	0.94	781.80	0.80
20	*trans*-4-Octene	784.10	783.99	0.11	783.72	0.38
21	*cis*-4-Octene	788.20	784.15	4.05	784.43	3.77
22	*trans*-3-Octene	788.20	788.89	−0.69	789.01	−0.81
23	*cis*-3-Octene	789.80	789.82	−0.02	789.72	0.08
24	*trans*-2-Octene	797.50	797.89	−0.39	800.61	−3.11
25	*cis*-2-Octene	803.20	804.17	−0.97	801.32	1.88
26	1-Nonene	882.50	880.80	1.70	880.93	1.57
27	*trans*-4-Nonene	884.20	884.30	−0.10	884.03	0.17
28	*cis*-4-Nonene	885.40	884.46	0.94	884.74	0.66
29	*trans*-3-Nonene	886.40	887.23	−0.83	887.35	−0.95
30	*cis*-3-Nonene	887.50	888.16	−0.66	888.06	−0.56
31	*trans*-2-Nonene	896.40	896.17	0.23	898.91	−2.51
32	*cis*-2-Nonene	901.90	902.47	−0.57	899.62	2.28
33	*cis*-5-Decene	981.60	978.99	2.61	981.67	−0.07
34	*trans*-4-Decene	982.50	982.64	−0.14	982.37	0.13
35	1-Decene	982.50	980.48	2.02	980.62	1.88
36	*cis*-4-Decene	982.80	982.80	−0.00	983.09	−0.29
37	*trans*-5-Decene	984.10	983.63	0.47	980.96	3.14
38	*trans*-3-Decene	985.80	985.53	0.27	985.65	0.15
39	*cis*-3-Decene	985.80	986.46	−0.66	986.36	−0.56
40	*trans*-2-Decene	996.70	995.31	1.39	998.04	−1.34
41	*cis*-2-Decene	1001.70	1001.61	0.089	998.76	2.94

TABLE I (*continued*)

No.	*n*-Alkene	Kováts index				
		Exptl. *(a)*	*Calc.* *(b)*	*Difference* *(a) − (b)*	*Calc.* *(c)*	*Difference* *(a) − (b)*
Correlation:						
	Number of compounds used		84		84	
	Correlation coefficient, R		0.999		0.999	
	Standard deviation, σ		1.64		2.78	
42	*cis*-5-Undecene	1078.20	1077.33	0.87	1080.02	−1.82
43	*cis*-4-Undecene	1080.50	1081.10	−0.60	1081.39	−0.89
44	*trans*-4-Undecene	1081.10	1080.94	0.16	1080.67	0.43
45	*trans*-5-Undecene	1081.80	1081.97	−0.17	1079.31	2.50
46	1-Undecene	1082.40	1080.65	1.75	1080.79	1.61
47	*cis*-3-Undecene	1085.30	1085.60	−0.30	1085.50	−0.20
48	*trans*-3-Undecene	1085.40	1084.67	0.73	1084.78	0.62
49	*trans*-2-Undecene	1096.60	1094.99	1.61	1097.73	−1.13
50	*cis*-2-Undecene	1101.50	1101.30	0.20	1098.44	3.06
51	*cis*-6-Dodecene	1175.00	1173.02	1.98	1176.36	−1.36
52	*cis*-5-Dodecene	1175.60	1175.63	−0.03	1178.32	−2.72
53	*trans*-6-Dodecene	1179.60	1178.98	0.62	1175.65	3.95
54	*cis*-4-Dodecene	1179.60	1180.24	−0.64	1180.52	−0.92
55	*trans*-5-Dodecene	1180.60	1180.27	0.33	1177.60	3.00
56	*trans*-4-Dodecene	1180.60	1180.08	0.52	1179.81	0.79
57	1-Dodecene	1183.00	1181.26	1.74	1181.39	1.61
58	*cis*-3-Dodecene	1185.10	1185.29	−0.19	1185.18	−0.08
59	*trans*-3-Dodecene	1185.10	1184.35	0.75	1184.47	0.63
60	*trans*-2-Dodecene	1196.90	1195.16	1.74	1197.90	−1.00
61	*cis*-2-Dodecene	1201.70	1201.46	0.24	1198.61	3.09
62	*cis*-6-Tridecene	1271.20	1271.32	−0.12	1274.66	−3.46
63	*cis*-5-Tridecene	1273.80	1274.77	−0.97	1277.45	−3.65
64	*trans*-6-Tridecene	1277.40	1277.28	0.12	1273.95	3.45
65	*cis*-4-Tridecene	1278.60	1279.92	−1.32	1280.21	−1.61
66	*trans*-5-Tridecene	1279.50	1279.41	0.09	1276.74	2.76
67	*trans*-4-Tridecene	1279.90	1279.77	0.13	1279.50	0.40
68	1-Tridecene	1283.10	1282.74	0.36	1281.45	1.65
69	*cis*-3-Tridecene	1284.40	1285.45	−1.05	1285.35	−0.95
70	*trans*-3-Tridecene	1284.90	1284.52	0.38	1284.64	0.26
71	*trans*-2-Tridecene	1297.00	1295.77	1.23	1298.50	−1.50
72	*cis*-2-Tridecene	1301.60	1302.07	−0.47	1299.22	2.38
73	*cis*-7-Tetradecene	1366.70	1366.69	0.01	1370.96	−4.26
74	*cis*-6-Tetradecene	1368.60	1370.45	−1.85	1373.80	−5.20
75	*cis*-5-Tetradecene	1372.00	1374.45	−2.45	1377.14	−5.14
76	*trans*-7-Tetradecene	1374.50	1374.49	0.01	1370.25	4.25
77	*trans*-6-Tetradecene	1375.70	1376.42	−0.72	1373.09	2.61
78	*cis*-4-Tetradecene	1377.70	1380.09	−2.39	1380.38	−2.68
79	*trans*-5-Tetradecene	1378.40	1379.09	−0.69	1376.43	1.97
80	*trans*-4-Tetradecene	1379.30	1379.93	−0.63	1379.66	−0.36
81	1-Tetradecene	1383.20	1383.19	0.01	1383.20	−0.00
82	*cis*-3-Tetradecene	1384.10	1386.06	−1.96	1385.96	−1.86
83	*trans*-3-Tetradecene	1384.60	1385.13	−0.53	1385.24	−0.64
84	*trans*-2-Tetradecene	1396.90	1397.25	−0.35	1398.56	−1.66

for the different sub-populations: reference *n*-alkanes, 1-alkenes and six pairs of *cis*- and *trans*-alkenes from 2-alkenes up to 7-alkenes. Two information contents of Fig. 2d and such a graph in a two-dimensional space would seem similar at first glance. On such a graph only macro-variations due, for example, to the non-linearity of the deviation for the first members of a homologous series could appear. However, micro-variations of about 3 or 4 KI would be lost. For a detailed study it is better to discuss relative variations of small amplitude instead of discussing absolute experimental data. The deviation used will be the isotopology factor, τI (refs. 13 and 14), identical in this case to Schomburg's[21] homeomorphism factor H^A, that is, to the difference between data relative to an alkene and its isotopological alkane.

Study of the first development direction, DD_1

We must remember that the first development direction, DD_1, according to the well defined law of generation of the topological sites, inside the imprint, corresponds here to lengthening of the *n*-alkyl chain R in compounds $CH_2{=}CH{-}R$ or $R'{-}CH{=}CH{-}R$ with $R > R'$. The contribution of every topological site, determined on statistical bases, is represented more clearly in Fig. 4a, which gives the trend in the variations.

An alternating effect appears up to A_1 in E_B^3 (such a site occurs first in 1-heptene for compounds $CH_2 = CH{-}R$), and after that a regular increase is observed. The most important variations are near the focus. The larger value of 113.9 for site A_1 in E_B^1 in DD_1 expresses the drastic change in the π net charge[15] and dispersion forces brought about by replacing a hydrogen atom at an sp^2 carbon atom with a methyl group.

This alternating effect is found also when R increases in the 1-alkenes $CH_2{=}$ $CH{-}R$, as is shown by plotting experimental τI values *versus* the carbon number, *n*, of these alkenes (Fig. 4b). From the topology–information diagram (Fig. 2d) it is easy to calculate the contribution of every topological site, $\delta(\tau I)$, to the isotopology factor (τI) of particular compounds. $\delta(\tau I)$ equals the difference between the calculated perturbation term (P_i) for a particular site (S_i) and 100 KI. To obtain τI for a particular 1-alkene these partial contributions must be added:

$$\tau I = \Sigma\delta(\tau I)$$

for 1-butene $\tau I = (-21.7) + (13.9) + (-6.1) = -13.9$ KI. These calculated τI values are given *versus* the carbon atom number in Fig. 4b. The curves corresponding to experimental values and calculated values obtained by using the topology–information correlation are closely similar. These variations are also in good agreement with the variation of the vapour pressure of 1-alkenes relative to their isotopological alkanes.

These comparisons show that the perturbation terms associated with every topological site in DD_1 (Figs. 2d and 4a) express adequately the small variations in the observed physico-chemical properties. Differences between the curves in Fig. 4b correspond to differences between experimental and calculated values in Table I. It must be noted that for the heavier alkenes the maximum observed difference is 2 KI, that is, a relative deviation lower than $2 \cdot 10^{-3}$.

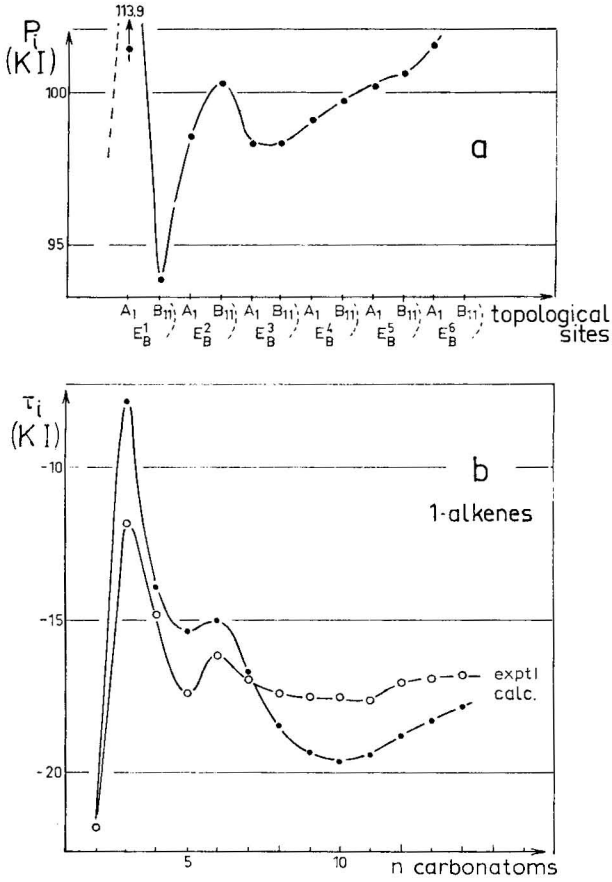

Fig. 4. Influence of chain lengthening in the first development direction, DD_1. (a) Contribution to the Kováts index of the perturbation term, P_i, associated with every topological site in DD_1, by lengthening of *n*-alkyl chain R in $CH_2=CH-R$ or $R'-CH_2=CH-R$ with $R \geqslant R'$. (b) τI for 1-alkenes ($\tau I = I_{\text{alkene}} - I_{\text{isotopological alkane}}$) *versus* number of carbon atoms in every alkene. Comparison of experimental and calculated values. Calculated value for a given alkene corresponds to the sum of elementary contributions of every carbon atom, taken from Fig. 2d.

Study of the second development direction, DD_2

The topological sites in DD_2 are first occupied in the *trans* geometrical isomers from *trans*-2 up to *trans*-7. The average contribution of these topological sites for these isomers is given in Fig. 2d and trends are summarized in Fig. 5a.

The non-equivalence of both development directions DD_1 and DD_2 must be stressed. This non-equivalence reflects the specificity in the behaviour of *trans* and *cis* geometrical isomers relative to the corresponding 1-alkenes.

An alternating effect is also clearly shown in direction DD_2 (Figs. 2d and 5a). The important contribution of site A_1 in E_B^1 (114.5 KI) underlines the great difference between 2-alkenes and 1-alkenes. It shows, once more, the large change in behaviour brought about by replacing a hydrogen atom at an sp^2 carbon atom by a methyl group. But site B_{11} in E_B^1 has a low contribution of only 89.4 KI because the Kováts

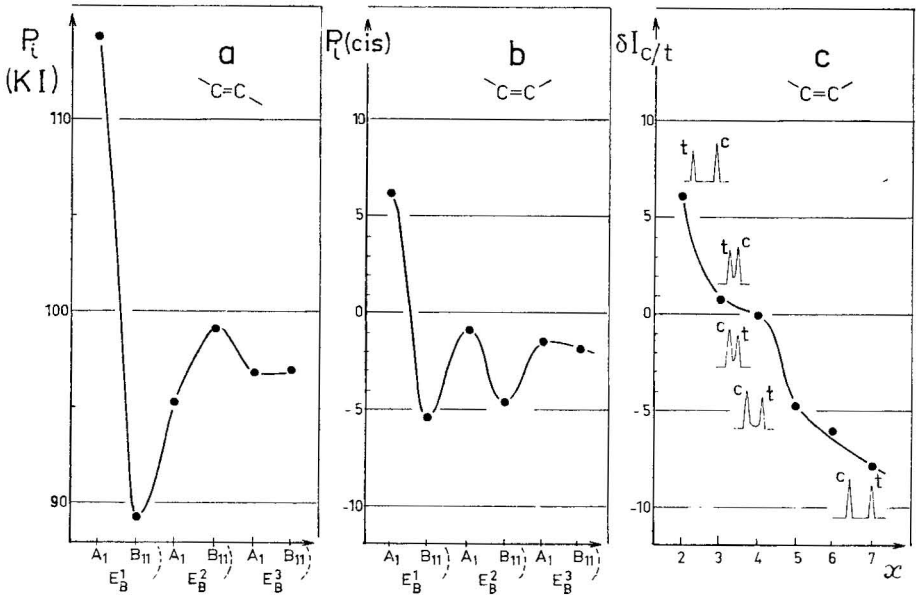

Fig. 5. Statistical behaviour of linear geometrical isomers and contribution of topological sites in the second development direction, DD_2. (a) Contribution of the sites (P_i) calculated with the *trans*-alkenes; (b) corresponding supplementary parameter, $P_i(cis)$, for *cis*-alkenes; (c) possibilities of separation of different pairs of *cis*/*trans* isomeric linear x-alkenes for different positions x of the double bond (*e.g.*, $x = 4$ in 4-octene, 4-nonene, ...)

indices of 3-alkenes are systematically lower than those of *trans*-2 alkenes. After this decrease the contributions of topological sites A_1 in E_B^2 (introduced by 4-alkenes) and B_{11} in E_B^2 (introduced by 5-alkenes) increase to 95.4 and 99.3 KI, respectively. Then another decrease is observed for sites A_1 and B_{11} in E_B^3, introduced by *trans*-6- and *trans*-7-alkenes, respectively.

The perturbation terms associated with the *cis* isomers are calculated relative to the *trans* isomers. They are given in Fig. 2d and corresponding trends are summarized in Fig. 5b. An alternating effect is also evident.

For *cis*-2 alkenes, the positive perturbation term ($P_i = 6.3$ KI) indicates that the Kováts index of *cis*-2 alkenes is about 6.3 KI greater than that for the *trans*-2 alkenes. The *cis* parameter related to B_{11} in E_B^1 is introduced by 3-alkenes, and the corresponding perturbation term decreases markedly, $P_i = -5.4$ KI. This term indicates that Kováts indices of *cis*-3-alkenes are systematically much lower than those of the corresponding *cis*-2-alkenes. However, for *cis*-4-alkenes the difference is less important, only -0.8 KI on average. A large decrease, -4.8 KI, is observed for the *cis*-5-alkenes. A small further decrease is observed for the subsequent *cis*-6- and *cis*-7-alkenes. In Fig. 5b and 5c, the zero values on the ordinate correspond to the contribution of *trans*-*n*-alkenes, taken as reference compounds.

These perturbation terms, P_i (*cis*), for the *cis* isomers are defined relative to the *trans* isomers but also to the preceding *cis* isomers, due to the definition of a perturbation term. By making the sum of this elementary contribution, P_i (*cis*), for every type of *cis* isomer, from *cis*-2 up to *cis*-7 we obtain the values $\delta I_{c/t}$ indicated in Fig. 5c

for every *cis*-alkene. For example, the average behaviour of *cis*-5-alkenes (*c*) defined relative to *trans*-5-alkenes (*t*) only is characterized by:

$$\delta I_{c/t} = \Sigma P_i\ (cis) = (+\ 6.3) + (-5.4) + (-0.8) + (-4.8) = -4.7\ \text{KI}$$

This value corresponds to the average calculated difference between the Kováts indices of *cis*-5-alkenes and *trans*-5-alkenes, by using the topology–information diagram. Fig. 5c, which describes the behaviour of *cis*-*x*-alkenes relative to the *trans*-*x*-alkenes only (with $x = 2$ up to 7), shows clearly the following, on statistical bases:

(a) the difficulties of separating pairs of *cis*- and *trans*-3- or *trans*-4-alkenes;

(b) despite chain lengthening, pairs of *cis*- and *trans*-5-, *cis*- and *trans*-6- and *cis*- and *trans*-7-alkenes are easier to separate;

(c) *cis*-2-alkenes have higher retention times than the corresponding *trans*-2-alkenes, but for heavier alkenes (*cis*-5-, *cis*-6- and *cis*-7-) the reverse is observed, the *cis*-alkenes having lower retention times than the corresponding *trans*-alkenes.

Study of differences between experimental and calculated values for every compound

Differences between the experimental and calculated values (Table I) correspond to the deviation between the real property and the average behaviour calculated on a statistical basis. These differences also show interesting regular trends, which are for the most part understandable even if these differences are taking place in a narrow range of about 3 or 4 KI. These trends are shown in Fig. 6.

The larger deviation observed for 1-propene and *cis*-2-butene underlines the way in which properties of ethene are changed by replacing a hydrogen atom at an sp^2 carbon atom by one and two methyl groups. Nevertheless, part of this relatively abnormal behaviour for the first term of a homologous series is taken into account by the weight attributed to the corresponding perturbation term and has been discussed previously (for example, the experimental Kováts index of *cis*-2-butene is 12 KI higher than that of *trans*-2-butene. Half of this value is accounted for by the *cis* perturbation term associated with A_1 in E_B^1, in DD_2. The other half appears in the difference between the experimental and calculated values for this compound).

Molecular symmetry is an important factor and explains the particular behaviour of the first members of a homologous series: *cis*-2-butene, *cis*-3-hexene, *cis*-3-heptene, *cis*-4-octene and *cis*-5-decene. The greatest deviations are observed for these first terms of the corresponding homologous series of geometrical isomers. These deviations do not follow a random distribution but show regular trends. In Fig. 6b, in agreement with previous observations[2], *trans*-2-hexene deviates from the trend followed by the other *trans*-2-alkenes. This deviation has been attributed to a "propyl effect"[17].

The deviations are greater for the *cis* isomers than for the *trans* isomers (Fig. 6b–e). This difference is due to the fact that the observed τI variations for the *cis* isomers are greater than those for the corresponding *trans* isomers. For example, $\Delta\tau I = 9.6$ KI for *cis*-5-tetradecene and *cis*-5-decene, whereas it is only 5.7 KI for the corresponding *trans* isomers. For the latter the deviations between experimental and calculated values are lower than 1 KI and show that for these *trans*-5-alkenes variation due to increasing chain length is well described by the perturbation term of the

topological sites in DD_1. The above difference between $\Delta\tau I$ for *cis*-5- and *trans*-5-alkenes explains the observed maximum amplitude of $\pm$ 2.5 KI for the differences between the experimental and calculated values (Fig. 6e).

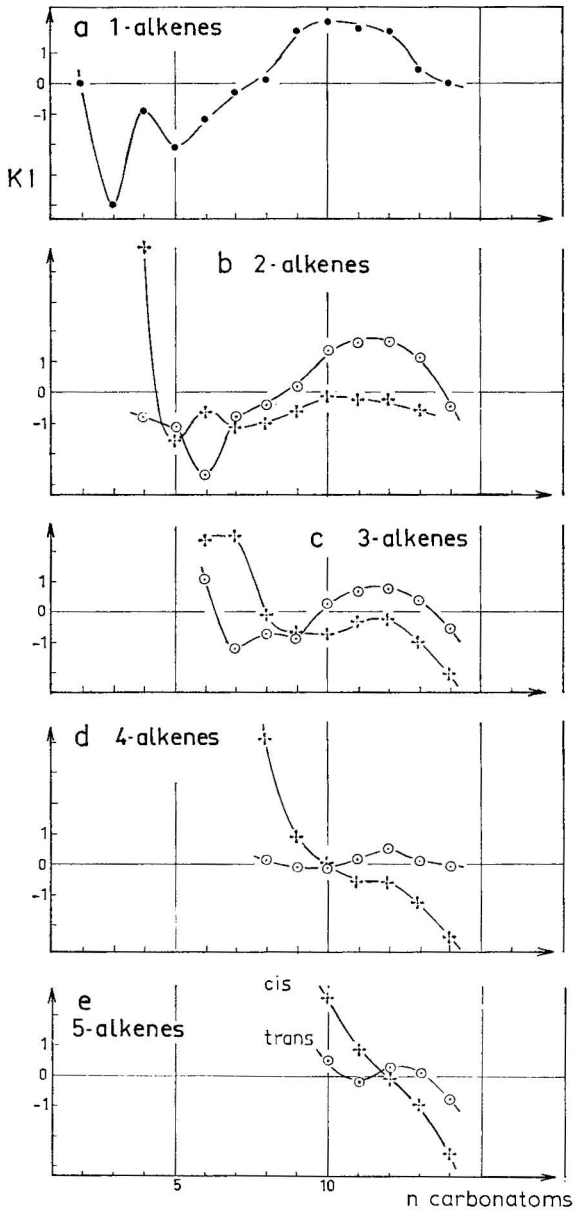

Fig. 6. Study of differences between experimental and calculated Kováts indices of alkenes for homologous series *versus* their carbon atom number. This shows regular trends for all types of *x*-alkenes and differentiates well the *cis* and *trans* variations for each group of *cis*/*trans* isomers as a function of their chain lengthening.

The more central the double bond, the smaller are the differences between the experimental and calculated values for the *trans* isomers, from *trans*-2-alkenes up to *trans*-7-alkenes.

The principles for calculating the contribution of topological sites in the form of an average perturbation term, with the help of multiple regression analysis, are reflected also by the analysis of differences. The smaller differences for *cis*-4- and *cis*-5-alkenes are observed for compounds of average molecular weight. More or less evident similar trends are seen also in Fig. 6a–c.

CONCLUSION

Topological analysis (DTA) based on the DARC topological system summarizes, on a statistical basis, Kováts indices of 84 alkenes for high-performance capillary gas chromatography on squalane. The topology–information diagram gives information at the skeletal carbon atom level of the solute molecules.

As in every mathematical method, our structural model is partly conventional. Use of such a diagram needs a minimum of training which is easily obtained with the help of some examples showing how to calculate Kováts indices for different types of alkenes whose graphs are included in the imprint of the population studied. The results presented in the topology–information diagram and the differences between the experimental and calculated values for every alkene show the trends which have been discussed.

The very precise data used here have been discussed at a second-order level of precision, on statistical bases. These results confirm that the Kováts rule[22], stating that every CH_2 group in a homologous series contributes 100 KI, is valid only to a first approximation. From a methodological point of view, when very precise data are used, the present results show the necessity for taking into account the small differences of behaviour between different kinds of *cis*-*x*-alkenes, *i.e.*, for every value of *x*. Retention data of higher *n*-alkenes can be predicted only by structural interpolation in this instance[12].

This model of *n*-alkenes is particularly interesting as a severe test of the analytical and physico-chemical potentialities of DTA. This study shows the links between the well known behaviour of these compounds and the consequences on the contribution of the topological site in the topology–information diagram. It offers a good basis for determining the influence of the polarity at the carbon atom level[14] or for determining if the influence of an apolar stationary phase (squalane, hydrocarbon C_{87}) is limited to a mass effect[23] or if structural effects of the stationary phase also intervene. It would offer also a good basis for the study of long-chain dienes where two double bonds are present in different places and can interact together. Work along these lines in connection with the analysis of unsaturated hydrocarbons of petrochemical interest is currently under way.

REFERENCES

1 L. Soják and P. Skalak, *Ropa-Uhlie*, 21 (1979) 485.
2 L. Soják, J. Hrivňák, P. Majer and J. Janák, *Anal. Chem.*, 45 (1973) 293.
3 L. Soják, J. Hrivňák, I. Ostrovský and J. Janák, *J. Chromatogr.*, 91 (1974) 613.

4 L. Soják, J. Krupčik and J. Janák, *J. Chromatogr.*, 195 (1980) 43.
5 M. Ryba, *Chromatographia*, 5 (1972) 23.
6 O. Eisen, A. Orav and S. Rang, *Chromatographia*, 5 (1972) 229.
7 S. Rang, K. Kuningas, A. Orav and O. Eisen, *Chromatographia*, 10 (1977) 55.
8 J. C. Bonnet and J. E. Dubois, *Anal. Chim. Acta*, 112 (1979) 245.
9 J. E. Dubois, D. Laurent and H. Viellard, *C.R. Acad. Sci., Ser. C*, 263 (1966) 764.
10 J. E. Dubois, in A. Balaban (Editor), *The Chemical Applications of Graph Theory*, Academic Press, New York, 1976, p. 330.
11 J. E. Dubois, D. Laurent and A. Aranda, *J. Chim. Phys.*, 70 (1973) 1608 and 1616.
12 J. E. Dubois and J. Chrétien, *J. Chromatogr. Sci.*, 12 (1974) 811.
13 J. R. Chrétien and J. E. Dubois, *J. Chromatogr.*, 126 (1976) 171.
14 J. R. Chrétien, *C.R. Acad. Sci., Ser. C*, 281 (1975) 151.
15 J. R. Chrétien and J. E. Dubois, *Anal. Chem.*, 49 (1977) 747.
16 J. R. Chrétien and J. E. Dubois, *J. Chromatogr.*, 158 (1978) 43.
17 L. Soják, P. Zahradnik, J. Leška and J. Janák, *J. Chromatogr.*, 174 (1979) 97.
18 R. A. Hively and R. E. Hinton, *J. Gas Chromatogr.*, 6 (1968) 203.
19 J. A. Rijks and C. A. Cramers, *Chromatographia*, 7 (1974) 99.
20 P. Souter, *J. Chromatogr. Sci.*, 12 (1974) 418 and 424.
21 G. Schomburg, *J. Chromatogr. Sci.*, 11 (1973) 151.
22 E. Sz. Kováts, *Advan. Chromatogr.*, 1 (1965) 229.
23 G. A. Huber and E. Sz. Kováts, *Anal. Chem.*, 45 (1973) 1155.

Journal of Chromatography, 194 (1980) 135–144
Elsevier Scientific Publishing Company, Amsterdam — Printed in The Netherlands

CHROM. 12,726

SYN–ANTI ISOMERISATION OF 2,4-DINITROPHENYLHYDRAZONES OF VOLATILE CARBONYL COMPOUNDS IN CAPILLARY GAS CHROMATOGRAPHIC–MASS SPECTROMETRIC ANALYSES

V. P. URALETS*
Institute of Organo-Element Compounds, Academy of Sciences, Moscow (U.S.S.R.)
and
J. A. RIJKS and P. A. LECLERCQ*
Laboratory of Instrumental Analysis, Eindhoven University of Technology, Eindhoven (The Netherlands)
(Received January 31st, 1980)

SUMMARY

Dinitrophenylhydrazone derivatives of volatile aldehydes and ketones were investigated by high-performance liquid chromatography (HPLC) and by gas chromatography–mass spectrometry (GC–MS). HPLC separations were slightly better than those obtained by existing procedures, but high-resolution GC is the method of choice.

The equilibrium of the *syn–anti* isomerization of the compounds is influenced by the nature of the solvent, the deactivation of the column and the injection and column temperatures. The GC profile can therefore be controlled by careful selection of the experimental conditions. It is shown that this phenomenon, in addition to the occurrence of characteristic values of the difference in the retention indices of *syn* and *anti* isomers for a given compound, can facilitate the identification.

Chemical ionization (methane) mass spectra of the compounds were found to contain more information than conventional electron impact spectra. Characteristic fragment ions are tabulated.

INTRODUCTION

Volatile carbonyl compounds are important flavour ingredients in many food products. For analytical purposes, these compounds are often converted into stable 2,4-dinitrophenylhydrazones (DNPHs), which can be selectively isolated from complex mixtures of flavour components.

After isolation of the DNPHs, the mixture can be separated chromatographically either as such or after regeneration of the free carbonyl compounds. Gas chromatographic (GC) studies on the liberated compounds[1–5] show that this method is not suitable for quantitative trace analyses. Moreover, reactions with the liberating agents may give artefacts[2,3].

* Present address: Institute of Nutrition, Academy of Medical Sciences, Ustinsky projezd 2/14, Moscow 109240, U.S.S.R.

0021-9673/80/0000–0000/$02.25

Many attempts to analyse DNPHs directly by GC have been reported[6–20]. In the gas chromatograms doubling of peaks has been observed in several instances[8,11,16,17], even when low-resolution packed columns were used. Obvious double peaks have been recorded with high-resolution capillary columns[18,19]. Purification of carbonyl compounds before derivatization to avoid peak doubling was not successful[18]. The doubling effects were attributed to either decomposition[10,16,20] or isomerization[17,18] of the compounds.

The occurrence of *syn* and *anti* isomers of DNPHs of aliphatic aldehydes was observed in 1961 by Van Duin[21], who studied these phenomena by conventional liquid chromatography. Published as a thesis, this work was apparently overlooked in the more recent GC studies cited above.

High-performance liquid chromatography (HPLC) has also been applied to the analysis of DNPHs[16,22,23]. This method is very attractive because the separation can be carried out at low temperature and the compounds can be detected with relatively high sensitivity. However, HPLC has a poor separation power in comparison with capillary GC.

Electron impact (EI) mass spectrometry (MS) has been applied to the identification of DNPHs[24–26] after separation by thin-layer or conventional column chromatography. EI mass spectral data are available for many DNPHs of saturated and unsaturated aldehydes and ketones[26–29]. Chemical ionization (CI) mass spectra of DNPHs were not found in the literature.

Although some attempts were made to optimize HPLC for the separation of DNPHs, the main purpose of this work was to study the GC behaviour of DNPHs on glass capillary columns. In particular, factors influencing isomerization phenomena, such as the nature of the solvent, deactivation of the column wall and the injection and column temperatures were investigated. CI mass spectra, using methane as reagent gas, are discussed.

EXPERIMENTAL

2,4-Dinitrophenylhydrazine was used as a reagent for preparing derivatives of aldehydes and ketones. The following procedures were applied for the preparation of DNPHs: (a) the conventional method and recrystallization from ethanol[30]; (b) derivatization on a column filled with neutral sorbent and the reagent[21]; (c) derivatization in pyridine solution[21].

Liquid chromatography

The HPLC equipment used is described elsewhere[31]. A variable-wavelength Model PM 2D LC UV detector (Carl Zeiss, Jena, G.D.R.) was applied. Absorbances were measured at 358 nm. The stationary and mobile phase systems were similar to those described earlier for the separation of DNPHs[22]. Adsorption chromatography was performed on LiChrosorb SI-60 with ethyl acetate–isooctane (1:49) or isooctane–methylene chloride (3:2) as solvents. Reversed-phase chromatography was carried out on LiChrosorb RP-8 with acetonitrile–water (3:2) or dimethylformamide–water (3:1). Before use the solvents were degassed in an ultrasonic bath.

Gas chromatography

An Intersmat IGC 120 FB gas chromatograph (Intersmat Instruments, Pavillons sous Bois, France) equipped with a flame-ionization detector and an all-glass "moving needle" injector[32] was used at injection block temperatures of 200–400 °C (mainly 225 °C). Four Duran 50 glass capillary columns (40 m × 0.4 mm I.D.), rinsed with dry methylene chloride and dried with a gentle stream of dry nitrogen, were coated by a static procedure with SE-30 stationary phase using a 0.4% (w/w) solution in *n*-hexane[33]. Different treatments of the glass surface were applied before coating, in order to deactivate the column wall, with the exception of column 1, which was coated without prior treatment. Column 2 was deactivated with a 1% solution of benzyltriphenylphosphonium chloride (BTPPC) in methylene chloride, as described by Rutten and Luyten[34]. Column 3 was deactivated with a 5% solution of Carbowax 20M in methylene chloride according to Blomberg[35]. Column 4 was deactivated by Carbowax 20M vapour[36,37]. In all experiments the injector was deactivated essentially according to the same procedure as the column. The columns were operated isothermally between 200 and 260 °C, but mainly at 225 °C. The carrier gas was nitrogen at a flow-velocity of 10–20 cm/sec, the detector temperature was 280 °C and the sample size was $5 \cdot 10^{-7}$ to $5 \cdot 10^{-10}$ g per component in 1 μl of an appropriate solvent.

Mass spectrometry

A Finnigan Model 4000 quadrupole mass spectrometer (Finnigan, Sunnyvale, CA, U.S.A.) was used in the CI mode. The mass spectral data presented were acquired under the following conditions: ionizing electron energy, 79 eV; electron current, 0.20 mA; scan time, 1 sec per scan; and source temperature, 250 °C. Methane reactant gas was introduced via the make-up gas line. The ion source pressure was maintained at 0.15 Torr gauge reading. Samples were analysed by GC–MS using column No. 2 and helium as carrier gas. The column was coupled directly to the ion source via a platinum–iridium capillary (60 cm × 0.1 mm I.D.). The column was operated isothermally at 230 °C and the platinum–iridium interface was maintained at 250 °C. Samples were injected on to the column as described above at 250 °C.

RESULTS AND DISCUSSION

Fig. 1 shows part of a representative gas chromatogram of DNPHs derived from pentanal and heptanone-3 on capillary column No. 1. Two distinct peaks correspond to each compound. The baseline in between the pairs is elevated and has a slope. The composition of these complicated chromatographic zones was studied by GC–MS in the EI and CI (methane, isobutane) mode for DNPHs of different aldehydes and ketones. The mass spectra recorded at different points of one pair of peaks and in between were identical with and similar to those obtained by direct insertion of the sample into the mass spectrometer. Therefore, the peak doubling cannot be attributed to decomposition[10,16,20].

Preparative separation of the isomers of acetaldehyde DNPH was achieved by HPLC on LiChrosorb SI-60, using isooctane–ethyl acetate (49:1) as solvent. The identity of the isomers was established by proton NMR. The isomer eluting first in both GC and HPLC appeared to be the *syn* isomer:

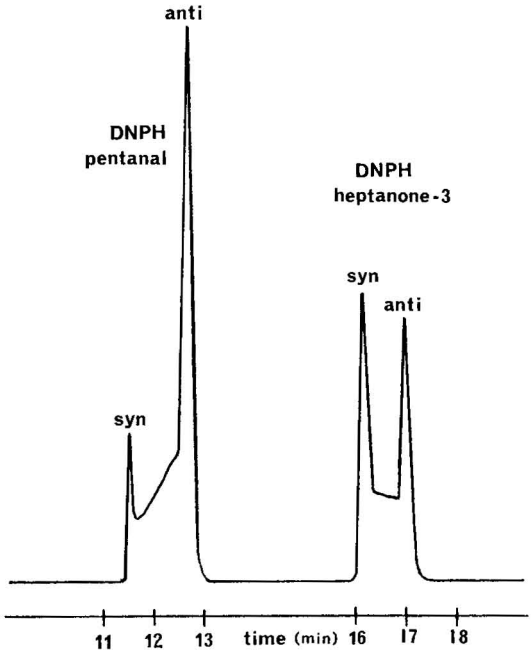

Fig. 1. Separation of *syn* and *anti* isomers of 2,4-dinitrophenylhydrazones of pentanal and heptanone-3 on a glass capillary column coated with SE-30 (column No. 1). Column and injector temperature, 225 °C; linear carrier gas (nitrogen) velocity, 200 mm/sec.

$R_1 = H$ (aldehydes)
$R_1 < R_2$ (ketones)

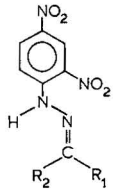

SYN

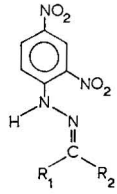

ANTI

The occurrence of a single peak for DNPHs of formaldehyde, acetone, diethyl ketone and other symmetrical carbonyl compounds will be easily understood.

The raised baseline between two DNPH isomers is evidently due to isomerization in the column during chromatography. This results in intermediate retention for components passing one part of the column as a *syn* and the other as an *anti* isomer.

Attempts have been made to suppress isomerization in the chromatographic column. Fig. 1 shows significant on-column isomerization (elevated baseline between DNPH isomers) on column No. 1, which was not treated with deactivating agents. Less isomerization was observed with column No. 2, which was treated with BTPPC as described above. Fig. 2 represents the separation of a DNPH mixture on this column. The column efficiency for heptanone-2 DNPH (capacity ratio, $k' = 6.5$) was 1500 theoretical plates per metre (2300 for n-$C_{24}H_{50}$, $k' = 5.4$). In contrast, Carbowax treatment (columns No. 3 and 4) decreased the column performance with respect to

the separation of DNPHs. Rapid isomerization was observed, resulting in enormous peak broadening, although separations of other compounds (hydrocarbons, pesticides, steroids) were successful. Column No. 2 was used in further experiments.

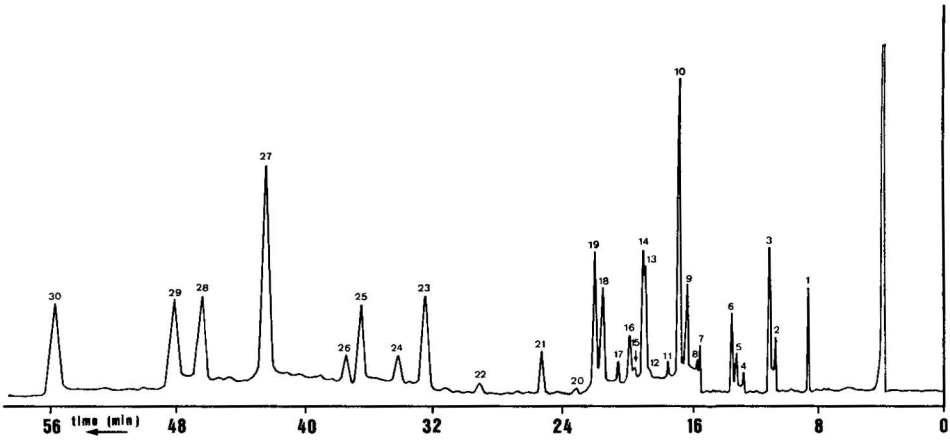

Fig. 2. Chromatogram of a mixture of 2,4-dinitrophenylhydrazones from a glass capillary column coated with SE-30 (column No. 2). Column and injector temperature, 225 °C; linear carrier gas (nitrogen) velocity, 160 mm/sec. Peaks: 1 = methanal; 2 = ethanal (*syn*); 3 = ethanal (*anti*); 4 = propanal (*syn*); 5 = acetone; 6 = propanal (*anti*); 7 = butanal (*syn*); 8 = butanone (*syn*); 9 = butanone (*anti*); 10 = butanal (*anti*) + 2-methylbutanal (*syn*); 11 = = 3-methylbutanal (*syn*); 12 = pentanone-2 (*syn*); 13 = 2-methylbutanal (*anti*); 14 = 3-methylbutanal (*anti*); 15 = pentanal (*syn*); 16 = pentanone-2 (*anti*); 17 = 4-methylpentanone-2 (*syn*); 18 = pentanal (*anti*); 19 = 4-methylpentanone-2 (*anti*); 20 = hexanone-2 (*syn*); 21 = hexanone-2 (*anti*); 22 = heptanone-2 (*syn*); 23 = heptanone-2 (*anti*) + heptanal (*syn*); 24 = hexenal-2; 25 = heptanal (*anti*); 26 = octanone-2 (*syn*); 27 = octanone-2 (*anti*); 28 = heptenal-2; 29 = octanal (*anti*) + nonanone-2 (*syn*); 30 = nonanone-2 (*anti*).

Within the column temperature range of 200–260 °C, increasing temperature promotes the isomerization rate. The slope between the pairs of isomer peaks increases significantly more than can be accounted for by decreasing retention times at higher temperatures. Temperatures of 220–235 °C are preferable, providing reasonable elution times and acceptable isomerization.

The injector temperature significantly influences the *syn/anti* ratio, as shown in Fig. 3 for derivatives of propanal, pentanal and heptanal. It should be noted that the injected sample contained mainly *anti* isomers, corresponding approximately to the ratios as in chromatogram A at a low injector temperature. Rapid isomerization was observed at 400 °C (Fig. 3B), which resulted in increased amounts of the *syn* isomers.

The initial ratio of isomers depends substantially on the derivatization procedure[21]. Conversions using a neutral adsorbent[21] yield high fractions of *syn* DNPHs (70%). Derivatives obtained from a pyridine solution[21] were mainly *anti* isomers (96%). The percentages given refer to butanal DNPH, as determined with GC column No. 2 at 225 °C and the injector also at 225 °C.

Kallio *et al.*[17] reported an influence of the solvent on the size of the secondary (*syn*) peak, although later this effect was not observed[18]. We examined several solvents to investigate this phenomenon. Isooctane and carbon disulphide did not change,

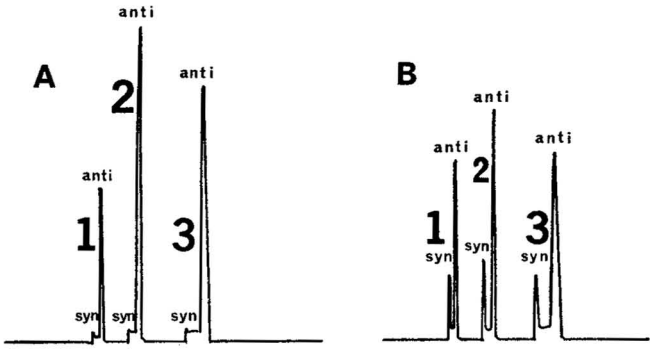

Fig. 3. Influence of injector temperature on the relative amounts of *syn*- and *anti*-DNPH isomers of propanal (1), pentanal (2) and heptanal (3). Glass capillary column coated with SE-30 (column No. 2) operated at 225 °C. Injector temperature: A, 235 °C; B, 400 °C.

over a period of 2 weeks, the *syn/anti* ratio of two samples of butanal DNPH, containing 70 and 4% of the *syn* isomer, respectively. In acetic acid, however, rapid isomerization was observed, resulting in an equilibrium corresponding to 25% of the *syn* and 75% of the *anti* isomer for both samples. Similar results were initially obtained with chloroform. After removal of hydrochloric acid, however, this solvent no longer promoted isomerization. Hence the isomerization in solutions is connected with the solvent acidity, as also follows from Van Duin's data[21]. It can be concluded that acid-catalysed interconversion leads to an equilibrium in the *syn–anti* composition. Thus, DNPH derivatives obtained in acidic medium show a constant *syn/anti* ratio in solutions[18].

Consequently, it is also apparent that glass capillary column and injector deactivation procedures have to eliminate the surface acidity (Duran 50 is slightly acidic) to suppress isomerization during chromatography.

The results obtained allow one to control the appearance of the chromatograms. To simplify the chromatograms, derivatization procedures should be applied that yield mainly *anti* isomers. Neutral solvents (isooctane or carbon disulphide) must be used for further treatment and low injector temperatures (approximately equal to the column temperature) have to be chosen to minimize the formation of *syn* isomers. On the other hand, the identification can be aided by the presence of *syn*-DNPH isomers in defined quantitative ratios and with appropriate retention data. This can easily be achieved by dissolving the DNPH mixture in acetic acid or by increasing the injector temperature. Thus, for analysis of an unknown mixture of DNPHs two chromatographic runs are advisable: one with suppressed *syn* isomer formation and another with both isomers present.

Retention indices of *syn*- and *anti*-DNPHs of 40 aldehydes and ketones are presented in Table I. *anti*-DNPH isomers of *n*-alkanals were used as reference compounds for the calculation of retention indices. Derivatives of the symmetrical carbonyl compounds, having only one isomer, and of methyl isopropyl ketone, methyl *tert.*-butyl ketone and α-unsaturated aldehydes producing negligible amounts of the *syn* isomer, are characterized by only one retention index value.

anti Isomers, having the (larger) alkyl group in the *anti* position with respect to the N–H group, are more exposed to stationary phase molecules than the corre-

TABLE I

RETENTION INDICES (*I*) OF 2,4-DINITROPHENYLHYDRAZONES OF CARBONYL COMPOUNDS ON SE-30 AT 225 °C

The *anti*-DNPH isomers of *n*-alkanals serve as reference compounds.

DNPHs of aldehydes	*I*		*ΔI**	*DNPHs of ketones*	*I*		*ΔI**
	syn	*anti*			*syn*	*anti*	
Methanal	100			Acetone	292		
Ethanal	188	200	12	Butanone	370	386	16
Propanal	272	300	28	Pentanone-2	442	468	26
Butanal	366	400	34	Hexanone-2	529	562	33
Pentanal	463	500	37	Heptanone-2	616	658	42
Hexanal	559	600	41	Octanone-2	709	755	46
Heptanal	657	700	43	Nonanone-2	805	851	46
Octanal	755	800	45	3-Methylbutanone-2		436	
Nonanal	854	900	46	Pentanone-3	451		
2-Methylpropanal	298	346	48	4-Methylpentanone-2	481	509	28
2-Methylbutanal	399	449	50	3,3-Dimethylbutanone-2		485	
3-Methylbutanal	418	451	33	3-Methylpentanone-2	493	517	24
2-Methylpentanal	476	533	57	2-Methylpentanone-3	488	503	15
3-Methylpentanal	523	561	38	2,4-Dimethylpentanone-3	529		
2-Ethylbutanal	469	526	57	2-Methylhexanone-3	547	574	27
Propenal		298		Heptanone-4	591		
Butenal-2		468		5-Methylhexanone-3	552	565	13
Hexanal-2		676		Heptanone-3	600	620	20
Heptenal-2		787		5-Methylhexanone-2	586	624	38
2,4-Hexadienal		749		6-Methylheptanone-3	649	666	17
				2,6-Dimethylheptanone-4	657		
				Nonanone-5	737		
				Nonanone-4	758	773	15
				Nonanone-3	776	806	30

* $\Delta I = I_{anti} - I_{syn}$.

sponding *syn* isomers. Therefore isomers with a higher retention index have the *anti* structure.

The elution sequence of DNPHs is similar to that observed for free carbonyl compounds on non-polar stationary phases[38]. However, hydrazones give twice as much retention data from one column as do free carbonyls, thus considerably increasing the possibilities of identification. The ΔI values in Table I are a measure of the distinction between the hydrocarbon groups attached to the (converted) carbonyl group. For compounds with the same number of carbon atoms, the ΔI value decreases in the order *n*-alkanals, methyl *n*-alkyl ketones, ethyl *n*-alkyl ketones and so on (*cf.*, 2-methylbutanal, pentanal, 3-methylbutanal). Within homologous series the ΔI value increases with increasing number of carbon atoms, and approaches a constant value. These regularities may facilitate the identification of unknown components.

Separations of DNPH mixtures using HPLC were similar to those reported by Selim[22]. A higher selectivity was obtained in the separation of DNPHs of alkanals and 2-alkanones with the same number of carbon atoms. This was accomplished by

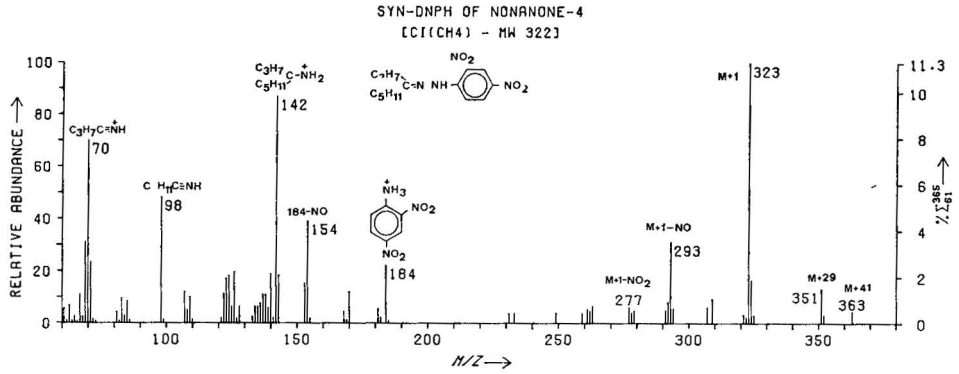

Fig. 4. Chemical ionization mass spectrum of the 2,4-dinitrophenylhydrazone of nonanone-4.

using a LiChrosorb RP-8 column with dimethylformamide–water (3:1) as solvent system. However, the relatively low separation power of this method, in comparison with capillary GC, restricts the use of HPLC for the analysis of DNPHs in complex mixtures.

CI (methane) mass spectra of many DNPHs were recorded. Fig. 4 shows, as an example, the CI spectrum of the nonanone-4 derivative. The spectra of the *syn* and *anti* isomers of the investigated compounds were found to be identical. The masses and relative abundances of characteristic ions from the CI spectra of DNPH derivatives are given in Tables II and III.

Protonated molecular ions, MH^+, appear to be the base peaks in most

TABLE II

SELECTED IONS FROM THE CI (METHANE) MASS SPECTRA OF 2,4-DINITROPHENYLHYDRAZONES OF ALDEHYDES

Ions with a mass below *m/z* 60 were not measured.

DNPH	*(m/z) relative abundance*						
	MH^+	$[MH - NO]^+$	$[MH - NO_2]^+$	*m/z* 184	*m/z* 154	$R_2HC{=}\overset{+}{N}H_2$	$R_2C{\equiv}\overset{+}{N}H$
Methanal	(211)100	(181) 5	(165)12	23	8		
Ethanal	(225)100	(195) 6	(179) 2	24	9		
Propanal	(239)100	(209)10	(193) 5	21	10		
Butanal	(253)100	(223)13	(207) 5	26	19	(72)29	(70) 64
2-Methylpropanal	(253)100	(223)15	(207) 3	45	28	(72)61	(70) 95
Hexanal	(281)100	(251) 5	(235) 2	25	4	(100)11	(98) 14
2-Methylpentanal	(281)100	(251) 3	(235) 1	27	1	(100) 6	(98) 8
2-Ethylbutanal	(281)100	(251) 4	(235) 1	20	2	(100) 8	(98) 9
Heptanal	(295)100	(265) 5	(249) 2	20	5	(114)15	(112) 14
Octanal	(309) 51	(279)19	(263) 5	28	65	(128)56	(126)100
Propenal	(237)100	(207) 7	(191) 3	13	4	(56)13	
Butenal-2	(251)100	(221) 3	(205) 1	5	1	(70)12	(68) 9
Hexenal-2	(279)100	(249) 3	(233) 1	4	1	(98) 8	(96) 6
Heptenal-2	(293)100	(263) 3	(247) 1	4	1	(112) 8	(110) 6
Hexadienal	(277) 48	(247)21	(231) 1	23	46	(96)92	(94)100

TABLE III

SELECTED IONS FROM THE CI (METHANE) MASS SPECTRA OF 2,4-DINITROPHENYLHYDRAZONES OF KETONES

Ions with a mass below *m/z* 60 where not measured. Alkyl group R_1 is smaller than or equal to R_2.

DNPH	*(m/z) relative abundance*							
	MH^+	$[MH-NO]^+$	$[MH-NO_2]^+$	*m/z* 184	*m/z* 154	$R_1-C(=\overset{+}{N}H_2)-R_2$	$R_2C\equiv\overset{+}{N}H$	$R_1C\equiv\overset{+}{N}H$
Pentanone-2	(267)100	(237) 4	(221) 2	7	8	(86) 28	(70) 7	
Hexanone-2	(281)100	(251) 5	(235) 1	8	2	(100) 9	(84) 2	
3-Methyl-pentanone-2	(281) 86	(251)28	(235)10	12	21	(100)100	(84) 39	
4-Methyl-pentanone-2	(281)100	(251) 5	(235) 1	8	1	(100) 7	(84) 2	
3,3-Dimethyl-butanone-2	(281)100	(251) 4	(235) 2	9	2	(100) 4	(84) 1	
Heptanone-2	(295)100	(265) 4	(249) 1	5	0	(114) 4	(98) 5	
Heptanone-3	(295)100	(265) 4	(249) 2	6	1	(114) 4	(84) 5	
2,4-Dimethyl-pentanone-3	(295) 29	(265)13	(249) 3	4	8	(114) 31	(70)100	—*
Heptanone-4	(295)100	(265) 4	(249) 2	4	0	(114) 3	(70) 12	—*
Octanone-3	(309)100	(279)29	(263) 6	24	26	(128) 43	(98) 45	
Nonanone-4	(323)100	(293)31	(277) 6	22	39	(142) 87	(98) 48	(70)70
2,6-Dimethyl-heptanone-4	(323) 48	(293)14	(277) 4	13	22	(142) 84	(84)100	—*

* Ions R_1CNH^+ and R_2CNH^+ are coincident ($R_1 = R_2$).

instances. Exceptions include branched-chain and high-molecular-weight compounds. The high abundance of MH^+ ions is a great advantage over EI-MS, especially for the analysis of trace components by GC–MS. Adductions $[M + C_2H_5]^+$ and $[M+C_3H_5]^+$ (not included in Tables II and III) are always present, with abundances of 11–14% and 3–4% relative to MH^+, respectively. The DNPHs of methanal, ethanal and propanal, however, give significantly lower $[M + C_2H_5]^+$ peaks (5% of MH^+).

Common fragment ions are $[MH-NO]^+$, $[MH-NO_2]^+$, protonated dinitroaniline (*m/z* 184) and its product ion formed by loss of NO (*m/z* 154). Their peak heights are generally lower than 10% of the base peak with the following exceptions. Derivatives of saturated aldehydes yield more abundant *m/z* 184 ions (20–28%) than the DNPHs of alkenals and of lower ketones up to octanone (4–13%). DNPHs of 2-methylpropanal, octanal and hexadienal, as well as 3-methylpentanone-2, the branched heptanone, the octanone and both nonanones, show increased fragmentation. While most product ions are more abundant in these instances, the enhanced fragmentation apparently does not affect the formation of $[MH-NO_2]^+$ ions.

The occurrence of the ions $R_1-C(=\overset{+}{N}H_2)R_2$, $R_1-C\equiv\overset{+}{N}H$ and $R_2-C\equiv\overset{+}{N}H$ is of diagnostic value, enabling one to distinguish aldehydes from isomeric ketones.

ACKNOWLEDGEMENTS

This work was supported by the Scientific Exchange Agreement (S.E.A.). Thanks are due to Dr. J. H. Dhont, Dr. S. van Straten, Dr. H. Maarse (Central Institute for Nutrition and Food Research TNO, Zeist, The Netherlands) and Dr. H. T. Badings and Dr. H. van Duin (Netherlands Institute for Dairy Research NIZO, Ede, The Netherlands) for discussions on the analysis of carbonyl compounds. We also thank Dr. J. W. de Haan and Mr. L. J. M. van de Ven (Eindhoven University of Technology) for the NMR analyses.

REFERENCES

1 M. Keeney, *Anal. Chem.*, 29 (1957) 1485.
2 J. W. Ralls, *Anal. Chem.*, 32 (1960) 332.
3 L. A. Jones and R. J. Monroe, *Anal. Chem.*, 37 (1965) 935.
4 R. V. Golovnya and V. P. Uralets, *Nahrung*, 16 (1972) 497.
5 H. Halvarson, *J. Chromatogr.*, 57 (1971) 406.
6 R. J. Soukup, R. J. Scarpellino and E. Danielczik, *Anal. Chem.*, 36 (1964) 2255.
7 E. Fedeli and M. Cirimele, *J. Chromatogr.*, 15 (1964) 435.
8 R. E. Leonard and J. E. Kiefer, *J. Gas Chromatogr.*, 4 (1966) 142.
9 W. G. Galetto, R. E. Kepner and A. D. Webb, *Anal. Chem.*, 38 (1966) 34.
10 R. Barrera, L. Gasco and F. de la Crus, *An. Quim*, 64 (1968) 517.
11 K. Shibasaki and S. Iwabuchi, *Nippon Shokuhin Kogyo Gakkai-Shi (J. Food Sci. Technol., Tokyo)*, 17 (1970) 193.
12 Y. Shimizu, S. Matsuto, Y. Mizunuma and J. Okada, *Nippon Shokuhin Kogyo Gakkai-Shi (J. Food Sci. Technol., Tokyo)*, 17 (1970) 385.
13 M. F. Fracchita, F. J. Schuette and P. K. Mueller, *Environ. Sci. Technol.*, 1 (1967) 915.
14 M. M. E. Metwalley, C. H. Amundson and T. Richardson, *J. Amer. Oil Chem. Soc.*, 48 (1971) 149.
15 M. Deki and M. Yoshimura, *Chem. Pharm. Bull.*, 23 (1975) 1374.
16 L. J. Papa and L. P. Turner, *J. Chromatogr. Sci.*, 10 (1972) 744.
17 H. Kallio, R. R. Linko and J. Kaitaranta, *J. Chromatogr.*, 65 (1972) 355.
18 Y. Hoshika and Y. Takata, *J. Chromatogr.*, 120 (1976) 379.
19 R. R. Linko, H. Kallio and K. Rainio, *J. Chromatogr.*, 155 (1978) 191.
20 J. B. Pias and L. Casco, *Chromatographia*, 8 (1975) 270.
21 H. van Duin, *Ph.D. Thesis*, Free University of Amsterdam, Amsterdam, 1961.
22 S. Selim, *J. Chromatogr.*, 136 (1977) 271.
23 M. A. Carey and A. F. Persinger, *J. Chromatogr. Sci.*, 10 (1972) 537.
24 D. P. Schwartz and A. I. Wirtanen, *Acta Chim. Scand.*, 22 (1968) 1717.
25 D. F. Brown, V. J. Senn, F. G. Dollear and L. A. Goldblatt, *J. Amer. Oil Chem. Soc.*, 50 (1973) 16.
26 H T. Badings, *Ph.D. Thesis*, Agricultural University of Wageningen, Wageningen, 1970.
27 J. B. Stanley, D. F. Brown, V. J. Senn and F. J. Dollear, *J. Food Sci.*, 40 (1975) 1134.
28 R. J. C. Kleipool and J. T. Heins, *Nature* (London), 203 (1964) 1280.
29 S. R. Heller and G. W. A. Milne, *EPA/NIH Mass Spectral Data Base*, Vols. I–IV, U.S. Department of Commerce, Washington, D.C., 1978.
30 R. J. Shriner, R. C. Fuson and D. Y. Curtin, *The Systematic Identification of Organic Compounds. A Laboratory Manual*, Wiley, New York, 4th ed., 1956, p. 219.
31 R. S. Deelder and P. J. Hendricks, *J. Chromatogr.*, 83 (1973) 343.
32 P. M. J. van den Berg and Th. Cox, *Chromatographia*, 5 (1972) 301.
33 G. A. F. M. Rutten and J. A. Rijks, *J. High Resolut. Chromatogr. Chromatogr. Commun.*, 1 (1978) 279.
34 G. A. F. M. Rutten and J. A. Luyten, *J. Chromatogr.*, 74 (1972) 177.
35 L. Blomberg, *J. Chromatogr.*, 115 (1975) 365.
36 J. J. Franken, R. C. M. de Nijs and F. L. Schulting, *J. Chromatogr.*, 144 (1977) 253.
37 R. C. M. de Nijs, J. J. Franken, R. P. M. Dooper, J. A. Rijks, H. J. J. M. de Ruwe and F. L. Schulting, *J. Chromatogr.*, 167 (1978) 231.
38 V. P. Uralets and R. V. Golovnya, *Zh. Anal. Khim.*, 33 (1978) 782.

Journal of Chromatography, 194 (1980) 145–152
Elsevier Scientific Publishing Company, Amsterdam — Printed in The Netherlands

CHROM. 12,731

SUPPORT TREATED WITH CARBOWAX FOR A STANDARD, NON-POLAR PACKING IN GAS–LIQUID CHROMATOGRAPHY

A. N. KOROL*, G. M. BELOKLEYTSEVA and G. V. FILONENKO

Institute of Physical Chemistry, Academy of Sciences of the Ukrainian SSR, pr. Nauki 31, Kiev 252028 (U.S.S.R.)

(First received December 3rd, 1979; revised manuscript received January 30th, 1980)

SUMMARY

The molar heat of solutions, entropic selectivities of the packings and the relative retentions of many solutes of different polarity were determined for two non-polar packings with squalane: these packings were prepared by using silanized and modified supports. The modified support was shown to be the best for preparing non-polar packings for gas–liquid chromatography.

INTRODUCTION

Inter-laboratory reproducibility of retention data remains a problem in gas–liquid chromatography (GLC), especially for non-polar stationary phases and polar solutes. Interfacial adsorption on a solid–liquid surface is the main reason for the lack of reproducibility because of the poorly reproducible properties of chromatographic supports. Although tailor-made paraffinic stationary phase C_{87} seems to have become a standard non-polar stationary phase for GLC[1–3], no choice among the available support materials for the non-polar packing has yet been made. Demands for an ideal support have been reported earlier[4], but even the best modern commercially available support materials have marked adsorption activity towards polar solutes. This activity is non-reproducible from batch to batch of the support material, with two main disadvantages: (a) the retention data depend on the amount of stationary phase in the column; (b) because of a non-linear adsorption isotherm the retention data depend on the amount of sample and some peak tailing occurs on the chromatograms. Although the amount of the stationary phase in the column can be reproduced, injection of a reproducible liquid sample remains a serious technical problem for routine analysis. Also, the peak tailing decreases considerably the column performance.

Hence, the non-linearity of the adsorption isotherm seems to be a more deleterious effect for analytical GLC than the presence of interfacial adsorption itself. Moreover, it is impossible from a theoretical point of view to develop a support without any adsorption activity; therefore, the only real solution to the

0021-9673/80/0000–0000/$02.25

support problem is to develop a support with minimal adsorption activity and with a linear adsorption isotherm for all solutes.

The most widely used white supports are of diatomaceous origin; their surface has some different active centres, which lead to non-linear adsorption isotherms. Only one technique has been generally accepted after the evaluation of different treatments of diatomites, *viz.*, silanization of the supports with dimethyldichlorosilane, with subsequent special thermal treatment; this procedure allowed the development of supports such as Chromosorb W HP. Unfortunately, these supports seem to have non-silanized parts of the surface, which can be demonstrated by non-linear adsorption isotherms for polar solutes.

It seems that supports of the HP series are the best modifications for silanized supports, and it therefore seems necessary to search for new techniques of support treatments. Some techniques of support modification have been described[5–10]: the surface is covered with a non-extractable polymer layer which is formed on heating at high temperature. These supports seem to have a homogeneous surface, as demonstrated by the resolution of highly polar solutes: the alcohol peaks have a symmetrical form. The separating power of these supports has been investigated for many polar solutes, but only a few papers have reported applications of the modified support in GLC[10–13]. Many examples of almost linear sorption isotherms for highly polar solutes have been reported for supports modified by Carbowax[5–9]. When using this support for GLC some new properties may be observed, because the adsorption properties of the modified support–non-polar stationary phase interface are not the same as those for the support–gas interface. Adsorption properties of the modified support with a non-polar stationary phase have to be evaluated by using thermodynamic functions of sorption, which allow an interpretation of the intermolecular interactions with the solutes.

Comparison of the best silanized support with one modified by Carbowax allows a recommendation to be made for a standard support for a non-polar stationary phase.

EXPERIMENTAL

Materials

Chromaton N super (Lachema, Brno, Czechoslovakia), which is similar to Chromosorb W HP, was chosen as a silanized support. Chromaton N AW is the initial raw material for the preparation of Chromosorb N super, and therefore the same substance was chosen for the modification based on the Aue *et al.* technique[7]. The difference between the Aue *et al.* technique and our procedure is elimination of the methanol extraction step. We assume that the minimal amount of the modifier needed to cover the whole support surface (0.2% for the white supports) is bonded entirely with the support surface.

The modification procedure was as follows. Chromaton N AW was coated with 0.2% of Carbowax 15,000 and the resulting packing was conditioned at 260 °C for 4 h; the conditioning temperature was increased from room temperature to 260 °C at a rate of 1 °C/min. A commercial squalane sample was purified through a silica gel column in order to eliminate trace amounts of unsaturated hydrocarbons. A 5% coating of the stationary phase was used with both Chromaton N super (packing S)

and Chromaton N AW modified by Carbowax (packing M). These freshly prepared packings were conditioned at 100 °C for 8 h. Because the same amount of stationary phase was used on the supports, all differences in retention data for the two packings relate only to the differences in the supports.

Different standard solutes were used to evaluate the packings (Table I), which enabled the adsorption properties of the supports to be compared.

Apparatus and calculations

The experiments were carried out with Chrom-31 and Chrom-41 gas chromatographs (Laboratorni Přistroje, Prague, Czechoslovakia) with flame-ionization detectors at column temperatures ranging from 40 to 80 °C. The samples were injected as vapours (100-μl Hamilton syringe) or as liquids (1-μl Hamilton syringe). Glass columns (1 m × 3 mm I.D.) were used. Helium was used as the carrier gas at a flow-rate of about 20 ml/min, which is about the optimal value in order to achieve the minimal HETP.

The following retention parameters were determined: relative retention (r), relative molar heat of solution* (ΔH_s^0) and the entropic selectivity (F^0)[14] (n-heptane was chosen as the standard). The last parameter was calculated by using the equation

$$F^\circ = R \ln r + \frac{0.565 \Delta H_s^0}{T}, \tag{1}$$

where ΔH_s^0 is in cal/mole, T is the column temperature (°K) and R is the gas constant.

We shall use the thermodynamic scale of ΔH_s^0, *i.e.*, the more negative the ΔH_s^0 value the stronger is the intermolecular interaction. We chose 50 °C as a standard temperature for entropy and relative retention calculations. The relative retention data were calculated from the relationship between ln r and $1/T$ at the standard temperature.

The entropic selectivity (F°) relates to the rotational entropy changes when the solute passes from the gas phase to the stationary phase, and this parameter expresses the entropic selectivity of the stationary phases. It should be noted that the experimental retention values relate to the whole sorption process, including solution in the stationary phase and adsorption on the solid–liquid interface. Adsorption on the gas–liquid interface is negligible for the systems under study.

When the sorption isotherm is non-linear, the retention volume depends on the amount of sample and the isobaric (for a fixed peak height, h) retention data are calculated as in ref. 15. The following equation is used in order to determine the relationship between the net retention volume, V_N, and h:

$$V_N = A/\log h + B \tag{2}$$

where A and B are constants. The slope of this line may be expressed as

$$\delta A^* = \frac{V_N' - V_N''}{V_N^*} \tag{3}$$

* The difference between the molar heats of solution for the solute under study and the standard solute (n-heptane).

where the primes refer to the net retention volumes, which were determined for two different values of h (for $1/\log h = 0.4$ and $1/\log h = 0.3$; h is measured in millimetres on the 250-mm recorder chart, the full scale of the recorder being $1 \cdot 10^{-11}$A). The V_N value for $1/\log h = 0.3$ was chosen as the standard isobaric retention volume and the isobaric thermodynamic functions of sorption were calculated from the isobaric retention volumes; the thermodynamic functions depend on the peak height chosen for the determinations and these functions actually are differential thermodynamic functions. The δA^* term expresses non-linearity of the sorption isotherm; the greater the δA^* value, the greater is the non-linearity of the sorption isotherm. When comparing δA^* values for the same solute on different packings (S and M), it is possible to determine the non-linearity of the adsorption isotherm on the solid–liquid interface. As the retention volume depends on the amount of sample, solute samples in different amounts were injected into the column and the relationship between V_N or t_N (net retention time) and $1/\log h$ was plotted; all the necessary retention data were determined from this graph.

ΔH_s^0 was calculated by using the temperature dependence of $\log r$ for four or five different column temperatures. The mean standard deviation for ΔH_s^0 is 0.03 kcal/mole and the mean relative standard deviation for the r values is about 0.1%.

RESULTS AND DISCUSSION

The main results are given in Table I. These data show marked differences for polar solutes on the compared packings which are related to adsorption on the liquid–solid interface.

Linearity of adsorption isotherm (δA^*)

Dependence of the retention volume on the amount of sample was observed for only three solutes, ethyl acetate, methyl ethyl ketone and 1-propanol, on packing S. When using packing M, only 1-propanol showed a marked dependence of V_N on amount of sample (Fig. 1). The δA^* value for 1-propanol is about 10 times smaller on packing M than on packing S, which illustrates the better homogeneity of the support surface modified by Carbowax. The difference relates to the treatment techniques for the basic Chromaton N AW.

The diatomaceous surface has relatively small amounts of hydroxyl groups; these groups react with silanizing agents and are then shielded by trimethylsilyl groups. The latter groups cover only part of the support surface; therefore, dichlorodimethylsilane is used in order to form a dimer chain (with traces of water) on the support surface around the contact point on the hydroxyl group location. In our opinion, this process is the reason for the greater effectiveness of dimethyldichlorosilane than hexamethyldisilazane, because the latter agent does not dimerize. Unfortunately, the support surface is not covered entirely even with the best silanization procedures; the δA^* values confirm this assumption. Some additional evidence was obtained on modification of the silanized supports with Carbowax[16].

The modification process with Carbowax also occurs on hydroxyl groups[17,18], but the presence of C–O–Si bonds is not definitely established, because these bonds must be broken when the modified support is washed with methanol at high temperatures[18]. The long polymer molecules of Carbowax seem to be polymerized

TABLE I

RELATIVE RETENTIONS AND RELATIVE THERMODYNAMIC FUNCTIONS OF SOLUTIONS ON PACKINGS M AND S

Solute	*Packing M*			*Packing S*			*r*
	r	ΔH_s^0 *(kcal/mole)*	F° *(e.u.)*	*r*	ΔH_s^0 *(kcal/mole)*	F° *(e.u.)*	*(ref.19)*
n-Hexane	0.370	1.20	0.12	0.380	1.15	0.10	0.380
n-Octane	2.63	−1.20	−0.18	2.650	−1.20	−0.16	2.635
n-Nonane	7.02	−2.20	0.02	7.09	−2.20	0.04	7.03
Hexene-1	0.308	1.50	0.28	0.332	1.40	0.20	0.318
Cyclohexane	0.690	0.75	0.57	0.720	0.75	0.66	0.703
Benzene	0.550	1.15	0.83	0.572	1.25	1.08	0.556
Toluene	1.54	0	0.86	1.60	0.05	1.02	1.575
p-Xylene	4.25	−1.10	1.02	4.320	−1.05	1.12	4.31
Chloroform	0.311	1.45	−0.21	0.324	1.30	−0.02	—
1,2-Dichloroethane	0.386	1.10	0.03	0.398	1.00	−0.08	—
Carbon tetrachloride	0.574	1.15	0.91	0.607	1.15	1.02	—
Isoamyl chloride	0.916	0.40	0.53	0.930	0.40	0.56	—
Diisopropyl ether	0.307	0.85	−0.86	0.320	0.85	−0.78	—
Ethyl acetate	0.246	1.30	−0.57	0.257	1.25	−0.51	—
Methyl ethyl ketone	0.215	1.00	−1.31	0.231	1.65	−0.03	—
1-Propanol	0.160	0.90	−2.07	0.153	2.00	−0.25	—

additionally at high temperatures, and the non-extractable polymer layer covers the support with a homogeneous film. Hence, the experimental data show that the chromatographic properties of packing M are better than those of packing S, based on δA^* values.

The "self-modification" effect occurs in GLC when polar solutes are separated on a non-polar packing[16]: the long tail of the peak modifies the liquid–solid inter-

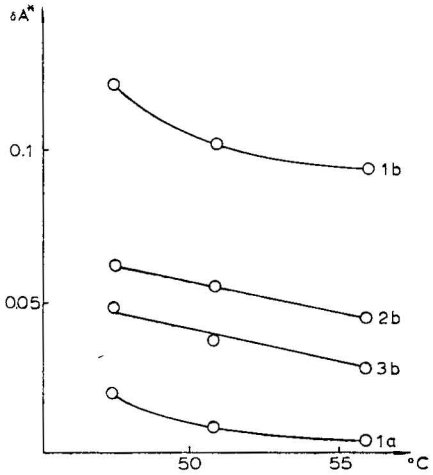

Fig. 1. Relationship between δA^* and column temperature on (a) packing M and (b) packing S: 1, 1-propanol; 2, methylethyl ketone; 3, ethyl acetate.

face and decreases the retention volume for polar solutes. This "self-modification" phenomenon is not reproducible and changes all of the retention parameters markedly. Because of this effect only pure solutes are needed in order to determine reproducible retention data for systems including a polar solute and a non-polar stationary phase. The length of the tail of the peak is proportional to the δA^* value, and therefore a decrease in the δA^* value on passing from packing S to packing M is preferable in the GLC of polar solutes. This phenomenon is illustrated in Fig. 2. The time between two injections of *n*-propanol is denoted *T*. *r* and δA^* were measured for the second injection (this relates to the influence of the first injection on the data for the second sample). The data show that the parameters change even with 20-min intervals between successive injections on packing S. Fig. 2 shows no "self-modification" effects for packing M, owing to the more polar nature of the interface. These data show that packing M is better for the determination of reproducible retention dat for mixtures with polar solutes; the column performance also seems to be better for packing M.

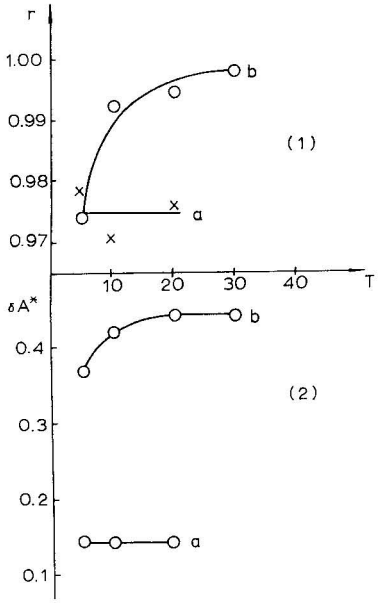

Fig. 2. Relationship between time of injection and (1) relative retention and (2) δA^* for 1-propanol on (a) packing M and (b) packing S.

Retention data

Because of the differences in the nature of the surfaces of the supports, a change in retention is observed when comparing packing S with packing M.

ΔH_s^0 values are related to the energy of intermolecular forces and allow one to evaluate the differences in intermolecular forces for the two types of supports. These values are virtually identical for *n*-paraffins for both packings, but the *r* values are lower for packing M than packing S. These small differences may be due to the hydrocarbon nature of the Chromaton N super support. The data in ref. 19 confirm

this explanation: these data were determined on the stainless-steel capillary column with a non-hydrocarbon nature. The r values determined on packing M are lower than those on the capillary column.

Some low-polar solutes have more positive ΔH_s^0 values on packing M than on packing S: this indicates a decrease in the intermolecular forces with the interface for packing M. Hexene-1, dichloroethane and chloroform belong to this group of solutes. In general, solutes of low and moderate polarity have nearly the same ΔH_s^0 values on both packings.

The aromatic hydrocarbons are high polarizable solutes, and therefore the intermolecular forces of these solutes with the interface are greater on the more polar packing M. Highly polar solutes (methyl ethyl ketone) have stronger intermolecular forces with packing M. The same effect was observed for solutes that can form hydrogen bonds (1-propanol). Hence, the polar nature of the modified support is observed only for highly polar solutes. This effect has to be taken into account when the thermodynamics of solution are determined by GLC. The silanized support allows one to determine more accurate thermodynamic values for highly polar solutes.

The r values on packing M are lower than those on packing S with only one exception (1-propanol). The r values for highly polarizable hydrocarbons on packing M are lower than those on the capillary column. The F° values are the main reason for this difference. This may be explained by the differences in adsorption on homogeneous and non-homogeneous surfaces. The latter surface has active centres of different activity; the solute molecule bonds with the more active adsorption centre at one point. The remaining groups in the solute molecule bond with less active adsorption centres; rotation of the solute molecule is possible for the groups that bond with the less active centres. The adsorption centres on a homogeneous surface have the same activity and all groups in the solute molecule have the same degree of hindrance for rotation. Hindrance of rotation is greater for packing M (this can be seen from the F° values). Hence, the adsorption entropy on a homogeneous surface is lower than that for a non-homogeneous surface.

When expressing the "polarity" term in Rohrschneider or McReynolds units, packing M is less polar than packing S. Actually, the intermolecular forces with polar solutes are greater for packing M and, therefore, this packing is more polar from the physico-chemical point of view.

The next point for comparison is the variation with temperature of the relative retentions, which is related to the ΔH_s^0 value. The difference between the ΔH_s^0 values for the two packings is small, except for very polar solutes. This causes a more rapid increase in the r values on packing M than on packing S when the column temperature is decreased.

Bleeding for support M is observed at 260 °C[9]; this is the upper limit for use of packing M, whereas the silanized packings may be used up to 350 °C. This restricts the application of the modified supports in high-temperature separations.

In conclusion, the results show that the Carbowax-modified support is the best for reproducible GLC analysis with non-polar stationary phases, and this support can be recommended as a standard for non-polar packings. Precautions are necessary when thermodynamic data are determined for highly polar solutes because of the polarity of the support surface modified with Carbowax.

REFERENCES

1 F. Riedo, D. Fritz, G. Tarján and E. Kováts, *J. Chromatogr.*, 126 (1976) 63.
2 L. Boksányi and E. Kováts, *J. Chromatogr.*, 126 (1976) 87.
3 A. N. Korol, *J. Chromatogr.*, 172 (1979) 77.
4 D. M. Ottenstein, *J. Gas Chromatogr.*, 1, No. 4 (1963) 11; *J. Chromatogr. Sci.*, 11 (1973) 136.
5 W. A. Aue, C. R. Hastings, K. O. Gerhardt, J. O. Pierce II, H. H. Hill and R. F. Moseman, *J. Chromatogr.*, 72 (1972) 259.
6 W. A. Aue, C. R. Hastings and S. Kapila, *J. Chromatogr.*, 77 (1973) 299.
7 W. A. Aue, C. R. Hastings and S. Kapila, *Anal. Chem.*, 45 (1973) 725.
8 W. A. Aue, C. R. Hastings and K. O. Gerhardt, *J. Chromatogr.*, 99 (1974) 45.
9 W. A. Aue and D. R. Younker, *J. Chromatogr.*, 88 (1974) 7.
10 W. L. Winterlin and R. F. Moseman, *J. Chromatogr.*, 153 (1978) 409.
11 R. F. Moseman, *J. Chromatogr.*, 166 (1978) 397.
12 R. C. M. de Nijs, J. J. Franken, R. P. M. Dooper, J. A. Rijks, H. J. J. M. de Ruwe and F. L. Schulting, *J. Chromatogr.*, 167 (1978) 231.
13 C. R. Fontan and H. H. Hill, Jr., *J. Chromatogr.*, 170 (1979) 249.
14 A. N. Korol, *Chromatographia*, 8 (1975) 385.
15 L. S. Lysyuk and A. N. Korol, *Chromatographia*, 10 (1977) 712.
16 A. N. Korol, G. M. Belokleytseva and G. V. Filonenko, *Chromatographia*, 12 (1979) 95.
17 M. M. Daniewski and W. A. Aue, *J. Chromatogr.*, 147 (1978) 395.
18 F. W. Karasek and H. H. Hill, *Res./Develop.*, 26, No. 12 (1975) 30.
19 R. A. Hively and R. E. Hinton, *J. Gas Chromatogr.*, 6 (1968) 203.

Journal of Chromatography, 194 (1980) 153–161
Elsevier Scientific Publishing Company, Amsterdam — Printed in The Netherlands

CHROM. 12,742

PREPARATION AND SORPTION BEHAVIOUR OF CYCLODEXTRIN POLYURETHANE RESINS

YOSHIKAZU MIZOBUCHI, MINORU TANAKA and TOSHIYUKI SHONO*

Department of Applied Chemistry, Faculty of Engineering, Osaka University, Yamadakami, Suita, Osaka 565 (Japan)

(Received February 6th, 1980)

SUMMARY

The interactions between cyclodextrin polyurethane resins and various organic compounds have been estimated by gas–solid chromatography. Cyclodextrin polyurethane resins were obtained by the polymerization of cyclodextrins with diisocyanates in pyridine and/or N,N-dimethylformamide. The cyclodextrin resins exhibit strong interactions with guest molecules containing π-electrons or heteroatoms. The resins can be used to distinguish between the configurations of xylene isomers and pyridine derivatives.

INTRODUCTION

Cyclodextrins are torus-shaped oligosaccharides composed of α-(1,4)-linkages of a number of D(+)-glucopyranose units, where the Greek letter denotes the number of glucose units, *e.g.* α for 6, β for 7, γ for 8, etc. In these compounds the primary hydroxyl groups lie on one side of the torus and the secondary hydroxyl groups on the other side. The cavities which exist in cyclodextrins are slightly "V" shaped, with the secondary hydroxyl side more open than the primary hydroxyl side.

It is well known that cyclodextrins form inclusion complexes with a variety of (guest) compounds and have attracted much interest as models for enzymes. The better the guest fits into the cavity, the more stable is the inclusion complex. Since their cavities are spatially restricted, cyclodextrins exhibit many interesting features such as rate effects, stereospecificity, enantiometric specificity, etc. Many of these have described by Bender and Komiyama[1]. By using this specificity, the epichlorohydrin cross-linked cyclodextrin gels have been used for the chromatographic separation of benzoic acid derivatives[2], nucleic acids[3], mandelic acid derivatives[4], etc.

Solid sorbents, particularly porous organic polymers (*e.g.*, Amberlite XAD-2, Porapak Q, Tenax GC, etc.), have recently been used for concentrating trace organic compounds, because these polymers are hydrophobic in nature and retard the progress of organic compounds through a column. The degree of interaction between organic compounds and these polymers generally increases with increasing boiling point of

0021-9673/80/0000–0000/$02.25

the organic compounds. Therefore, these polymers do not sorb various kinds of organic compounds selectively. There is thus a need in environmental analysis to find sorbents that will sorb these compounds selectively.

We have started a study of insoluble porous polymers containing cyclodextrins. In this paper, we describe the preparation and preliminary sorption behaviour of cyclodextrin polyurethane resins cross-linked with diisocyanates.

EXPERIMENTAL

Materials

α- and β-Cyclodextrins were obtained from Hayashibara Biochemical Laboratories (Shimoishii, Okayama, Japan), 1,3-bis(isocyanatomethyl)cyclohexane and 1,3-bis(isocyanatomethyl)benzene from Takeda Chemical Industries (Osaka, Japan); all other chemicals were from Wako (Osaka, Japan).

α- and β-Cyclodextrins were recrystallized from water and dried *in vacuo* at 80°C for 24 h. Diisocyanates were carefully distilled under reduced pressure. Pyridine and N,N-dimethylformamide and *n*-hexane were dried over potassium hydroxide and calcium hydride, respectively, and distilled before use. Other reagents were used without any purification.

Preparation of cyclodextrin polyurethane resins

β-Cyclodextrin polyurethane resins were prepared by a reaction similar to that of corn starch with phenyl isocyanate in pyridine[5]. β-Cyclodextrin ($8.8 \cdot 10^{-3}$ mol; 10 g) was dissolved in 300 ml of pyridine in a 1000-ml round-bottomed flask at room temperature. Trace amounts of water in this solution was distilled off azeotropically. The volume of pyridine distilled off was 100 ml. (The pyridine solution was cooled to 80°C with constant vigorous stirring.) The calculated amount of the diisocyanate was added. Then, the solution was stirred at 115°C for 4 h. The cyclodextrin polyurethane resin was precipitated from a large excess of methanol or acetone. The resin was purified by thorough Soxhlet extraction and dried *in vacuo* at 80°C for 24 h.

Alternatively, α-cyclodextrin ($8.8 \cdot 10^{-3}$ mol; 8.6 g) or β-cyclodextrin (10 g) was dissolved in 200 ml of N,N-dimethylformamide. (The solution was heated to 50°C for α-cyclodextrin or 80°C for β-cyclodextrin.) The diisocyanate was added without azeotropic distillation. The subsequent treatment was the same as that described above.

The cyclodextrin polyurethane resins thus obtained were granulated to a particle size of 177–250 μm with an agate mortar and sieved. The unreacted hydroxyl groups in the resin particles were silanized with trimethylchlorosilane in *n*-hexane at 60°C for 4 h.

Apparatus

A Shimadzu Model GC-3BF dual-column gas chromatograph equipped with a flame ionization detector was used. All chromatograms were recorded on a Shimadzu Model R-101 recorder. Chromatographic columns were made of Pyrex glass (80 cm × 3 mm I.D.) unless stated otherwise. Nitrogen was used as the carrier gas at a constant flow-rate of 30 ml/min. The column and detector temperatures were maintained at 150°C or 170°C. The samples were injected with a 1-μl Terumo microsyringe.

Specific surface areas of the resins were estimated by the B.E.T. method; the upper temperature limit was determined thermogravimetrically.

The desorption patterns were measured on a Shimadzu Model ADS-1B sorptograph with automatic temperature-programming equipment connected to a thermal conductivity gas chromatograph, Shimadzu Model GC-3BT.

RESULTS AND DISCUSSION

Physical properties of cyclodextrin polyurethane resins

Table I shows the monomer feed, solvent and precipitant used in the preparation of cyclodextrin polyurethane resins, together with those for butanediol–hexamethylene diisocyanate polyurethane resin.

TABLE I

POLYMERS USED IN THIS STUDY

Solvents: P = pyridine; DMF = N,N-dimethylformamide. Diisocyanates: HDI = hexamethylene diisocyanate; H6XDI = 1,3-bis(isocyanatomethyl)cyclohexane; XDI = 1,3-bis(isocyanatomethyl)-benzene. Precipitants: M = methanol; A = acetone.

Symbol	*Feed composition*
β-HDI-I-P-5.5-M	
β-HDI-P-5.5-M-Si*	β-Cyclodextrin (10 g; $8.8 \cdot 10^{-3}$ mol)–HDI (5.5 g; $3.27 \cdot 10^{-2}$ mol)
β-HDI-P-5.5-A	
β-HDI-DMF-5.5-A	
β-HDI-P-18.6-M	β-Cyclodextrin (10 g; $8.8 \cdot 10^{-3}$ mol)–HDI (18.6 g; $11.06 \cdot 10^{-2}$ mol)
β-HDI-P-18.6-A	
β-H6XDI-P-6.0-M	β-Cyclodextrin (10 g; $8.8 \cdot 10^{-3}$ mol)–H6XDI (6.0 g; $3.09 \cdot 10^{-2}$ mol)
β-XDI-P-5.8-A	β-Cyclodextrin (10 g; $8.8 \cdot 10^{-3}$ mol)–XDI (5.8 g; $3.08 \cdot 10^{-2}$ mol)
α-HDI-DMF-5.9-A	α-Cyclodextrin (8.6 g; $8.8 \cdot 10^{-3}$ mol)–HDI (5.9 g; $3.5 \cdot 10^{-2}$ mol)
α-HDI-DMF-13.3-A	α-Cyclodextrin (8.6 g; $8.8 \cdot 10^{-3}$ mol)–HDI (13.3 g; $7.9 \cdot 10^{-2}$ mol)
BDOL-HDI-P-M	1,4-Butanediol (BDOL) (8.3 g; $9.2 \cdot 10^{-2}$ mol)–HDI (15.5 g; $9.2 \cdot 10^{-2}$ mol)

* β-HDI-P-5.5-M was silanized with trimethylchlorosilane.

The physical properties of the resins obtained are listed in Table II. Each cyclodextrin resin has an upper temperature limit of 200–230°C, defined here as the temperature on the thermogravimetric curve where the resin begins to degrade slowly. A rapid weight loss was seen at *ca.* 250°C. The specific surface area of a resin depends upon the treatment used after precipitation. Consequently, the values in Table II are the average ones for several separate batches of resins.

The number of free hydroxyl groups which did not react with the diisocyanate was calculated from elemental analysis. The hydroxyl groups of cyclodextrins could not be made to react with the diisocyanates.

It is found that porous polyurethane resins containing cyclodextrin units can be prepared which have comparable physical properties to commercial porous polymers.

Retention behaviour of cyclodextrin polyurethane resins

The interactions of cyclodextrin polyurethane resins with typical organic com-

TABLE II

PHYSICAL PROPERTIES OF CYCLODEXTRIN POLYURETHANE RESINS

Adsorbent	*Temperature limit (°C)*	*Surface area (m^2/g)*	*OH Residues per cyclodextrin molecule*
β-HDI-P-5.5-M	200	170	14.4
β-HDI-P-5.5-M-Si	200	150	—
β-HDI-P-5.5-A	200	260	13.5
β-HDI-DMF-5.5-A	200	170	13.5
β-HDI-P-18.6-M	200	420	4.4
β-HDI-P-18.6-A	200	350	4.8
β-H6XDI-P-6.0-M	230	250	15.5
β-XDI-P-5.8-A	210	170	14.6
α-HDI-DMF-5.9-A	230	180	10.1
α-HDI-DMF-13.3-A	230	280	0.9
BDOL-HDI-P-M	250	160	—

pounds (adsorbates) were estimated from retention times measured by gas chromatography.

First, five adsorbates with similar boiling points were injected on columns packed with β-cyclodextrin resins prepared using different diisocyanates in order to minimize the vapour pressure effect of adsorbates on their retention times. These β-cyclodextrin resins exhibit similar interactions as shown in Table III: the interaction with benzene or methyl ethyl ketone is strong and that with cyclohexane is the weakest. The strong interaction seems to proceed through the π-electrons of the adsorbates. Silylation of hydroxyl groups in the resin does not affect the interactions with the adsorbates. The absolute interaction with benzene, for example, is strongly dependent upon the cross-linking diisocyanate and increases in the order:

$$\beta\text{-HDI-P-5.5-M} < \beta\text{-XDI-P-5.8-A} < \beta\text{-H6XDI-P-6.0-M}$$

The cyclodextrin resins obtained from hexamethylene diisocyanate seem to reflect most the effect of cyclodextrin units because of the presence of the linear

TABLE III

RETENTION TIMES (RELATIVE TO BENZENE) OF ADSORBATES WITH SIMILAR BOILING POINTS ON β-CYCLODEXTRIN POLYURETHANE RESINS

Carrier gas: nitrogen, 30 ml/min. Column temperature: 170°C. Actual retention times (min) are given in parentheses.

Adsorbate	*β-HDI-P-5.5-M*	*β-HDI-P-5.5-M-Si*	*β-H6XDI-P-6.0-M*	*β-XDI-P-5.8-A*
Benzene	1.00 (28.76)	1.00 (22.32)	1.00 (101.00)	1.00 (88.85)
Cyclohexane	0.13	0.15	0.18	0.16
Ethanol	0.31	0.32	0.25	0.23
Methyl ethyl ketone	0.81	0.60	0.88	0.85
Methyl propionate	0.54	0.37	0.36	0.72

methylene linkages. Thus, the interactions of resins from β-cyclodextrin and hexamethylene diisocyanate with various adsorbates were investigated. The relative retention times are shown in Table IV together with those on BDOL-HDI-P-M and on Tenax GC. The interactions of the cyclodextrin resins are very weak with the aliphatic hydrocarbons and extraordinarily strong with pyridine, compared with the other classes of adsorbates. *p*-Xylene is retained more strongly than the *m*- and *o*-isomers. The retention behaviours of the xylene isomers and the pyridine derivatives are discussed later in this paper. The precipitants have little effect on the absolute values of the retention times. However, the use of N,N-dimethylformamide as solvent instead of pyridine results in a large decrease in the absolute retention times and a variation of elution order. This seems to reflect the difference in the porosity of the resin to the solvent[6,7]. The retention times of benzene, for example, increase with increasing cyclodextrin content in the resins. Neither BDOL-HDI-P-M nor Tenax GC interacts strongly with benzene, compared with the other adsorbates with similar

TABLE IV

RETENTION TIMES (RELATIVE TO BENZENE) ON CYCLODEXTRIN POLYURETHANE RESINS

Carrier gas: nitrogen, 30 ml/min. Column temperature: 150°C. Actual retention times (min) are given in parentheses. Column length of β-HDI-P-18-6-M and Tenax GC is 120 cm.

Adsorbate	*β-HDI-P-5.5-M*	*β-HDI-P-5.5-A*	*β-HDI-DMF-5.5-A*	*β-HDI-P-18.6-M*	*β-HDI-P-18.6-A*	*BDOL-HDI-P-M*	*Tenax GC*
Hexane	0.07	0.04	0.04	0.12	0.06	0.47	0.44
Heptane	0.10	0.09	0.06	0.12	0.06	0.53	0.72
Octane	0.18	0.15	0.10	0.20	0.07	0.61	1.62
Methanol	0.09	0.12	0.36	0.29	0.19	0.96	0.16
Ethanol	0.29	0.35	0.78	0.57	0.50	1.07	0.21
Propanol	1.16	1.33	1.96	1.80	1.67	1.44	0.35
Butanol	3.37	—	4.63	4.14	4.00	2.08	0.66
Acetone	0.37	—	0.67	0.37	0.54	0.80	0.25
Methyl ethyl ketone	0.84	1.03	1.24	1.10	1.02	1.01	0.55
Methyl propyl ketone	1.80	—	2.02	1.71	1.81	1.29	1.06
Methyl butyl ketone	*	—	3.64	2.70	3.46	1.82	2.09
Methyl propionate	0.57	0.69	0.85	0.64	0.63	0.89	0.64
Methyl butyrate	1.36	—	1.49	1.07	1.16	1.10	1.30
Methyl valerate	3.40	—	2.93	1.47	2.05	1.49	2.88
Ethyl propionate	1.06	—	1.11	0.75	0.84	0.99	1.04
Cyclohexane	0.08	0.05	0.05	0.27	0.04	0.59	0.75
Benzene	1.00 (70.36)	1.00 (60.52)	1.00 (16.68)	1.00 (24.42)	1.00 (22.80)	1.00 (1.52)	1.00 (4.25)
Toluene	1.46	—	1.20	1.12	1.26	—	1.96
o-Xylene	*	—	0.60	2.17	1.58	2.35	5.12
m-Xylene	*	—	1.08	2.00	1.48	1.91	4.38
p-Xylene	*	—	1.87	2.65	1.95	1.87	4.34
Pyridine	*	—	9.00	6.80	5.36	3.16	1.94

* This peak is too broad.

boiling points. Therefore, it is reasonable that the β-cyclodextrin units in the resins result in the strong interactions with the adsorbates.

It is of interest to investigate the polyurethane resins containing α-cyclodextrin whose cavity diameter is smaller than that of β-cyclodextrin. Table V shows the retention times on the polyurethane resins of α- and β-cyclodextrins prepared in N,N-dimethylformamide. The difference in the cavity diameter between α- and β-cyclodextrins is reflected in the retention behaviours of adsorbates. Bulky adsorbates such as the aromatic ones interact with β-HDI-DMF-5.5-A more strongly than with α-HDI-DMF-A; most adsorbates with a linear group, such as aliphatic hydrocarbons, esters and ketones, exhibit the opposite trend. This behaviour may be explained on the basis that the adsorbates with a linear group are less bulky and fit better into the α-cyclodextrin cavity than the aromatic adsorbates.

TABLE V

RETENTION TIMES (RELATIVE TO BENZENE) ON CYCLODEXTRIN POLYURETHANE RESINS

Carrier gas: nitrogen, 30 ml/min. Column temperature: 150°C. Actual retention time (min) are given in parentheses.

Adsorbate	*β-HDI-DMF-5.5-A*	*α-HDI-DMF-5.9-A*	*α-HDI-DMF-13.3-A*
Hexane	0.04	0.16	0.27
Heptane	0.06	0.24	0.33
Octane	0.10	0.29	0.45
Methanol	0.36	0.53	1.06
Ethanol	0.78	0.83	1.53
Propanol	1.96	2.03	2.80
Butanol	4.63	6.01	6.23
Acetone	0.67	0.71	0.98
Methyl ethyl ketone	1.24	1.61	1.65
Methyl propyl ketone	2.02	5.44	3.32
Methyl butyl ketone	3.64	11.68	6.58
Diethyl ketone	1.75	6.09	2.97
Methyl propionate	0.85	1.84	1.20
Methyl butyrate	1.49	6.43	2.51
Methyl valerate	2.93	—	5.61
Ethyl propionate	1.11	6.80	1.90
Cyclohexane	0.05	0.07	0.12
Benzene	1.00	1.00	1.00
	(16.68)	(6.59)	(4.16)
Toluene	1.20	2.73	1.96
o-Xylene	0.60	0.89	2.62
m-Xylene	1.08	2.22	2.77
p-Xylene	1.87	6.53	3.41
Pyridine	9.00	7.23	6.80

Table VI shows the retention times of the aromatic adsorbates on the cyclodextrin resins from hexamethylene diisocyanate at the column temperature of 170°C. On the resins of BDOL-HDI-P-M and Tenax GC containing no cyclodextrin units, the xylene isomers are eluted in the order of the *p*-, *m*- and *o*-isomers, as shown in Table IV. This order parallels that of the boiling points of the isomers. The *m*- and

TABLE VI

RETENTION TIMES (RELATIVE TO BENZENE) OF AROMATIC ADSORBATES ON CYCLODEXTRIN POLYURETHANE RESINS

Carrier gas: nitrogen, 30 ml/min. Column temperature: 170°C. Actual retention times (min) are given in parentheses.

Adsorbate	*β-HDI-P-5.5-M*	*β-HDI-DMF-5.5-A*	*β-HDI-P-5.5-M-Si*	*α-HDI-DMF-5.9-A*
Benzene	1.00 (28.76)	1.00 (7.25)	1.00 (22.32)	1.00 (3.88)
Toluene	1.19	1.11	1.00	1.25
o-Xylene	1.59	1.00	1.32	1.53
m-Xylene	1.42	1.09	1.10	2.20
p-Xylene	2.07	1.49	1.55	4.93

o-isomers interact with the β-cyclodextrin resins almost to the same extents, considering their boiling points. The *o*-isomer interacts the least with the α-cyclodextrin resin. The *p*-isomer is eluted last on the resins containing α- or β-cyclodextrin. This effect of the structure of xylene isomers may be reasonably interpreted as follows. *p*-Xylene can enter deep into the cavity of β-cyclodextrin with one of the methyl groups first, but the benzene ring of *m*- or *o*-xylene cannot enter so deeply because of the steric hindrance of the methyl groups. As seen from the retention times of benzene, the smaller cavity of α-cyclodextrin is unable to interact with a benzene ring as strongly as the β-cyclodextrin cavity. The entrances of the cross-linked cyclodextrins are more rigid and more crowded than of native cyclodextrins. Therefore, the α-cyclodextrin resin interacts more strongly with a less bulky isomer and with the three xylene isomers to different extents.

As shown in Tables IV and V, pyridine gives very long retention times on the cyclodextrin resins. This is also true for tetrahydrofuran and 1,4-dioxan. This fact suggests a strong hydrogen-bonding interaction between the heteroatoms and the polyurethane resins in addition to the hydrophobic guest–host interaction. The retention behaviours of pyridine derivatives, picolines and lutidines, on the resins were therefore investigated. The results in Table VII may be interpreted as follows. If we consider that the pyridine ring of a picoline enters the β-cyclodextrin cavity deeply like benzene or pyridine, the introduction of a methyl group into the pyridine ring will cause the position of the nitrogen atom in the cavity to change. The nitrogen atom of α-picoline is included inside the cavity and greatly shielded from the hydrogen-bonding interaction. γ-Picoline, on the other hand, interacts in the same way as pyridine. In the case of the α-cyclodextrin cavity, the pyridine rings are not able to enter the cavity deeply. All the nitrogen atoms of pyridine and picolines are situated in similar environments. They are, therefore, eluted in the order of increasing boiling point.

A similar argument is presumably true for the retention behaviours of lutidine isomers. The nitrogen atom of 2,6-lutidine cannot participate in hydrogen-bonding and 2,6-lutidine cannot enter deep into the β-cyclodextrin cavity, because of the introduction of two methyl groups at the 2- and 6-positions. Consequently, 2,6-lutidine is eluted faster on the β-cyclodextrin resins than any of the other pyridine derivatives discussed. 2,5-Lutidine is able to enter the β-cyclodextrin cavity as deeply

TABLE VII

RETENTION TIMES (RELATIVE TO PYRIDINE) OF PYRIDINE DERIVATIVES ON CYCLODEXTRIN POLYURETHANE RESINS

Carrier gas: nitrogen, 30 ml/min. Column temperature: 170°C. Actual retention times (min) are given in parentheses.

Adsorbate	*β-HDI-P-5.5-M*	*β-HDI-DMF-5.5-A*	*α-HDI-DMF-5.9-A*
Pyridine	1.00 (142.09)	1.00 (48.95)	1.00 (19.36)
α-Picoline	0.90	0.93	1.49
β-Picoline	1.60	1.55	2.76
γ-Picoline	2.19	1.84	2.33
2,3-Lutidine	1.94	1.65	2.37
2,4-Lutidine	1.74	1.65	2.33
2,5-Lutidine	1.73	1.62	3.68
2,6-Lutidine	0.58	0.67	1.13

as *p*-xylene, and its hydrophobic guest–host interaction is the strongest. The interaction due to hydrogen-bonding, however, is reduced considerably, for the nitrogen atom is situated inside the cavity. 2,5-Lutidine is thus eluted faster than the 2,4- or 2,3-isomer (Table VII). All the isomers cannot enter into the cavity of α-cyclodextrin so deeply as into that of β-cyclodextrin, as the cavity of the former is smaller and more crowded as mentioned above. Except for 2,6-lutidine, these isomers have almost equal hydrogen-bonding effects. 2,5-Lutidine with the least bulky structure is eluted last. The cyclodextrin polyurethane resins thus have the ability to distinguish between the configurations of picoline and lutidine isomers.

In order to confirm the strong interactions of the cyclodextrin cavities in the resins with guest molecules containing π-electrons and/or heteroatoms, the desorption patterns for benzene were measured by means of the temperature-programmed des-

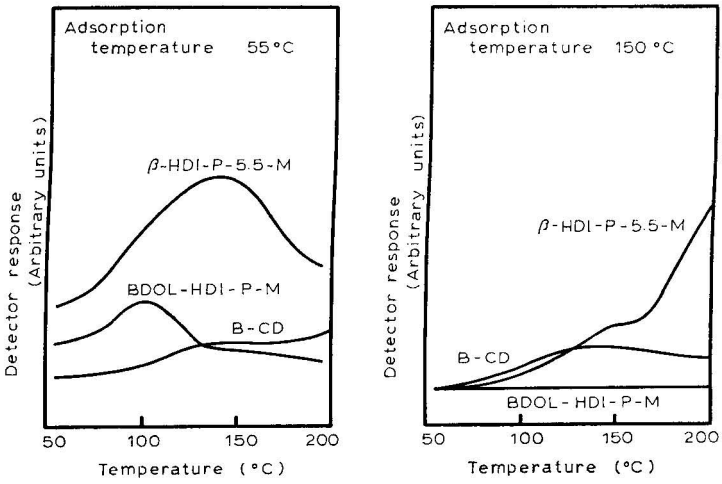

Fig. 1. Desorption patterns for benzene. Particle size, 60–80 mesh. Programmed at 3.1°C/min. Carrier gas, helium.

orption method (Fig. 1). At the adsorption temperature of 55°C, β-HDI-P-5.5-M and native β-cyclodextrin exhibit the peak of benzene at 140°C, while BDOL-HDI-P-M has it at 110°C. At the adsorption temperature of 150°C, the desorption peaks on β-HDI-P-5.5-M and native β-cyclodextrin appear above 200°C; on the other hand, BDOL-HDI-P-M shows no peak at all. These results strongly suggest that the cyclodextrin cavities in the resins take part in interactions with guest molecules.

This preliminary study of cyclodextrin polyurethane resins was carried out to investigate the specific interactions between the resins and organic compounds for the purpose of using these resins for selective concentration of organic compounds. The cyclodextrin resins prepared here strongly interact with guest molecules containing heteroatoms and can be used to distinguish between the configurations of the guest molecules. The results obtained indicate the possibility of using the cyclodextrin polyurethane resins as adsorbents that can selectively adsorb organic compounds in the gas phase.

ACDNOWLEDGEMENT

This work was partially supported by a Grant-in-Aid for Scientific Research from the Ministry of Education.

REFERENCES

1 M. L. Bender and M. Komiyama, *Cyclodextrin Chemistry*, Springer, Berlin, Heidelberg, 1978.
2 N. Wiedenhof, *Die Stärke*, 21 (1969) 163.
3 J. L. Hoffman, *J. Macromol. Sci., Chem.*, A7 (1973) 1147.
4 A. Harada, M. Furue and S. Nozakura, *J. Polym. Sci.*, 16 (1978) 189.
5 I. A. Wolff and C. E. Rist, *J. Amer. Chem. Soc.*, 70 (1948) 2779.
6 W. Heitz, *J. Chromatogr.*, 53 (1970) 37.
7 M. Kraus and H. Kopecká, *J. Chromatogr.*, 124 (1976) 360.

Journal of Chromatography, 194 (1980) 163–173
Elsevier Scientific Publishing Company, Amsterdam — Printed in The Netherlands

CHROM. 12,751

DETERMINATION OF THE COMPOSITION OF COPOLYMERS AS A FUNCTION OF MOLECULAR WEIGHT BY PYROLYSIS GAS CHROMATOGRAPHY–SIZE-EXCLUSION CHROMATOGRAPHY

SADAO MORI

Department of Industrial Chemistry, Faculty of Engineering, Mie University, Tsu, Mie 514 (Japan)

(First received January 15th, 1980; revised manuscript received February 11th, 1980)

SUMMARY

A sample of acrylonitrile–styrene copolymer was fractionated into ten portions by using analytical scale size-exclusion chromatography and the composition of the copolymer fractions was determined by using pyrolysis gas chromatography. A 0.12-ml volume of each fraction was collected in a platinum boat and the copolymer on the boat was pyrolyzed at 700°C after the removal of solvent. The amount of copolymer pyrolyzed at a time ranged from 0.004 mg to 0.022 mg. The copolymer fractions have an average acrylonitrile content of 24%, the composition ranges from 21% to 30%, with the acrylonitrile content decreasing with increasing molecular weight. These data are in fair agreement with those determined by a dual-detector method, using ultra-violet and differential refractive index detectors. This system can be applied to the determination of both distributions, molecular weight and composition, of copolymers for which a dual-detector method is inadequate.

INTRODUCTION

The physical properties of copolymers are dependent on their composition and molecular weight. Several studies have been made of the determination of the copolymer composition as a function of molecular weight. Size-exclusion chromatography (SEC) (conventionally gel permeation chromatography, GPC) has been used in combination with ultraviolet (UV) and differential refractive index (RI) detectors for molecular weight and composition analysis of copolymers such as styrene–butadiene[1,2] and 4-vinylphenyl–isoprene[3]. The relationship between copolymer composition and molecular weight for a poly(styrene–vinyl stearate) copolymer has been investigated by preparative SEC and infrared (IR) analysis of the fractions[4], and by the rapid stop-and-go GPC–IR technique[5]. Molecular weight and composition distributions of a poly(vinyl chloride–vinyl acetate) copolymer have been determined by SEC and IR analysis[6,7]. An on-line IR spectrophotometric detector has been used to monitor individual functional groups in a poly(styrene–*tert.*-butyl methacrylate) by repeated injections of the solute, and changing the wavelength setting[8].

0021-9673/80/0000–0000/$02.25

The use of a UV detector in series with a RI detector for simultaneous determination of the composition and the molecular weight of a binary copolymer requires the restriction that one component should absorb UV radiation and the other should not. This limits the number of copolymers that can be examined by this UV–RI system. Appropriate selection of the wavelength setting in an IR detector may significantly expand its range of applicability to copolymer analysis, but the limited choice of solvent as the mobile phase to match the wavelength setting for functional groups in copolymers restricts the versatility of the detector.

Pyrolysis gas chromatography (PGC) has been widely used for copolymer composition analysis. Conditions essential to quantitative reproducibility in PGC have been studied and reproducibility can be achieved provided parameters such as pyrolysis-temperature rise time, sample size and sample thickness are carefully prescribed[9]. PGC may offer many advantages over other techniques such as the UV–RI system and IR detection in SEC. One of these advantages is the small sample size, and polymer amounts of less than 0.1 mg are occasionally pyrolyzed at a time. Sample size injected in high-performance SEC is usually 0.5 mg or less, and preparative-scale SEC may be required in order to determine the copolymer composition by an off-line IR detector[7]. Therefore, the utilization of PGC on the SEC fractions may permit the compositional analysis of copolymers the components of which do not absorb UV radiations, or of copolymers for which the application of IR detection is difficult. One example is a combination of SEC, thin-layer chromatography and PGC which has been used for the investigation of a polymethyl methacrylate–polystyrene–polymethyl methacrylate block copolymer[10].

In this paper, the evaluation of the precision and applicability of combined PGC–SEC was undertaken and compared with the dual-detector method, a combination of UV and RI detectors in SEC, in the determination of the percent composition of copolymers as a function of molecular weight. Acrylonitrile–styrene copolymers (ASR) were employed, a small amount of ASR being fractionated by SEC followed by determination of the composition of the fractions by PGC.

EXPERIMENTAL

Apparatus

SEC. Two sets of liquid chromatographs were used. One was a JASCO (Japan Spectroscopic Co., Tokyo, Japan) Trirotar high-performance liquid chromatograph equipped with a JASCO Uvidec-100 variable-wavelength UV detector and a Shodex SE-11 RI detector (Showa Denko Co., Ltd., Minato-ku, Tokyo, Japan). The UV detector was operated at 254 nm with a 10-mm path length microcell. Two Shodex A 80M GPC columns (500 × 8 mm I.D.) packed with a mixture of polystyrene gels of nominal porosity 10^3, 10^4, 10^5, and 10^6 Å were used. The other set was a Model LC-08 high-speed preparative liquid chromatograph (Japan Analytical Industry Co., Tokyo, Japan) equipped with UV and RI detectors and two preparative GPC columns (600 × 20 mm I.D.) packed with Jaigel 3H (corresponding to Shodex H203). Chloroform was used as solvent (the mobile phase).

PGC. A Yanaco (Yanagimoto Seisakusho Co., Kyoto, Japan) G-80 gas chromatograph equipped with a flame ionization detector was used. A Shimadzu Model PYR-2A furnace-type pyrolyzer was employed. The stainless-steel column

(150 cm × 3 mm I.D.) was packed with Diasolid L (100–120 mesh) coated with 5% PEG 6000.

Samples

Two grades of acrylonitrile–styrene copolymers (ASR) were used. One was prepared in our laboratory by solution polymerization in benzene using α,α'-azobisisobutyronitrile as an initiator. The nitrogen content in the polymers was determined by Dumas' method. The acrylonitrile contents ranged from 22.2 to 46.4 wt.%. The average molecular weight ranged from 5000 to 10,000 as determined by SEC. The acrylonitrile content of the sample (ASR-5) used for SEC fractionation and PGC analysis was 28.6 wt.%. The other grade was obtained from Mitsubishi Monsanto, Tokyo, Japan. The acrylonitrile contents ranged from 20.0 to 29.0 wt.%, and the average molecular weight from 100,000 to 200,000. The acrylonitrile content of the sample (ASR-24) used for SEC fractionation and PGC analysis was 24.0 wt.%.

Procedures

Calibration curve for PGC. About 5 mg copolymer material of known composition were weighed into a 20-ml volumetric flask and dissolved in 20 ml chloroform. A 20-μl volume of this solution was placed in a platinum boat (capacity *ca.* 40 μl) and dried using a 250-W IR lamp. This procedure was repeated twice, *ca.* 10 μg of the copolymer material being collected in the boat. The platinum boat was then inserted into the pyrolyzer. The pyrolysis temperature was 700°C. Operating conditions for GC analysis: nitrogen flow, 15 ml/min; column oven temperature, 140°C; flame ionization detector, range 10^{-1} with 1/256 attenuation. The ratio of peak area of acrylonitrile monomer to that of styrene monomer was plotted against the copolymer composition and a calibration curve was thus constructed. The product of peak height and peak half-width was used as peak area.

Fractionation of copolymer. The sample ASR-5 (*ca.* 25 mg) was weighed and dissolved in 5 ml chloroform. A 1.5-ml volume of this solution was injected into a Model LC-08 liquid chromatograph. Eleven 10-ml fractions were collected over the elution range of the sample.

The sample ASR-24 (*ca.* 10 mg) was weighed and dissolved in 5 ml chloroform. A 0.5-ml portion of this solution was injected into a Trirotar liquid chromatograph, the flow-rate being 1.0 ml/min. Collection of fractions was carried out at intervals of 80 sec (every 1.33 ml) and ten fractions were collected over the elution range of the sample.

PGC of the fractions. For fractions of the sample ASR-5, a 30-μl portion of each fraction, except Nos. 1 and 11, was placed in a platinum boat and allowed to dry. This procedure was repeated six times and a total of 180 μl of the fraction were collected on the boat. Fractions 1 and 11 were concentrated to one-fourth by volume before being placed in a platinum boat, and then a total of 180 μl of the concentrastes were collected on the boat.

For fractions of the sample ASR-24, a total of 120 μl of each fraction, except Nos. 1 and 10, were collected on the boat. For fractions 1 and 10, 360 μl were collected in total. PGC conditions were the same as for the calibration curve.

Distributions of molecular weight and composition

Step 1. A calibration curve of log molecular weight *vs.* elution volume was constructed using polystyrene standards.

Step 2. A copolymer calibration curve of log molecular weight *vs.* elution volume was constructed from the known compositions of the fractions of ASR-5 or ASR-24 copolymers and by using the polystyrene calibration curve. The copolymer molecular weight obtained from the polystyrene calibration curve was converted into the so-called "working" molecular weight[5] using

$$M_c = M_s\,(1 - 4.9 \times 10^{-3}\ \text{AN mol}\%)$$

$$= M_s(1 - \frac{51\ \text{AN wt.}\%}{5300 + 51\ \text{AN wt.}\%} \qquad (1)$$

where M_c = "working" molecular weight of the copolymer, M_s = molecular weight from the polystyrene calibration curve and AN mol% and AN wt.% = acrylonitrile content in mol% and wt.%.

First, the value of M_s for each fraction was determined from the average elution volume of the fraction using the polystyrene calibration curve. Then, the value of M_c for the fraction was calculated from eqn. 1, followed by plotting the value and the average elution volume of the fraction.

Step 3. The RI response of the SEC chromatogram of the copolymer sample was corrected using

$$H_{\text{corr.}} = H_{\text{uncorr.}}\,(1 + 0.011\ \text{AN wt.}\%) \qquad (2)$$

where $H_{\text{corr.}}$ and $H_{\text{uncorr.}}$ are the corrected and uncorrected heights of each increment of the elution volume.

Step 4. The molecular weight averages of the copolymer sample were calculated from the values of $H_{\text{corr.}}$ obtained in Step 3 and using the copolymer calibration curve in Step 2.

Step 5. The differential molecular weight distribution curve was constructed after converting the values of dW/dV of the normalized SEC chromatogram in to those of $dW/d\log M$ using the copolymer calibration curve.

Step 6. By plotting the relation between M_c and acrylonitrile content of each fraction on the same chart obtained in Step 5, both distribution curves, molecular weight and composition, were visualized.

RESULTS AND DISCUSSION

Fundamentals of PGC

Quantitative analysis of pyrolysis products requires much more stringent control than qualitative identification techniques. Differences in, for example, sample size and sample features, can often significantly affect the decomposition pattern[11]. The major product of degradation of polystyrene and polyacrylonitrile is the

respective monomer and the yield is dependent on temperature and sample size. The copolymer concentration of SEC fractions is variable and the content of copolymers subjected to PGC might be very small. For these reasons, preliminary investigations of experimental factors must be performed before analysis of SEC fractions.

A chloroform solution (0.5%, w/v) of ASR-5 was prepared and various volumes of this solution from 10 μl to 100 μl were loaded into a platinum boat, followed by evaporation of the chloroform. Polymer contents loaded were between 0.05 mg and 0.5 mg. PGC was carried out at various pyrolysis temperatures and peak-height ratios of acrylonitrile monomer to styrene monomer were plotted against polymer weight pyrolyzed. The results are shown in Fig. 1. Both the yields and peak-height ratios of the respective monomers increased with rising pyrolysis temperatures except that the maximum yield of styrene monomer was attained at 650°C. This suggests that sensitive analysis may be performed at higher pyrolysis temperatures. Pyrolysis of lower sample weights gave similar results as shown in Fig. 2. A 0.05% (w/v) chloroform solution of ASR-5 was prepared and the polymer contents

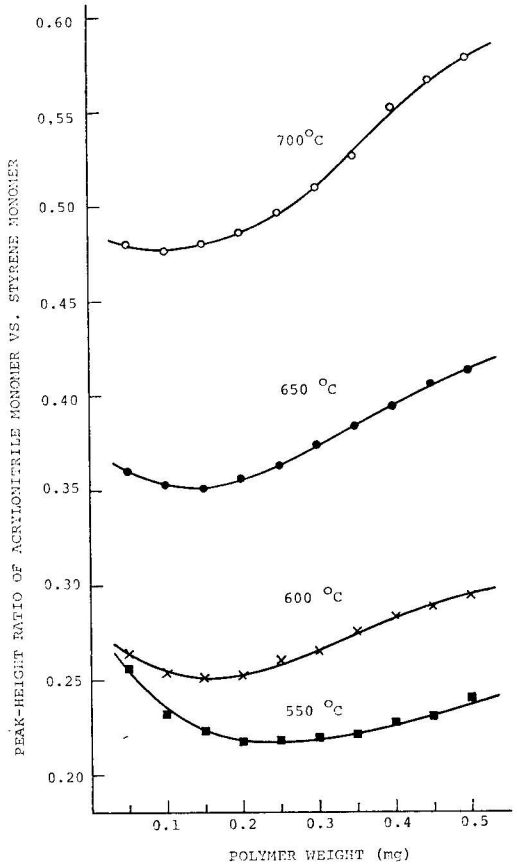

Fig. 1. Variation of ratio of monomer yields with sample weight pyrolyzed. Sample, ASR-5.

loaded into a platinum boat were between 0.005 mg and 0.05 mg. The curves of peak-height ratio against polymer weight exhibit a minimum, which demonstrates that the peak-height ratio is dependent on the weight of the pyrolyzed sample. On the other hand, the peak-area ratio is independent of the sample weight (see Fig. 2).

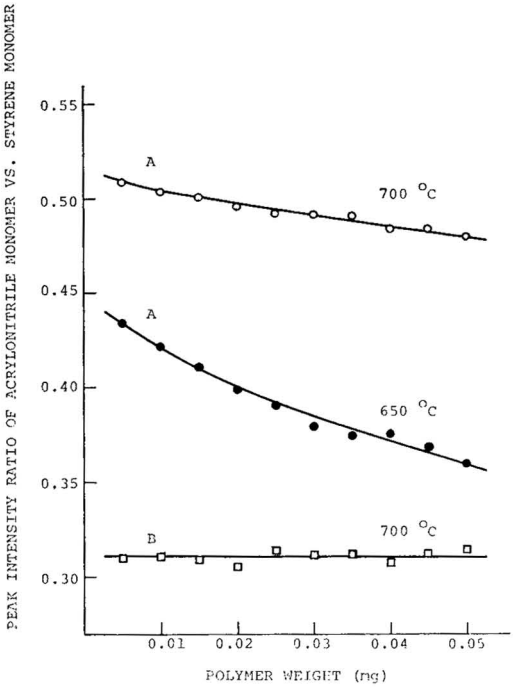

Fig. 2. Variation of ratio of monomer yields with lower sample weight pyrolyzed and comparison of peak height and peak area. A, Peak-height ratio; B, peak-area ratio. Sample, ASR-5.

A PGC calibration curve of the ratio of peak areas of acrylonitrile and styrene monomers *versus* acrylonitrile content obtained from physical mixtures of homopolymers (polystyrene and polyacrylonitrile) differed significantly from that obtained from copolymers of known composition as shown in Fig. 3. This difference may be due to the difference in rates of degradation between copolymers and homopolymers. The yield of acrylonitrile monomer from the physical mixture was 50% less than that from the copolymer of the same composition, and that of styrene monomer 25% more. The peak positions of styrene monomer and other products from polystyrene were delayed by *ca.* 7 sec compared with those from the styrene unit of the copolymer. In this study a PGC calibration curve has been constructed by using copolymers of known composition.

The repeatability of pyrolysis is excellent and the relative standard deviation of the ratio of peak areas ranges from 1.0% to 1.5%. The reproducibility at different sample loads is also good and the relative standard deviation is less than 1.5%. The standard deviation of the acrylonitrile content is 0.15 wt.%. The calibration data were not affected by the molecular weight difference in the range studied.

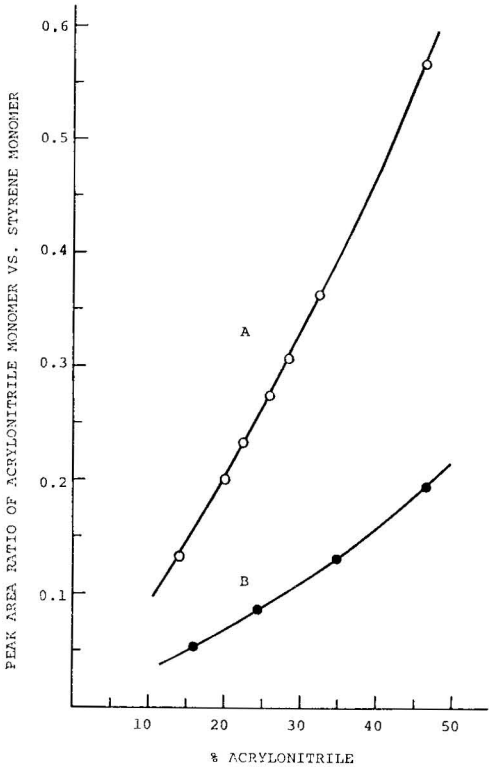

Fig. 3. Comparison of the ratio of respective monomer yields between copolymers (A) and physical mixtures of homopolymers (B). Sample weigth pyrolyzed, 2 mg.

Composition and molecular weight of fractions

ASR-5. The copolymer material (7.5 mg; 1.5 ml of 0.5% solution) was fractionated into eleven portions and the copolymer content in each solution fractionated ranged from 0.045 mg to 1.545 mg. The copolymer amount pyrolyzed at a time ranged from 0.0027 to 0.0278 mg. The variation of the pyrograms with polymer weight pyrolyzed is shown in Fig. 4 for fractions 1 and 2. For fraction 2, the pyrolysis patterns are somewhat different, but the numerical value of the ratios of peak area of acrylonitrile and styrene monomers does not change with sample size except A in Fig. 4 which is about two-thirds that of the others. In addition, hydrocarbons such as methane, ethane and ethylene increased in yield. The minimum sample amount pyrolyzed should by 0.002 mg under the present experimental conditions. Therefore, a volume of 180 μl for fraction 1 is too small to obtain an accurate value for the peak ratio.

For comparison purposes, known weights of the copolymer fraction were collected on the boat. The copolymer content in each solution fractionated was estimated from the area on the SEC chromatogram occupied by each fraction and *ca.* 0.006 mg (from 40 μl to 330 μl for fractions 2–10) of the copolymer were pyrolyzed. The compositions of copolymer fractions as determined by both procedures are summarized in Table I, together with the values calculated by a dual-detector method

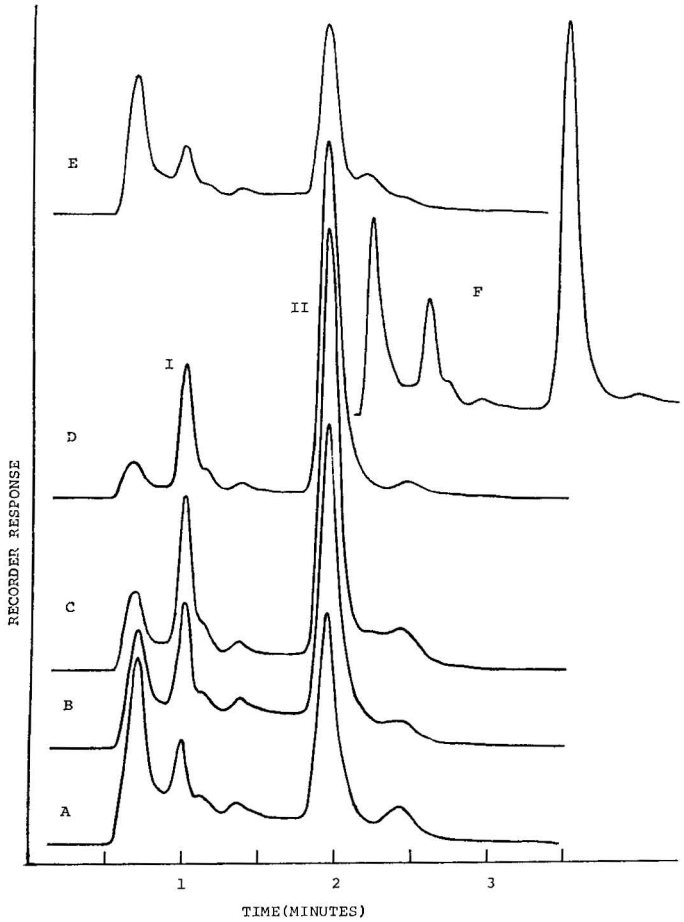

Fig. 4. Pyrolysis gas chromatograms of fractionated copolymer ASR-5 at different pyrolysis amounts. A–D, Fraction 2; E–F, fraction 1. Sample volume, weight and GC sensitivity: A, 40 μl, 1.0 μg, $10^{-1} \times 1/32$; B, 60 μl, 1.5 μg, $10^{-1} \times 1/32$; C, 180 μl, 4.6 μg, $10^{-1} \times 1/64$; D, 300 μl, 7.7 μg, $10^{-1} \times 1/128$; E, 180 μl, 1.2 μg, $10^{-1} \times 1/32$; F, 180 μl (a concentrate), 4.8 μg, $10^{-1} \times 1/64$. Peaks: I = acrylonitrile; II = styrene.

which will be discussed elsewhere. These results are in good agreement with each other. The average acrylonitrile content for the whole copolymer as calculated from the acrylonitrile content and the weight percent of each fraction is listed in the same column. These values are in fair agreement with the analysis of the unfractionated sample (28.6 wt.%).

The weight percent of each fraction was calculated from the area of the SEC chromatogram defined by the dotted line (see Fig. 5). A correction was made for the difference in response factors between polystyrene and polyacrylonitrile using eqn. 2. In the range of chemical compositions studied, the correction does not significantly influence the results of the weight percent for each fraction. The molecular weight of each fraction was calculated from the average elution volume of the fraction using the polystyrene calibration curve and eqn. 1. Molecular weight averages

TABLE I

ACRYLONITRILE CONTENT AND MOLECULAR WEIGHT OF ASR-5 FRACTIONS

Fraction No.	*Acrylonitrile content (wt.%)*			*Weight percent fraction (%)*		*Molecular weight* $\times 10^{-3}$
	By definite volume	*By definite weight*	*By D-D method**	*Uncorrected*	*Corrected*	
1	24.2	(24.2)	25.6	0.9	0.9	54
2	25.5	26.0	25.9	3.5	3.4	27.5
3	27.2	27.0	27.2	10.0	9.9	16.6
4	27.7	27.7	28.2	17.1	16.9	11.1
5	28.8	28.6	29.1	20.6	20.6	7.5
6	29.3	29.3	28.9	18.1	18.2	5.0
7	30.1	30.3	29.9	13.7	13.8	3.35
8	30.7	30.8	30.5	8.8	8.9	2.25
9	31.3	31.5	31.5	4.7	4.8	1.55
10	31.6	31.9	30.9	2.0	2.0	1.02
11	33.3	(33.3)	33.9	0.6	0.6	0.66
Calculated average composition	28.9	29.0	29.0			

* Dual-detector method.

of the whole copolymer, calculated by using the corrected SEC chromatogram (Step 3) and the copolymer calibration curve (Step 2), are $\overline{M}_w = 8.01 \cdot 10^3$ and $\overline{M}_n = 4.38 \cdot 10^3$.

ASR-24. The copolymer material (1.0 mg; 0.5 ml of 0.2% solution) was fractionated into ten portions and the copolymer amount pyrolyzed at a time ranged from 0.0019 mg to 0.0220 mg. The normalized size exclusion chromatogram, the polystyrene calibration curve (Step 1) and the copolymer calibration curve (Step 2) are shown in Fig. 5. Fractionation of the copolymer was carried out at indicated by the dotted lines on the chromatogram.

The SEC chromatogram of the copolymer must be corrected using eqn. 2 when a differential refractometer is used as a detector. This equation has been derived from the assumption that the response factor of polystyrene is 2.1 times that of polyacrylonitrile.

The molecular weight averages for the copolymer calculated according to Step 4 are $\overline{M}_w = 1.79 \cdot 10^5$, $\overline{M}_n = 6.44 \cdot 10^4$ and $\overline{M}_w/\overline{M}_n = 2.78$. The values calculated assuming a constant composition are slightly higher: $\overline{M}_w = 1.81 \cdot 10^5$, $\overline{M}_n = 6.63 \cdot 10^4$ and $\overline{M}_w/\overline{M}_n = 2.73$. In the range of chemical compositions and molecular weights studied, the chemical composition does not significantly influence the results of SEC analysis.

Fig. 6 shows a normalized differential molecular-weight distribution curve calculated by Step 5, and the acrylonitrile content as a function of molecular weight. The composition distribution curve calculated by a dual-detector mehtod is also shown. The comparison of these methods will be discussed elsewhere. The average acrylonitrile content for the whole copolymer as calculated from the composition and

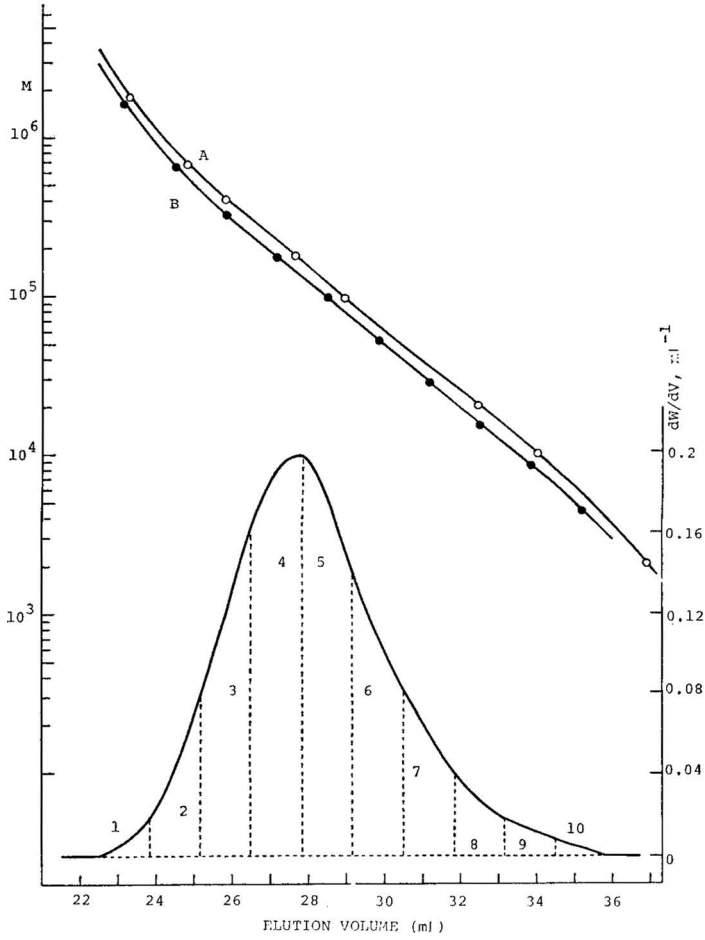

Fig. 5. Normalized size exclusion chromatogram, polystyrene calibration curve (A) and copolymer calibration curve (B) for ASR-24 copolymer.

the weight percent of each fraction was 24.4 wt.%, which is in good agreement with the value for the unfractionated sample (24.0 wt.%).

Eqn. 1 has been derived from

$$M_c = M_s \times \frac{53\ \text{AN mol\%} + 104\ \text{ST mol\%}}{104 \times 100} \tag{3}$$

where 53 and 104 are the molecular weights of monomer units of acrylonitrile and styrene, respectively. This equation is based on the concept of "working" molecular weight[12], and its validity will be discussed elsewhere.

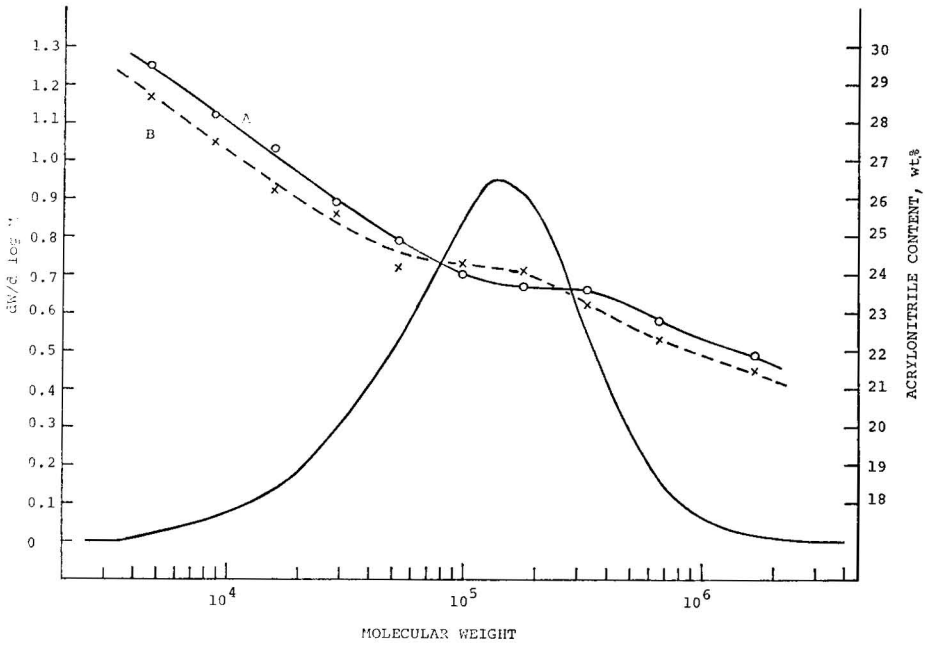

Fig. 6. Normalized molecular weight and composition distribution curves of ASR-24 copolymer, obtained by PGC (A) and by a dual-detector method (B).

ACKNOWLEDGEMENT

The author is grateful to Mr. F. Iioka for technical assistance.

REFERENCES

1 H. E. Adams, *Separ. Sci.*, 6 (1971) 153.
2 J. R. Runyon, D. E. Barnes, J. F. Rudd and L. H. Tung, *J. Appl. Polym. Sci.*, 13 (1969) 2359.
3 J. Heller, J. F. Schimscheimer, R. A. Pasternak, C. B. Kingsley and J. Moacanin, *J. Polym. Sci., Part A-1*, 7 (1969) 73.
4 F. M. Mirabella, Jr., E. M. Barrall, II and J. F. Johnson, *J. Appl. Polym. Sci.*, 20 (1976) 959.
5 F. M. Mirabella, Jr., E. M. Barrall, II and J. F. Johnson, *J. Appl. Polym. Sci.*, 20 (1976) 581.
6 J. Janča and M. Kolínský, *J. Appl. Polym. Sci.*, 21 (1977) 83.
7 S. Mori, *J. Chromatogr.*, 157 (1978) 75.
8 J. V. Dawkins and M. Hemming, *J. Appl. Polym. Sci.*, 19 (1975) 3107.
9 J. Q. Walker, *J. Chromatogr. Sci.*, 15 (1977) 267.
10 B. G. Belenkii, E. S. Gankina, P. P. Nefedov, M. A. Lazareva, T. S. Savitskaya and M. D. Volchikhina, *J. Chromatogr.*, 108 (1975) 61.
11 R. S. Lehrle and J. C. Robb *J. Gas Chromatogr.*, 5 (1967) 89.
12 F. M. Mirabella, Jr., E. M. Barrall, II and J. F. Johnson, *J. Appl. Polym. Sci.*, 19 (1975) 2131.

Journal of Chromatography, 194 (1980) 175–181
Elsevier Scientific Publishing Company, Amsterdam — Printed in The Netherlands

CHROM. 12,721

INTERACTION OF TRYPSIN WITH IMMOBILIZED *p*-AMINOBENZAMIDINE DERIVATIVES STUDIED BY MEANS OF AFFINITY ELECTROPHORESIS

V. ČEŘOVSKÝ and M. TICHÁ*

Department of Biochemistry, Charles University, Albertov 2030, 128 40 Prague 2 (Czechoslovakia)

J. TURKOVÁ

Institute of Organic Chemistry and Biochemistry, Czechoslovak Academy of Sciences, 166 10 Prague 6 (Czechoslovakia)

and

J. LABSKÝ

Institute of Macromolecular Chemistry, Czechoslovak Academy of Sciences, 162 06 Prague 6 (Czechoslovakia)

(Received January 28th, 1980)

SUMMARY

The strength of the interaction of trypsin with immobilized *p*-aminobenzamidine derives was studied by affinity electrophoresis on polyacrylamide gel in Tris–diethylbarbituric acid buffer (pH 8). *p*-Aminobenzamidine was coupled to two kinds of soluble macromolecular carrier: (i) periodate-oxidized Dextran T-500 and (ii) a synthetic copolymer of N-(2-hydroxypropyl)methacrylamide and 4-nitrophenyl esters of 6-(methacroyl)aminohexanoic acid. The enzyme inhibitor was attached to the periodate oxidized dextran either directly or through glycine, 6-aminohexanoic acid or 12-aminododecanoic acid spacer. The strength of the interaction of trypsin with immobilized *p*-aminobenzamidine did not depend on the type of macromolecular carrier that the ligand was bound to but it did depend on the length of the spacer arm. The dissociation constants of the trypsin–immobilized *p*-aminobenzamidine complexes decreased with increasing length of the spacer arm.

INTRODUCTION

Affinity electrophoresis is a type of electrophoretic separation of proteins based on their different affinities to ligands immobilized in the separating gel. This technique is convenient for the quantitative study of interactions of proteins with immobilized and free ligands. So far, affinity electrophoresis in polyacrylamide gels has been used for the study of interactions of phosphorylases with glycogen[1,2], lectins[3–5], enzymes[6] and antibodies[7] with immobilized and free sugars and some enzymes with Blue Dextran[8].

Using this method, the ligand in question can be coupled with dextran or other

0021-9673/80/0000–0000/$ 02.25

high-molecular-weight water-soluble polymers, and the bound ligand is added to the polymerization mixture used for the preparation of the polyacrylamide gel. Affinity electrophoresis of proteins interacting with Gibacron Blue reported in a previous paper[8] was the first example of the application of this method.

In this work the applicability of affinity electrophoresis for the quantitative study of the interactions of trypsin with its immobilized inhibitor, *p*-aminobenzamidine (PAB), was studied. Two kinds of macromolecular carrier of this ligand were used: periodate-oxidized Dextran T-500 and a synthetic copolymer of N-(2-hydroxypropyl)methacrylamide and 4-nitrophenyl esters of 6-(methacroyl)aminohexanoic acid.

EXPERIMENTAL

Lyophilized trypsin was supplied by Léčiva (Dolní Měcholupy, Czechoslovakia); the activity was determined using benzoyl-L-arginine-*p*-nitroanilide as a substrate according to Erlanger *et al.*[9].

PAB was purchased from Serva (Heidelberg, G.F.R.), Dextran T-500 (molecular weight *ca.* 500,000) from Pharmacia (Uppsala, Sweden) and 1-cyclohexyl-3-(2-morpholinoethyl)carbodiimide metho-*p*-toluenesulphonate from Fluka (Buchs, Switzerland).

Polyacrylamide gel electrophoresis was performed using the apparatus designed by Davis[10] in Tris–diethylbarbituric acid buffer (pH 8.0)[11] or in an acidic buffer system (pH 3.8) as described by Reisfeld *et al.*[12] omitting the large pore gel layers.

Protein samples (50 μg) in 25% glycerol solution (20 μl) were applied per tube (5 × 75 mm). Electrophoresis in the alkaline buffer system[11] was run at 4 mA per tube towards the cathode for 2 h at room temperature. In the acidic buffer system[12] the electrophoresis was carried out at 7 mA per tube for 1.5 h. Migration distances were measured with an accuracy of $\pm$ 0.5 mm after staining with Amido Black.

Dissociation constants (K_i) of the trypsin-immobilized PAB complex were obtained by a modification of our original method[3]. The values of $1/d_0 - d$ were plotted against $1/c_i$ (where d_0 = mobility on a control gel and d = mobility on affinity gel containing a molar concentration c_i of the immobilized ligand). The straight line yields $-1/K_i$ as the intercept with the abscissa and the value of its intercept with the ordinate is $1/d_0 - D_i$ (where D_i = mobility of the enzyme–"immobilized" ligand complex), thus providing information on the degree of immobilization of the ligand[13].

Affinity gels were prepared by addition of appropriate amounts of the solution of PAB-coupled polymer to the polymerization mixture to give the required concentration (c_i) of immobilized enzyme inhibitor; c_i was chosen within the range of concentrations from $5 \cdot 10^{-5}$ to $3 \cdot 10^{-4}$ M. The PAB concentration in the polymer solution was determined spectrophotometrically at 292 nm assuming that the absorptivity of PAB did not change during immobilization.

Preparation of polymers containing coupled PAB

Periodate oxidation of Dextran T-500. To the Dextran T-500 solution (1%), sodium periodate was added to give a final concentration of 0.1 M. The oxidation proceeded at 25 °C for 1 h; the reaction mixture was exhaustively dialysed against distilled water.

Coupling of amino acids to oxidized dextran. A solution of an appropriate amino acid in 0.2 *M* borate buffer (pH 9.0) (100 mg in 20 ml of the buffer) was mixed with a 1 % solution of periodate-oxidized dextran (20 ml) and stirred at room temperature for 2 h. Then sodium borohydride (10 mg) was added in two portions within 10 min. After stirring for a further 10 min, two drops of acetone were added. The reaction mixture was dialysed exhaustively against distilled water and then lyophilized.

Coupling of PAB to oxidized dextran. A PAB solution in borate buffer (pH 9.0) (10 mg in 10 ml of the buffer) was added to a 1 % solution of the oxidized dextran (10 ml). After stirring for 2 h at room temperature, the precipitate formed was discarded and the supernatant was reduced with sodium borohydride (10 mg), which was added in several portions within 30 min. After exhaustive dialysis against distilled water, the reaction mixture was lyophilized. The content of coupled PAB in the dextran derivative was 3.9 %.

Coupling of PAB to dextran containing bound amino acid residue. Dextran coupled with the amino acid residue (100 mg) was dissolved in water (10 ml) and then PAB (10 mg) was added; the pH of the reaction mixture was maintained at 4.7 using 0.1 *N*-sodium hydroxide solution. After addition of 1-cyclohexyl-3-(2-morpholinoethyl)carbodiimide metho-*p*-toluenesulphonate (50 mg), the mixture was stirred for 20 h at room temperature, then dialysed against distilled water and lyophilized. The content of PAB in the dextran derivatives was in the range 1.6–3.4 %.

Coupling of PAB to synthetic polymers. Copolymers of the 4-nitrophenyl ester of 6-(methacroyl)aminohexanoic acid (for polymer of molecular weight 39,000) or the N-hydroxyphthalimide ester of 6-(methacroyl)aminohexanoic acid (for polymer of molecular weight 82,000) with N-(2-hydroxypropyl)methacrylamide were prepared as described by Labský and Kálal[14,15]. The molecular weight of the polymers was determined by the light-scattering method.

Coupling of PAB to these polymers was performed by heating the polymer (200 mg) with PAB (100 mg) dissolved in 3 ml of dimethyl sulphoxide in a closed vessel at 50 °C for 5 h. The resulting polymer derivative was dialysed exhaustively against 1 % acetic acid in water. The content of coupled PAB in the prepared polymers was about 3 mol. %.

RESULTS

The interaction of trypsin with immobilized PAB was studied in the alkaline Tris–diethylbarbituric acid buffer system. The alkaline buffer system used has been shown not to affect the trypsin activity in the solution. In an acidic buffer system the mobility of trypsin on any type of affinity gel was identical with that on a control gel, indicating an apparent lack of interaction of the enzyme with immobilized PAB at the low pH (3.8). This is in agreement with the pH dependence of trypsin activity.

In the Tris–diethylbarbituric acid buffer system trypsin yielded a single zone, usually accompanied by a faint zone with lower electrophoretic mobility (Fig. 1). The control gels were prepared by addition of an appropriate polymer derivative without coupled PAB, *i.e.*, derivatives substituted by the corresponding ω-amino acid. Addition of these polymer derivatives to the gels had no effect on the trypsin mobility in comparison with gels containing either no macromolecular additions or underivatized dextran or hydroxypropylmethacrylamide polymer. Thus, no "non-specific" inter-

Fig. 1. Affinity electrophoresis of trypsin on polyacrylamide gels containing hydroxypropylmethacrylamide copolymers with coupled PAB. 1, Control gel containing hydroxypropylmethacrylamide copolymer without coupled PAB ($c_i = 0$); 2 and 3, affinity gels containing hydroxypropylmethacrylamide copolymer (mol. wt. 39,000) containing coupled PAB through C_6 spacer ($c_i = 3.0 \cdot 10^{-5}$ and $1.0 \cdot 10^{-4}$ *M*); 4, affinity gel containing hydroxypropylmethacrylamide copolymer (mol. wt. 82,000) containing coupled PAB through C_6 spacer. Electrophoresis was carried out in Tris–diethylbarbituric acid buffer (pH 8.0).

action of these polymeric derivatives with trypsin was observable (Fig. 1). With dextrans substituted with ω-amino acids the trypsin zone was rather diffuse with a sharp frontal edge; the mobility of the frontal edge was identical with that observed on gels containing hydroxypropylmethacrylamide polymer derivatives or on other controls gels. Similarly, the zones on affinity gels prepared from dextran substituted by PAB bound through an amino acid spacer were diffuse with a sharp frontal edge.

TABLE I

DISSOCIATION CONSTANTS OF TRYPSIN–IMMOBILIZED *p*-AMINOBENZAMIDINE COMPLEXES

*Polymer**	K_i *(M)*
Dextran–PAB	$2.13 \cdot 10^{-3}$
Dextran–glycine–PAB	$4.71 \cdot 10^{-4}$
Dextran–6-aminohexanoic acid–PAB	$2.89 \cdot 10^{-4}$
Dextran–12-aminododecanoic acid–PAB	$1.47 \cdot 10^{-4}$
HPMA–6-aminohexanoic acid–PAB (mol. wt. 39,000)	$2.88 \cdot 10^{-4}$
HPMA–6-aminohexanoic acid–PAB (mol. wt. 82,000)	$2.67 \cdot 10^{-4}$

*PAB = *p*-aminobenzamidine; HPMA = hydroxypropylmethacrylamide copolymer

Incorporation of all of the prepared macromolecular derivatives of PAB into polyacrylamide gel caused a decrease in the electrophoretic mobility of trypsin in the alkaline Tris–diethylbarbituric acid buffer system. The decrease in electrophoretic mobility was dependent on the concentration of immobilized PAB in the gel. The dissociation constants of the trypsin-immobilized PAB complexes obtained on various types of affinity gels are given in Table I.

Clearly, the strength of the interaction of trypsin with immobilized PAB does not depend on the type of macromolecular carrier used: very similar values of K_i were obtained using the hydroxypropylmethacrylamide copolymers and periodate-oxidized dextran substituted with PAB bound through a hexamethylene spacer. On the other hand, K_i decreases with increasing spacer length.

Surprisingly, effective immobilization of PAB was achieved even with relatively low-molecular-weight hydroxypropylmethacrylamide copolymer derivatives; a negligible mobility of D_i of the enzyme complex with immobilized ligand is obtained from the $1/d_0-d$ *versus* $1/c_i$ plot (Fig. 2) for both types of polymer used. Moreover, no leakage of the polymers from the gel into the electrode buffer compartments during the electrophoresis was observable by spectrophotometric examination.

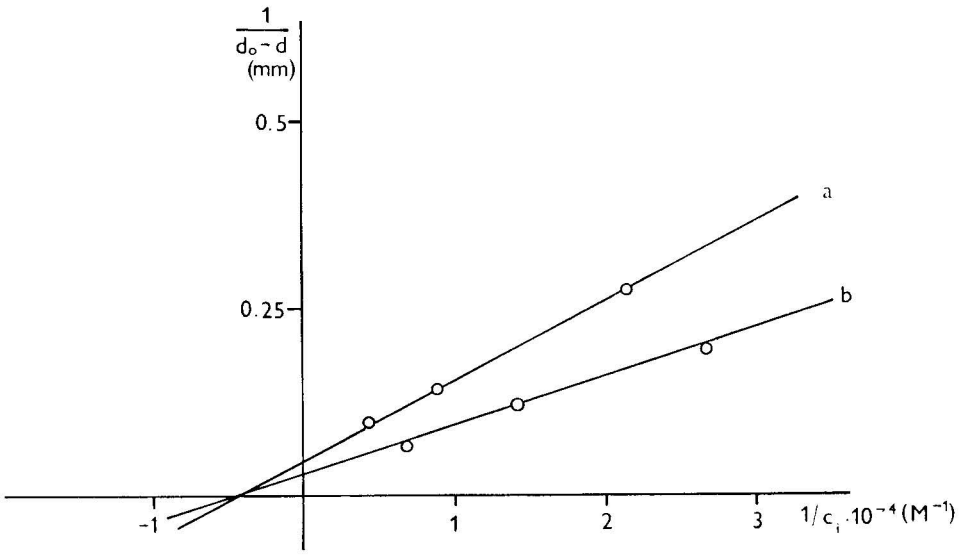

Fig. 2. Determination of dissociation constant of the trypsin–immobilized PAB complex. d_0 = electrophoretic mobility of trypsin on control gel ($c_i = 0$); d = electrophoretic mobility of trypsin on affinity gels containing immobilized PAB; c_i = concentration of immobilized PAB in affinity gels. (a) PAB coupled to periodate-oxidized dextran through 6-aminohexanoic acid residue (Dex–C_6–PAB); (b) PAB coupled to hydroxypropylmethacrylamide copolymer through 6-aminohexanoic acid residue (HPMA–C_6–PAB)

DISCUSSION

The results demonstrate that affinity electrophoresis can be used for the quantitative study of the interaction of trypsin with immobilized inhibitors. This technique seems to be a convenient tool for rapid and simple comparisons of the

effects of carrier macromolecules and spacer arms on the strength of an interaction of an enzyme with an immobilized ligand.

The increase in strength of the interaction of an enzyme with an immobilized ligand with increasing spacer length is a general phenomenon observed in affinity chromatographic experiments, and can be explained either by an improved steric accessibility of the ligand bound through a longer spacer and/or by an interaction of the enzyme with the spacer itself[16]. In our study no non-specific interaction of trypsin with the spacer molecules coupled to the polymer was observed.

It is interesting that relatively low-molecular-weight synthetic hydroxypropylmethacrylamide copolymers (molecular weight 39,000) served well for the effective immobilization of PAB. The immobility of these copolymers cannot be explained by simple entrapment in the gel network, but some kind of interaction of these copolymers with polyacrylamide gel must be assumed.

The interactions of trypsin with immobilized PAB under the conditions of affinity electrophoresis are, even in optimal cases (long spacers), approximately one order of magnitude weaker than those with free PAB (measured by affinity chromatography or from kinetic data[17]. Unfortunately, we were not able to measure the interaction of trypsin with free PAB by affinity electrophoresis because of the high electrophoretic mobility of free PAB in the buffer system used. The decrease in trypsin affinity towards immobilized PAB in comparison with free PAB (2–5-fold) has been observed by other workers[18].

In contrast to these findings, the reverse relationship between the affinity of trypsin towards immobilized and free PAB was found using quantitative affinity chromatography[17].

The weaker interaction of trypsin with immobilized PAB in comparison with free inhibitor might be explained by the possible inaccessibility of a fraction of the immobilized PAB residues to trypsin molecules. Also, the possible effect of the presence of by-products being formed in the reaction of inhibitor binding to polymer could be considered. In general, attachment of PAB to activated esters or carboxyl groups on polymers is assumed to occur simply through an amino group with amide formation[19].

Differences in the relationship of the interaction of trypsin with immobilized and free inhibitor determined by quantitative affinity chromatography[17] and by affinity electrophoresis are given by the different values of the concentration of immobilized ligand (c_i) used in the two methods. The dissociation constant of the enzyme–immobilized ligand complex (K_i) is greatly dependent on the value of c_i used for the K_i calculations. In quantitative affinity chromatography[17] the effective concentration calculated on the basis of the working capacity[20] was used, whereas in affinity electrophoresis the total concentration of immobilized ligand was employed. At present there is apparently no direct method that allows the determination of the effective concentration of immobilized ligands in affinity gels. The concentration of immobilized ligand calculated on the basis of the working capacity[20] is much lower than the total concentration of enzyme inhibitor determined analytically.

Although the values of dissociation constants of protein–immobilized ligand complexes obtained by affinity electrophoresis, as well as by affinity chromatography, are less exactly defined, their usefulness for comparative purposes is nevertheless obvious.

ACKNOWLEDGEMENT

The authors thank Dr. V. Hořejší for helpful discussions.

REFERENCES

1 R. Siepmann and H. Stegemann, *Naturwissenschaften*, 54 (1967) 116.
2 K. Takeo and S. Nakamura, *Arch. Biochem. Biophys.*, 153 (1972) 1.
3 V. Hořejší, M. Tichá and J. Kocourek, *Biochim. Biophys. Acta*, 499 (1977) 290.
4 V. Hořejší, M. Tichá and J. Kocourek, *Biochim. Biophys. Acta*, 499 (1977) 301.
5 K. Hauzer, M. Tichá, V. Hořejší and J. Kocourek, *Biochim. Biophys. Acta*, 583 (1979) 103.
6 V. Hořejší, *Biochim. Biophys. Acta*, 577 (1979) 383.
7 K. Takeo and E. A. Kabat, *J. Immunol.*, 121 (1978) 2305.
8 M. Tichá, J. Barthová and V. Hořejší, *Biochim. Biophys. Acta*, 534 (1978) 58.
9 B. F. Erlanger, N. Kokowsky and W. Cohen, *Arch. Biochem. Biophys.*, 95 (1961) 271.
10 B. J. Davis, *Ann. N.Y. Acad. Sci.*, 121 (1964) 404.
11 D. E. Williams and R. A. Reisfeld, *Ann. N.Y. Acad. Sci.*, 121 (1964) 373.
12 R. A. Reisfeld, V. S. Lewis and D. E. Williams, *Nature (London)*, 195 (1962) 281.
13 V. Hořejší, *J. Chromatogr.*, 178 (1979) 1.
14 J. Labský and J. Kálal, *Eur. J. Polym.*, 15 (1979) 167.
15 J. Labský and J. Kálal, *Eur. J. Polym.*, 15 (1979) 603.
16 P. O'Carra, S. Barry and T. Griffin, *Methods Enzymol.*, 34 (1974) 108.
17 M. Malaníková and J. Turková, *J. Solid-Phase Biochem.*, 2 (1978) 237.
18 H. F. Hixson and A. H. Nishikawa, *Methods Enzymol.*, 34 (1974) 440.
19 H. F. Hixson and A. H. Nishikawa, *Arch. Biochem. Biophys.*, 154 (1973) 501.
20 B. M. Dunn and I. M. Chaiken, *Biochemistry*, 14 (1975) 2343.

Journal of Chromatography, 194 (1980) 183–189
Elsevier Scientific Publishing Company, Amsterdam — Printed in The Netherlands

CHROM. 12,740

DETERMINATION OF THE INTERACTION OF LACTATE DEHYDROGENASE WITH HIGH-MOLECULAR-WEIGHT DERIVATIVES OF AMP BY AFFINITY ELECTROPHORESIS

M. TICHÁ and J. BARTHOVÁ*
Department of Biochemistry, Charles University, Albertov 2030, 128 40 Prague 2 (Czechoslovakia)
J. LABSKÝ
Institute of Macromolecular Chemistry, Czechoslovak Academy of Sciences, 162 06 Prague 6 (Czechoslovakia)
and
M. SEMANSKÝ
Department of Biochemistry, Charles University, Albertov 2030, 128 40 Prague 2 (Czechoslovakia)
(Received February 5th, 1980)

SUMMARY

The interaction of lactate dehydrogenase with high-molecular-weight derivatives of AMP was studied by affinity electrophoresis in an alkaline buffer system and by means of kinetic measurements. AMP was coupled to synthetic hydroxypropylmethacrylamide copolymers through glycine, 6-aminohexanoic and 12-aminododecanoic spacer arms. The values of the dissociation constants (K) of the lactate dehydrogenase isoenzymes–immobilized AMP complexes determined by affinity electrophoresis decreased with increasing length of the spacer arm. Lactate dehydrogenase was competitively inhibited by high-molecular-weight derivatives of AMP; values of the inhibition constants (K_i) also depended on the spacer arm: the longer the spacer arm the stronger was the interaction between the enzyme and the inhibitor. K_i values for high-molecular-weight derivatives of AMP were lower than those obtained for free AMP.

INTRODUCTION

Affinity electrophoresis is a type of electrophoretic separation of proteins based on their different affinities for ligands immobilized in the separating gel. This method represents a convenient tool for the quantitative study of the interaction of proteins with immobilized and free ligands.

So far, affinity electrophoresis in polyacrylamide gels has been used for the study of the interaction of phosphorylases with glycogen[1,2], lectins[3–6], α-galactosidase[7] and antibodies[8] with immobilized and free sugars and trypsin with immobilized *p*-aminobenzamidine derivatives[9]. Affinity electrophoresis in polyacrylamide gel has been also used for the qualitative and quantitative study of the interaction of several

0021-9673/80/0000–0000/$02.25

enzymes, mostly possessing a dinucleotide fold in their structure, with Blue Dextran[10]. Dissociation constants of complexes of lactate dehydrogenase with immobilized Cibacron Blue obtained using affinity electrophoresis were in good agreement with the inhibition constants of the enzyme and Blue Dextran obtained by kinetic measurements[11,12], as well as with association constants of enzyme–Cibacron Blue complexes determined using differential spectroscopy[13]. However, Blue Dextran as a group-specific affinity medium interacts both with enzymes containing a dinucleotide fold and with some other proteins[10]. The possibility of applying affinity media containing more specific ligands for the study of protein–ligand interactions is in some instances more advantageous, using both affinity chromatography and affinity electrophoresis.

For the affinity chromatography of lactate dehydrogenase, immobilized NAD or part of its molecule are currently used[14]. In this work the applicability of affinity electrophoresis for the quantitative study of interactions of the enzyme with its immobilized inhibitor was employed. The data obtained characterizing the binding parameters were compared with the inhibition constants of lactate dehydrogenase by high-molecular-weight derivatives of AMP and with those of free AMP.

EXPERIMENTAL

Bovine heart lactate dehydrogenase was prepared by the precipitation of an aqueous extract of heart muscle with ammonium sulphate to 65% saturation and, after dialysis, was lyophilized. AMP was purchased from Reanal (Budapest, Hungary).

Preparation of AMP coupled to hydroxypropylmethacrylamide copolymer

Copolymers of the 4-nitrophenyl ester of N-methacroyl derivatives of ω-amino acids were prepared as described by Labský and Kálal[15,16]. The molecular weight of the polymers was determined by the light-scattering method.

Coupling of AMP to these polymers was performed by heating the polymer (300 mg) with AMP (100 mg) in 3 ml of dimethyl sulphoxide in a closed vessel at 50 °C for 5 h. The resulting polymer derivative was dialysed exhaustively against 50% ethanol. The dialysed solution was evaporated to dryness, the residue was dissolved in methanol (2 ml) and the AMP derivative was precipitated with acetone (30 ml).

Affinity electrophoresis

Polyacrylamide gel electrophoresis was performed using the apparatus designed by Davis[17] in a discontinuous alkaline buffer system[18] according to the standard procedure (omitting large-pore gel layers).

Protein samples (80 μg) in 20% glycerol solution (20 μl) were applied to each tube (5 × 75 mm) and electrophoresis was run at 4 mA per tube for 1.5–2 h. Gels were stained specifically[19]. The migration distances of the zones of lactate dehydrogenase isoenzymes were measured with an acuracy ± 0.5 mm.

The dissociation constants (K) of the complexes of the lactate dehydrogenase isoenzymes and immobilized AMP were obtained by a modification of our original method[3,9]. The values of $1/d_0 - d$ were plotted against $1/c_i$ (d_0 = mobility on control gel, d = mobility on an affinity gel containing a molar concentration c_i of immobilized ligand). The straight line yields $-1/K$ as the intercept with the abscissa.

Affinity gels were prepared by addition of an appropriate amount of the solu-

tion of AMP-containing polymer to the polymerization mixture to give a desired concentration c_i of immobilized enzyme inhibitor; c_i was used in the range $3.2 \cdot 10^{-5}$–$6.4 \cdot 10^{-4}$ *M*.

The AMP concentration in the polymer solution was determined spectrophotometrically at 259 nm using a molar extinction coefficient of 15.4 $mmol \cdot l^{-1} \cdot cm^{-1}$.

Measurement of the rate of the reaction catalysed by lactate dehydrogenase

The determination of the rate of reaction in the direction of lactate oxidation was based on the spectrophotometric measurement of the hydrazone formed in alkaline medium by pyruvate and 2,4-dinitrophenylhydrazine. The reaction mixture contained, in 0.6 ml of 0.1 *M* Tris–acetate buffer (pH 9.1), 0.12 mmole of sodium lactate, 0.5–2 μmole of NAD and an appropriate amount of inhibitor. The reaction was started by addition of 1 μg of enzyme dissolved in 50 μl of buffer. The type of inhibition and values of the inhibition constants were determined both by the method of Lineweaver and Burk and that of Dixon.

RESULTS

Coupling of AMP to hydroxypropylmethacrylamide copolymer

By means of copolymerization of N-(2-hydroxypropyl)methacrylamide with 4-nitrophenyl esters of N-methacroyl derivatives of ω-amino acids, copolymers were obtained, in which the content of reactive 4-nitrophenyl esters was about 3 mole% (Fig. 1, $n = 1, 5, 11$; R = 4-nitrophenyl residue). The molecular weight of the prepared copolymers was 37,000 for $n = 5$ and 11 and 42,000 for $n = 1$.

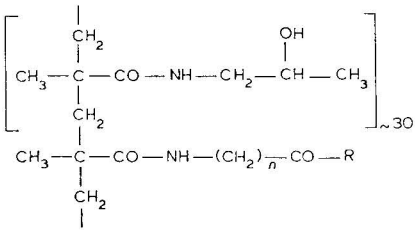

Fig. 1. Structure of AMP derivatives. R: (A) AMP immobilized through the 6-amino group of adenine; (B) $-NH(CH_2)_5CH_3$.

For coupling of AMP to soluble polymers, the reaction of 4-nitrophenyl esters with the 6-amino group of AMP was employed. AMP was bound to the polymer through different spacer arms (Fig. 1, R = A, $n = 1, 5, 11$). The same reaction was used for the preparation of polymer containing coupled hexylamine (Fig. 1, R = B, $n = 5$).

Affinity electrophoresis

The addition of hydroxypropylmethacrylamide copolymers containing coupled AMP to polyacrylamide gels caused a decrease in the electrophoretic mobility of lactate dehydrogenase isoenzymes in comparison with control gels. The decrease in electrophoretic mobility is dependent on the concentration of immobilized AMP in the polyacrylamide gels.

The control gels were prepared by an addition of hydroxypropylmethacrylate copolymer containing no AMP to polyacrylamide gels. The presence of the copolymer without a ligand did not affect the mobility of lactate dehydrogenase isoenzymes, indicating no "non-specific" interaction of the polymer with the enzyme. To eliminate the possible effect of interaction of lactate dehydrogenase with the spacer arms, hydroxypropylmethacrylamide copolymer containing coupled hexylamine was tested. The presence of this alkyl polymer derivative in polyacrylamide gel in the same concentration as the polymer AMP derivatives did not affect the electrophoretic mobility of lactate dehydrogenase isoenzymes under the experimental conditions. Similar results were obtained with the alkyl derivatives of dextran which were prepared according to Nakamura *et al.*[20], used for the detection of hydrophobic interactions in the case of lactate dehydrogenase[21].

In the preparation of bovine heart lactate dehydrogenase, three isoenzymes were detected, which differ slightly in their interaction with immobilized AMP. The apparent dissociation constants of lactate dehydrogenase–immobilized AMP complexes calculated from the dependence of the electrophoretic mobility on AMP concentration are given in Table I.

TABLE I

DISSOCIATION CONSTANTS OF LACTATE DEHYDROGENASE ISOENZYMES AND IMMOBILIZED AMP COMPLEXES DETERMINED BY MEANS OF AFFINITY ELECTROPHORESIS

*Polymer**	*K(M)*		
	Isoenzyme 1	*Isoenzyme 2*	*Isoenzyme 3*
HPMA		No interaction observed	
HPMA-C_6-hexyl		No interaction observed	
HPMA-C_2-AMP		Weak interaction	
HPMA-C_6-AMP	$2.7 \cdot 10^{-3}$	$2.3 \cdot 10^{-3}$	$1.9 \cdot 10^{-3}$
HPMA-C_{12}-AMP	$3.9 \cdot 10^{-3}$	$3.7 \cdot 10^{-3}$	$2.7 \cdot 10^{-3}$

*HPMA = hydroxypropylmethacrylate polymer; C_2 = glycine residue; C_6 = 6-aminohexanoic acid residue; C_{12} = 12-aminododecanoic acid residue.

Kinetic measurement of inhibition of lactate dehydrogenase by AMP and its high-molecular-weight derivatives.

Free AMP and AMP coupled to hydroxypropylmethacrylamide copolymer through spacer arms of different length were found to decrease the rate of the reaction catalysed by lactate dehydrogenase from bovine heart muscle. The dependence of the reaction rate either on the concentration of coenzyme (NAD) or on the concentration of inhibitor indicated that all derivatives of AMP as well as free AMP acted as competitive inhibitors to coenzyme (Fig. 2). From these dependences the values of the inhibition constants were calculated (Table II). As can be seen, all high-molecular-weight derivatives of AMP were characterized by a higher affinity to the enzyme than free AMP; values of the inhibition constants were one order of magnitude lower for high-molecular-weight derivatives than for free AMP. Values of the inhibition constants depended on the length of the spacer arm. The lowest affinity of the enzyme was observed with the shortest spacer arm. The rate of the enzyme reaction was not influen-

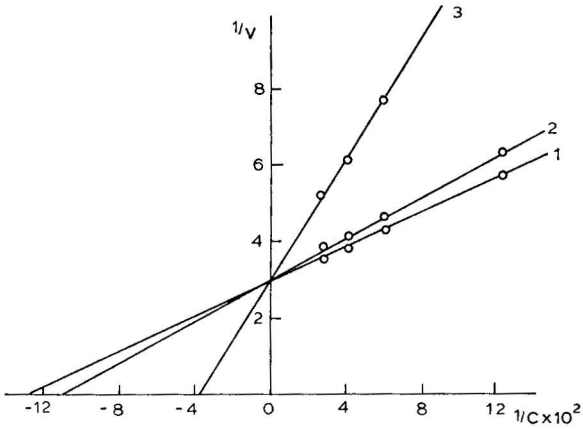

Fig. 2. Determination of inhibition constants for bovine heart lactate dehydrogenase and derivatives of AMP. 1, No inhibition; 2, inhibition by free AMP ($5.7 \cdot 10^{-4}$ *M*); 3, inhibition by HPMA-C_6-AMP (concentration of coupled AMP, $5 \cdot 10^{-4}$ *M*). *C* = concentration of NAD (*M*); *V* = rate of reaction (in International Units).

TABLE II

INHIBITION OF LACTATE DEHYDROGENASE FROM BOVINE HEART MUSCLE BY AMP AND ITS HIGH-MOLECULAR-WEIGHT DERIVATIVES

Values of K_i determined from kinetic measurements.

*Inhibitor**	K_i *(M)*
AMP	$5.4 \cdot 10^{-3}$
HPMA-C_2-AMP	$5.9 \cdot 10^{-3}$
HPMA-C_6-AMP	$2.0 \cdot 10^{-4}$
HPMA-C_{12}-AMP	$1.0 \cdot 10^{-4}$
HPMA	No inhibition
HPMA-C_6-hexyl	No inhibition

*HPMA = hydroxypropylmethacrylate polymer; C_2 = glycine residue; C_6 = 6-aminohexanoic acid residue; C_{12} = 12-aminododecanoic acid residue.

ced by hydroxypropylmethacrylamide copolymer alone, or by this copolymer containing coupled hexyl residues.

DISCUSSION

The results show that the strength of the interaction of lactate dehydrogenase with derivatives of AMP increased with increasing spacer arm length from C_2 to C_6, whereas almost no difference was observed between C_6 and C_{12} spacer arms. These observation are in a good agreement with the results of Hipwell *et al.*[22] on the affinity chromatography of lactate dehydrogenase on homologous series of immobilized N^6-aminoalkyl-AMP. This phenomenon could be explained by an improved steric accessibility of the ligand bound through a longer spacer arm and/or by the fact that the spacer arm contributes to the binding of the enzyme. However, our results have shown that high-molecular-weight derivatives containing coupled hexyl residues without AMP do not interact with the enzyme studied. The contribution of the spacer

arm to the binding of lactate dehydrogenase to AMP derivatives was also suggested by Hipwell *et al.*[22]

In a previous paper[10] we described the application of affinity electrophoresis to a quantitative study of the interaction of lactate dehydrogenase isoenzymes with immobilized Cibacron Blue. Dissociation constants of complexes of lactate dehydrogenase and immobilized Cibacron Blue determined by affinity electrophoresis agreed satisfactorily with values of inhibition constants (K_i) determined kinetically[11] and also with dissociation constants measured spectrophotometrically[13]. In the case of high-molecular-weight derivatives of AMP used in the present work, values of the dissociation constants of enzyme–immobilized inhibitor complexes determined by means of affinity electrophoresis are in good agreement with the constants of inhibition of lactate dehydrogenase by free AMP (our results and ref. 23) determined kinetically. However, interesting data were obtained from kinetic measurements of the inhibition of lactate dehydrogenase by AMP derivatives coupled to hydroxypropylmethacrylamide copolymer. In this instance inhibition constants were about by one order of magnitude lower than with free AMP. This fact could be explained by non-biospecific interference of the spacer arms and/or of hydroxypropylmethacrylamide copolymer, which could contribute to the binding of the inhibitor to the enzyme, even though hydroxypropylmethacrylamide copolymer alone or with a coupled spacer arm does not interact with the protein and does not affect its enzyme activity. Such non-biospecific contributions of the spacer arm are known to be affected by the nature of a spacer arm and by the composition of buffer solution used, mainly by ionic strength[24].

The difference between the dissociation constants of enzyme–immobilized inhibitor complexes determined by affinity electrophoresis and constants of inhibition of the lactate dehydrogenase activity by high-molecular-weight derivatives of the inhibitor might be attributed to several factors: (i) the conditions for the determination of inhibition constants by kinetic measurements differed from those in the determination of dissociation constants by affinity electrophoresis. (ii) Kinetic measurements of inhibition constants were performed in the presence of the substrate lactate, whereas in affinity electrophoresis only the interaction of lactate dehydrogenase with immobilized AMP was followed; the presence of the second substrate might influence the binding of inhibitor. Analogous phenomena were described for the precipitation of lactate dehydrogenase with a bifunctional NAD coupound; affinity precipitation of the enzyme occurred only in the presence of substrate[25]. This fact is also used for the specific elution of lactate dehydrogenase from an affinity column[14]. (iii) Interaction of lactate dehydrogenase with immobilized AMP under the conditions of affinity electrophoresis could be stronger than with free AMP, as was determined from kinetic measurements; however, higher values of the dissociation constants of enzyme–immobilized AMP complexes in comparison with inhibition constants determined kinetically might be also caused by the lower effective concentration of immobilized ligand in polyacrylamide gel than the analytical concentration used for the calculation of the dissociation constants.

REFERENCES

1 R. Siepmann and H. Stegemann, *Naturwissenschaften*, 54 (1967) 116.
2 K. Takeo and S. Nakamura, *Arch. Biochem. Biophys.*, 153 (1972) 1.

3 V. Hořejší, M. Tichá and J. Kocourek, *Biochim. Biophys Acta*, 499 (1977) 290.
4 V. Hořejší, M. Tichá and J. Kocourek, *Biochim. Biophys. Acta*, 499 (1977) 301.
5 K. Hauzer, M. Tichá, V. Hořejší and J. Kocourek, *Biochim. Biophys. Acta*, 583 (1979) 103.
6 V. Čeřovský, M. Tichá, V. Hořejší and J. Kocourek, *J. Biochem. Biophys. Methods*, in press.
7 V. Hořejší, *Biochim. Biophys. Acta*, 577 (1979) 383.
8 K. Takeo and E. A. Kabat, *J. Immunol.*, 121 (1978) 2305.
9 V. Čeřovský, M. Tichá, J. Turková and J. Labský, *J. Chromatogr.*, 194 (1980) 175.
10 M. Tichá, J. Barthová and V. Hořejší, *Biochim. Biophys. Acta*, 534 (1978) 58.
11 J. E. Wilson, *Biochem. Biophys. Res. Commun.*, 72 (1976) 816.
12 E. Stellwagen, R. Cass, S. T. Thompson and M. Woody, *Nature* (London), 257 (1975) 716.
13 S. T. Thompson and E. Stellwagen, *Proc. Nat. Acad. Sci. U.S.*, 73 (1976) 361.
14 K. Mosbach, *Methods Enzymol.*, 34B (1974) 229.
15 J. Labský and J. Kálal, *Eur. Polym. J.*, 15 (1979) 167.
16 J. Labský and J. Kálal, *Eur. Polym. J.*, 15 (1979) 603.
17 B. J. Davis, *Ann. N.Y. Acad. Sci.*, 121 (1964) 404.
18 F. C. Steward, R. F. Lyndon, and J. T. Barber, *Amer. J. Bot.*, 52 (1965) 155.
19 J. King, *Can. J. Bot.*, 48 (1970) 533.
20 K. Nakamura, A. Kuwahara and K. Takeo, *J. Chromatogr.*, 171 (1979) 89.
21 J. Barthová and M. Tichá, unpublished results.
22 M. C. Hipwell, M. J. Harvey and P. D. G. Dean, *FEBS Lett.*, 42 (1974) 355.
23 A. McPherson, *J. Mol. Biol.*, 51 (1970) 39.
24 P. O'Carra, S. Barry and T. Griffin, *FEBS Lett.*, 43 (1974) 169.
25 P. O. Larsson and K. Mosbach, *FEBS Lett.*, 98 (1979) 333.

Journal of Chromatography, 194 (1980) 191–197
Elsevier Scientific Publishing Company, Amsterdam — Printed in The Netherlands

CHROM. 12,745

GAS CHROMATOGRAPHIC ANALYSIS OF ALIPHATIC AND AROMATIC ALDEHYDES AS TRIMETHYLSILYLATED DITHIOACETALS OF 2-MERCAPTOETHANOL

SUSUMU HONDA*, NORIO TANIMITSU and KAZUAKI KAKEHI
Faculty of Pharmaceutical Sciences, Kinki University, Kowakae, Higashi-osaka (Japan)
(First received January 3rd, 1980; revised manuscript received February 6th, 1980)

SUMMARY

A new general method has been devised for the gas chromatographic analysis of aldehydes as their trimethylsilylated dithioacetal derivatives of 2-mercaptoethanol. The sequential derivatization reactions of mercaptalation and trimethylsilylation allow rapid and convenient analysis of both aliphatic and aromatic aldehydes with high accuracy and precision. A few applications of this method to products of enzymatic reactions are presented.

INTRODUCTION

Direct gas chromatography (GC) may be unprofitable for the analysis of aldehydes because of tailing of peaks and instability of samples. Recently we reported a convenient method for gas chromatographic analysis of monosaccharides[1,2] and conjugated aldehydes in products of periodate oxidation of carbohydrates[3,4] as their trimethylsilylated diethyl dithioacetals. This method gives a single peak for each aldehyde, unlike the hydrazone and oxime methods[5] which give dual peaks of steric isomers, and the derivatization procedure is simple and rapid. Further, the flame photometric detector is selectively sensitive to the dithioacetal derivatives. However, this method is not suitable for the analysis of aldehydes of small molecules, since the derivatives are extremely volatile, and ethanethiol has a pungent odour. This paper describes a new general method for the analysis of aliphatic and aromatic aldehydes by use of 2-mercaptoethanol, and odourless mercaptan.

EXPERIMENTAL

Materials

An extra pure sample of 2-mercaptoethanol was purchased from Tokyo Kasei Kogyo (Tokyo, Japan). The authentic sample of the dithioacetal of *n*-octanal was prepared by mercaptalation of *n*-octanal with 2-mercaptoethanol in the presence of trifluoroacetic acid, followed by purification of the crude product on a column of silica gel with diethyl ether–*n*-hexane (1:1, v/v). Proton magnetic resonance (PMR)

0021-9673/80/0000–0000/$02.25

data ($CDCl_3$,δ) in ppm: 0.90 (triplet-like, $-CH_3$), 1.3 (multiplet, $C-CH_2-C \times 6$), 2.55 (broadened singlet, $OH \times 2$), 2.83 (triplet, $-S-CH_2-$), 2.87 (triplet, $-S-CH_2-$), 3.80 (triplet, $-CH_2-OH \times 2$), 3.8 (triplet-like, -C-CH-S). The refined sample as its trimethylsilyl derivative gave a single peak on GC. All other chemicals, solvents and samples of aldehydes were of the highest grade commercially available. The specimens of alcohol dehydrogenase (yeast, 322 U/mg) and monoamine oxidase (beef plasma, 25 U/mg) were obtained from Sigma (St. Louis, MO, U.S.A.) and Miles Labs. (Elkhart, IN, U.S.A.), respectively.

Apparatus

Gas chromatography was performed on a Shimadzu 4BMPF instrument equipped with a flame ionization detector (FID). The flow-rate of the carrier gas (nitrogen) was 50 ml/min.

Recommended procedure for the analysis of aldehydes

Dissolve a sample of an aldehyde or a mixture of aldehydes (total amount, 10^{-8}–10^{-6} mole) in 1,2-dichloroethane (50 μl). Add a 4:1 (v/v) mixture (20 μl) of 2-mercaptoethanol and trifluoroacetic acid, and keep the mixture for 30 min at 25°C. Add a pyridine solution (50 μl) of D-glucitol (internal standard), hexamethyldisilazane (100 μl) and chlorotrimethylsilane (50 μl) in this order, and incubate the mixture for 30 min at 50°C with occasional shaking. Centrigufe the mixture, and analyze the aldehydes by injecting the supernatant (1–5 μl) to the gas chromatography column. Standard column conditions are as follows: column, 3% OV-1 on Chromosorb W (2 m, glass); column temperature, 180°C (aliphatic aldehydes) or 210°C (aromatic aldehydes); flow-rate of carrier gas (nitrogen), 50 ml/min; detector FID (240°C).

Enzymatic oxidation of alcohols with dehydrogenase

A 0.015 *M* nicotine–adenine dinucleotide (1.5 ml), 0.05 *M* pyrophosphate buffer (pH 8.5, 1.3 ml) and a solution (0.1 ml) of alcohol dehydrogenase in 0.01 *M* phosphate buffer (pH 7.5) were added to a sample solution (0.1 ml) of ethanol or to a mixture of alcohols, and the reaction mixture was kept for 20 min at 25°C. Then the mixture was extracted with 1,2-dichloroethane (0.5 ml), and a 50 μl-portion of the organic layer was subjected to aldehyde analysis as described above.

Assay of the activity of monoamine oxidase

An aqueous solution (0.1 ml) of a mixture of substrate amines (each 10^{-5} mole) and 0.2 *M* phosphate buffer (pH 7.4, 2.80 ml) were added to a sample solution (0.1 ml) of monoamine oxidase, and the mixture was kept for 1 h at 25°C. Then the mixture was extracted with 1,2-dichloroethane (500 μl), and a 50 μl-portion of the organic layer was subjected to aldehyde analysis as described above.

RESULTS AND DISCUSSION

Table I gives the retention times of the trimethylsilylated dithioacetals of straight-chain aliphatic aldehydes, measured on various kinds of liquid phase. These derivatives were well separated on all the silicone phases at the given temperatures in *ca.* 1.5 h. The polyethylene glycol succinate column, however, gave

TABLE I

RETENTION TIMES OF THE DERIVATIVES OF STRAIGHT-CHAIN ALIPHATIC ALDEHYDES

Aldehyde	*Retention time (min)*			
	3% OV-1, 2 m, 180°C	*3% OV-17, 2 m, 200°C*	*10% SF-96, 2 m, 200°C*	*15% PEG succinate, 2 m, 145°C*
Methanal	—	7.56	—	—
Ethanal	6.81	7.69	7.35	11.48
Propanal	8.10	9.04	9.26	12.37
n-Butanal	10.57	11.26	11.72	14.37
n-Pentanal	14.47	14.89	15.54	18.36
n-Hexanal	19.94	20.87	21.41	24.14
n-Heptanal	29.24	28.33	29.53	33.13
n-Octanal	40.93	39.84	41.07	46.14
n-Nonanal	61.41	56.32	58.01	64.55
n-Decanal	88.00	79.44	81.98	90.32

broadened peaks, especially for the derivatives of higher aldehydes, and this tendency was common to other polar phases.

Fig. 1 shows the relationship between the number (n) of carbon atoms and the logarithm of the retention time (t'_R) adjusted for that of the solvent (1,2-dichloroethane). Good linearity was observed for all the liquid phases for n values between 4 and 10.

The dithioacetal derivatives of aromatic aldehydes were also well separated on silicone columns. Table II gives an example of separation of the derivatives of several substituted benzaldehydes, together with those of phenylacetaldehyde and cinnamaldehyde.

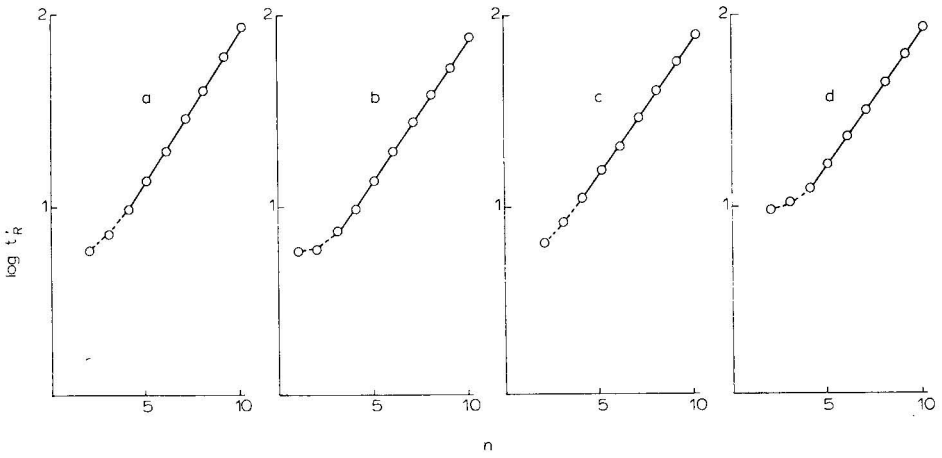

Fig. 1. Relationship between the number (n) of carbon atoms and the adjusted retention time (t'_R) for straight-chain aliphatic aldehydes. Phases: a = 3% silicone OV-1; b = 3% silicone OV-17; c = 10% silicone SF-96; d = 15% polyethylene glycol succinate.

TABLE II

RETENTION TIMES OF THE DERIVATIVES OF SELECTED AROMATIC ALDEHYDES

Aldehyde		*Retention time (min) on 3% OV-1, 2 m, 210°C*
Benzaldehyde		8.21
Substituted benzaldehyde		
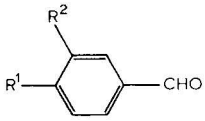	$R^1 = OH, R^2 = H$	21.43
	$R^1 = R^2 = OH$	31.93
	$R^1 = OCH_3, R^2 = OH$	28.16
	$R^1 = R^2 = OCH_3$	24.54
Phenylacetaldehyde		10.65
Cinnamaldehyde		18.99

The derivatization procedure of the present method consists of the mercaptalation process with 2-mercaptoethanol and the subsequent trimethylsilylation process.

$$CH_3(CH_2)_6CHO \rightarrow CH_3(CH_2)_6CH(SCH_2CH_2OH)_2 \quad (1)$$

$$CH_3(CH_2)_6CH(SCH_2CH_2OH)_2 \rightarrow CH_3(CH_2)_6CH(SCH_2CH_2OTMS)_2 \quad (2)$$

The first process is affected by various factors. Therefore, an optimization study was performed by using *n*-octanal as the model aldehyde. The PMR spectrum of the product of mercaptalation gave a methine proton at *ca.* 3.8 ppm, indicative of the presence of a dithioacetal bond. An acetal bond would give its methine proton at lower field at *ca.* 5 ppm. This evidence confirms that the product was the dithioacetal, but not the acetal, of *n*-octanal. The methylene protons adjacent to the sulphur atom are split into a couple of two-proton triplets at 3.83 and 3.87 ppm, presumably due to restricted rotation of the S–CH_2 bond.

The dithioacetal formed gave a single GC peak of presumably the bis(trimethylsilyl) ether of the dithioacetal on treatment with chlorotrimethylsilane and hexamethyldisilazane in pyridine. Table III shows the influence of reaction solvent on mercaptalation, expressed as the yield of the trimethylsilylated dithioacetal

TABLE III

INFLUENCE OF REACTION SOLVENT ON THE MERCAPTALATION OF *n*-OCTANAL

Solvent	*Yield (%) of the dithioacetal derivative*
Diethyl ether	0.0
Diisopropyl ether	0.7
Ethyl acetate	25.1
Carbon tetrachloride	46.7
Toluene	47.2
Chloroform	47.8
Benzene	51.7
n-Hexane	88.6
1,2-Dichloroethane	100.6

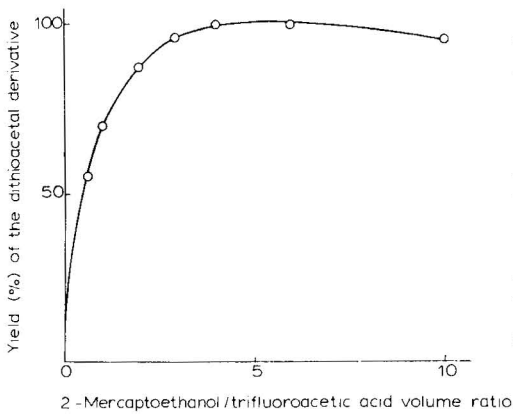

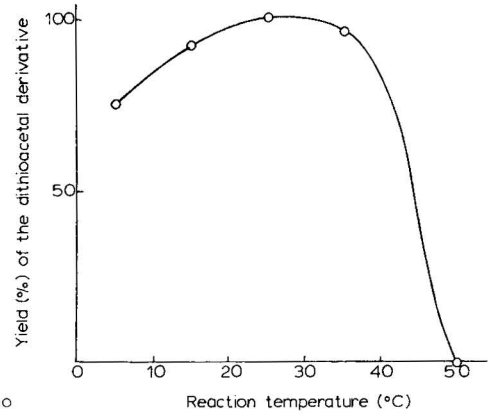

Fig. 2. Influence of the 2-mercaptoethanol: trifluoroacetic acid volume ratio on the yield of the derivative of *n*-octanal. Reaction temperature, 25°C; reaction time, 30 min.

Fig. 3. Effect of reaction temperature on the yield of the dithioacetal derivative of *n*-octanal. Volume ratio of 2-mercaptoethanol to trifluoroacetic acid, 4; reaction time, 30 min.

derivative. 1,2-Dichloroethane gave almost quantitative yields of the dithioacetal derivative, whereas other solvents gave lower yields. The difference in yield among solvents is probably due to the difference in affinity of solvents toward the proton supplied by the acid catalyst. The most suitable catalyst proved to be trifluoroacetic acid; similar results were obtained for the determination of monosaccharides[1,2] and the aldehydes in products of periodate oxidation of carbohydrates[3,4]. The yield of the dithioacetal derivative increased with increasing volume ratio of 2-mercaptoethanol to trifluoroacetic acid, giving a quantitative yield between the volume ratios of 4 and 10, as shown in Fig. 2. Fig. 3 shows the effect of reaction temperature on mercaptalation. The maximal yield of the dithioacetal derivative was obtained at 25°C. Lower and higher temperatures were disadvantageous for dithioacetal formation. Fig. 4 shows the course of mercaptalation of *n*-octanal. The reaction was complete in 30 min at 25°C.

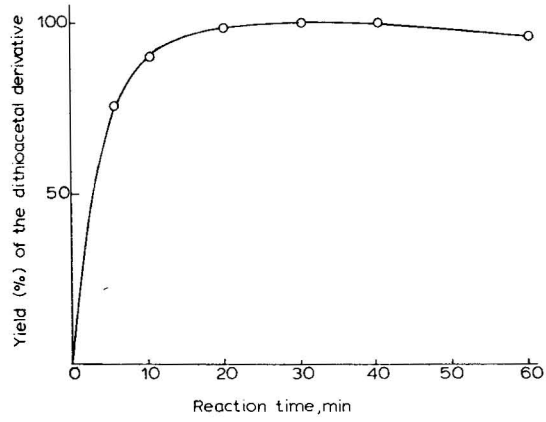

Fig. 4. Course of mercaptalation of *n*-octanal. Volume ratio of 2-mercaptoethanol to trifluoroacetic acid, 4; reaction temperature, 25°C.

On the basis of the results mentioned above, a recommended procedure was devised for the determination of aliphatic aldehydes and is described in the Experimental section. The analysis time was only 2 h, including the GC operation, significantly shorter than that required for the acetalation method[6]. Under the conditions described above, the calibration curve of *n*-octanal was linear for sample amounts ranging from 10^{-8} to 10^{-6} mole, and the coefficient of variation was 2.2% ($n = 10$) at the 10^{-7} mole level. Similar results were obtained for other aliphatic aldehydes. For aromatic aldehydes, the same reaction conditions were applicable, as substantiated by the average yield (99.6%) of the dithioacetal derivative of *p*-hydroxybenzaldehyde. Its calibration curve was also linear in the same range of sample amount.

Since the dithioacetal method thus developed is simple and rapid, it is widely applicable to both aliphatic and aromatic aldehydes, and suitable especially for those from biochemical sources. Fig. 5 shows an example of its application to the products of enzymatic reaction of alcohols with yeast alcohol dehydrogenase. Under the specified conditions, the product from a mixture of ethanol, *n*-propanol and *n*-butanol contained all the corresponding aldehydes, whose derivatives were well separated, as shown in Fig. 5a. The yield of each aldehyde increased, giving parabolic curves with increasing reaction time, and the yield increased with decrease in the number of carbon atoms (Fig. 5b). The calibration curve of ethanol obtained for the reaction time of 20 min was linear in the range of sample concentration, 0.1–1.5%. The use of a flame photometric detector will allow the determination of lower concentrations.

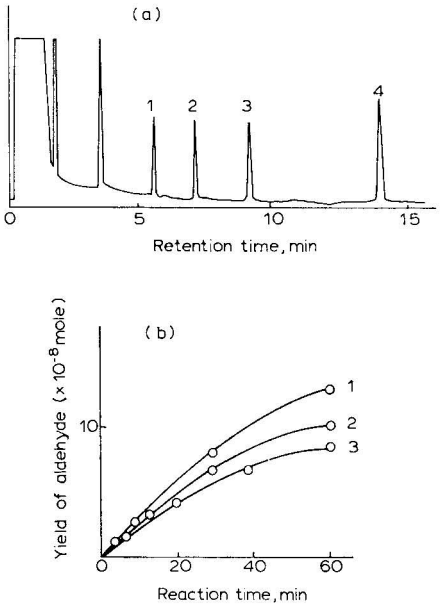

Fig. 5. a, Gas chromatogram for the products of enzymatic oxidation of a mixture of ethanol, *n*-propanol and *n*-butanol with yeast alcohol dehydrogenase. Peaks 1, 2, 3 and 4 are assigned to the trimethyl silylated dithioacetals of ethanal, propanal and *n*-butanal and trimethylsilylated D-glucitol (internal standard), respectively. b, Course of formation of aldehydes from an equimolar mixture of ethanol (1), *n*-propanol (2) and *n*-butanol (3).

Fig. 6 shows another example of application. Monoamine oxidase converts various bioamines into corresponding aldehydes. Based on substrate preferences, it has been claimed that there are two types of isozyme, monoamine oxidase A and B. The former type has a high affinity for serotonin and norepinephrine, while the latter is specific to benzylamine and phenylethylamine. Therefore, analysis of the products from a mixture of these amines will serve for classification of the type of isozyme and estimation of the enzyme activity. In the experiment reported herein, which used a mixture of these four bioamines as substrate, only the derivatives of benzaldehyde and phenylacetaldehyde were detected; no other aldehyde derivatives were found even at elevated temperatures. This evidence indicates that the enzyme used belonged to the B-type monoamine oxidase. The amounts of the aldehyde derivatives were also consistent with the activity described for this preparation.

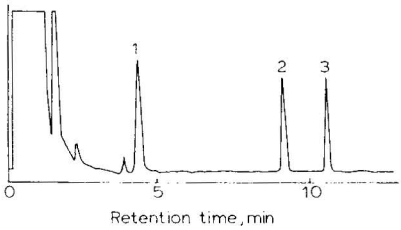

Fig. 6. Gas chromatogram for the products of enzymatic oxidation of a mixture of benzylamine, phenylethylamine, serotonin and norepinephrine with beef plasma monoamine oxidase. Peaks 1, 2 and 3 are assigned to trimethylsilylated D-glucitol (internal standard), the trimethylsilylated dithioacetal of benzaldehyde and the trimethylsilylated dithioacetal of phenylacetaldehyde, respectively.

The foregoing results demonstrate that the dithioacetal method described is useful for the determination of biochemical compounds related to aldehydes. Further applications of this method will be described elsewhere.

REFERENCES

1 S. Honda, N. Yamauchi and K. Kakehi, *J. Chromatogr.*, 169 (1979) 287.
2 S. Honda, K. Kakehi and K. Okada, *J. Chromatogr.*, 176 (1979) 367.
3 S. Honda, Y. Fukuhara and K. Kakehi, *Anal. Chem.*, 50 (1978) 55.
4 S. Honda, Y. Takai and K. Kakehi, *Anal. Chim. Acta*, 105 (1979) 153.
5 S. Honda, K. Kisaka and K. Kakehi, unpublished results.
6 G. M. Gray, *J. Chromatogr.*, 4 (1960) 52.

Journal of Chromatography, 194 (1980) 199–204
Elsevier Scientific Publishing Company, Amsterdam — Printed in The Netherlands

CHROM. 12,746

PRESENCE OF SQUALANE IN URBAN AQUATIC ENVIRONMENTS

GENKI MATSUMOTO* and TAKAHISA HANYA

Department of Chemistry, Faculty of Science, Tokyo Metropolitan University, Setagaya-ku, Tokyo 158 (Japan)

(First received January 3rd, 1980; revised manuscript received February 5th, 1980)

SUMMARY

Ethyl acetate extracts of river waters and sediments, night-soil and sewage treatment plant effluents and sludges from the Tokyo area were analysed for squalane using combined gas chromatography–mass spectrometry after separation by silica gel column chromatography. Squalane was identified in all the samples studied and the concentration in river waters and sediments ranged from 0.46 to 1.7 μg/l and from 0.86 to 15 μg per g dry sediment, respectively. Squalane is presumably derived from artificial materials rather than from natural sources, with the exception of fossil fuel products.

INTRODUCTION

Much attention has been paid to isoprenoid hydrocarbons as a biological marker in various sediments ranging in age from recent to precambrian rocks and petroleum. It is well known that pristane and phytane are widely distributed in sediments and petroleum. The entire series of acyclic regular (head-to-tail linked) isoprenoid hydrocarbons from C_5 to C_{40} have also been found in petroleum[1–6]. Biological substances such as squalene(C_{30}), lycopene(C_{40}), solanesol(C_{45}) and phytyl side chain of chlorophyll have been suggested as the precursors of these regular isoprenoid alkanes[1–6]. The irregular isoprenoid hydrocarbon squalane has been found in the Soudan shale[7], an African cretaceous shale[8] and a Nigerian petroleum[4]. In the modern environment, regular isoprenoid hydrocarbons such as C_{18} (ref. 9), pristane and phytane have been found, but very little is known on the occurrence of irregular isoprenoid hydrocarbons, except for squalene, other than in living organisms. We report here the identification and estimation of squalane in river waters and sediments and some related samples collected from the Tokyo area.

EXPERIMENTAL

Apparatus

Care was taken to avoid contamination of samples, as described previously[10,11]. The gas chromatographic–mass spectrometric (GC–MS) measurements were

0021-9673/80/0000-0000/$02.25

performed using a Shimadzu LKB 9000 instrument. A silanized glass column (2 m × 3 mm I.D.) was packed with 1% silicone OV-1 on Chromosorb W AW DMCS (80–100 mesh). The flow-rate of carrier gas (helium) was 30 ml/min. The column temperature was programmed from 100°C to 285°C at 6°C/min. The injection block, molecular separator and ion source were maintained at 290, 300 and 330°C, respectively. The mass fragmentogram was recorded for the mass number *m/e* 57 ($C_4H_9^+$) at 20 eV. Mass spectra were taken at 70 eV with an accelerator voltage of 3.5 kV.

Chemicals

Chemicals were used after treatment as described in previously[10,11]. Authentic squalane and squalene were purchased from Wako (Osaka, Japan).

Samples

During 1975–1977, water samples were collected from the downstream (Chohfu) of Tama river and its tributaries (Ohkuri and Nogawa rivers) and Sumida river (Kototoi) in the Tokyo area, which are highly polluted by sewage[10]. Sediments were taken from the upper (Hamura) and downstreams (Chohfu and Gasu) of Tama river. F night-soil and T sewage treatment plant effluents and F night-soil and S and M sewage treatment plant sludges were collected from the Tama river basin, as possible sources of squalane in the rivers.

Water samples were collected using a 5-l stainless-steel bucket or with a 2-l glass bottle with glass stopper. The sample was immediately acidified (pH < 2) with concentrated hydrochloric acid and stored at *ca.* 5°C until analysis. Sediments were collected with an Eckman-Berge Dredge and stored in polyethylene bags at temperatures of *ca.* 5°C or −20°C, together with sludge.

Analysis of squalane

The water sample (1.0 l) was extracted three times with ethyl acetate (200 ml, 150 ml × 2). The ethyl acetate extract was evaporated to dryness, redissolved in 50 μl benzene–ethyl acetate (1:1) and then chromatographed on a silica gel column (160 × 4 mm I.D., 100 mesh, 5% water). Two column volumes of hexane eluate (hydrocarbon fraction) were analysed using GC–MS. The method of extraction of organic matter from sediment (sludge) is described in detail elsewhere[11,12] and will be noted here only briefly. Wet sediment or sludge (2–5 g) was extracted with ethyl acetate after saponification with 0.5 *M* potassium hydroxide in methanol. The ethyl acetate extract was analysed by the same method as the water sample.

The identification of squalane was based on the comparison of retention time and mass spectrum with that of the authentic compound. The estimation was performed by measurement of peak height on the mass fragmentogram. In addition, for *n*-alkanes, the peak height on the mass fragmentogram was calibrated with C_{16}, C_{20}, C_{24}, C_{28} and C_{36} alkanes. Based on four replicate addition experiments using authentic squalane, the recoveries of squalane for water and sediment were 85% (standard deviation, S.D. = 5.8%) and 92% (S.D. = 10%), respectively. A blank test showed that the contamination of squalane was less than 2 ng/l or 2 ng per g dry sample. Its presence does not affect the analytical results for our samples.

RESULTS

Identification

A typical mass fragmentogram of the hydrocarbon fraction obtained from the Tama river water sample is given in Fig. 1. Squalane occurs as the most prominent peak in the chromatogram, together with *n*-alkanes, pristane, phytane and an unresolved envelope of a complex mixture of hydrocarbons (UCMH) comprised of substituted naphthenic and aromatic compounds. The mass spectrum of squalane found in the river water sample is shown in Fig. 2, together with that of authentic

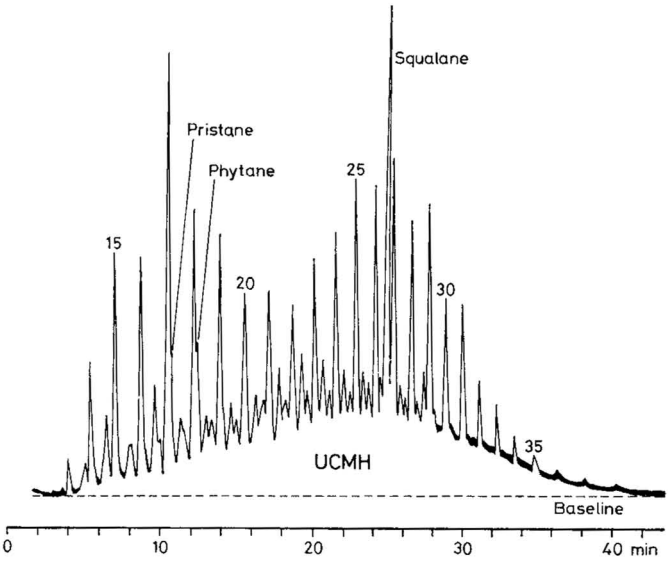

Fig. 1. Mass fragmentogram of the hydrocarbon fraction obtained from the Tama river water (Chohfu, December 21, 1977). Numbers at the peaks indicate the carbon chain length of *n*-alkanes. UCMH = Unresolved complex mixture of hydrocarbons.

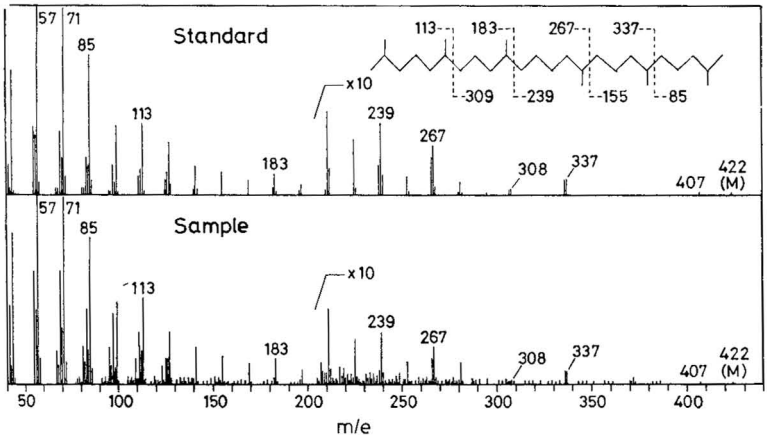

Fig. 2. Mass spectrum of squalane.

squalane. The major fragments of the sample coincide with those of authentic squalane, although there are several peaks due to UCMH.

Concentration

Squalane is found generally as the major constituent of the hydrocarbon fraction and its concentration in river waters ranges from 0.46 to 1.7 μg/l, depending upon the sampling locations (Table I). Squalane has also been identified in night-soil and sewage treatment plant effluents. In the river sediments, the concentrations of squalane range from 0.86 to 15 μg per g dry sample. Large amounts of squalane are also found in sludges.

TABLE I

SQUALANE FOUND IN URBAN AQUATIC ENVIRONMENTS

Sample	*Sampling data*	*Concn.*	*Squalane/ n-alkanes* ratio*
Water			
Tama R. (Chohfu)	Dec. 21, 1977	0.92 μg/l	0.10
Ohkuri R.	Aug. 29, 1977	0.46 μg/l	0.21
Nogawa R.	Dec. 16, 1975	1.7 μg/l	0.13
Sumida R. (Kototoi)	July 9, 1975	1.3 μg/l	0.093
F night-soil treatment plant effluent	Dec. 16, 1975	5.3 μg/l	0.35
T sewage treatment plant effluent	June 26, 1975	0.23 μg/l	0.37
Sediment and sludge			
Tama R. (Hamura)	July 6, 1977	0.86 μg/g	0.054
(Chohfu)	July 21, 1977	15 μg/g	0.26
(Gasu)	Dec. 9, 1976	4.6 μg/g	0.065
F night-soil treatment plant sludge	Nov. 9, 1976	14 μg/g	0.13
S sewage treatment plant sludge	Nov. 6, 1976	84 μg/g	0.76
M sewage treatment plant sludge	Nov. 6, 1976	26 μg/g	0.24

* Sum of the C_{15}–C_{33} contents.

DISCUSSION

Squalane is known to be present in a Nigerian crude oil but its calculated concentration is very small (2 ppm)[4]. In addition, squalane is generally not a major constituent of petroleum and petroleum products. Thus the ratio squalane/*n*-alkanes (sum of the C_{15}–C_{33} contents) is assumed to be very small. However, the ratios for river waters and sediments are considerably higher, ranging from 0.093 to 0.21 and from 0.054 to 0.26, respectively (Table I). The ratios in night-soil and sewage treatment plant effluents and sludges are similar to those of the river waters and sediments. Therefore petroleum and petroleum products can hardly be the major source of squalane. Furthermore, squalane is rarely found in living organisms, thus the most probable source of squalane in our samples seems to be due to urban activities. Squalane is widely used as a lubricant, transformer oil, ingredient of watch and chronometer oils, perfume fixative, skin lubricant, ingredient of suppositories and carrier of lipid-soluble drugs[13].

Squalene is also a possible source of squalane if subsequent biotic and/or abiotic hydrogenation occurs in the natural environment. Squalene is present in large amounts in shark liver oil and in smaller amounts (0.1–0.7%) in olive oil, wheat germ oil, rice bran oil and yeast. It is also known to be an intermediate in the biosynthesis of cholesterol. Furthermore, squalene is used as a bactericide, as an intermediate in the manufacture of pharmaceuticals, organic colouring materials, rubber chemicals, aromatics and surface active agents[13]. However, no squalene has yet been found in our water and sediment samples, although it has been isolated from surface sea-water in a coastal region[14] and from a water sample collected at Chohfu on Tame river[15]. Besides, no squalane has been detected from areas unpolluted by man, even when the organic content of the sample was extremely high[12,16]. Therefore, the contribution of squalene to the content of squalane in aquatic environments is thought to be small.

These results imply strongly that squalane is largely derived from artificial sources with the exception of petroleum products, rather than from natural sources. Squalane may be introduced to urban river waters and sediments directly and/or through night-soil and sewage treatment plants by our daily activity. Consequently, squalane in the aquatic environment is considered to be one of the indicators of human activities.

CONCLUSION

Squalane was identified in river waters and sediments, night-soil and sewage treatment plant effluents and sludges obtained from the Tokyo area. Its concentration in river waters and sediments ranged from 0.46 to 1.7 μg/l and from 0.86 to 15 μg per g dry sediment, respectively. Squalane is most likely to be derived from artificial materials, except for fossil fuel products, rather than natural sources. This analytical method is also useful for determining very low concentrations (ng/l or ng per g dry sediment) of squalane in water and sediments.

REFERENCES

1 J. G. Bendoraitis, B. L. Brown and L. S. Hepner, *Anal. Chem.*, 34 (1962) 49.
2 K. E. H. Göhring, P. A. Schenck and E. D. Engelhardt, *Nature (London)*, 215 (1967) 503.
3 J. Han and M. Calvin, *Geochim. Cosmochim. Acta*, 33 (1969) 733.
4 P. M. Gardner and E. V. Whitehead, *Geochim. Cosmochim. Acta*, 36 (1972) 259.
5 E. J. Gallegos, in T. F. Yen and G. V. Chilingarian (Editors), *Developments in Petroleum Science, Vol. 5, Oil Shale*, Elsevier, Amsterdam, 1976, p. 149.
6 J. Albaigés, J. Barbón and P. Salagre, *Tetrahedron Lett.*, (1978) 595.
7 R. B. Johns, T. Belsky, E. D. McCarthy, A. L. Burlingame, P. Haug, H. K. Schnoes, W. Richter and M. Calvin, *Geochim. Cosmochim. Acta*, 30 (1966) 1191.
8 C. Spyckerelle, P. Arpino and G. Ourisson, *Tetrahedron*, 28 (1972) 5703.
9 W. E. Reed, *Geochim. Cosmochim. Acta*, 41 (1977) 1231.
10 G. Matsmoto, R. Ishiwatari and T. Hanya, *Water Res.*, 11 (1977) 693.
11 G. Matsumoto and T. Hanya, *J. Chromatogr.*, 193 (1980) 89.
12 G. Matsumoto, T. Torii and T. Hanya, in T. Nagata (Editor), *Proc. Seminar III on Dry Valley Drilling Project, 1978. Memoirs of National Institute of Polar Research, Special Issue No. 13, Tokyo, June 5–10, 1978*, National Institute of Polar Research, Tokyo, 1979, p. 103.
13 P. G. Stechter, *The Merck Index*, Merck & Co. Inc., Rahway, 8th ed., 1968, p. 977.

14 M. Blumer, in D. W. Hood (Editor), *Proc. Symp. on Organic Matter in Natural Waters, Alaska, Sept. 2–4, 1968*, Institute of Marine Science, University of Alaska, Alaska, 1970, p. 153.
15 *Water Quality Annual Report 1975 (Suishitsu Nenpo 1975)* (in Japanese), Tokyo Waterworks Bureau, Tokyo, 1978, p. 394.
16 G. Matsumoto and T. Hanya, *Ogasawara Research (Ogasawara Kenkyu) 1 & 2* (in Japanese), Ogasawara Research Committee of Tokyo Metropolitan University, Tokyo, 1978, p. 35.

Journal of Chromatography, 194 (1980) 205–212
Elsevier Scientific Publishing Company, Amsterdam — Printed in The Netherlands

CHROM. 12,723

HIGH-PERFORMANCE LIQUID CHROMATOGRAPHY AND MASS SPECTROMETRY OF TRANSFER RNA BASES FOR ISOTOPIC ABUNDANCE

PAUL F. AGRIS* and JULIA G. TOMPSON
Division of Biological Sciences, University of Missouri, Columbia, MO 65211 (U.S.A.)
and
CHARLES W. GEHRKE, KENNETH C. KUO and ROY H. RICE
Department of Biochemistry, University of Missouri, Columbia, MO 65211 (U.S.A.)
(Received February 1st, 1980)

SUMMARY

We present a quantitative analysis of the incorporation of stable isotopes into nucleic acids for verification of the site and determination of the abundance of the label. High-performance liquid chromatography and mass spectrometry of nucleic acid bases were used for quantitation of isotopic enrichment, with only μg amounts of available RNA. Conditions for acid hydrolysis of tRNA were optimized for quantitative yield of bases without destruction, and optimum conditions for the reversed-phase high-performance liquid chromatographic separation of the bases were determined. Three tRNA preparations, ^{13}C-enriched *in vivo* by incorporation of [$^{13}C_2$]adenine, [$^{13}C_2$]uracil and [^{13}C]methyl groups from methionine, were subjected to these procedures, followed by mass spectrometry of the bases. In natural abundance, ^{13}C is 1.08 atom%; in these tRNA preparations we found: 27% of all adenine was labeled at position 2 with ^{13}C atoms; 43 atom% ^{13}C at position 2 of uracil and 45 atom% ^{13}C at position 2 of cytosine; and 56.9 atom% ^{13}C at the methyl of thymine, respectively. The techniques described are important to the study of nucleic acid biosynthesis, modification and structure by nuclear magnetic resonance spectroscopy.

INTRODUCTION

Analysis of RNA nucleoside composition and sequences can now be accomplished with μg quantities of RNA when radiolabeling and gel sequencing techniques are utilized. Recently, we developed techniques for enzymatic hydrolysis and high-performance liquid chromatographic (HPLC) analysis of RNA nucleoside composition at less than μg level[1–3]. This sensitive method of analysis is especially suited to the identification of previously uncharacterized modified nucleosides. Modified nucleosides obtained in ng amounts from purified species of tRNA could be identified by mass spectrometry (MS)[4].

However, there was a need for related methodology applicable to investi-

gations of biosynthesis, biochemistry and biophysics of nucleic acids and their modified nucleosides. Information beyond that of identification and quantification of nucleosides could be obtained if the RNA is from cells grown in media containing a labeled precursor of nucleic acids, or the labeled presumed precursor of a nucleic acid modification. This labeling could be semi-specific, such as one particular carbon within a specific base, or extremely specific, such as the methyl carbon of ribothymidine, which occurs only once in a tRNA molecule. Verification of the site and abundance of the label would be applicable to the study of nucleic acid biosynthesis, modification and structural analyses. The methods presented here demonstrate that the incorporation of the stable isotope, ^{13}C, from specific nucleic acid precursors into RNA could be successfully identified and quantitated with only μg amounts of available RNA.

MATERIALS AND METHODS

Carbon-13-enriched tRNA

Enrichment of tRNA was accomplished at specific locations by addition of particular ^{13}C-enriched nucleic acid precursors to stringently defined media in which a selected strain of *Escherichia coli* was grown. The selection of *E. coli* C6 $cys^-met^-rel^-$strain M1 and details of the media components, culture growth characteristics and tRNA extraction procedures have been published[5]. Briefly, cells were grown in media (15-l cultures) containing the nucleic acid bases, adenine, guanine, uracil and cytosine and the donor of all methyl group modifications, methionine. In order to achieve specific enrichment, only one of these added precursors contained a ^{13}C-enriched carbon. For the experiments reported here, [$^{13}C_2$]adenine, [$^{13}C_2$]uracil, and [^{13}C-methyl]methionine were obtained from Merck (Quebec, Canada), with enrichments of at least 90 atom% at the specified location[5,6]. The media also contained 6-mercaptopurine, an inhibitor of both purine biosynthesis *de novo* and adenosine–guanosine interconversion. This drug forces the cells to grow by utilizing the exogenously provided precursors for nucleoside synthesis via the "salvage pathways". The strain M1 was selected for its ability to rapidly express and efficiently utilize the "salvage pathways" for nucleoside synthesis. The tRNA was extracted by a method employing phenol denaturation of proteins, ethanol precipitation of nucleic acids, DEAE-cellulose column chromatographic separation of tRNA, and urea–polyacrylamide gel electrophoretic analysis of tRNA purity[5–7]. Yeast tRNA (Sigma, St. Louis, MO, U.S.A.) was used for comparison of ^{13}C abundance in bases.

Acid hydrolysis of nucleosides

Stock standards[1,2] were weighed on a microgram balance to afford working solutions of fine accuracy: adenosine, 1.02 m*M*; cytosine, 1.00 m*M*; guanosine, 0.42 m*M*; and uridine, 1.00 m*M*. The hydrolysis procedure reported earlier[8] entailed placing 100 μl of the stock nucleoside solution into a 100 × 16 mm screw-cap culture tube. The solvent was removed with a stream of pure nitrogen while the tube was kept at 45°C in a heating block. When dryness was confirmed, 1 ml of trifluoroacetic acid (TFA)–formic acid (1/1, v/v) was added, the tube was capped, and the solution was mixed and placed in a 150°C heating block. Times for the hydrolysis were varied between 0.5 and 8 h. After removing the tube from the heating block, it was placed

in a freezer at –20°C for *ca.* 10 min to allow condensation of the TFA and formic acid. The acids from the hydrolysate were removed with a stream of pure nitrogen gas in a heating block maintained at 45°C. Exactly 1 ml of double-distilled water was added to the dry hydrolysate followed by sonication before HPLC of 0.1-ml aliquots.

Acid hydrolysis of tRNA

The aqueous tRNA sample of *ca.* 15 μg was quantitatively transferred into a 100 × 16 mm Pyrex culture tube. The water was removed by placing the tube in a heating block at 50°C under a gentle stream of purified nitrogen gas. Then 1 ml of the TFA–formic acid mixture was added to the tube, and a PTFE-lined screw cap was firmly attached. This solution was mixed and placed in a heating block at 150°C for 4 h, no more than one-third of the tube being placed in the block. When hydrolysis was complete, the tube was carefully placed in the freezer for at least 15 min before opening the screw cap. The acids were then evaporated to dryness on the 50°C heating block under a gentle stream of nitrogen gas. Care was taken not to bake the dry hydrolysate. Redistilled nanopure water (0.4 ml) was added and sonicated to dissolve all of the residue. An aliquot (0.2 ml) of this solution was injected on to the HPLC column for separation of major and modified bases.

HPLC of bases

Major and modified bases from acid hydrolysates of tRNA were separated by reversed-phase HPLC. A μBondapak C_{18} column (600 × 4 mm) maintained at 35°C was used for the separation. Bases were eluted with a linear gradient of methanol (0 to 10%) in 0.10 *M* $NH_4H_2PO_4$ (pH 5.1). The flow-rate was 1.0 ml/min, with the methanol concentration increasing at a rate of 0.5%/min. The ultraviolet absorption of the bases was measured at 254 nm. An analytical run was made for the bases in each of the samples, then a preparative run was made, and *ca.* 60% of the central portion of the peak of interest was collected. This fraction (1.5 ml) was further purified by re-injection into the same chromatographic system. However, the elution solution was changed to 10% methanol in water, in order to remove the $NH_4H_2PO_4$. Use of a higher concentration of methanol not only gave a more concentrated base fraction, but also changed the retention characteristics of the bases. Thus, the purity of the final material was further ensured. Again, only 60% of the central portion of the peak was collected. An aliquot of this collection was used for the MS measurement.

Mass spectrometry

The MS equipment consisted of a modified CEC 21-110B high-resolution mass spectrometer, operating in conjunction with a Japan Electron Optics Laboratory JEC-6 spectrum-computer and a JMA-IC-O automatic data analyzer for photoplate detection. The instrument has a demonstrated resolution in excess of 1/30,000. Before MS analysis, detection thresholds were established for the RNA bases. Enough of each base was isolated from the tRNA for a complete mass spectrum and single-ion monitoring of the M^+ and $M^+ + 1$ peak height ratios.

The electron multiplier on our mass spectrometer is of the 16-stage Allen type with beryllium–copper dynodes and is inherently noisy. Therefore, after a period of testing by which we were assured we could routinely achieve $\pm$ 10% accuracy when

the ratio of $M^+ + 1$ to M^+ was $<10\%$, and $\pm 5\%$ accuracy at ratios $>10\%$, measurements were made in the following manner. Half of each sample, purified by and collected from the HPLC, was introduced by direct probe into the mass spectrometer source, and a complete low-resolution spectrum was made to determine if any impurities were present. After the low-resolution runs, the instrument was tuned to a resolution of 1/10,000 to further ensure that there would be no contribution from ions other than M^+ and $M^+ + 1$ (the 1/10,000 resolution still allowed ample sensitivity for our purpose). Channel "A" of the high-resolution mass measurement section was then focused on the pertinent M^+ ion, while channel "B" was focused on the corresponding $M^+ + 1$ ion. The sample was then introduced into the instrument, and, as it began to volatilize, the two channels were scanned alternately at 1-sec intervals. The signals were recorded on a CEC-5-124 recording oscillograph. The three "sets" (channels "A" and "B") of signals just prior to and just after the maximum signal strength were then averaged, and the enrichment was calculated by the following formula.

$$\text{Mole}\% \text{ of labeled species} = \frac{[(M^+ + 1) - A^*(M^+)]}{M^+ + [(M^+ + 1) - A^*(M^+)]} \times 100$$

where A* is the normal isotopic abundance of $M^+ + 1$ calculated separately for each non-enriched sample.

The percentage enrichment of ^{13}C in each of the tRNA bases was calculated according to the following example for thymine. The thymine molecular ion (*m/e* 126) peak height (designated M^+) and the molecular ion plus one (*m/e* 127) peak height ($M^+ + 1$) were used to determine the enrichment. In a natural-abundance sample of thymine, $M^+ + 1$ should be 6.3% of the peak height, M^+. Thymine has the molecular formula $C_5H_6N_2O_2$, and the percentages of natural abundance for ^{13}C, ^{15}N and ^{17}O are 1.08, 0.37 and 0.037, respectively. Hence, the percent natural abundance of the $M^+ + 1$ peak from non-labelled thymine is calculated as percent isotopes at $M^+ + 1$: $(5 \times 1.1\%) + (2 \times 0.37\%) + (2 \times 0.037\%) = 6.314\%$. The percent enrichment would be calculated for thymine as follows:

$$\text{Mole}\% \text{ of labeled species} = \frac{[(M^+ + 1) - 6.3(M^+)]}{M^+ + [(M^+ + 1) - 6.3(M^+)]} \times 100$$

RESULTS AND DISCUSSION

The ability to quantify isotopic enrichment within specific bases of tRNA is very much dependent on complete hydrolysis of the nucleosides to bases[8], quantitative separation and purification of the bases and MS. The combined chromatographic–MS procedures must be made applicable to small amounts, (μg quantities) of tRNA, because only limited amounts of sample are available. Therefore, verification of complete hydrolytic release of bases is important.

Release of bases from μg quantities of the four major ribonucleosides, ribothymidine (5-methyluridine) and 2-methylguanosine was investigated. Bases were separated and quantitated by reverse-phase HPLC and UV absorbance measurements under conditions specified in Materials and methods. Fig. 1A is a chromato-

gram of the base separation we have achieved. The release of bases from nucleosides by acid hydrolysis was quantitated over an 8-h period. Yields of the bases are shown in Fig. 2A, B. The major purine nucleosides were quantitatively hydrolysed to bases in less than 1 h; whereas pyrimidine nucleosides required at least 4 h of hydrolysis. This difference between purine and pyrimidine nucleoside hydrolysis was also evident for the two modified nucleosides. The 2-methylguanosine hydrolysis was complete in less than 1 h; ribothymidine hydrolysis required 4 h.

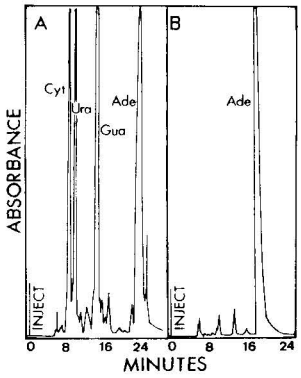

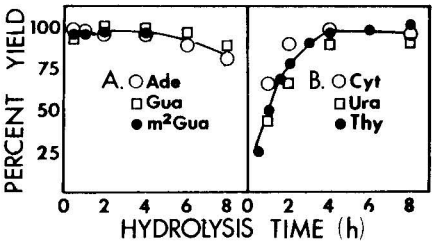

Fig. 1. Reversed-phase HPLC of bases. A: tRNA that had been acid hydrolysed to bases (see Materials and methods) was injected on to a μBondapak C_{18} column (600 × 4 mm) and bases were eluted with a 0–10% methanol gradient in phosphate buffer. Absorption at 254 nm was measured with a full-scale deflection of 0.5 absorbance units. B: The central 60% of the adenine fraction from an initial chromatography, such as that shown in A, was subjected to re-chromatography on the same column but with elution by 10% methanol in water. Ade = adenine; Cyt = cytosine; Gua = guanine; Ura = uracil.

Fig. 2. Release of bases from acid hydrolysis of nucleosides. Major and modified nucleosides [adenosine, cytosine, guanosine, uridine, 2-methylguanosine (m^2G) and ribothymidine] were acid hydrolysed. Aliquots taken at various time intervals were assessed for the amount of base released. Release of bases was quantitated by HPLC and UV absorption and is plotted as percent yield.

Since release of pyrimidines from nucleosides required the longer time, release of thymine from μg quantities of tRNA was studied in detail. *E. coli* unfractionated tRNA (13.7 μg) was subjected to acid hydrolysis as described in Materials and methods. Release of thymine over an 8-h period is depicted in Fig. 3. At 4 h, the release of thymine was complete and continued at the same level for the remaining 4 h of hydrolysis. An assessment of recovery was determined by addition of 121.6 ng of thymine to 13.7 μg of tRNA. This mixture, hydrolysed and chromatographed, resulted in 99.6% recovery of the added thymine.

With the appropriate conditions successfully achieved for the tRNA hydrolysis and quantification of bases, analysis of isotopically enriched tRNA was accomplished. Unfractionated tRNA was obtained from a strain of *E. coli* grown in stringently defined media that contained either [$^{13}C_2$]adenine, [$^{13}C_2$]uracil or [^{13}C-methyl]-methionine[5]. The ^{13}C-enrichment of these nucleic acid precursors was ascertained by nuclear magnetic resonance (NMR) spectroscopy and MS to be site-specific and greater than 90 atom%[5,6,9]. Unlabeled yeast tRNA was extensively dialyzed against glass-distilled water and used for comparison of the ^{13}C content of bases. Unlabeled

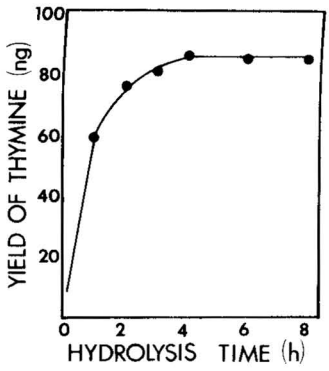

Fig. 3. Release of thymine from tRNA. tRNA was acid hydrolysed, and aliquots of the hydrolysate were taken at various time intervals and subjected to HPLC. The release of thymine from the tRNA over 8 h is plotted in nanograms.

and ^{13}C-enriched tRNAs were acid hydrolysed, and the bases were separated by HPLC. The base of interest was subjected to chromatography a second time and eluted with 10% methanol in water. This procedure further purified the base and removed all salts from the first chromatography before MS analysis; Fig. 1B is the elution profile of adenine during the second chromatography. The retention time for each base was shorter during the second chromatography under conditions of 10% methanol, as seen by comparison of adenine in Figs. 1A and 1B.

The purified bases were subjected to MS analysis. Due to the non-volatility of guanine in the mass spectrometer ion source, a trimethylsilyl (TMS) derivative was made by reacting the purified base with 0.5 ml of bis(trimethylsilyl)trifluoroacetamide (BSTFA) in 0.5 ml of acetonitrile for 15 min at 150°C. Both a complete mass spectrum and single-ion monitoring of the molecular ion (M^+) and the molecular ion plus one mass unit ($M^+ + 1$) were accomplished for each base. For the mass spectrum of TMS-guanine, *m/e* 208 and 209 were used to find the ^{13}C atom% enrichment, because this pair contained the least spectral background when compared to other measurable fragments. The MS analyses of M^+ and $M^+ + 1$ of bases from unlabeled and ^{13}C-enriched tRNA preparations are shown in Fig. 4. Unlabeled tRNA contained bases with ^{13}C abundance comparable to the theoretical values based on 1.1 atom% natural abundance. The tRNA obtained from cultures grown with $^{13}C_2$-enriched adenine was found to contain enrichment only within adenine, and to the extent of 27 atom%. tRNA obtained from cultures grown with [$^{13}C_2$]uracil was found to contain enrichment within both uracil and cytosine and to the extents of 43 and 45 atom%, respectively. *E. coli* was cultured in the presence of 6-mercaptopurine, which blocks *de novo* purine biosynthesis and adenosine–guanosine interconversions. This drug is incapable of blocking the interconversion of pyrimidines. Thus, both uracil and cytosine were labeled in the tRNA of cells grown on [$^{13}C_2$]uracil. By NMR spectroscopy of the adenine and uracil/cytosine tRNA preparations, the base location of the labels was verified, and it was shown that the labels were present only at the C_2-positions (Fig. 5).

The most successful labeling of tRNA occurred with cells grown on [^{13}C-methyl]methionine. This may be due to the strain's methionine auxotrophy. Thymine

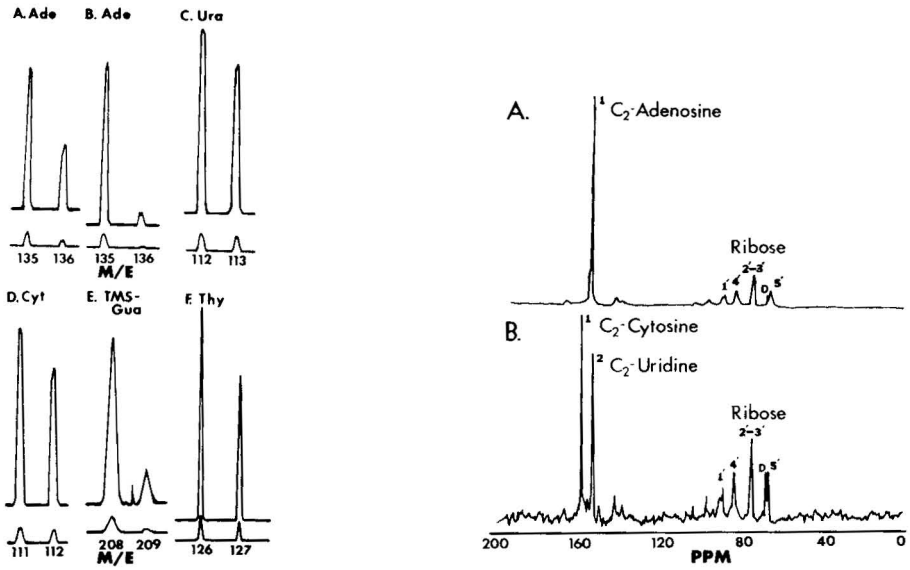

Fig. 4. Mass spectometry of bases from labeled and unlabeled tRNA samples. Bases obtained from unlabeled and ^{13}C-enriched tRNA samples were subjected to mass spectral analysis. The figures show the results of single-ion monitoring in which the molecular ion (M^+) and the molecular ion plus one mass unit ($M^+ + 1$) are detected. A, adenine from tRNA of cultures grown with $^{13}C_2$-enriched adenine; B, adenine from unlabeled tRNA; C, uracil from tRNA of cultures grown with $^{13}C_2$-enriched uracil; D, cytosine from tRNA of cultures grown with [$^{13}C_2$]uracil; E, TMS-guanine from tRNA of cultures grown with [$^{13}C_2$]adenine; F, thymine from tRNA of cultures grown with methionine, ^{13}C-enriched in the methyl group.

Fig. 5. Carbon-NMR spectroscopy of [$^{13}C_2$]adenine and [$^{13}C_2$]uracil/cytosine tRNA. Carbon-NMR spectra of ^{13}C-enriched tRNA were taken on a Varian XL100 FT NMR spectrometer equipped with a Nicolet 1180 computer and Varian temperature control. Samples (2 ml) of *ca.* 2 m*M* tRNA were placed in 12-mm tubes and for the spectra shown were kept at 76.5°C for the time-averaged acquisition of 8192 scans. Chemical shifts (ppm) are relative to tetramethylsilane with the internal standard dioxane (signal designated D in the figures) located at 67.4 ppm. Resonance signals 1′, 2′–3′, 4′ and 5′ emanate from the natural-abundance ^{13}C of the five ribose carbons. A, tRNA from cultures grown with $^{13}C_2$-enriched adenine exhibited only one enriched signal (number 1 in the figure); this signal corresponds in chemical shift to that of C_2 of adenine, adenosine and polyA[6]. B, tRNA from cultures grown with [$^{13}C_2$]uracil exhibited two enriched signals (numbered 1 and 2); signal 2 corresponds in chemical shift to that of the C_2 of uracil, uridine, UMP and polyU and signal 1 to the C_2 of cytosine, cytidine and CMP[6].

isolated from tRNA of this culture was labeled to the extent of 56.9 atom%; NMR spectroscopy of this tRNA verified that ^{13}C-enrichment occurred only at methyl groups and not in base-ring carbons[5,6].

ACKNOWLEDGEMENTS

This work was supported by a grant from the National Institute of Health (USPH 1 R01 GM23037) to Paul F. Agris and by the University of Missouri Division of Biological Sciences, Research Council, and Experiment Station Chemical Laboratories. Our appreciation is extended to Mark Nace, senior student chemist,

and Roy McCune, graduate student chemist, for technical assistance and to Rosemary Crane, Nancy Rice and Karla Cook for aid in preparation of the manuscript.

REFERENCES

1 G. E. Davis, C. W. Gehrke, K. C. Kuo and P. F. Agris, *J. Chromatogr.*, 173 (1979) 281.
2 C. W. Gehrke, K. C. Kuo, G. E. Davis, R. D. Suits, T. P. Waalkes and E. Borek, *J. Chromatogr.*, 150 (1978) 455.
3 C. W. Gehrke, K. C. Kuo and R. W. Zumwalt, *J. Chromatogr.*, 188 (1980) 129.
4 A. Rafalski, J. Kohli, P. Agris and D. Soll, *Nucleic Acids Res.*, 6 (1979) 2683.
5 J. G. Tompson and P. F. Agris, *Nucleic Acids Res.*, 7 (1979) 765.
6 J. G. Tompson, F. Hayashi, J. V. Paukstelis, R. N. Loeppky and P. F. Agris, *Biochemistry*, 18 (1979) 2079.
7 P. F. Agris, T. Powers, D. Soll, F. Ruddle, *Cancer Biochem. Biophys.*, 1 (1975) 69.
8 D. B. Lakings and C. W. Gehrke, *Clin. Chem.*, 18 (1972) 810.
9 P. F. Agris, F. G. Fujiwara, C. F. Schmidt and R. N. Loeppky, *Nucleic Acids Res.*, 2 (1975) 1503.

Journal of Chromatography, 194 (1980) 213–216
Elsevier Scientific Publishing Company, Amsterdam — Printed in The Netherlands

CHROM. 12,729

Note

Zur Abhängigkeit des relativen molaren Response-Faktors isomerer Alkane von der Molekülform

KURT ALTENBURG

Zentralinstitut für physikalische Chemie der Akademie der Wissenschaften der D.D.R., Rudower Chaussee 5, DDR-1199 Berlin (D.D.R.)

(Eingegangen am 30. Januar 1980)

In vorangegangenen Mitteilungen war gezeigt worden, dass für isomere Alkane der Kovatssche Retentionsindex[1,2] und seine Temperaturabhängigkeit[3] Funktionen des quadratischen Mittelwertes des Radius[4] sind. Im folgenden soll dargestellt werden, dass auch der mit einem Wärmeleitfähigkeitsdetektor gemessene "relative molare Response-Faktor" (RMR) eine eindeutige Funktion des quadratischen Mittelwertes des Radius ist.

Der RMR-Faktor vermittelt den Zusammenhang zwischen der molaren Konzentration einer Komponente i und der experimentell bestimmten Peakfläche des Gaschromatogramms. Er ist wie folgt definiert:

$$(\mathrm{RMR})_i = \frac{\varphi_i/[V_i(\varrho_i/M_i)]}{\varphi_0/[V_0(\varrho_0/M_0)]} \cdot 100 \qquad (1)$$

φ ist die Peakfläche, V das Probenvolumen, M die (relative) Molekülmasse und ϱ die Dichte (Lit. 5). Durch den Index i bzw. 0 wird die zu untersuchende Substanz bzw. eine Vergleichssubstanz, im allgemeinen Benzen, gekennzeichnet.

DER QUADRATISCHE MITTELWERT DES RADIUS EINES MOLEKÜLS

Der quadratische Mittelwert des Radius eines Moleküls ist wie folgt definiert[4]:

$$\overline{R^2} = \frac{1}{m} \sum_i m_i \overline{r_i^2} \text{ mit } m = \sum_i m_i \qquad (2)$$

m ist die Gesamtmasse des Moleküls, m_i die Masse des i-ten Atoms und r_i der Abstand dieses Atoms vom Schwerpunkt des Moleküls. Bei nichtstarren Molekülen ist über allé möglichen Konformationen des Moleküls zu mitteln. Der quadratische Mittelwert des Radius ist proportional dem mittleren Trägheitsmoment eines Moleküls, er wird umso kleiner je kompakter ein Molekül gebaut ist. Ersetzt man ein Molekül näherungsweise durch gleichartige Bausteine, die die gleiche sterische Anordnung haben wie die Kohlenstoffatome des Alkanmoleküls, so kann man für bestimmte Molekülmodelle den quadratischen Mittelwert des Radius mittels ein-

0021-9673/80/0000–0000/$02.25

facher Abzählverfahren berechnen[4,6,7]. Die für das Modell der frei drehbaren Valenzwinkelkette (freie Drehbarkeit um jede Einfachbindung unter Berücksichtigung des Tetraederwinkels) berechneten quadratischen Mittelwerte der auf die Länge einer C–C-Bindung a_1 bezogenen Radien $K^2 = \bar{R}^2/a_1^2$ der acyclischen isomeren Alkane C_5

TABELLE I

DIE AUF DIE LÄNGE EINER C–C-BINDUNG a_1 BEZOGENEN QUADRATISCHEN MITTELWERTE DER RADIEN $K^2 = \bar{R}^2/a_1^2$, EXPERIMENTELL BESTIMMTE[5] $(RMR)_{ex}$ UND MITTELS GLEICHUNG 5 BZW. 6 BERECHNETE $(RMR)_{th}$ RELATIVEN MOLAREN RESPONSE-FAKTOREN DER ACYCLISCHEN ALKANE C_5 BIS C_8 UND DER DIMETHYLCYCLOPENTANE

Verbindung	K^2	$(RMR)_{ex}$	$(RMR)_{th}$
n-Pentan	1.1048	106.8	107.8
2-Methylbutan	0.9511	104.5	103.1
2,2-Dimethylpropan	0.8000	97.6	98.5
n-Hexan	1.4132	122.6	124.3
2-Methylpentan	1.2510	120.4	119.4
3-Methylpentan	1.1965	118.8	117.7
2,2-Dimethylbutan	1.0370	112.9	112.8
2,3-Dimethylbutan	1.0895	114.8	114.4
n-Heptan	1.7271	139.4	140.9
2-Methylhexan	1.5672	136.7	136.1
3-Methylhexan	1.4865	134.1	133.6
3-Ethylpentan	1.4059	132.1	131.2
2,2-Dimethylpentan	1.3288	129.4	128.8
2,3-Dimethylpentan	1.3273	130.9	128.8
2,4-Dimethylpentan	1.4074	130.7	131.2
3.3-Dimethylpentan	1.2487	125.4	126.4
2,2,3-Trimethylbutan	1.1701	122.2	124.0
n-Oktan	2.0449	155.7	157.7
2-Methylheptan	1.8913	152.8	153.0
3-Methylheptan	1.7984	151.2	150.2
4-Methylheptan	1.7673	149.9	149.3
3-Ethylhexan	1.6744	148.3	146.4
2,2-Dimethylhexan	1.6464	146.2	145.6
2,3-Dimethylhexan	1.6142	146.2	144.6
2,4-Dimethylhexan	1.6449	146.4	144.5
2,5-Dimethylhexan	1.7377	147.6	148.4
3,3-Dimethylhexan	1.5230	141.4	141.8
3,4-Dimethylhexan	1.5525	143.5	142.7
2-Methyl-3-Ethylpentan	1.5214	141.9	141.8
3-Methyl-3-Ethylpentan	1.4306	137.6	139.0
2,2,3-Trimethylpentan	1.4010	137.5	138.1
2,2,4-Trimethylpentan	1.4931	141.5	140.9
2,3,3-Trimethylpentan	1.3698	135.1	137.1
2,3,4-Trimethylpentan	1.4612	138.6	139.9
Ethyl-cyclopentan	1.2929	127.7	126.6
1,1-Dimethylcyclopentan	1,1235	120.9	120.0
cis-1,2-Dimethylcyclopentan	1.1266	119.6	120.1
trans-1,2-Dimethylcyclopentan	1.1810	122.2	122.2
cis-1,3-Dimethylcyclopentan	1.2196	122.8	123.7
trans-1,3-Dimethylcyclopentan	1.2741	125.0	125.8

bis C_8 und der Dimethylcyclopentane sind in Tabelle I zusammengestellt[4,7] (bei diesen Berechnungen wird der Ring als eben vorausgesetzt).

In einer Reihe von Veröffentlichungen konnte gezeigt werden, dass zahlreiche physikalische Eigenschaften Y reiner isomerer Alkane und von Gemischen einfacher Funktionen von N (der Zahl der Kohlenstoffatome) und K^2 sind[8–13]:

$$Y = Y(N; K^2) \tag{3}$$

Diese Beziehung kann man in eine Reihe entwickeln[14] und erhält schliesslich einen Ausdruck der Form

$$Y = A_0 + A_1 N + A_2 K^2 + A_{11} N^2 + A_{22} (K^2)^2 + A_{12} N K^2 + \ldots \tag{4}$$

Die A_{ij} sind Konstante, die aus empirischen Daten mittels der Methode der kleinsten Quadrate bestimmt werden können.

Einige Eigenschaften hängen noch von der "Platt-number" n_3 ab; sie gibt an, wieviel Paare von C-Atomen existieren, die jeweils durch drei Bindungen voneinander getrennt sind. In diesem Falle sind in Gleichung 4 noch Terme der Form n_3, n_3^2, $n_3 N$, $n_3 K^2$ usw. zu berücksichtigen.

DIE ABHÄNGIGKEIT DES RMR-FAKTORS VOM QUADRATISCHEN MITTELWERT DES RADIUS

Systematische Messungen des RMR-Faktors isomerer Alkane sind in letzter Zeit von Carson und Lege[5] durchgeführt worden. In Tabelle I sind diese Daten zusammengestellt. Die Autoren[5] haben jeweils zwei unabhängige Bestimmungen des RMR-Faktors durchgeführt. Die Tabelle I enthält die auf eine Stelle nach dem Komma gerundeten Mittelwerte. In Fig. 1 und 2 sind diese Werte für die isomeren Heptane und Oktane und als Beispiel für Cyclo-Alkane, für die Dimethylcyclo-

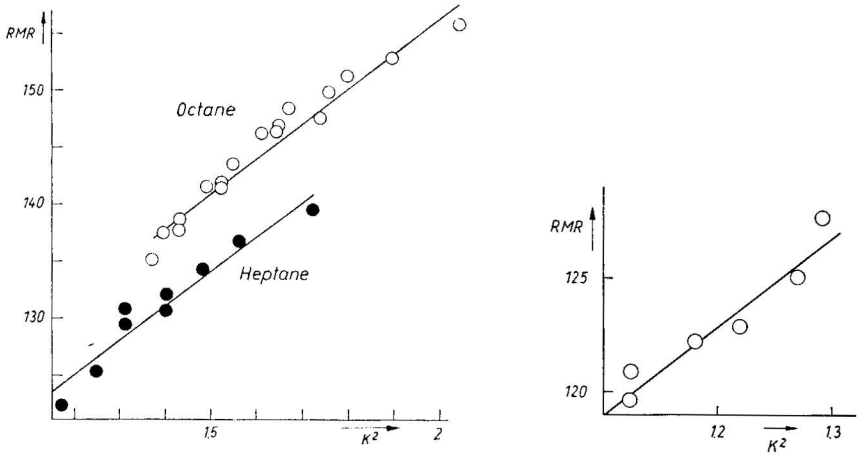

Fig. 1. Abhängigkeit des RMR-Faktors der isomeren Heptane ● und Octane ○ von K^2.

Fig. 2. Abhängigkeit des RMR-Faktors der isomeren Dimethylcyclopentane von K^2.

pentane als Funktion von K^2 dargestellt. Innerhalb der Reihen der isomeren Verbindungen besteht weitgehend ein linearer Zusammenhang. Zur analytischen Darstellung (s. Gleichung 4) genügt es, die linearen Terme dieser Gleichung zu berücksichtigen. Eine Ausgleichsrechnung ergibt für die acyclischen isomeren Alkane C_5 bis C_8:

$$(RMR)_{C_5 \ldots C_8} = 38.73 + 7.08\,N + 30.49K^2 \qquad (5)$$

Für die Dimethylcyclopentane erhält man entsprechend

$$(RMR)_{\text{Dimethylcyclopentane}} = 76.13 + 39.00\,K^2 \qquad (6)$$

Die Standardabweichung beträgt bei den isomeren Alkanen C_5 bis C_8 1.2 Einheiten und bei den Dimethylcyclopentanen 0.9 Einheiten. Sie liegt damit in der gleichen Grössenordnung wie die Unsicherheit der experimentellen Ergebnisse.

Auch für andere Reihen der Cycloalkane ergeben sich lineare Zusammenhänge zwischen RMR und K^2; die Neigung der Geraden ist jedoch für die Reihen unterschiedlich. Eine signifikante Abhängigkeit der Eigenschaften von der "Plattnumber" n_3 konnte in keinem Falle festgestellt werden. Die mittels Gleichungen 5 und 6 berechneten RMR-Werte sind in Tabelle I den experimentellen Daten gegenübergestellt.

ZUR DEUTUNG DER ERGEBNISSE

Der RMR Faktor hängt von der unterschiedlichen Differenz der Wärmeleitfähigkeit Substanz-Trägergas ab. Die Wärmeleitfähigkeit ihrerseits wird massgeblich durch die zwischenmolekulare Wechselwirkung bestimmt. Die Untersuchung der Abhängigkeit anderer Eigenschaften von quadratischen Mittelwert des Radius haben gezeigt[8–13], dass diese Abhängigkeit im wesentlichen durch die unterschiedliche zwischenmolekulare Wechselwirkung der verschiedenen Isomeren bedingt ist.

LITERATUR

1 K. Altenburg, in H. G. Struppe (Herausgeber), *Gas Chromatographie Berlin*, Akademie-Verlag, Berlin, 1968, S. 1.
2 K. Altenburg, *J. Chromatogr.*, 45 (1969) 306.
3 K. Altenburg, *J. Chromatogr.*, 44 (1969) 167.
4 K. Altenburg, *Kolloid-Z.*, 178 (1961) 112.
5 J. W. Carson und G. Lege, *J. Chromatogr. Sci.*, 16 (1978) 507.
6 K. Altenburg, *Z. Phys. Chem. (Leipzig)*, 260 (1979) 981.
7 K. Altenburg, *Z. Phys. Chem. (Leipzig)*, 228 (1965) 120; desgl., 230 (1965) 13; desgl., 231 (1966) 77.
8 K. Altenburg, *Proc. 1st Int. Conf. Calorimetry and Thermodynamics*, Warsaw, 1969, p. 575; und frühere Arbeiten.
9 H. Richter, *Chem.-Ztg.*, 95 (1971) 916.
10 H. Bauer, *VDI-Forschungsbericht 556*, VDI-Verlag, Düsseldorf, 1973, p. 1.
11 E. Kuss, *DGMK-Forschungsbericht 4510*, Deutsche gesellschaft für Mineralöl wissenschaft und Kohlechemie e.V., Hamburg, 1976, p. 1.
12 D. Richon, D. Patterson und G. Turrell, *Chem. Phys.*, 16 (1976) 61.
13 P. Tancrede, P. Bothorel, P. De St.Romain und D. Patterson, *J. Chem. Soc., Farad. Trans. II*, 73 (1977) 15, 29.
14 K. Altenburg, *Chem. Techn.*, im Druck.

Journal of Chromatography, 194 (1980) 217–223
Elsevier Scientific Publishing Company, Amsterdam — Printed in The Netherlands

CHROM. 12,732

Note

Sample-solvent-induced peak broadening in the reversed-phase high-performance liquid chromatography of Aspirin and related analgesics

K. J. WILLIAMS, A. LI WAN PO and W. J. IRWIN*

Department of Pharmacy, University of Aston in Birmingham, Gosta Green, Birmingham B4 7ET (Great Britain)

(First received November 13th, 1979; revised manuscript received January 30th, 1980)

Acetylsalicylic acid (Aspirin; 3) is a widely used analgesic, both alone and in combination. On exposure to moisture the drug undergoes hydrolysis to yield salicylic acid (4), the content of which must not exceed pre-determined specifications[1,2]. Many methods have been described for the assay of salicylic acid in the presence of Aspirin and in Aspirin-containing analgesics[3–5], and high-performance liquid chromatography (HPLC) is of proven value for the determination of Aspirin[6,7] and for the trace determination of salicylic acid[8] and other impurities[9]. We have previously developed an HPLC method for the detection of salicylic acid in Aspirin products containing phenacetin which have had reduced turnover due to legislation restricting sales to medical prescription only[8]. Sensitivity and specificity were achieved by ultraviolet detection at 310 nm. The chromatographic separation itself, however, was only partially achieved and we now present a method which allows resolution and simultaneous quantification of Aspirin and salicylic acid in the presence of paracetamol, caffeine and phenacetin.

Substantial improvements in chromatographic performance may be also achieved by optimisation of the sample solvent composition.

In reversed-phase liquid chromatography, the sample is normally prepared as a solution in water or in the mobile phase. However, it is often more convenient to use some other miscible solvent because of stability or solubility considerations. For example, when assaying Aspirin formulations it is usually preferable to prepare solutions in methanol or a similar non-aqueous solvent to avoid hydrolysis. Similarly on occasions there may be some component of a sample matrix which is capable of altering the nature of the sample-solvent. Thus, it is important in quantitative work to consider the effect of injection technique[10] and sample solvent on peak profiles. It is well recognised that the volume of sample solvent injected is important in maintaining column efficiency and that large volumes will cause volume overload with consequent loss in performance[11]. It appears less well recognised that peak asymmetry and column efficiency are also dependent upon the *nature* of the sample solvent. With normal adsorption HPLC it has been stated that sample solvents of higher polarity than the mobile phase (used, for example, to increase solubility) yield asymmetric peaks due to band broadening at the point of injection[12]. Reversed-phase chromatography is also susceptible to these effects and it has been shown that methanol is

0021-9673/80/0000–0000/$02.25

superior to aqueous methanolic systems for aromatic hydrocarbons[13]. Small sample volumes reduce, but do not remove, these problems. When the polarities of the mobile phase and sample solvent are grossly different an extreme effect may be observed such that a single component may be eluted as two distinct peaks. Thus dihydroxybenzene isomers dissolved in methanol and eluted with water appeared as doublets[14]. Broad peaks[14] or shoulders[15] may also result. Clearly, calibration lines constructed from peak height data alone are particularly susceptible to these problems, and one possible cause for deviations from linearity[16] may be associated with sample-solvent problems.

In this paper we have illustrated the effect of sample solvent-induced peak broadening. This has important implications in quantitative analysis and it will be shown that such effects should be considered during the choice of internal standards.

EXPERIMENTAL

Apparatus

Analyses were performed using a high-performance liquid chromatograph constructed from an Altex 100A constant-flow solvent-metering pump, a Rheodyne 7120 valve injector fitted with a 20-μl loop and a Pye LC3 variable wavelength ultraviolet monitor, equipped with a 8-μl flow cell and operated at 275 nm with a sensitivity of 0.32 a.u.f.s. Chromatography was performed using a 25 cm $\times$ 4.6 mm I.D. OD2-2 column (Whatman; Partisil PXS 10/25 ODS-2) with a mobile phase consisting of acetonitrile–acetic acid–water (25:5:70, v/v/v) which was delivered at a flow-rate of 1 ml min^{-1} at a pressure of 110 bar.

Materials

Acetonitrile (HPLC grade) and methanol (analytical reagent grade) were obtained from Fisons, Loughborough, Great Britain. Acetic acid, salicylic acid, caffeine citrate, phenacetin, paracetamol, ethanol, propan-2-ol, propan-1-ol and propane-1,2-diol (all analytical reagent grade) were obtained from BDH, Poole, Great Britain. Aspirin was obtained from Reckitt and Colman, Hull, Great Britain.

Procedures

Unless otherwise stated, the injected mixtures contained the following components in the stated concentrations: paracetamol, 0.20 mg ml^{-1}; caffeine citrate, 0.20 mg ml^{-1}; salicylic acid, 1.00 mg ml^{-1}; Aspirin, 1.00 mg ml^{-1}; phenacetin, 0.50 mg ml^{-1}. All solutions were freshly prepared and injected immediately to avoid any appreciable hydrolysis of aspirin.

The solutions prepared in various solvents were each chromatographed at least twice, and in all cases the peak heights of the replicates were not significantly different, suggesting that the injection volumes (20 μl unless otherwise stated) were consistent. Also, since the experiments tended to take several hours to complete, care was taken to avoid changes in mobile phase composition and other instrumental parameters. As an extra precaution peak areas were determined by the cut–weigh method using traces obtained with a fast chart recorder speed (1 min cm^{-1}). The changes in peak areas were not significant throughout each experiment and so instrumental response was assumed to be constant. The coefficients of variation of

the peak areas for each experiment were measured and 2% was found to be a typical value.

Calibration curves for each component were obtained by two methods. Initially 20-μl injections (using a fixed loop) of solutions containing various concentrations of solutes in methanol–water (25:75, v/v) were chromatographed. The experiment was repeated using a standard methanolic solution of the analgesics and in this case injections of various volumes were made using a calibrated syringe.

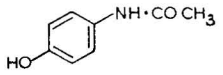

(1) Paracetamol

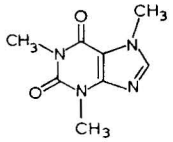

(2) Caffeine

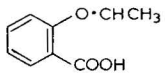

(3) Aspirin

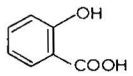

(4) Salicylic acid

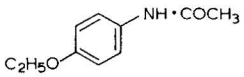

(5) Phenacetin

RESULTS AND DISCUSSION

Typical chromatograms obtained during the analysis of the analgesic mixture are illustrated in Fig. 1. This figure shows a normal chromatogram (A) where the solutes are dissolved in mobile phase, and a comparable chromatogram (B) in a sample solvent which has considerably more acetonitrile than the mobile phase. Other sample-solvent combinations give analogous results. Thus methanol–water (30:70, v/v) gives a chromatogram similar to Fig. 1A, while methanol alone causes peak broadening and is similar to Fig. 1B. The chromatographic system described gives a good separation of all the components, and the capacity ratios were found to be: paracetamol, 1.39; caffeine, 2.35; Aspirin, 3.27; salicylic acid, 4.72; phenacetin, 6.66. It can be seen that although peak area remains constant, there is a considerable change in peak profile and peak height which may be attributed to the change in the nature of the sample solvent. The dependence of peak height upon the composition of the sample solvent is illustrated in Fig. 2 and in Table I. Little change in chromatographic performance is observed until the acetonitrile content exceeds that the mobile phase, at which point efficiency is dramatically degraded. Fig. 3 shows similar peak

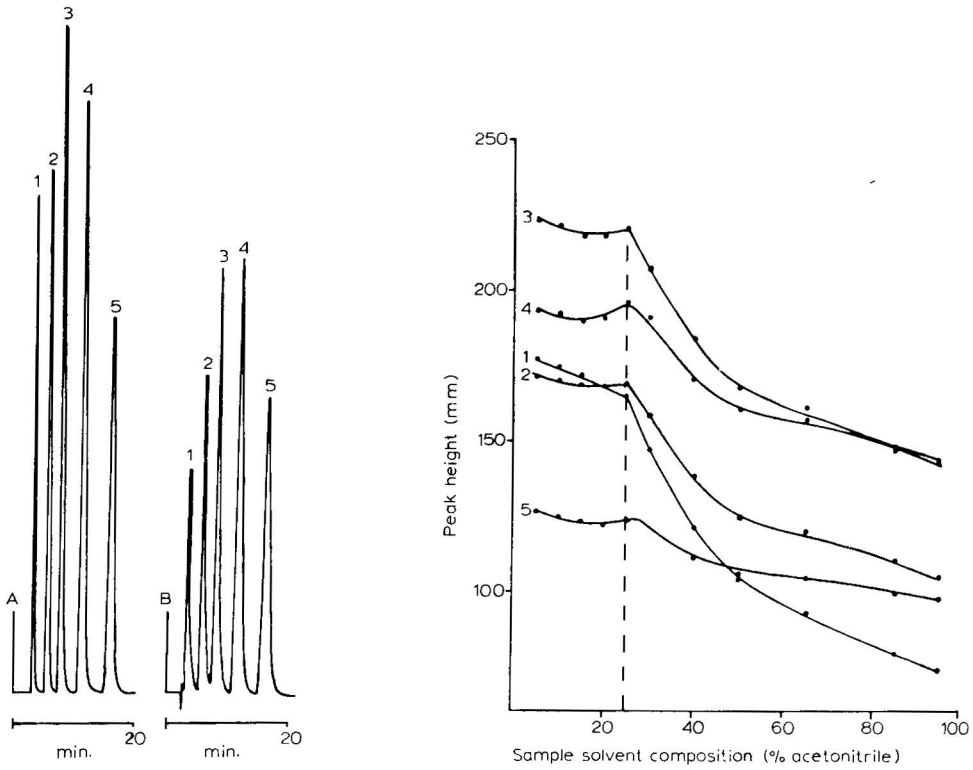

Fig. 1. Chromatograms of mixtures of paracetamol (1), caffeine (2), Aspirin (3), salicylic acid (4) and phenacetin (5). The first chromatogram (A) shows the trace obtained using mobile phase as the sample solvent (25% acetonitrile, 5% acetic acid, in water). The second trace (B) is for a mixture of identical composition prepared in an acetonitrile–acetic acid (95:5) mixture.

Fig. 2. Acetonitrile–acetic acid–water mixtures as sample solvents —the effect on peak heights. The solutes were prepared in solutions containing 5% (v/v) acetic acid and varying proportions of acetonitrile and water. The dotted line corresponds to the mobile phase composition.

TABLE I

COLUMN EFFICIENCY AS MEASURED BY THE NUMBER OF THEORETICAL PLATES FOR SAMPLE SOLVENTS OF VARIOUS COMPOSITION

Sample solvent (% acetonitrile, v/v) *	*Paracetamol*	*Caffeine*	*Aspirin*	*Salicylic acid*	*Phenacetin*
10	809	1024	1521	1418	1924
25	718	924	1400	1444	1960
40	629	855	1037	1378	1561
65	329	653	999	1220	1600
95	185	407	702	826	1363

* All the samples listed contained 5% (v/v) acetic acid and were made up to volume with distilled water.

height data for the analgesic mixture as a function of sample solvent–methanol composition. This curve exhibits a maximum at a methanol concentration of *ca.* 30% (v/v) and it is probable that at this point on the curve the polarity of the sample solvent is similar to that of the mobile phase.

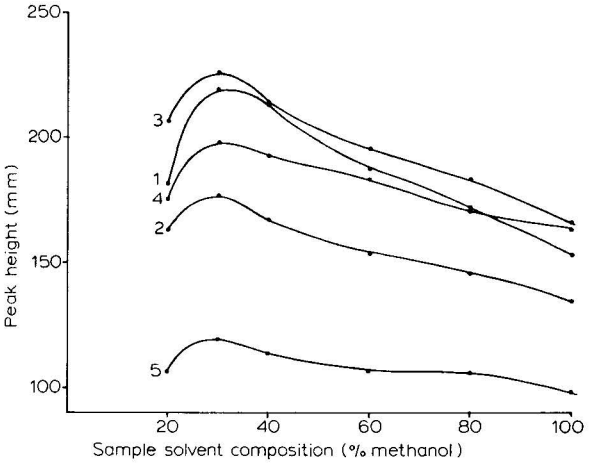

Fig. 3. Methanol–water mixtures as sample solvents —the effect on peak heights. Mixtures of the five solutes were prepared in sample solvents containing varying amounts of methanol and water. The peak height values are mean values from duplicate injections.

The causes for the observed effects are most probably associated with the length of column required for equilibration of the initial injection volume. Giddings[17] has related injection volume peak broadening to the square root of the number of theoretical plates occupied by the injected sample. It would appear that a similar mechanism is in operation here with the more polar solvents increasing the number of theoretical plates occupied by the sample and hence decreasing separation efficiency. This effect may also be observed with solvents which are less polar than the mobile phase. Fig. 4 illustrates the effect of various other sample solvents on the peak profile of salicylic acid (1 mg ml^{-1}) and shows that the peak height increases with increasing polarity[18] and that using the mobile phase as sample solvent does not necessarily maximise column efficiency.

The change in peak-height ratios which occurs, when changing sample solvent composition are important in quantitative analysis even if internal standards are used. Here it is often assumed that the peak-height ratio for two components will be dependent only upon the relative amounts of the two components. However, when the sample solvent composition changes, peak-height ratios can also change (Fig. 5). This variation may be significant and there is a potential error when the sample is of uncertain composition or where samples and standards are not prepared in the same manner. Solutes with a high capacity ratio were found to exhibit a lesser degree of peak broadening than poorly retained solutes. It is thus preferable to avoid internal standards with very short retention times and to ensure that internal standard and analyte have similar capacity ratios if sample solvent composition is liable to variation. However, provided the sample solvent is kept constant, peak height

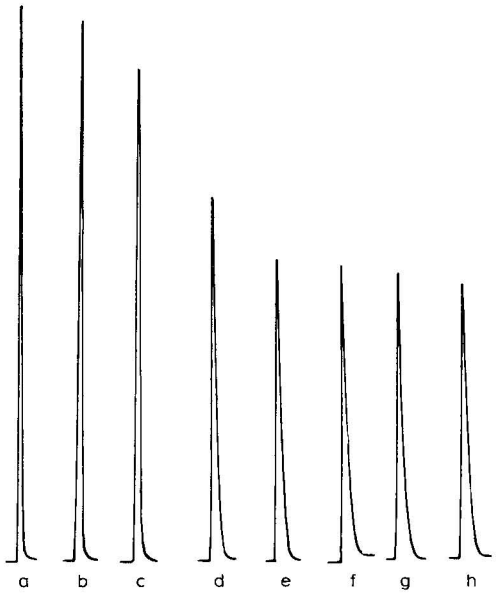

Fig. 4. The effect of various sample solvents on peak profile. Salicylic acid (1.00 mg ml^{-1}) was injected on to the column in a variety of sample-solvents. The solvents were: (a) water, (b) mobile phase, (c) propane-1,2-diol, (d) methanol, (e) acetonitrile, (f) ethanol, (g) propan-2-ol, (h) propan-1-ol.

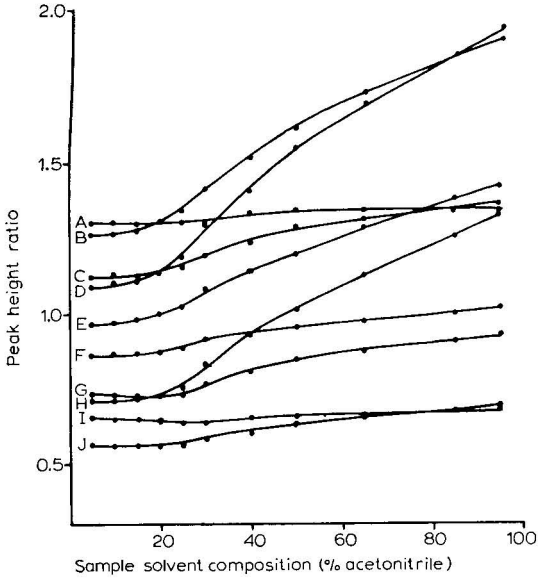

Fig. 5. The relationship between peak height ratios and sample solvent composition. A, Aspirin/caffeine; B, Aspirin/paracetamol; C, salicylic acid/caffeine; D, salicylic acid/paracetamol; E, caffeine/paracetamol; F, salicylic acid/Aspirin; G, phenacetin/caffeine; H, phenacetin/paracetamol; I, phenacetin/salicylic acid; J, phenacetin/Aspirin.

measurements produce satisfactory calibration lines. This was found to be the case when varying concentrations of the analgesics in 25% methanol were injected (constant volume, 25 μl) or when different volumes (5–20 μl) of a standard solution in methanol were analysed, although significant response differences were observed. This linearity of response indicates that small sample volume changes have an insignificant effect upon peak spreading and that little mixing of the sample solvent and mobile phase occurs. Thus provided that both standard and sample are treated in exactly the same way, quantitative measurements will be satisfactory. However, resolution and sensitivity are dependent upon the nature of the sample solvent, which may require optimisation for maximum chromatographic efficiency.

REFERENCES

1 *British Pharmacopoeia*, $HMSO_2$, London, 1973, p. 37.
2 *The Pharmaceutical Codex*, Pharmaceutical Press, London, 1979, p. 63.
3 N. Shane and D. Miele, *J. Pharm. Sci.*, 59 (1970) 397.
4 C. I. Miles and G. H. Schenk, *Anal. Chem.*, 42 (1970) 656.
5 S. Patel, J. H. Perrin and J. J. Windheuser, *J. Pharm. Sci.*, 61 (1972) 1974.
6 S.-O. Jansson and I. Andersson, *Acta Pharm. Suecica*, 14 (1977) 161.
7 P. P. Ascione and G. P. Chrekian, *J. Pharm. Sci.*, 64 (1975) 1029.
8 W. J. Irwin, A. Li Wan Po and D. K. Scott, *J. Clin. Pharm.*, 4 (1979) 25.
9 H. Bundgaard, *Arch. Pharm. Chem. (Sci. Ed.)*., 4 (1976) 103.
10 C. F. Simpson, *Proc. Anal. Chem. Soc.*, 16 (1979) 222.
11 P. A. Bristow, *Liquid Chromatography in Practice*, hetp, Wilmslow, 1976, p. 170.
12 D. L. Saunders, *J. Chromatogr. Sci.*, 15 (1977) 372.
13 N. A. Parris, *Instrumental Liquid Chromatography*, Elsevier, Amsterdam, Oxford, New York, 1976, p. 231.
14 P. K. Tseng and L. B. Rogers, *J. Chromatogr. Sci.*, 16 (1978) 436.
15 L. J. Lorenz, personal communication.
16 W. C. Chiou, R. L. Nation, G. W. Pery and S. M. Huang, *Clin. Chem.*, 24 (1978) 1846.
17 J. C. Giddings, *Dynamics of Chromatography*, Part 1, Marcel Dekker, New York, 1965.
18 L. R. Snyder, in E. S. Perry and A. Weissberger (Editors), *Separation and Purification*, Wiley-Interscience, New York, 1978, p. 55.

Journal of Chromatography, 194 (1980) 224–227
Elsevier Scientific Publishing Company, Amsterdam — Printed in The Netherlands

CHROM. 12,747

Note

Determination of dissolved carbohydrates in natural water by gas–liquid chromatography

MASAHIRO OCHIAI

Department of Chemistry, Faculty of Science, Tokyo Metropolitan University, Fukazawa 2-1-1, Setagaya-Ku, Tokyo 158 (Japan)

(First received December 27th, 1979; revised manuscript received February 5th, 1980)

Dissolved carbohydrates (DCHO) are *ca.* 10–40% of the dissolved organic matter in natural water and play an important role in the aquatic ecosystem. DCHO in natural water have been measured by the anthrone–sulphuric acid, phenol–sulphuric acid and orcinol–sulphuric acid methods[1–5]. However, it was not possible to obtain information concerning the monosaccharide composition from the results of these colorimetries, and compounds other than DCHO may interfere with the colour development.

Monosaccharides can be determined by gas–liquid chromatography (GLC) after the formation of their acetyl, trimethylsilyl or trifluoroacetyl derivatives[6–8]. Josefsson[9] and Stabel[10] estimated the monosaccharides of DCHO in natural water by the use of trimethylsilylation. Eklund *et al.*[8] developed a method for sensitive GLC analysis of monosaccharides in sea-water using trifluoroacetyl derivatization and electron capture detection. It was difficult to determine accurately the monosaccharide concentrations using this method because a number of chromatographic peaks result from the anomers of each monosaccharide. Alditol-acetylation is suitable for natural water samples containing a complex mixture of organic matter, because only one peak appears for each monosaccharide. Good results were obtained with GLC using alditol-acetylation after hydrolysis of the DCHO in lake-water.

EXPERIMENTAL

The analysis of monosaccharides by GLC followed the method of Crowell and Burnett[7]. To determine its usefulness for the analysis of DCHO in natural water, the time of hydrolysis was studied.

The water samples were filtered through Whatman GF/C glass fibre filter, previously baked in a furnace at 450°C for 2 h. A 100- or 200-ml volume of filtered water sample was dried in a freeze dryer. Inositol was added to the dried sample as internal standard and dissolved in 1 *N* HCl. This material was transferred to a 10-ml glass ampoule and sealed under nitrogen. The sample was hydrolysed under nitrogen in 1 *N* HCl at 100°C. The hydrolysate was again dried and reduced with sodium borohydride for 1 h at 60°C. The reduced sample was applied to the top of a column (150 × 8 mm) of Dowex 50W-X8 cation exchange resin, which had previously been

0021-9673/80/0000–0000/$02.25

cleaned with 1 *N* sodium chloride solution, regenerated (to H^+) with 1 *N* HCl and rinsed to neutrality with distilled water. The monosaccharides were eluted with 25 ml of distilled water. The solution was evaporated to dryness, 20 ml of methanol added and re-evaporated to dryness. The dehydrated residue was transferred to a 1-ml glass ampoule with methanol and evaporated to dryness under vacuum. The residue was acetylated with 100 μl of acetic anhydride–pyridine (1:1) for 2 h at 100°C. The acetylation mixture was evaporated and the residue dissolved in 30 μl of chloroform. An aliquot of this solution was injected into the gas chromatograph for analysis.

The gas chromatograph used was a Shimadzu Model GC-6AM instrument equipped with a flame ionization detector. Chromatographic peak area measurements were made with a Shimadzu Model C-R1A chromatopac integrator. A glass column (2 m × 3 mm I.D.) packed with 5% OV-275 on Chromosorb W was employed at a nitrogen flow-rate of 40 ml/min. A temperature-programmed analysis from 160°C to 240°C at 2°C/min required 40 min to eluate the acetyl derivatives of eight monosaccharides and the internal standard inositol.

RESULTS

The alditol acetates of monosaccharides have been determined generally by GLC using Gas-Chrom Q with ECNSS-M as column packing[7,11]. Chromosorb W with silicone OV-275 was used in this experiment. The maximum temperature of use was 220°C in the case of ECNSS-M and 250°C for OV-275. Since the gas chromatography could be performed at higher temperature, the determination was completed in a shorter time.

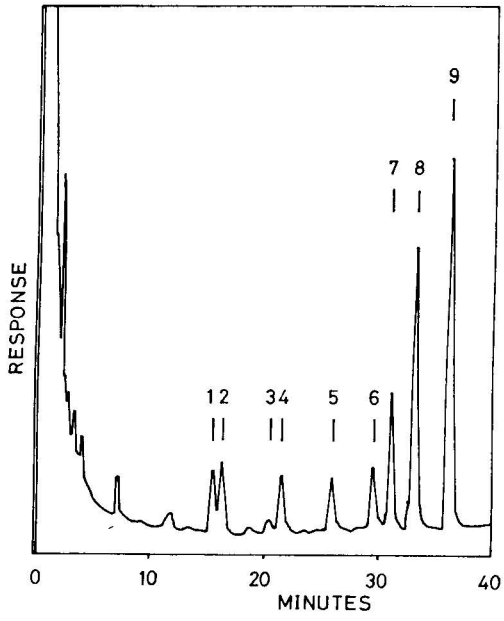

Fig. 1. Gas–liquid chromatography of alditol acetates of monosaccharides, formed by hydrolysis of DCHO in lake-water (taken from the surface of Lake Nakanuma, Japan, on May 26th, 1978). Peaks: 1 = rhamnose; 2 = fucose; 3 = ribose; 4 = arabinose; 5 = xylose; 6 = mannose; 7 = galactose; 8 = glucose; 9 = inositol internal standard.

Although there are lipids, amino acids, humic substances, etc., in addition to carbohydrates in natural water, the monosaccharides of the DCHO could be measured without clean-up. A typical chromatogram of monosaccharides of the DCHO in natural water is shown in Fig. 1.

The hydrolysis times of the DCHO in lake-water with 1 *N* HCl are shown in Table I. Stabel[10] analysed monosaccharide trimethylsilyl derivatives after hydrolysis of the DCHO in distrophic lake-water for 12 h with 1 *N* HCl. Handa[12] measured monosaccharide acetyl derivatives after hydrolysing the carbohydrates in lake sediment for 15 h with 1 *N* HCl. Hecky *et al.*[13] analysed the sugar composition of diatoms after hydrolysis for 4 h with 1.8 *N* HCl. After 7 h the hydrolysate of the DCHO with 1 *N* HCl had little effect on the colour developing activity of anthrone–sulphuric acid, but after 12 h it slightly decreased the activity. Three hydrolysis times, 7, 12 and 24 h, were studied. The results indicated that hydrolysis times of 12 and 24 h were too long for the DCHO in the lake-water. Thus, the concentrations of total monosaccharides after 12 and 24 h of hydrolysis were only 76% and 33% of those after 7 h.

TABLE I

LIBERATION OF MONOSACCHARIDES FROM DCHO IN LAKE-WATER AFTER DIFFERENT TIMES OF HYDROLYSIS WITH 1 *N* HCl

R = Rhamnose; F = fucose; Rb = ribose; A = arabinose; X = xylose; M = mannose; Ga = galactose; G = glucose.

Time (h)	*% liberated*								
	Total	*R*	*F*	*Rb*	*A*	*X*	*M*	*Ga*	*G*
7	100	100	100	100	100	100	100	100	100
12	76	91	93	11	70	70	89	98	83
24	33	43	39	10	66	15	36	40	30

The reproducibility of the concentrations of monosaccharides in the DCHO of Lake Suwako surface water by this method is shown in Table II. The average of the total monosaccharide concentrations was 4350 μg/l, the standard deviation 80 μg/l and the coefficient of variation 1.8%. The reproducibility for each mono-

TABLE II

REPRODUCIBILITY OF DETERMINATION OF MONOSACCHARIDES OF DCHO IN LAKE-WATER

$\bar{x}$ = Average; S.D. = standard deviation; C.V. = Coefficient of variation.

Sample No.	*Concentration (μg/l)*								
	Total	*R*	*F*	*Rb*	*A*	*X*	*M*	*Ga*	*G*
1	4270	523	287	140	64	238	259	1059	1698
2	4340	518	289	156	62	212	261	1085	1757
3	4430	546	296	167	69	264	287	1034	1766
$\bar{x}$	4350	529	291	154	65	238	269	1059	1740
S.D.	80	14.9	4.7	13.6	3.6	26.0	15.6	25.5	36.9
C.V. *(%)*	1.8	2.8	1.6	8.8	5.5	10.9	5.8	2.4	2.1

saccharide, fucose, glucose, galactose and rhamnose, was good; that of xylose was poorer but satisfactory. The results indicated the potential of this analytical method for the determination of dissolved carbohydrates in natural water.

ACKNOWLEDGEMENT

The author acknowledges Dr. Atsuo Tanaka, Mitsubishi-Kasei Institute of Life Sciences, for technical advise on carbohydrate analysis by gas chromatography.

REFERENCES

1 M. Ochiai, T. Nakajima and T. Hanya, *Jap. J. Limnol.*, 40 (1979) 185.
2 G. E. Walsh, *Limnol. Oceanogr.*, 10 (1965) 570.
3 K. Sugawara and E. Kamata, *J. Chem. Soc. Jap.*, 85 (1965) 1275.
4 N. Handa, *J. Oceanogr. Soc. Jap.*, 22 (1966) 79.
5 H. de Haan and T. de Boer, *Arch. Hydrobiol.*, 85 (1979) 30.
6 C. C. Sweeley, R. Bentley, M. Makita and W. W. Wells, *J. Amer. Chem. Soc.*, 85 (1963) 2497.
7 E. P. Crowell and B. B. Burnett, *Anal. Chem.*, 39 (1967) 121.
8 G. Eklund, B. Josefsson and C. Roos, *J. Chromatogr.*, 142 (1977) 575.
9 B. O. Josefsson, *Anal. Chim. Acta*, 52 (1970) 65.
10 V. H-H. Stabel, *Arch. Hydrobiol.*, 80 (1977) 216.
11 J. S. Sawardeker, J. H. Sloneker and A. Jeanes, *Anal. Chem.*, 37 (1965) 1602.
12 N. Handa, *Proc. Japan Acad.*, 53 (1977) 51.
13 R. E. Hecky, K. Mopper, P. Kilham and E. T. Degens, *Mar. Biol.*, 19 (1973) 323.

Journal of Chromatography, 194 (1980) 228–233
Elsevier Scientific Publishing Company, Amsterdam — Printed in The Netherlands

CHROM. 12,766

Note

Determination of furfural in spent sulfite liquor by gas chromatography

HENRY T. HOFFMAN, Jr.
American Can Company, P.O. Box 50, 469 North Harrison Street, Princeton, NJ 08540 (U.S.A.)
(First received April 20th, 1979; revised manuscript received February 18th, 1980)

Spent sulfite liquor (SSL) is a waste by-product of the manufacture of wood pulp by the acid sulfite process. Furfural is formed in the pulping process by a two-step reaction. Initially, hydrolysis converts some of the pentosan content of the pulp to pentoses which in turn are partially converted to furfural by dehydration. Evaporation of the sulfite liquor to increase its solids content results in additional conversion to furfural which collects in the condensate. A rapid and convenient method for estimation of furfural content at any stage of the process is essential for study of parameters which influence furfural formation.

Analytical methods for furfural were reviewed by Madden[1]. Most methods are based on reactions of the ring or of the aldehyde function although there is a UV method based on the characteristic absorption of furfural at 276 nm. The gas chromatographic (GC) determination of furfural in condensates from the evaporation of SSL has been reported by Rexfelt and Samuelson[2,3]. Hrutfiord and McCarthy also used GC to determine furfural in the steam volatile fraction of SSL[4].

Initially, furfural analysis was attempted by direct injection of diluted SSL samples. Poor peak area reproducibility, due to ghosting was observed. It is believed that the ghosting arises from retention of furfural by sample solids residue deposited in the injection port. The source of the retained furfural may be either free furfural initially present in the SSL sample or may be previously unconverted pentoses which convert to furfural in the hot (260 °C) injection port.

The problem of peak area reproducibility, combined with the possibility that peak area may not be representative of the initial furfural content of the sample, led to the conclusion that extraction of the furfural would be necessary to eliminate these difficulties.

An extraction procedure using chloroform to extract the furfural quantitatively from the SSL was developed. The chloroform extracts give reproducible furfural peak areas, and the extraction step ensures that no additional furfural formation takes place in the injection port since chloroform will not extract significant quantities of pentoses from the SSL.

Method development included determination of the precision of the method at two concentration levels of furfural over a period of several days. Also included were studies to determine the effect of furfural concentration level and pH on efficiency of the chloroform extraction.

0021-9673/80/0000–0000/$02.25

EXPERIMENTAL

Instrumentation and operating parameters

A Perkin-Elmer 900 gas chromatograph with flame ionization detector and a Hewlett-Packard 3370B integrator were used. The column was 6 ft. × 1/8 in. O.D. stainless steel packed with 60–80 mesh Porapak Q. Operating parameters were: column temperature, 240 °C; injection port temperature, 260 °C; detector temperature, 300 °C; carrier gas, nitrogen at 30 ml/min; sensitivity, $5 \cdot 10^{-10}$ A f.s.

Reagents, standards and samples

Furfural was obtained from Aldrich (Milwaukee, WI, U.S.A.; 99%). This material was used for preparation of standards and known addition experiments without purification.

Chloroform was obtained from Burdick & Jackson Labs. (Muskegon, MI, U.S.A.). Ethanol preservative in the chloroform does not interfere with the determination.

Sodium chloride (reagent grade) was obtained from Baker (Phillipsburg, NJ, U.S.A.).

A master solution of furfural in chloroform (nominal concentration, 1 μg/μl) was prepared by accurately weighing about 100 mg of furfural in a 100-ml volumetric flask and diluting to volume with chloroform. Appropriate dilutions of this solution were used for standards. Including the master solution, the concentration range (0.02–1 μg/μl) of these standards brackets the expected concentration range of furfural in the chloroform sample extracts.

To establish a working concentration range for the method, a hardwood SSL, SSL-A, was used "as received" for the high furfural concentration level sample. SSL-B, the low concentration level sample, was prepared from SSL-A by steam stripping of a major portion of the furfural. Samples with known additions of furfural for recovery experiments were prepared from SSL-A and SSL-B.

For studies of the effect of pH on extraction efficiency, a series of samples with pH ranging from 1.03 to 5.03 were prepared from SSL-A by pH adjustment with 1 *M* sodium hydroxide or 1 *M* sulfuric acid and dilution with water to give a dilution factor of 0.5. A control sample, diluted without pH adjustment, was included.

Extraction procedure

If necessary, dilute SSL samples so that furfural concentration is below 0.8 mg/ml. The pH of solutions can range from 1.0 to at least 5.0. Use volumetric pipets to transfer the SSL sample and chloroform to a screw-cap test tube. The chloroform–SSL volume ratio can be varied, depending upon the furfural concentration of the sample. For the samples reported here, the ratio was 2:3 for the dilute sample, SSL-B, and 2:2 for the more concentrated sample, SSL-A. Add approximately 0.5 g sodium chloride to the mixture, cap tube, and mix contents of the tube on a tube mixer for 2 min. The sodium chloride is necessary to make extraction of the furfural quantitative. Centrifuge for 2 min. The excess salt collects at the liquid–liquid interface. Use a disposable pipet to transfer the chloroform (lower) layer to a sample vial and cap the vial tightly.

Measurement procedure

It is preferable to use the solvent flush method for sample injection[5]. Inject nominal 5 μl sample volumes for both furfural standard solutions and chloroform sample extracts. Determine weight of furfural injected in GC sample extracts from calibration curve prepared from standard solution data. Calculate the furfural concentration in the original SSL sample from the following equation:
Furfural concentration in SSL (μg/μl or mg/ml) = (Wt. furfural inj. (μg)/Vol. GC sample (μl))·(Vol. chloroform (ml)/Vol. SSL (ml)).

RESULTS AND DISCUSSION

A typical calibration curve is shown in Fig. 1. Fig. 2 shows a chromatogram of a chloroform extract of SSL-A. The furfural elutes on the tail of the chloroform peak, but uncertainties in area integration of this type peak were reduced by operating the integrator in the tangent skimming mode.

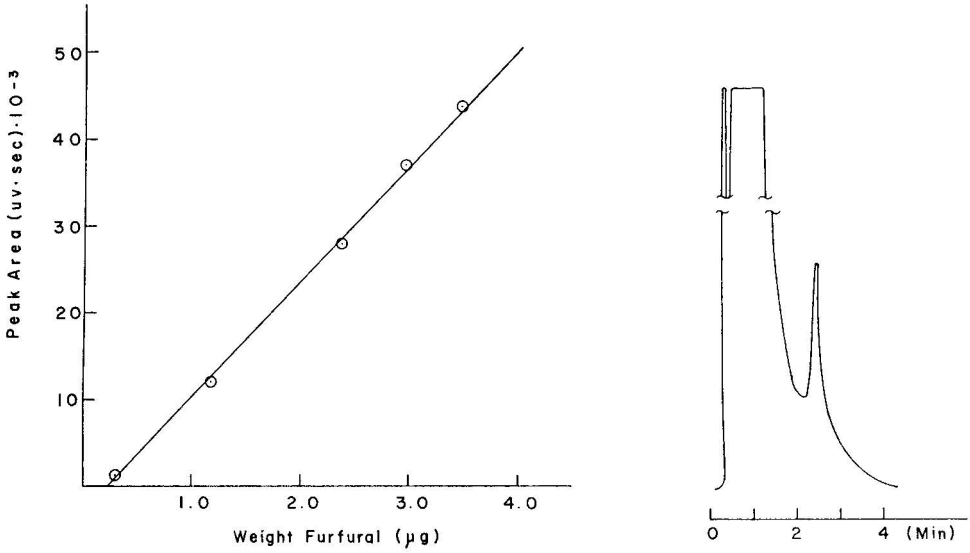

Fig. 1. Calibration curve, a plot of peak area *versus* weight of furfural, from furfural standards in chloroform.

Fig. 2. Gas chromatogram of chloroform extract of SSL. The retention time of furfural peak is 2.48 min.

A series of repeat runs were made in which SSL-A and SSL-B were analyzed on successive days to determine the precision of the method. A new calibration curve and fresh chloroform extracts were prepared at the start of each day's runs. Four replicate determinations on each sample were made each day. Results of these analyses are shown in Table I.

From Table I it is seen that the precision of the determination at the higher concentration level is about twice that of the lower concentration level (C.V., 6% *versus* 12.5%). This is expected because of the inevitable loss of precision that accompanies

TABLE I

RESULTS OF PRECISION STUDIES FOR THE DETERMINATION OF FURFURAL IN SSL

S.D. = Standard deviation; C.V. = coefficient of variation.

Furfural concentration (mg/ml)							
SSL-A				*SSL-B*			
Run	*Day 1*	*Day 2*	*Day 3*	*Run*	*Day 1*	*Day 2*	*Day 3*
1	0.47	0.51	0.56	1	0.041	0.053	0.045
2	0.49	0.51	0.49	2	0.044	0.053	0.045
3	0.45	0.52	0.49	3	0.045	0.055	0.038
4	0.48	0.50	0.47	4	0.045	0.057	0.046
Overall mean		0.50		Overall mean		0.047	
S.D.		0.030		S.D.		0.0059	
C.V.		6.0%		C.V.		12.5%	

determinations at lower concentration levels. SSL-B has a furfural concentration about tenfold lower than SSL-A. The furfural concentration of SSL-B probably represents the lower concentration limit that can be determined under the stated experimental conditions.

Furfural recovery experiments were carried out to determine the efficiency of the extraction procedure. The SSL samples with known furfural additions (described earlier) were used for this study. Four replicate runs were made for each sample. The analyses, including preparation of fresh extracts, were repeated the next day. The theoretical furfural concentration of each sample was assumed to be the sum of the average experimentally determined concentration of the original samples (Table I) plus the known addition. Results are summarized in Table II.

TABLE II

FURFURAL RECOVERY DETERMINATIONS OF SSL SAMPLES WITH KNOWN ADDITIONS

Furfural concentration (mg/ml)							
SSL-A with known addition (0.30 mg/ml added furfural)				*SSL-B with known addition (0.45 mg/ml added furfural)*			
Day 1	*Day 2*			*Day 1*	*Day 2*		
0.76	0.80			0.49	0.49		
0.73	0.76			0.46	0.53		
0.76	0.75			0.52	0.48		
0.78	0.74			0.52	0.48		
Overall mean			0.76	Overall mean			0.50
Theoretical conc.		(0.50 + 0.30)	0.80	Theoretical conc.		(0.047 + 0.45)	0.50
Recovery			95%	Recovery			100%

The recovery data in Table II show that the extraction efficiency ranged from 95 to 100% for the concentration range studied. The lower recovery at the higher concentration level indicates that this level is somewhat high for maximum quantitative

recovery by chloroform extraction under the experimental conditions. Therefore, it is recommended that SSL samples be diluted with water before extraction to give a furfural concentration less than 0.8 mg/ml to ensure that maximum extraction of fufural by chloroform is achieved.

The question was raised concerning the effect of pH on extraction efficiency because of possible interference from the furfural bisulfite addition compound (α-hydroxy-2-furanmethanesulfonic acid) which is known to exist in equilibrium with furfural in aqueous solutions containing bisulfite ions[6]. This equilibrium is pH dependent because bisulfite ion concentration varies markedly with pH[7,8]. To determine the effect of pH on extraction efficiency, furfural was determined in a series of pH adjusted solutions (described earlier) prepared from SSL-A. Results of these determinations are shown in Table III.

TABLE III

EFFECT OF pH ON EXTRACTION EFFICIENCY, SSL-A FURFURAL CONCENTRATION *versus* pH ADJUSTED SAMPLES

Values are the average of two determinations.

Sample pH	*SSL-A Furfural conc. (mg/ml)*
1.03	0.54
1.89 (Control)	0.53
2.93	0.55
5.03	0.51
	Mean 0.53

The mean value is within the range of the standard deviation of the previous determinations for this sample (Table I). It is concluded that pH does not affect extraction efficiency significantly in the pH range (1.03–5.03) investigated in this study. This is not unexpected because reduction of furfural concentration in the SSL by chloroform extraction will cause the equilibrium to shift towards furfural and reduce the concentration of the addition compound to insignificant levels.

A GC method for furfural in SSL which ensures that the furfural content of the sample is not altered by high temperatures of the instrument, has been described. The simple extraction procedure for sample preparation and rapidity of analysis make it particularly useful for monitoring the effect of process variables on furfural content of the SSL.

ACKNOWLEDGEMENTS

The author wishes to thank Mr. Harvey Pobiner for helpful discussion and support, Dr. Marcel Faber who pointed out the need for a rapid furfural method and furnished samples for analysis, and Miss Eddie Johnson, Mr. John Harrison, and Mr. Ronald Chen for experimental assistance.

REFERENCES

1 J. W. Madden, in F. D. Snell and L. S. Ettre (Editors), *Encyclopedia of Industrial Chemical Analysis*, Vol. 13, Interscience, New York, London, Sydney, Toronto, 1971, p. 232.
2 J. Rexfelt and O. Samuelson, *Sven. Papperstidn.*, 73 (1970) 689.
3 J. Rexfelt and O. Samuelson, *Sven. Papperstidn.*, 75 (1972) 299.
4 B. F. Hrutfiord and J. L. McCarthy, *Tappi*, 47 (1964) 381.
5 R. F. Kruppa and R. S. Henly, *Amer. Lab.*, 3 ,No. 5 (1971) 41.
6 E. Adler, *Sven. Papperstidn.*, 50, No. 11B (1947) 9.
7 *Instruction Manual, Sulfur Dioxide Electrode Model 94-65*, Orion Research, Cambridge, MA, 1973, p. 12.
8 J. F. Harris and L. L. Zoch, *Anal. Chem.*, 34 (1962) 201.

Journal of Chromatography, 194 (1980) 234–238
Elsevier Scientific Publishing Company, Amsterdam — Printed in The Netherlands

CHROM. 12,756

Note

Fluorimetric and high-performance liquid chromatographic determination of harmane alkaloids in *Peganum harmala* cell cultures

FLORENZ SASSE*, JOACHIM HAMMER and JOCHEN BERLIN
Gesellschaft für Biotechnologische Forschung, Mascheroder Weg 1, D-3300 Braunschweig (G.F.R.)
(Received February 15th, 1980)

Cultured cells, even when grown in one flask, are known to differ greatly in their biochemical potential for producing secondary compounds[1]. It has been shown that highly productive cell clones can be selected from wild-type populations by analytical means[1,2]. An analytical selection method should be as simple and as sensitive as possible for screening a large number of small samples in a short time. In connection with studies on cell cultures of *Peganum harmala*, it became necessary to establish a method for screening cell colonies for their harmane alkaloids contents.

According to Gröger[3], *Peganum* plants contain the harmane derivatives harmine, harmol, harmaline and harmalol, which can be divided in two groups according to their oxidation stage (Fig. 1).

The quantitative determination of the alkaloids in extracts by measuring their UV absorption is possible only after separation[4,5] and is not very sensitive. However, harmane alkaloids are fluorescent compounds with characteristic emission spectra. This fact was used to establish a rapid method for distinguishing between both groups of alkaloids in the same unpurified cell extract. To quantitate all four harmane derivatives of cell culture extracts the alkaloids were separated by high-performance liquid chromatography (HPLC).

EXPERIMENTAL

Materials

Alkaloids were obtained from Sigma (St. Louis, MO, U.S.A.). All other chemicals were purchased from different commercial sources. Cell cultures of *Peganum harmala* were initiated from different organs of sterile grown seedlings. The cultures were maintained on a Murashige–Skoog medium[6] with 1.8 μM 2,4-D. Methanolic cell extracts (25 mg dry weight per 25 ml) were centrifuged, filtered through a 0.45-μm cellulose filter and diluted with methanol or water.

Fluorescence measurement

A Jobin Yvon JY 3D spectrofluorimeter with excitation and emission monochromators was used.

0021-9673/80/0000–0000/$02.25

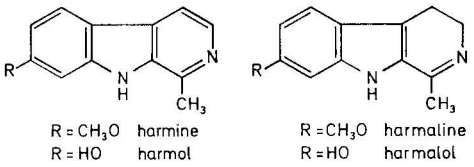

Fig. 1. The alkaloids of the harmane group.

High-performance liquid chromatography

An LDC Model II G Constametric pump in conjunction with a Rheodyne Model 7120 syringe-loading injector was used. Detection was effected by means of an LDC Model 1204 spectromonitor III set at 330 nm and a JY 3D spectrofluorimeter. Chromatography was carried out using a 25-cm Merck RP-8 column (7 μm) combined with an RP-2 pre-column (30 μm) and isocratic elution with methanol–water–formic acid (166:34:1) buffered with triethylamine at pH 8.5. The flow-rate was 1 ml/min, and the column pressure was 1670 p.s.i.

RESULTS AND DISCUSSION

Fluorimetric determination

The fluorescence spectra of the four harmane alkaloids are shown in Fig. 2. In methanolic solution harmine and harmol had nearly the same maximum at 355 nm with optimal excitation at 304 nm. Harmaline and harmalol showed no emission under these conditions. They fluoresced maximally at 475 nm, when excited at 396 nm, whereas in this instance harmine and harmol did not show any fluorescence. The spectra of harmaline and harmalol were similar. The different fluorescence spectra of harmine/harmol and harmaline/harmalol allowed the determination of the two groups of alkaloids in the parts per billion (10^9) range without separation.

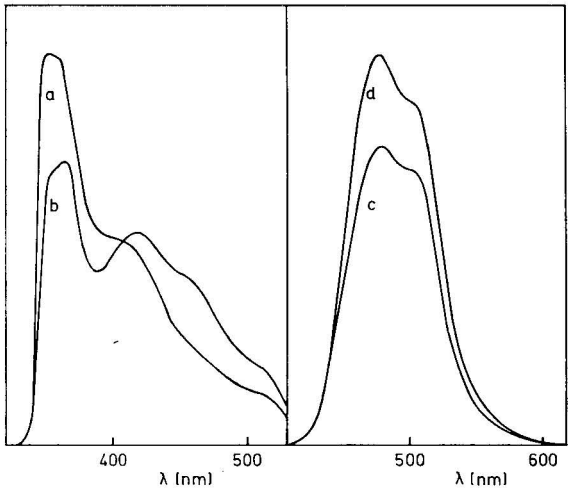

Fig. 2. Fluorescence spectra of harmine (a), harmol (b), harmaline (c) and harmalol (d) in methanol. Excitation at 304 nm (a,b) and 396 nm (c,d).

In the crude *Peganum* cell extracts tested, the fluorescence at 355 nm was masked by that of other compounds. However, dilution with water led to bathochromic shift of the fluorescence spectra of harmine and harmol (Fig. 3). Thus, solutions with a water to methanol ratio of 9:1 and higher did not fluoresce at 355 nm. The maximum shifted to 425 nm with optimal excitation at 324 nm. In this range other compounds of the cell extract did not interfere. The fluorescence spectra of harmaline and harmalol were not altered by dilution with water. Quenching effects were determined by measuring the fluorescence increase after the addition of a known amount of the alkaloid to a sample and comparing it with the expected value.

Changing the pH of the solution did not alter the fluorescence spectra, but the emission intensity decreased in solutions above pH 6.5. Therefore, the extracts were diluted with phosphate buffer (0.2 *M*, pH 5.0) to exclude errors caused by pH variations. The described conditions provided a simple method for screening a large number of samples for their harmane alkaloid contents. The relative standard deviation of rapid assays, *i.e.*, extraction with methanol, dilution with buffer and measuring the fluorescence with internal standardization, was less than 10%. Standard solutions of harmine and harmaline were prepared and the measured fluorescence values were expressed as harmine and harmaline equivalents. Systematic errors were thus introduced, because the emission intensity of harmine is higher than that of harmol, but it was negligible to purpose of our investigations, as in *Peganum* cultures the harmol concentration was only 5% that of harmine. Harmaline and harmalol were equal in intensity. Calibration graphs for harmine (425 nm) and harmaline (475 nm) were linear up to 1 and 3 μg/ml, respectively. The detection limit was below 0.5 μg/ml, at which concentration the signal-to-noise ratio was 4.

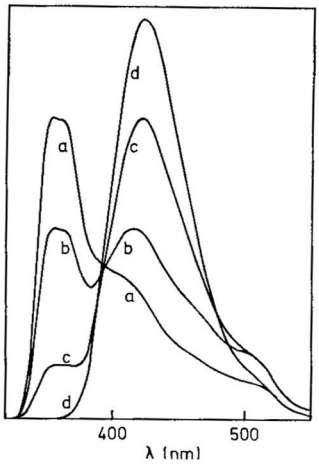

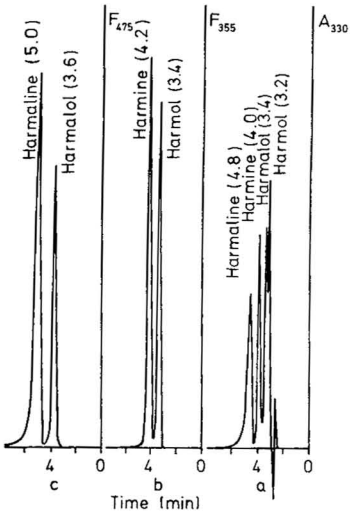

Fig. 3. Shift of harmine fluorescence with variation in the proportions of methanol and water in the solution (a, 10:0; b, 9:1; c, 7:3; d, 1:9). Excitation at 304 nm.

Fig. 4. HPLC separation of a standard mixture of harmane alkaloids on a reversed-phase column. Conditions as described in the text. Detection was effected by measuring absorbance (a, 330 nm) and fluorescence (b, 355 nm, excitation 304 nm; c, 475 nm, excitation 396 nm). Retention times (minutes) are given in parentheses.

High-performance liquid chromatography

Fig. 4 shows the separation of harmol, harmalol, harmine and harmaline. All four alkaloids could be detected by measuring the absorbance at 330 nm. This wavelength was chosen for measuring the four alkaloids in one chromatographic run. In methanol solution the absorbance maximum of harmine and harmol is at 240 nm and that of harmaline and harmalol at 380 nm. As for the fluorescence spectra, we found a bathochromic shift of the absorbance spectra of harmine and harmol in aqueous solutions. Using the above fluorimetric systems a better quantitative measurement was possible. Furthermore, fluorimetric determination increased the sensitivity by 100-fold. The detection limit was below 10 pg. For both methods the calibration graphs showed linear regression coefficients between 0.993 and 0.99998 in a tested range from 1 to 200 ng.

Fig. 5 shows a chromatogram of a methanolic extract of a *Peganum harmala* suspension culture. Harmalol, harmine and harmaline were clearly detected. However, at 355 nm we found another peak due to an unknown compound with a retention time 0.4 min less than that of harmol, which masked the small harmol signal. On measuring the above fluorescence maximum of harmine and harmol at 425 nm, the

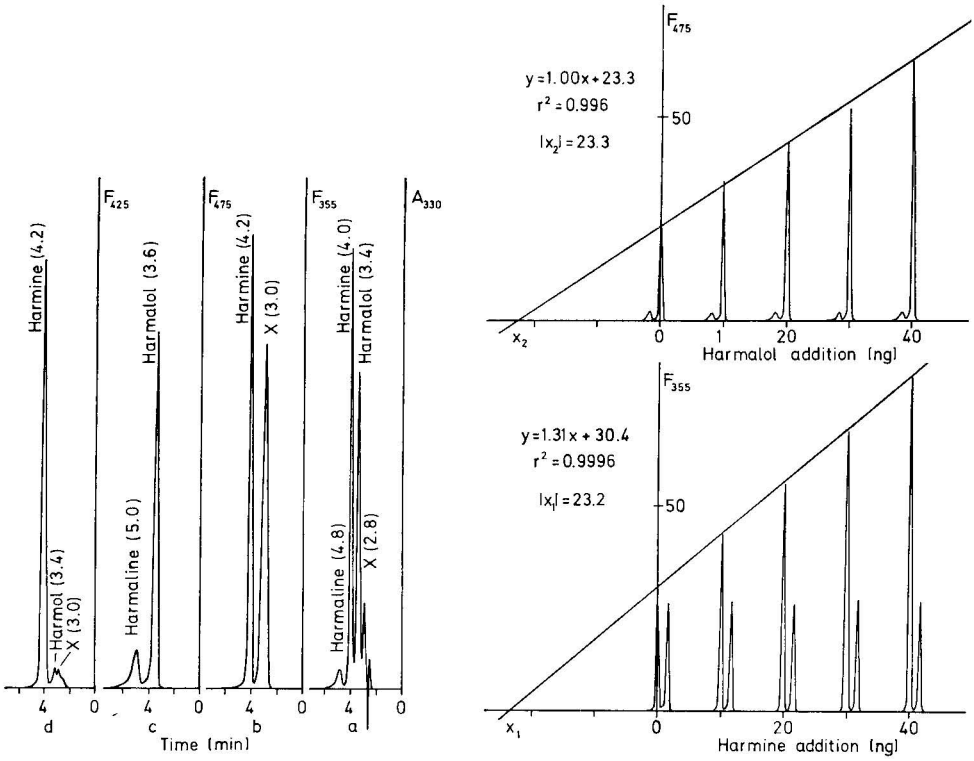

Fig. 5. Fluorimetric detection of HPLC-separated methanolic extract of a cell culture of *Peganum harmala*. Chromatographic conditions as in Fig. 4. Detection: a, absorbance (330 nm); b, c and d, fluorescence (b, 304/355 nm; c, 396/475 nm; d, 324/425 nm). Retention times (minutes) are given in parentheses.

Fig. 6. Determination of harmine (a) and harmalol (b) by internal calibration.

size of the unknown peak decreased considerably, and the small harmol signal could be detected.

The HPLC-separated alkaloids were quantitatively determined by internal calibration. Thus, the same conditions for the standard and the compound to be measured were provided. Fig. 6 shows the determination of fluorimetrically detected harmalol and harmine. It also provides proof of the identity of the measured compounds. The two other alkaloids could also be identified in this way. For routine determinations external calibration is preferable.

Peganum cells cultured on a standard medium contained mainly harmine and harmalol, and only trace amounts of harmol and harmaline. This is in agreement with results found by Nettleship and Slaytor[5], while in other *Peganum* cultures only harmine was detected[4].

The alkaloid pattern in seeds is different, harmaline and harmine being the predominant alkaloids[3,7]. The alkaloid patterns of intact plants seem to vary in a wide range[3–5], but harmine is always the main compound and harmalol is of lesser importance.

A comparison of the results obtained by determining the alkaloids in crude extracts and after HPLC showed good correspondence between the two methods and provided proof of the practicability of the simple fluorimetric method when screening of cell lines is needed. The determination of the individual alkaloids by HPLC is possible.

ACKNOWLEDGEMENTS

We thank Mrs. Annegret Bischoff for establishing the cultures, and Miss Marita Buchholz for skillful technical assistance.

REFERENCES

1 M. H. Zenk, in T. A. Thorpe (Editor), *Frontiers of Plant Tissue Culture 1978, Proc. 4th Int. Congress of Plant Tissue and Cell Culture*, The International Association for Plant Tissue Culture, Calgary, 1978, p. 1.
2 T. Ogino, N. Hiraoka and M. Tabata, *Phytochemistry*, 17 (1978) 1907.
3 D. Gröger, *Planta Med.*, 7 (1959) 461.
4 E. Reinhard, G. Corduan and O. H. Volk, *Phytochemistry*, 7 (1968) 503.
5 L. Nettleship and M. Slaytor, *J. Exp. Bot.*, 25 (1974) 1114.
6 T. Murashige and F. Skoog, *Physiol. Plant.*, 15 (1962) 473.
7 A. Schipper, *Untersuchungen an Peganum harmala, Dissertation*, University of Würzburg, Würzburg, 1960.

Journal of Chromatography, 194 (1980) 239–244
Elsevier Scientific Publishing Company, Amsterdam — Printed in The Netherlands

CHROM. 12,722

Note

Intermediate- and large-scale reversed-phase preparative high-performance liquid chromatography on an axially compressed column: a facile, quantitative separation of 7α- and 7β-methyl-17β-acetoxy-3-oxoandrost-4-enes*

F. GASPARRINI*, S. CACCHI, L. CAGLIOTI, D. MISITI and M. GIOVANNOLI
Istituto di Chimica Organica, Via Castro Laurenziano 9, 00161 Rome (Italy)
(Received February 4th, 1980)

Analytical high-performance liquid chromatography (HPLC) is a widely applied technique[1–3] and its obvious extension, preparative HPLC, is now well developed and a number of efficient commercial units are available. The high performance of this technique may be utilized successfully in the quantitative separation of complex reaction mixtures, purification of compounds with low α values being readily achieved. Some papers concerning the application of normal-phase preparative HPLC to a number of difficult separations, using radial compressed cartridges (5 × 30 cm), have been published[4–7].

Some separations on pre-packed commercially available semi-preparative columns using both normal and reversed phases have also been reported[8–12]. However, it must be emphasized that all of the above separation procedures use pre-packed commercially available cartridges or columns of fixed length and supports and therefore they are less versatile than a system which allows one to pack columns of convenient lengths with suitable supports.

Such a separation system, using axial compression[13,14], has recently been introduced with 2- and 4-cm I.D. columns by Jobin-Yvon.

Here we report the application of reversed-phase preparative HPLC on axially compressed columns to the separation of 7α- and 7β-methyl derivatives of 17β-acetoxy-3-oxoandrost-4-ene and side-reaction products obtained by reaction of 17β-acetoxy-3-oxoandrosta-4,6-diene with lithium dimethylcuprate.

EXPERIMENTAL

Solvents for analytical separations (methanol, ethyl acetate and *n*-hexane) were of LiChrosolv grade (Merck, Darmstadt, G.F.R.), and the water used was doubly distilled and deionized. Methanol for preparative purposes was of RPE-ACS grade (Carlo Erba, Milan, Italy).

Analytical separations were performed on columns pre-packed (Policonsult, Rome, Italy) with LiChrosorb Si-60 (10 μm), LiChrosorb RP-8 (10 μm) and LiChrosorb RP-18 (7 μm) (Merck) using a Waters Model ALC/GPC-202 chromatograph (Waters

* Dedicated to Professor L. Panizzi on the occasion of his 70th birthday.

0021-9673/80/0000–0000/$02.25

Assoc., Milford, MA, U.S.A.) equipped with a U6-K universal injector, a Model M6000 solvent delivery system, a Model 450 differential UV detector and a Model 401 refractive index (RI) detector.

Preparative separations were performed on columns packed with LiChrosorb RP-18 (10 μm) and LiChroprep RP-18 (25–40 μm) (Merck) using a Miniprep LC (2-cm I.D. column) or a Chromatospac Prep 10 chromatograph (4-cm I.D. column), both from Jobin-Yvon (Longjumeau, France), equipped with an RI detector.

The preparative column was packed as follows. A suspension of the desired amount of packing material [LiChrosorb RP-18 (10 μm), LiChroprep RP-18 (25–40 μm)] in methanol–0.1% sodium acetate solution (80:20) was maintained in a ultrasonic bath for 5 min, poured into the column, axially compressed until a selected packing pressure was reached, and finally conditioned by passing 2–3 times the interstitial volume of eluent. The same column can be used successfully for several injections and can be easily regenerated by passing 2–3 times the interstitial volume of methanol or acetonitrile. In order to recover the packing material, the injector was removed from the column and the piston was allowed to push out the compressed adsorbent.

Generally, the loading capacities for 2- and 4-cm I.D. columns lie in the ranges 1 mg–1 g and 50 mg–10 g, respectively.

RESULTS AND DISCUSSION

17β-Acetoxy-3-oxoandrosta-4,6-diene (1)[15] reacts with lithium dimethylcuprate (Me_2CuLi) to give 7α- and 7β-epimeric compounds (2) in 77% overall yield* (53:47 epimeric ratio) through regioselective 1,6-conjugate addition[16,17]. The main isolated by-products (15% overall yield)* are the two epimeric compounds (3), presumably derived from hydrolytic decomposition of (2) during the work-up (Scheme 1).

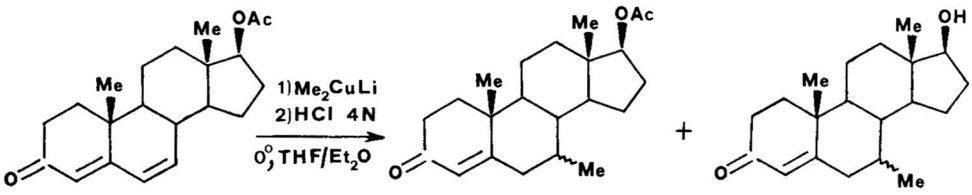

1 2: α (41%) + β (36%) 3: α (7%) + β (8%)

Scheme 1

In a typical small-scale run, to a stirred suspension of purified copper(I) iodide (2.32 g, 12.15 mmol) in anhydrous diethyl ether (13 ml), 1.64 *M* methyllithium (15 ml) in diethyl ether was added at a temperature not exceeding 0 °C and under argon. Then, at the same temperature, was added a tetrahydrofuran solution (5 ml) of 17β-acetoxy-3-oxoandrosta-4,6-diene (0.5 g, 1.52 mmol). After 10 min the reaction mixture was syphoned into stirred 4 *N* hydrochloric acid and extracted with diethyl ether.

* Yields were calculated using the external standard method.

The organic layer was separated, treated with ammonia–ammonium chloride buffer (pH 8), washed with water and dried over anhydrous sodium sulphate. The solvent was removed at reduced pressure to leave a solid residue (0.490 g), which was analysed by analytical normal- and reversed-phase HPLC under isocratic conditions (Figs. 1 and 2). The best separation of the components of the reaction mixture was obtained by using reversed-phase conditions mainly with an RP-18 support, as shown in Fig. 2a. Even using an RP-8 column a good separation was obtained (Fig. 2b); however, the utilization of an RP-18 column allows a shorter analysis time and a higher selectivity. As a further advantage, the separation on an RP-18 column utilized a mobile phase enriched in methanol; from a preparative standpoint this fact increases the loading of the column.

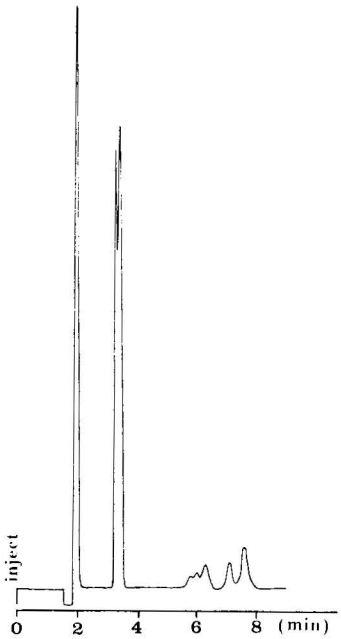

Fig. 1. Results for reaction mixture using normal-phase analytical LC conditions. Packing: LiChrosorb Si-60 (7 μm). Column: 25 cm × 3.0 mm. Solvent: *n*-hexane–ethyl acetate (85:15). Flow-rate: 1.0 ml/min. Detector: RI (×32) Temperature: ambient.

Even the preparative separation was effected by reversed-phase HPLC using axially compressed, high-efficiency 2- or 4-cm I.D. columns, packed with LiChrosorb RP-18 (10 μm) or LiChroprep RP-18 (25–40 μm), respectively. The separation attained with the 2-cm I.D. column is illustrated in Fig. 3a, while the corresponding analytical separation, using the same eluent, is shown in Fig. 3b.

It must be emphasized that the preparative chromatographic conditions were selected in order to achieve a good separation of the main components with the lowest waste of solvent and time (about 0.7 g of mixture were purified in less than 50 min on the 4-cm I.D. column). Under the reported conditions a 95% recovery of products with purity greater than 99% was attained.

The isolated compounds (2α) and (2β) were identified from elemental analysis

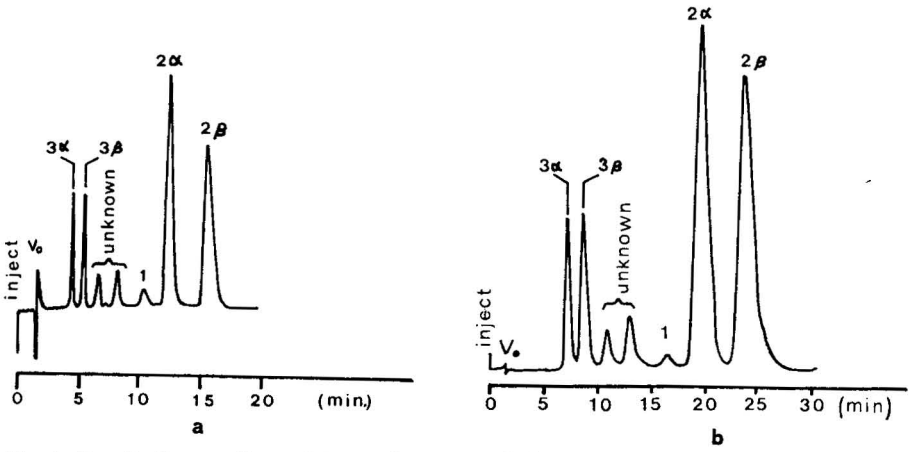

Fig. 2. Results for reaction mixture using reversed-phase analytical LC conditions. (a) Packing: LiChrosorb RP-18 (7 μm). Column: 25 cm × 4.6 mm I.D. Solvent: methanol–water (75:25). Flow-rate: 2.0 ml/min. Detector: RI (×8). Temperature: ambient. (b) Packing: LiChrosorb RP-8 (10 μm). Column: 25 cm × 4.6 mm I.D. Solvent: methanol–water (70:30). Flow-rate: 2.0 ml/min. Detector: RI (×8). Temperature: ambient.

and spectral data. The configuration of the 7-methyl groups was determined by comparison of ^{1}H and ^{13}C NMR spectra of the isolated products with those of known products of similar structure, such as 17β-hydroxy-7β,17-dimethyl-3-oxoandrost-4-ene (calusterone) (4β)[18] and 17β-hydroxy-7α,17-dimethyl-3-oxoandrost-4-ene (bolasterone) (4α)[18]. The data are listed in Table I.

The structures of the by-products (3α) and (3β) were determined from their mass and ^{1}H NMR spectra and by comparison with products derived from hydrol-

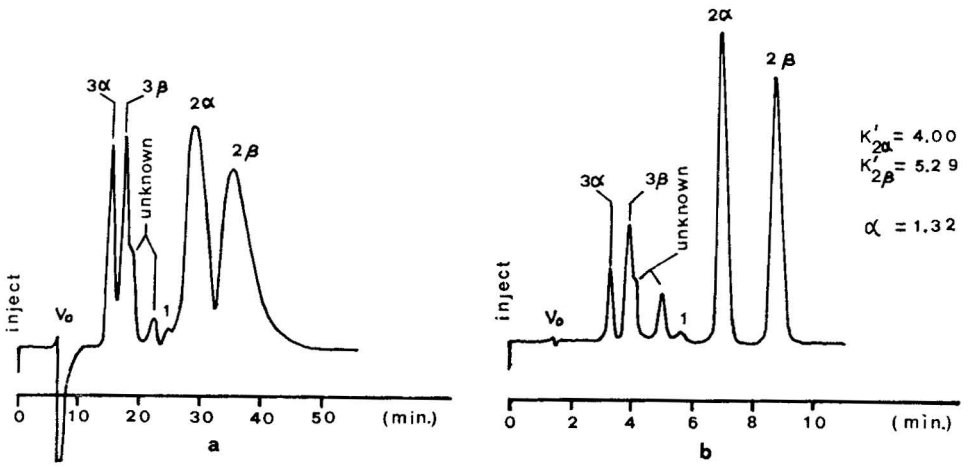

Fig. 3. (a) Result for reaction mixture using preparative LC conditions. Packing: LiChrosorb RP-18 (10 μm), 30 g. Column: 20 cm × 2.0 cm I.D. (P_i = 13 bar). Solvent: methanol–water (80:20). Detector: RI (×20). Flow-rate: 5.5 ml/min (P_e = 7.2 bar). Amount: 0.120 g (1.2 ml of methanol). Temperature: ambient. (b) Results for reaction mixture using analytical LC conditions. Packing: LiChrosorb RP-18 (10 μm). Column: 25 cm × 4.6 mm I.D. Solvent: methanol–water (80:20). Detector: RI (×8). Flow-rate: 2.0 ml/min. Temperature: ambient.

TABLE I

SIENIFICANT ^1H AND ^{13}C NMR CHEMICAL SHIFTS[19] OF THE MAIN PRODUCTS ISOLATED THROUGH PREPARATIVE HPLC

d = doublet; bs = broad singlet.

Compound No.	*^1H NMR ($CDCl_3$) (ppm, TMS)*		*^{13}C NMR ($CDCl_3$) (ppm, TMS)*			α_D*	*m.p.*** *(°C)*
	H-4	*7-CH_3*	*7-CH_3*	*CH_3-18*	*CH_3-19*		
4α	5.73 (d, J = 1.8 Hz)	0.75 (d, J = 7 Hz)	12.6	13.8	17.8	+88[18]	158–160[18]
2α	5.72 (d, J = 1.8 Hz)	0.81 (d, J = 7 Hz)	11.9 or 12.7	12.7 or 11.9	17.8	+89	Oil
4β	5.70 (bs, $W_{\frac{1}{2}}$ = 3 Hz)	1.03 (d, J = 5 Hz)	16.5	13.2	21.9	+56[18]	125–127[18]
2β	5.70 (bs, $W_{\frac{1}{2}}$ = 3 Hz)	1.03 (d, J = 5 Hz)	17.5	12.2	22.9	+79	142–143

* Rotations were determined in chloroform in 1-dm tubes at concentrations of 0.8–1.2 mg/ml.

** Melting points are uncorrected and were determined with a Büchi apparatus.

ysis of (2α) and (2β). The unreacted starting material was identified by its capacity factor (k') and the UV spectrum of the eluted peak in analytical HPLC (see Fig. 2a).

Analogous results were obtained in the purification of mixtures derived from 1,6-conjugate addition to 17β-hydroxy-17-methyl-3-oxoandrosta-4,6-diene[18,20] and 11β,17β-dihydroxy-17-methyl-3-oxoandrosta-4,6-diene[18].

CONCLUSIONS

The simple and fast separation procedure described may be proposed as useful substitute for pre-packed systems when complex reaction mixtures must be purified. The high efficiency of axially compressed columns allows a peak resolution comparable to that obtainable under analytical conditions; thus, the isolation of reaction products of high purity and in almost quantitative yield may be easily attained. Even by-products and trace amounts of impurities can be isolated. Further, as the utilization of 4- or 8-cm I.D. columns makes "large-scale" separations feasible, this method may be the separation procedure of choice for the purification of expensive fine chemicals.

Work is in progress to extend the application of axially compressed columns to the purication of complex mixtures of organometallic compounds, carbohydrates, antibiotics, etc., using a number of functionalized bonded phases (diol, CN, NH_2, etc.)[21].

ACKNOWLEDGEMENTS

We thank Dr. Giovanna Cancelliere and Dr. Antonio Arcadi for their technical assistance.

REFERENCES

1 L. R. Snyder and J. J. Kirkland, *Introduction to Modern Liquid Chromatography*, Wiley, New York, 1974.

2 S. G. Perry, R. Amos and P. I. Brewer, *Practical Liquid Chromatography*, Plenum/Rosetta, New York, 1973.

3 G. L. Hawk, *Biological/Biomedical Applications of Liquid Chromatography*, Marcel Dekker, New York, 1979.
4 M. J. Pettei, F. G. Pilkiewicz, K. Nakanishi, *Tetrahedron Lett.*, (1977) 2083.
5 M. A. Adams and K. Nakanishi, *J. Liquid Chromatogr.*, 2 (1979) 1097.
6 S. S. Singer and G. M. Singer, *J. Liquid Chromatogr.*, 2 (1979) 1219.
7 W. M. Waddel, M. M. Dawson, D. L. Hopkins, K. L. Rach, M. Vemura and J. L. Wost, *J. Liquid Chromatogr.*, 2 (1979) 1205.
8 B. B. Jones, B. C. Clark, Jr., and G. A. Iacobucci, *J. Chromatogr.*, 178 (1979) 575.
9 B. Coq, G. Cretier, C. Gonnet and J. L. Rocca, *Chromatographia*, 12 (1979) 139.
10 T. Yoshida, C. Shu and E. T. Theimer, *J. Chromatogr.*, 137 (1977) 461.
11 R. G. Berg and H. M. McNair, *J. Chromatogr.*, 131 (1977) 185.
12 J. Krupčík, J. Kříž, D. Prušová, P. Suchánek and Z. Čerenka, *J. Chromatogr.*, 142 (1977) 797.
13 E. Godbille and P. Devaux, *J. Chromatogr. Sci.*, 12 (1974) 564.
14 E. Godbille and P. Devaux, *J. Chromatogr.*, 122 (1976) 317.
15 C. Djerassi, G. Rosenkranz, J. Romo, S. Kaufmann and J. Pataki, *J. Amer. Chem. Soc.*, 72 (1950) 4534.
16 J. A. Marshall, R. A. Ruden and L. K. Hirsch, *Tetrahedron Lett.*, (1971) 3795.
17 E. J. Corey and R. H. K. Chen, *Tetrahedron Lett.*, (1973) 1611.
18 J. A. Campbell and J. C. Babcock, *J. Amer. Chem. Soc.*, 81 (1959) 4069.
19 H. J. Reich, M. Jautelat, M. T. Messe, F. J. Weigert and J. D. Roberts, *J. Amer. Chem. Soc.*, 91 (1969) 7445.
20 J. Montastier, S. Cacchi, F. Gasparrini, D. Misiti, L. Charles, J. Giglio and L. Caglioti, *Pittsburg Conference, Cleveland, Ohio, U.S.A., 5 March 1979.*
21 J. Montastier, L. Charles, J. Giglio, L. Caglioti, F. Gasparrini, M. Giovannoli and D. Misiti, *Pittsburg Conference, Atlantic City, NJ, U.S.A., March 1980.*

Journal of Chromatography, 194 (1980) 245–250
Elsevier Scientific Publishing Company, Amsterdam — Printed in The Netherlands

CHROM. 12,749

Note

Reversed-phase high-performance liquid chromatography for the determination of β-asarone

GIUSEPPE MICALI, PAOLA CURRO' and GIUSEPPE CALABRO'*
Istituto di Merceologia dell'Università degli Studi di Messina, Messina (Italy)
(First received January 2nd, 1980; revised manuscript received February 7th, 1980)

In drink and liquor formulations, aromatic substances play an important role because they introduce individual flavours that many affect consumer preferences. These aromatic substances originate mostly from natural sources (essential oils, extracts of roots, leaves, flowers, etc.), although these natural products are tending to be replaced with synthetic substances.

A natural aroma used in vermouths, bitters and liquors is calamus essential oil from *Acorus calamus*. This product is at present under close studied because recent investigations have revealed carcinogenic properties of one of its constituents, β-asarone (*cis*-2,4,5-trimethoxy-1-propenylbenzene). On account of this, the U.S. Food and Drug Administration has prohibited the use of calamus in any form (root, extract or oil) in any food or drug[1,2], and the Committee of experts for aromatic substances, including delegates from Great Britain, Belgium, Denmark, France, G.F.R., Italy, The Netherlands, Sweden, Switzerland, have recently fixed 0.1 mg/kg as the maximum content of β-asarone in foods and soft drinks and 1 mg/kg in alcoholic beverages.

Methods for the determination of β-asarone include gas–liquid chromatography[3–5] and thin-layer chromatography with densitometric valuation of the spots[6] and spectrofluorimetry[7]. These methods are unsatisfactory owing to the possibility of interferences, which are difficult to eliminate even with complex sample purification procedures; further, the sensitivity is not adequate for the requirements imposed by the above limits, which require the availability of very sensitive methods. The method described in this paper combines the high separation efficiency of high-performance liquid chromatography (HPLC) with the sensitivity and selectivity of the fluorimetric detector and allows the simple and rapid determination of β-asarone at concentrations down to 0.001 mg/l.

EXPERIMENTAL

A Perkin-Elmer Model 601 liquid chromatograph equipped with two 3000-p.s.i. pumps was used. For sample introduction a Rheodyne 7120 injection valve with a loop of 10 μl was used. The liquid chromatograph was connected in series with a spectrophotometric and a spectrofluorimetric detector. The spectrophotometric detector (Perkin-Elmer Model LC 55 UV-Vis, single beam with variable wavelength) was

0021-9673/80/0000–0000/$02.25

connected with a Perkin-Elmer Model 123 recorder and with the LC 55-S scanner for recording the spectra. The spectrofluorimetric detector was a Perkin-Elmer Model MPF 3 with a microcell of 20 μl (063-0547) equipped with a Perkin-Elmer Model 56 recorder. For spectrophotometric detection a wavelength of 254 nm was used, and for spectrofluorimetric detection an excitation wavelength of 310 nm and an emission wavelength of 355 nm were used.

The chromatographic separations were carried out with a stainless-steel column (25 cm $\times$ 2.6 mm I.D.) packed with octadecylsilane (HC-ODS/Sil-X, Perkin-Elmer, n 089-0716).

Reagents

All solvents were of analytical-reagent grade. Hexane (Carlo Erba, Milan, Italy) and absolute methanol (J. T. Baker, Phillipsburgh, NJ, U.S.A.) were used without further purification.

The mobile phase was methanol–water (6.2:3.8). The solvents were preliminarly filtered with Millipore filters. Pure α-asarone and β-asarone were supplied by C. Roth (Karlsruhe, G.F.R.).

A calibration graph was prepared by dilution of a standard solution containing 1 mg/ml of β-asarone in methanol. The solution remained stable for many months.

Preparations of samples

A 100-ml volume of an alcoholic beverage was placed in a 500-ml flask together with 200 ml of deionized water, the mixture was distilled and 250 ml of distillate were collected. The distillate was transferred into a separating funnel and 250 ml of saturated sodium chloride solution were mixed with it. Extraction was effected with two 25-ml volumes of *n*-hexane and the combined *n*-hexane phases were extracted with 20 ml of 1 *M* sodium hydroxide solution, 20 ml of 1 *M* hydrochloric acid and twice with 20 ml of water, in that order.

The *n*-hexane extract was dried with sodium sulphate and evaporated to dryness at room temperature under reduced pressure on a rotary evaporator. The residue was dissolved in 3 ml of methanol. The resulting solution was filtered on a FHLP 01300 Millipore filter directly into a glass vessel which was hermetically sealed via a perforable rubber septum. The sample was then ready for chromatographic analysis.

Chromatographic analysis

The analysis was carried out by reversed-phase HPLC, injecting 10-μl volumes of the sample by means of the injection valve, and by eluting with methanol–water (6.2:3.8). The column was thermostated at 65 °C. The flow rate was 0.75 ml/min at a pressure with of 1000 p.s.i.

β-Asarone was identified by comparing the chromatographic behaviour of the samples with that of a standard solution of β-asarone. Confirmation was obtained determining the excitation and emission spectra directly on the eluted fraction kept in the microcell, using the stopped-flow method.

The amount of β-asarone in the samples was obtained by interpolation on a calibration graph obtained by plotting the height of the β-asarone peak against the amount injected. A linear response of the detector was observed up to 5 mg/l.

TABLE I

RECOVERY OF β-ASARONE

Sample No.	*β-Asarone (mg/l)*				*Recovery (%)*
	Present	*Added*	*Total*	*Found*	
15	0.910	0.153	1.063	1.064	100.6
9	0	0.153	0.153	0.155	101.3
10	0	0.256	0.256	0.277	108.0
16	0	0.051	0.051	0.052	102.0
17	0	0.102	0.102	0.102	100.0
13	0.140	0.051	0.191	0.195	107.0
*	0	0.101	0.101	0.111	108.0
*	0	0.153	0.153	0.158	103.0

* Aqueous alcoholic solution.

The calibration graph was checked every time immediately before the analysis of a sample.

RESULTS AND DISCUSSION

Fig. 1 shows typical chromatograms obtained for a standard mixture of α- and β-asarone and for two samples of alcoholic drinks. For comparison, Fig. 1 also shows the chromatograms obtained simultaneously with the spectrophotometric detector connected in series with the spectrofluorimetric detector.

Comparison of the graphs clearly shows the superiority of the fluorimetric detector and indicates that the spectrophotometric detector cannot be used for the determination of β-asarone owing to its insufficient sensitivity and the presence of numerous interfering substances at 254 nm.

In order to evaluate the reproducibility accuracy of the proposed method, to the samples of commercial drinks that had previously been analysed for their

TABLE II

β-ASARONE CONCENTRATIONS DETERMINED IN COMMERCIAL SAMPLES

Sample		*β-Asarone (mg/l)*	*Sample*		*β-Asarone (mg/l)*
Type	*No.*		*Type*	*No.*	
Vermouth	1	0.018	Bitters	11	0.006
	2	0.005		12	0.003
	3	Absent		13	0.140
	4	Not measurable		14	0.004
	5	0.002		15	0.910
	6	Not measurable		16	Absent
	7	0.003			
	8	0.021	Alcoholic aperitif	17	Absent
	9	Absent			
	10	Absent			

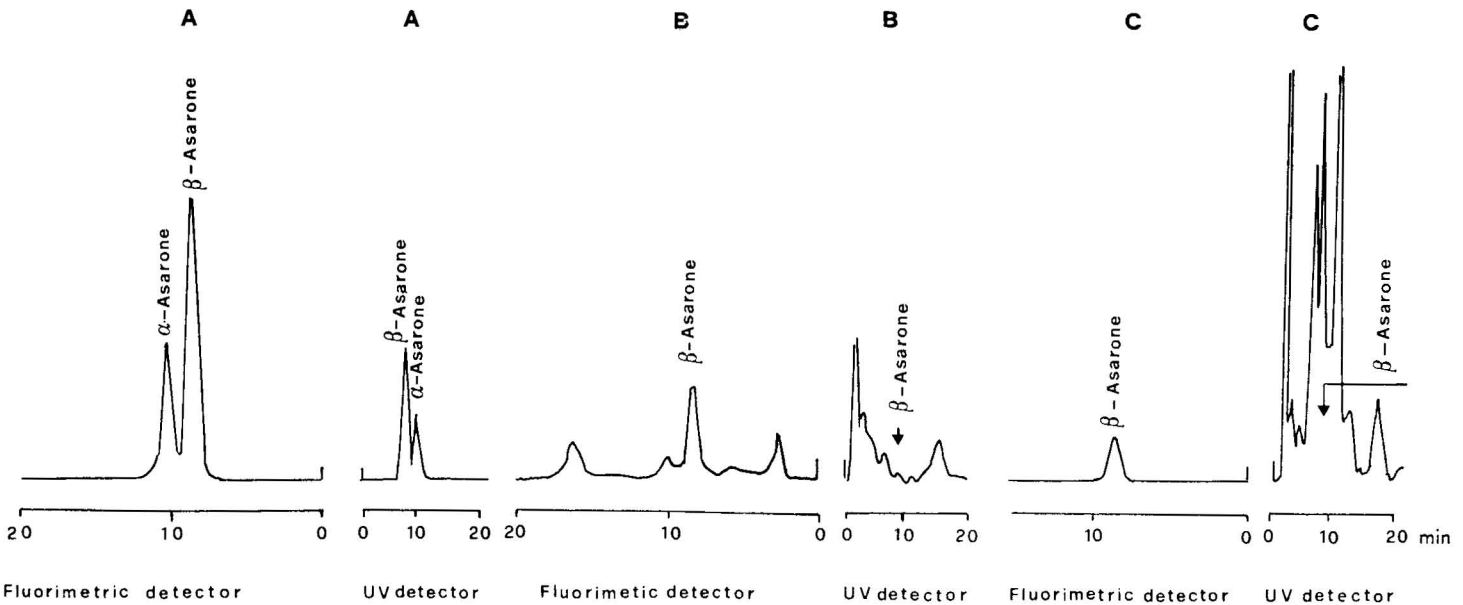

Fig. 1. Chromatograms obtained by spectrophotometric and spectrofluorimetric detectors connected in series: (A) standard α- and β-asarone mixture; (B) and (C) different samples of alcoholic beverages. The arrow shows the retention time of β-asarone. Column, HC-ODS/Sil-X (25 × 0.26 cm I.D.); mobile phase, methanol–water (6.2:3.8); flow rate, 0.75 ml/min; pressure, 1000 p.s.i.; temperature, 65°C; detection, UV (254 nm), fluorimetric ($\lambda_{exc.}$ 310 nm, λ_{em} 355 nm).

β-asarone contents were added known and variable amounts of pure β-asarone. The fortified samples were analysed using the described method. The results are summarized in Table I.

In Table II the β-asarone concentrations obtained by analysing some samples of vermouth and bitters purchased from local commercial sources are reported. The reported values are the averages of two determinations.

As is readily apparent from Table II, β-asarone was absent from or not measurable in 7 of the 17 examined samples; in two samples the β-asarone content was higher than 0.1 p.p.m., but in the remaining samples it was below this value.

The method was also applied to the analysis of a sample of European calamus oil, a solution in methanol ($1:2\cdot10^4$) being injected directly into the column. The β-asarone content found was 7.56 g per 100 ml.

The chromatogram obtained by both the fluorimetric and the spectrophotometric detectors is shown in Fig. 2. Also in this instance the complete separation of the two isomers is evident and the advantage of the spectrofluorimetric detector is also apparent. Confirmation of the peaks was obtained by the stopped-flow technique, measuring both excitation and emission fluorescence spectra and using "UV scanning" with the LC 55 spectrophotometer. Fig. 3 shows the UV spectra obtained for the two peaks of α- and β-asarone.

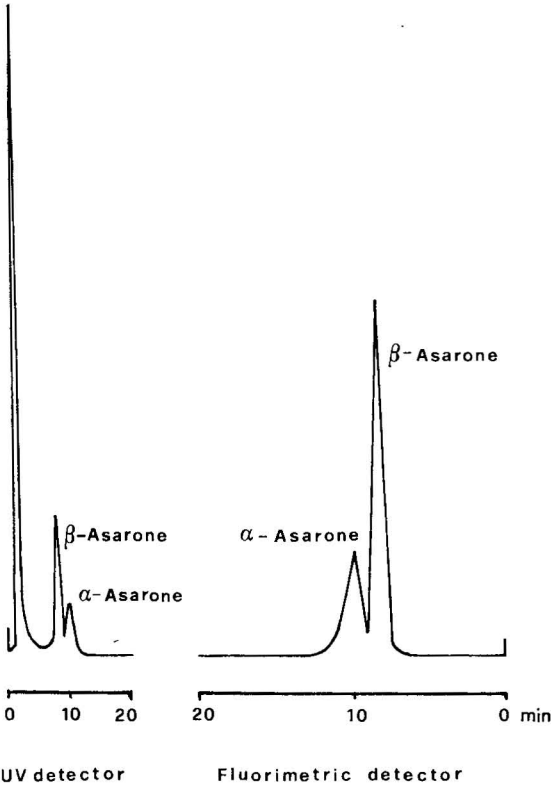

Fig. 2. Chromatograms of calamus oil in methanol ($1:2\cdot10^4$). Conditions as in Fig. 1.

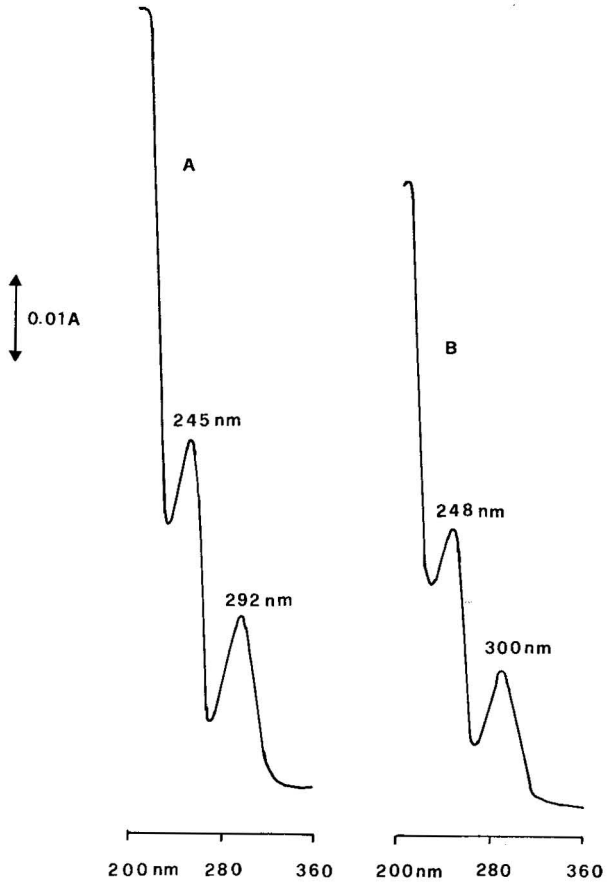

Fig. 3. UV spectra of β-asarone (A) and α-asarone (B) obtained by the stopped-flow technique on a calamus oil sample.

CONCLUSION

The obtained results show that the described method is rapid, accurate, reproducible and selective. The use of a fluorimetric detector enhances the sensitivity and lowers interferences, making possible the determination of β-asarone in complex mixtures.

ACKNOWLEDGEMENT

This work was supported by a C.N.R. grant.

REFERENCES

1 *Fed. Regist.*, 33 (1968) 6967.
2 *Code of Federal Regulations*, Title 21, 3.65 a, b, c (1974).
3 L. Usseglio-Tomasset, *Ind. Agr.*, 4 (1966) 153.
4 D. Larry, *J. Ass. Offic. Anal. Chem.*, 56 (1973) 1281.
5 R. H. Dyer, G. E. Martin and P. C. Buscemi, *J. Ass. Offic. Anal. Chem.*, 59 (1976) 675.
6 L. Usseglio-Tomasset, *Riv. Sci. Tec. Alim. Nutr. Um.*, 6 (1976) 115.
7 E. J. Wojtowicz, *J. Agr. Food Chem.*, 24 (1976) 526.

Journal of Chromatography, 194 (1980) 251–253
Elsevier Scientific Publishing Company, Amsterdam — Printed in The Netherlands

CHROM. 12,755

Note

Chromogenic reagent for vicine and convicine on thin-layer plates

E. HOEHN and S. I. KIM

Department of Food Science, University of Manitoba, Winnipeg, Manitoba R3T 2N2 (Canada)

and

N. A. M. ESKIN* and F. ISMAIL*

Department of Foods and Nutrition, University of Manitoba, Winnipeg, Manitoba R3T 2N2 (Canada)

(Received February 18th, 1980)

The aglycones of vicine and convicine have been implicated as the causative factors for favism in fababeans[1–4]. Separation of vicine and convicine by thin-layer chromatography (TLC) on cellulose plates was reported by Jamalian *et al.*[4] and Olsen and Andersen[5] who identified these compounds under UV light. This paper reports a new chromogenic reagent (2% titanium tetrachloride in conc. hydrochloric acid) for detecting vicine and convicine on cellulose coated sheets (Eastman-Kodak) based on the complex formation of the aglycones with titanium[6]. In order for the complex to form the aglycone must be produced by acid treatment of the glycosides (Fig. 1). This is required to release the hydroxyl group for interaction with the titanium salt. The titanium reagent has been developed in our laboratory to measure hydrogen peroxide[7],

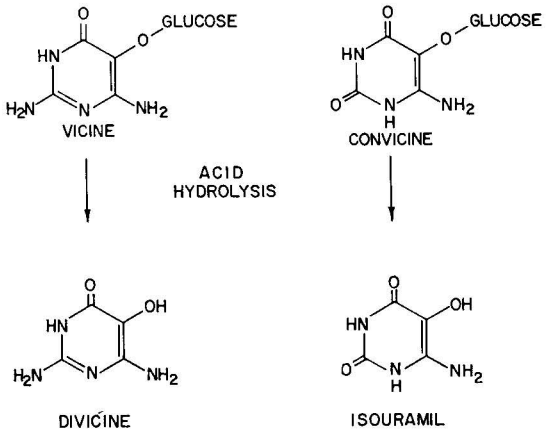

Fig. 1. Acid hydrolysis of vicine and convicine to their respective aglycones, divicine and isouramil.

* Present address: Department of Food Science & Technology, University of Cairo, Cairo, Egypt.

0021-9673/80/0000–0000/$02.25

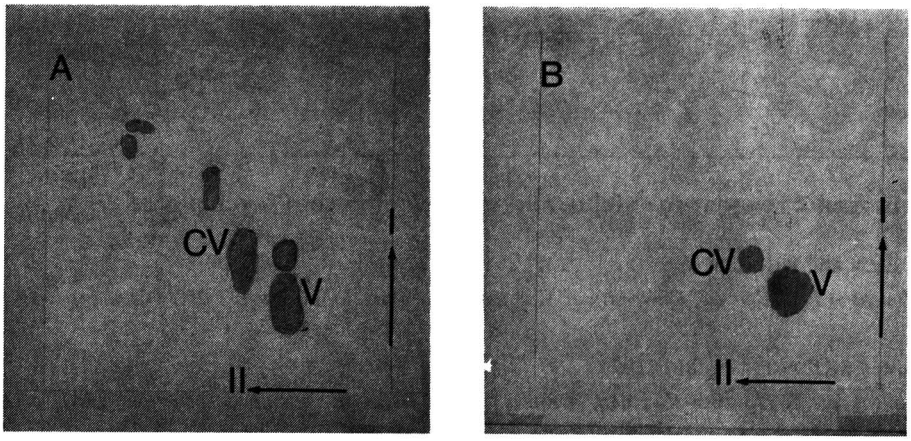

Fig. 2. Separation of vicine and convicine in fababean extracts by two-dimensional TLC. Dimension I: solvent 1, ethanol–water (95:5); dried then developed with solvent 2, methanol–25% ammonia–water (14:1:5); dimension II: solvent 3, methanol–0.02 *M* phosphate buffer pH 5.8 (7:3). A, 2% trichloroacetic acid extract; B, extract following aluminum oxide treatment. Abbreviations, V, vicine and CV, convicine.

organic hydroperoxides[8], phenolic compounds[9] and sinapine[10] as well as a chromogenic reagent for phenolics on thin-layer plates[11].

Pure vicine and convicine solutions ranging in concentration from 0.1–20 μg/2 μl were applied to cellulose plates and developed by TLC according to the procedure outlined by Olsen and Andersen[5]. The plates were air dried, sprayed with conc. hydrochloric acid and heated over a hot tray for 2 min to produce the aglycones followed by spraying with the titanium reagent. In both cases the limit of detection by the titanium reagent was 1 μg resulting in a brown spot of approximately 0.4 cm^2 area. The applicability of the reagent to detect vicine and convicine in 2% trichloroacetic acid extracts of fababean was examined before and after treatment with aluminum oxide by two-dimensional TLC. The chromatograms shown in Fig. 2 indicate that vicine and convicine could be readily detected in the fababean extracts. It is evident that interference by phenolic compounds can be eliminated by aluminum oxide treatment of the extract. No additional spots were evident in the fababean extract using the titanium reagent although additional ones were reported by Olsen and Andersen[5] using UV light as detector. Related pyrimidine and purine compounds did not react with the titanium reagent although they are known to respond to UV light. The titanium–aglycone spots were stable for several months. It is evident that the titanium reagent provides a simple and sensitive method for identifying vicine and convicine via their aglycones on thin-layer plates.

ACKNOWLEDGEMENTS

The authors appreciate the samples of pure vicine and convicine provided by W. J. Pitz, Department of Crop Science, University of Saskatchewan, Canada.

REFERENCES

1 J. Y. Ling and K. H. Ling, *J. Formosan Med. Assoc.*, 61 (1962a) 490.
2 J. Y. Ling, *J. Formosan Med. Assoc.*, 61 (1962b) 579.
3 J. Mager, G. Glaser, A. Razin, G. Izak, S. Bien and M. Noam, *Biochem. Biophys. Res. Commun.*, 20 (1965) 235.
4 J. Jamalian, F. A. Aylward and J. F. Hudson, *Qual. Plant Foods Hum. Nutr.*, 27 (1977) 213.
5 H. S. Olsen and J. H. Andersen, *J. Sci. Food Agr.*, 29 (1978) 323.
6 E. Hoehn, N. A. M. Eskin, S. I. Kim and F. Ismail, *J. Agr. Food Chem.*, in preparation.
7 C. B. Gupta, N. A. M. Eskin, C. Frenkel and A. Y. Sadovski, *J. Food Sci.*, 42 (1977) 537.
8 N. A. M. Eskin and C. Frenkel, *J. Amer. Oil Chem. Soc.*, 53 (1976) 74.
9 N. A. M. Eskin, E. Hoehn and C. Frenkel, *J. Agr. Food Chem.*, 26 (1978) 973.
10 F. Ismail and N. A. M. Eskin, *J. Agr. Food Chem.*, 27 (1979) 917.
11 N. A. M. Eskin and C. Frenkel, *J. Chromatogr.*, 150 (1978) 293.

Journal of Chromatography, 194 (1980) 254–261
Elsevier Scientific Publishing Company, Amsterdam — Printed in The Netherlands

CHROM. 12,743

Note

Studies of pyrazines as their n–π charge-transfer complexes with some nitro aromatic compounds

T. S. VASUNDHARA and D. B. PARIHAR*
Defence Food Research Laboratory, Mysore (India)
(First received September 24th, 1979; revised manuscript received February 6th, 1980)

Pyrazines are flavour compounds formed in roasted foods as a result of the interaction of carbonyls with amino compounds. Different techniques such as gas chromatography (GC) and mass, infrared and nuclear magnetic resonance spectroscopy have been employed for their separation, identification and determination[1–5]. In GC it is difficult to resolve isomeric pyrazines using a single column. Dietrich and Mavier[6] employed paper chromatography for the separation of pyrazine carboxylic acids. Sizer[7] tried to separate some isomeric alkylpyrazines that are difficult to resolve by GC by employing thin-layer chromatography (TLC).

Even with TLC, in spite of employing different solvent systems, difficulties are encountered in the separation of pyrazines that have the same or very close R_F values.

Pyrazines are n–π donors and are known to form charge-transfer complexes with iodine[8]. Nitro aromatic compounds are powerful π-acceptors. Silica gel G impregnated with π-acceptors such as 2,4,6-trinitroanisole (TNA), 2,4,6-trinitrotoluene (TNT), 2,4,6-trinitrobenzene (TNB), picric acid (PA) and picramide (PM) has been used for the TLC separation of a variety of basic compounds[9–11].

In this work advantage was taken of n–π complexation of pyrazines with 2,4,6-trinitroresorcinol (TNR), picryl chloride (PC), 2,4,6-trinitrophenetole (TNP) and TNT for their separation on TLC plates. Pyrazines form complexes both in solution and on thin-layer plates impregnated with these nitro compounds. The complexation results in a distinct spectral shift in solution and a change in the R_F values. The resolution as n–π complexes of 25 pyrazines that are generally found in roasted foods has been readily effected. In particular, the separation of those pyrazines which have the same or close R_F values in different solvent systems has been achieved as a result of complexation. The complexes have distinct UV maxima.

Pyrazines could be detected on the TLC plates by spraying with Dragendorff's reagent[12] followed by 0.5% sulphuric acid with a detection limit of 2.5 μg, and determined after liberating them from the complexes with ethanol at levels down to 5 μg by using a UV spectrophotometer.

0021-9673/80/0000–0000/$02.25

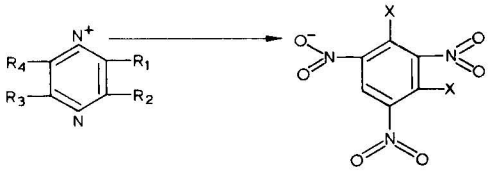

Pyrazine: Nitro aromatic compound
1:1 n–π complex
R_1, R_2, R_3, R_4 = H, alkyl, thioalkyl, alkoxy
X = H, OH, Cl, CH_3

EXPERIMENTAL

Authentic pyrazines (1–25, Table I) were received from Naarden International Research Centre (Naarden, The Netherlands) and Pyrazine Specialties (Atlanta, GA, U.S.A.). Styphnic acid, picryl chloride, trinitrotoluene and trinitrophenetole were of analytical-reagent grade.

Silica gel G (E. Merck, Darmstadt, G.F.R.) was used as the adsorbent. All solvents were dried and freshly distilled. The following eluting solvents were used with the ascending technique: I, chloroform–ethyl acetate–ethanol (60:38:2); II, benzene–acetone–ethanol (90:8:2).

Dragendorff's spray reagent was prepared as reported by Stahl[12].

A Perkin-Elmer Model 124 ultraviolet spectrophotometer was used for spectral measurements and a Chromatolite UV lamp (short-wave length radiation, 254 nm) for locating the compounds on the plates.

Preparation of plates, impregnation, spotting and elution

A fine slurry of silica gel G (50 g) in distilled water (100 ml) was poured on to glass plates (35 × 25 cm) and spread uniformly by tilting the plates from side to side. The plates were dried at room temperature overnight and activated at 110 °C in an oven for 1.5 h before use. The average coating thickness was 6.5 mg/cm^2. The plates were impregnated with a 0.01 % solution of the nitro aromatic compound in carbon tetrachloride by the ascending technique. The plates were dried at room temperature and standard solutions of pyrazines (5 μg in 10 μl of carbon tetrachloride) were spotted. The compounds were also spotted on an untreated plate, which served as a control. The control plates were eluted with solvents I and II, but for the elution of the impregnated plates these solvents also contained 0.01 % of the corresponding π-acceptor. After elution the plates were air dried. The compounds were located under UV light and by spraying with Dragendorff's reagent followed by 0.5 % sulphuric acid, appearing as pink spots on both unimpregnated and impregnated plates. Fig. 1 shows two typical chromatograms obtained on an impregnated plate for some pyrazines with very close R_F values; on the picryl chloride-impregnated plate they were well resolved. Table I gives the R_F values of 25 pyrazines, and of n–π complexes with four acceptors in two solvent systems.

Ultraviolet spectra of n–π complexes in solution

Solutions of $1 \cdot 10^{-6}$ *M* of each of the pyrazines and nitro aromatic compounds were prepared in carbon tetrachloride. The solutions were mixed in various pro-

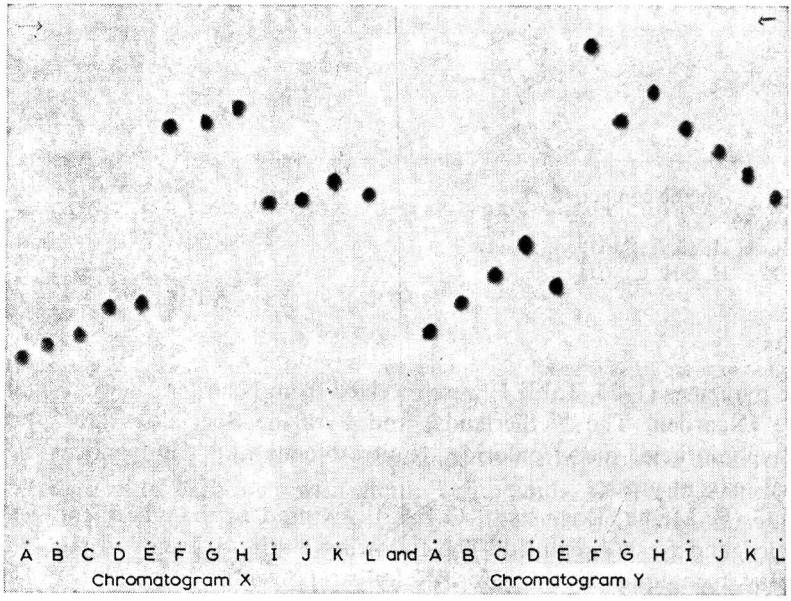

Fig. 1. Thin-layer chromatograms showing the separation of pyrazines having very close R_F values. Chromatogram X, without impregnation with picryl chloride; chromatogram Y, impregnated with picryl chloride. A = 2,3-Dimethylpyrazine; B = 2,5-dimethylpyrazine; C = 2,6-dimethylpyrazine; D = 2-ethyl-5-methylpyrazine; E = pyrazine; F = 2-methoxy-3-isopropylpyrazine; G = 2-methoxy-3-*sec.*-butylpyrazine; H = 2-methylthio-3-ethylpyrazine; I = 2-ethoxy-3-methylpyrazine; J = 2-acetyl-3-methylpyrazine; K = 2-propyl-3,6-dimethylpyrazine; L = 2-ethyl-6-methylpyrazine. Adsorbent: Silica gel G (E. Merck). Solvent system: Chloroform–ethyl acetate–ethanol (60:38:2) for chromatogram X; for Y the system also contained 0.01% of picryl chloride.

portions and the UV spectrum of each mixture was recorded together with those of the individual compounds. Table I gives the $\lambda_{max.}$ valves of the n–π complexes and of the individual compounds. Figs. 2–5 show the absorption patterns of some typical n–π complexes.

Micro-determination of pyrazines

Amounts of 5 μg of each pyrazine were doubly spotted on two half-sides of a picryl chloride-impregnated plate and eluted with solvent I containing 0.01% of this nitro compound. After elution the first half was sprayed with Dragendorff's reagent followed by 0.5% sulphuric acid. The spots corresponding to the first half of the plate were marked on the second half of the plate. The spots on the second half (unsprayed) portion were also visible under UV light. These were scraped with a micro-spatula into a sintered-glass funnel (I.D. 0.5 cm). Pyrazines were liberated from their complexes by treatment with ethanol, the pyrazines being found in the filtrate whereas the nitro compound remained adsorbed on the silica gel. The solvent was carefully removed from the filtrate under a partial vacuum, the residue was dissolved in carbon tetrachloride and the volume made up to 10 ml. The absorbance at the $\lambda_{max.}$ values were measured. The amounts were calculated from previously drawn standard absorption graphs for each pyrazine. The recovery of the pyrazines was 97–98% and the results were reproducible.

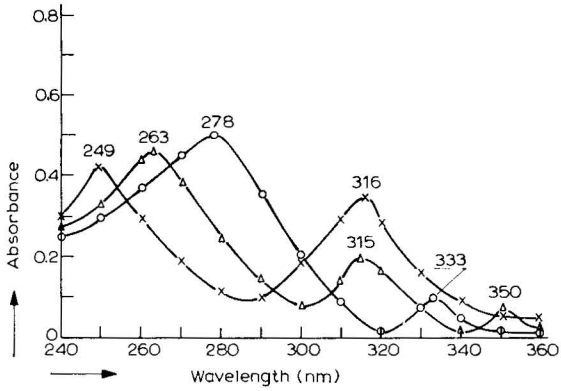

Fig. 2. UV spectra of 2-methylthio-3-isopropylpyrazine (×), styphnic acid (○) and their n–π complex (△).

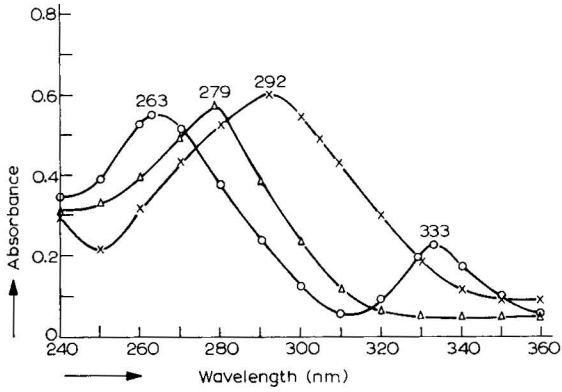

Fig. 3. UV spectra of 2-methoxy-3-ethylpyrazine (×), picryl chloride (○) and their n–π complex (△).

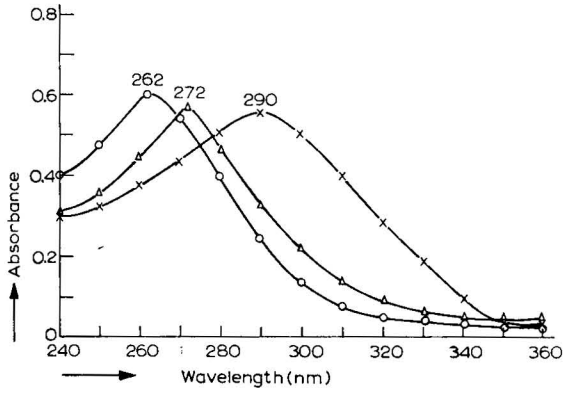

Fig. 4. UV spectra of 2-ethyl-5-methylpyrazine (×), TNT (○) and their n–π complex (△).

TABLE I

R_F VALUES OF PYRAZINES AND THEIR n–π COMPLEXES WITH STYPHNIC ACID, PICRYL CHLORIDE, TRINITROTOLUENE AND TRINITROPHENETOLE, AND ABSORPTION MAXIMA IN CARBON TETRACHLORIDE

Solvent systems: I = chloroform–ethyl acetate–ethanol (60:38:2); II = benzene–acetone–ethanol (90:8:2). Adsorbent: silica gel G (E. Merck). When the nitro compound-impregnated plates were eluted, the solvent also contained 0.01% of the respective nitro compound. $\lambda_{max.}$ values in carbon tetrachloride: styphnic acid, 278 and 333 nm; picryl chloride, 263 and 333 nm; trinitrotoluene, 262 nm; trinitrophenetole, 269 nm.

No.	*Compound*	*Pure pyrazines*			*$\lambda_{max.}$ of styphnic acid complexes in solution (nm)*	*R_F values on styphnic acid impregnated plate*		*$\lambda_{max.}$ of picryl chloride complexes in solution (nm)*	*R_F values on picryl chloride-impregnated plate*		*$\lambda_{max.}$ of trinitrotoluene complexes in solution (nm)*	*R_F values on trinitrotoluene-impregnated plate*		*$\lambda_{max.}$ of trinitrophenetole complexes in solution (nm)*	*R_F values on trinitrophenetole impregnated plate*	
		$\lambda_{max.}$ (nm)	*R_F values*													
			Solvent I	*Solvent II*		*Solvent I*	*Solvent II*		*Solvent I*	*Solvent II*		*Solvent I*	*Solvent II*		*Solvent I*	*Solvent II*
1	2-Methylpyrazine	266	0.30	0.35	274, 335	0.26	0.32	275	0.40	0.39	269, 315	0.41	0.43	260, 315	0.34	0.36
2	2,3-Dimethylpyrazine	274	0.36	0.37	271	0.38	0.35	270, 310	0.41	0.40	271, 309	0.43	0.40	271, 310	0.39	0.40
3	2,5-Dimethylpyrazine	275	0.38	0.39	276	0.40	0.37	270, 310	0.45	0.42	272, 314	0.46	0.45	272, 314	0.43	0.42
4	2,6-Dimethylpyrazine	275	0.40	0.39	276, 334	0.42	0.39	280	0.49	0.44	271, 314	0.49	0.48	270, 313	0.44	0.43
5	2-Ethyl-5-methylpyrazine	290	0.44	0.52	272, 335	0.53	0.57	275	0.53	0.58	272	0.52	0.59	273	0.48	0.49
6	2,3,5-Trimethylpyrazine	278	0.36	0.55	273, 335	0.40	0.61	274	0.44	0.63	271	0.40	0.50	282	0.32	0.59
7	2,3,5,6-Tetramethylpyrazine	279	0.41	0.37	281, 337	0.54	0.32	282	0.46	0.42	282	0.45	0.41	284	0.37	0.38

8	2-Methoxy-3-methylpyrazine	291	0.82	0.56	280, 340	0.91	0.50	293	0.86	0.66	279	0.71	0.51	286	0.89	0.69
9	2-Methoxy-3-isobutylpyrazine	290	0.87	0.70	280, 335	0.92	0.74	279	0.83	0.95	280	0.79	0.60	281	0.84	0.67
10	Pyrazine	261	0.44	0.51	274	0.40	0.55	270	0.46	0.56	263, 321	0.37	0.44	258, 316	0.40	0.46
11	2-Ethylpyrazine	266	0.58	0.50	270, 335	0.61	0.62	269	0.61	0.64	267, 315	0.53	0.42	268, 315	0.65	0.60
12	2-Methoxy-3-ethylpyrazine	292	0.90	0.81	276, 335	0.93	0.75	279	0.80	0.93	280	0.84	0.73	278	0.85	0.77
13	2-Methoxy-3-isopropylpyrazine	280	0.80	0.64	276, 331	0.84	0.84	275	0.93	0.58	275	0.75	0.56	274	0.77	0.59
14	2-Ethyl-3-methylpyrazine	274	0.48	0.37	270, 333	0.43	0.47	270	0.53	0.34	270	0.34	0.40	270, 312	0.52	0.41
15	2-Acetylpyrazine	271	0.75	0.34	268	0.78	0.40	266, 310	0.79	0.37	264	0.70	0.38	270, 310	0.70	0.38
16	2-Ethoxy-3-ethylpyrazine	285	0.86	0.60	280, 335	0.80	0.72	280	0.90	0.55	280	0.59	0.63	280	0.82	0.55
17	2-Ethoxy-3-methylpyrazine	290	0.66	0.53	277, 336	0.56	0.64	276	0.78	0.50	280	0.51	0.56	278	0.60	0.50
18	2-Methoxy-3-*sec.*-butyl pyrazine	280	0.80	0.65	284, 335	0.76	0.81	290	0.81	0.60	274	0.76	0.55	276	0.74	0.61
19	2-Acetyl-3-methylpyrazine	274, 222	0.67	0.53	277, 331	0.50	0.63	270	0.74	0.49	259, 312	0.59	0.45	271	0.61	0.59
20	2-Methylthio-3-ethylpyrazine	243, 316	0.81	0.66	275, 333	0.67	0.84	256, 317	0.85	0.56	259, 316	0.77	0.54	260, 315	0.78	0.61
21	2-Methylthio-3-isopropylpyrazine	249, 316	0.92	0.72	263, 315, 350	0.84	0.96	260, 315	0.88	0.62	260	0.88	0.58	317	0.86	0.76
22	2-Butyl-3-methylpyrazine	270	0.66	0.47	276, 310	0.76	0.63	266, 310	0.73	0.43	280	0.59	0.36	270, 312	0.61	0.40
23	2-Propyl-3,6-dimethylpyrazine	279	0.69	0.51	274, 331	0.63	0.66	284	0.70	0.46	284	0.61	0.42	284	0.60	0.44
24	2-Ethoxy-3-isopropylpyrazine	220, 278	0.96	0.81	271, 333	0.90	0.88	280	0.88	0.74	280	0.93	0.66	280	0.92	0.85
25	2-Ethyl-6-methylpyrazine	276	0.68	0.51	270, 333	0.52	0.63	282	0.66	0.52	272, 310	0.58	0.37	272, 310	0.64	0.53

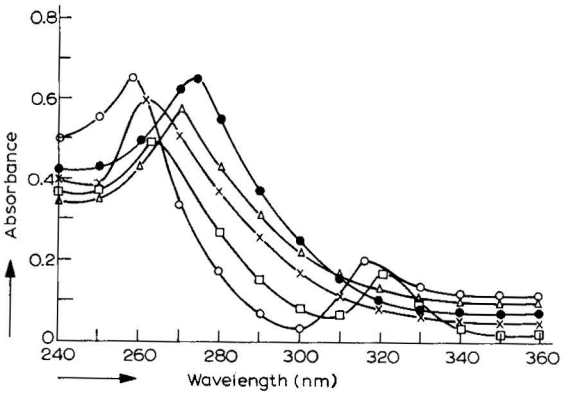

Fig. 5. UV spectra of pyrazine (×) and n–π complexes of pyrazine with styphnic acid (●), picryl chloride (△), TNT (□) and trinitrophenetole (○).

RESULTS AND DISCUSSION

As is evident from Table I, pyrazines form charge-transfer complexes with nitro aromatic compounds both in solution and on TLC plates, which is reflected in the spectral shifts and in the R_F values. For most of the compounds a large spectral shift is accompanied by a significant change in their R_F values.

Pyrazines are n donors. The nitrogen atoms in the ring deactivate all of the ring carbon atoms towards electrophilic substituents and activate them towards nucleophilic substituents. Hence nucleophilic substituents such as alkyl, alkoxy and thioalkyl groups on the pyrazine ring further modify the donor capacity of the molecule.

Of the four nitro aromatic compounds tried as acceptors, *viz.*, styphnic acid, PC, TNT and TNP, PC gave the best separation of the complexes. The chlorine atom attached to the nitro-aromatic ring further enhanced the acceptor properties.

Theoretically, pyrazines could form 1:1, 1:2 and 2:1 complexes with nitro aromatic compounds. From a Job's plot in solution it was observed that all of the pyrazines formed only 1:1 complexes. In some instances the complexes showed more than one absorption band in solution. This could be due to multiple charge transfer occurring between the closely related filled orbitals of the donor molecule and closely related unfilled orbitals of the acceptor molecule.

Silica gel G was suitable as an adsorbent. Of the two solvent systems examined, solvent I gave better resolutions of the complexes. The compounds could be detected with Dragendorff's reagent both on unimpregnated plates and on plates impregnated with nitro aromatic compounds.

This property of n–π complexation on TLC plates was found to be of great utility in the resolution of those pyrazines which had either identical or very close R_F values. For example, the following groups of pyrazines had very close R_F values in both solvent systems (Table I). Group I —2,3-dimethylpyrazine, 2,5-dimethylpyrazine, 2,6-dimethylpyrazine; Group II —2-ethyl-5-methylpyrazine, pyrazine; Group III —2-methoxy-3-isopropylpyrazine, 2-methoxy-3-*sec.*-butylpyrazine; 2-methylthio-3-ethylpyrazine; Group IV —2-ethoxy-3-methylpyrazine, 2-acetyl-3-meth-

ylpyrazine, 2-propyl-3,6-dimethylpyrazine, 2-ethyl-6-methylpyrazine. However, as can be seen from Fig. 1, as the n–π complexes they gave very distinct separations.

The procedure described is very useful for the separation of pyrazines that are difficult to resolve. It is possible to detect and determine them with limits of 2.5 and 5 μg, respectively.

ACKNOWLEDGEMENTS

The authors are grateful to Dr. P. K. Vijayaraghavan, Director, Defence Food Research Laboratory, Mysore, for his keen interest and encouragement. The generous help rendered by Dr. H. J. Takken, Naarden International Research Laboratory, The Netherlands and Dr. M. A. Gianturco, Coca Cola Company, U.S.A., in supplying authentic pyrazines as gifts is gratefully acknowledged.

REFERENCES

1 R. C. Buttery, R. M. Seifert, D. G. Guadagni and L. C. Ling, *J. Agr. Food Chem.*, 19 (1971) 969.
2 P. E. Koehler, M. E. Mason and J. A. Newell, *J. Agr. Food Chem.*, 17 (1969) 393.
3 J. P. Walradt, A. O. Pitet, T. E. Kinlin, R. Murali Dhara and A. Sanderson *J. Agr. Food Chem.*. 19 (1971) 972.
4 H. A. Bondarovich, P. Friedel, V. Krampl, J. A. Renner, F. W. Shephard and M. A. Gianturco, *J. Agr. Food Chem.*, 15 (1967) 1093.
5 M. van Praag, H. S. Stein and M. S. Tibbets, *J. Agr. Food Chem.*, 16 (1968) 1005.
6 P. Dietrich and D. Mavier, *J. Chromatogr.*, 1 (1958) 67.
7 C. E. Sizer, unpublished results.
8 V. G. Krishna and Mihir Chowdhry, *J. Phys. Chem.*, 67 (1963) 1067.
9 A. K. Dwivedy, D. B. Parihar, S. P. Sharma and K. K. Verma, *J. Chromatogr.*, 29 (1967) 120.
10 D. B. Parihar, S. P. Sharma and K. K. Verma, *J. Chromatogr.*, 31 (1967) 120.
11 D. B. Parihar, S. P. Sharma and K. K. Verma, *J. Forensic Sci. Soc.*, 10 (1970) 77.
12 E. Stahl, *Thin Layer Chromatography*, Springer Verlag, New York, 1969.

Journal of Chromatography, 194 (1980) 262–269
Elsevier Scientific Publishing Company, Amsterdam — Printed in The Netherlands

CHROM. 12,725

Note

Thin-layer chromatography of the acid hydrolysis products of nineteen benzodiazepine derivatives

E. ROETS and J. HOOGMARTENS*

Katholieke Universiteit Leuven, Instituut voor Farmaceutische Wetenschappen, Laboratorium voor Farmaceutische Chemie, Van Evenstraat 4, 3000 Leuven (Belgium)

(Received January 31st, 1980)

Thin-layer chromatography (TLC) of the benzophenones obtained by acid hydrolysis of benzodiazepine derivatives is widely used for the identification of members of this group of psychopharmacological agents. As already stated previously, this method is not specific, as different benzodiazepines can give the same benzophenone, nor is it a general method[1]. Indeed, benzodiazepines such as triazolam, alprazolam and clobazam do not form benzophenones when they are treated in the usual way, and medazepam is stable towards hydrolysis. The advantage of TLC of the benzophenones rather than of the benzodiazepines themselves is that different metabolites of the same benzodiazepine can give the same benzophenone on hydrolysis, which makes this method more suitable for identification of these products in biological fluids. Work up to 1974 has already been reviewed[2,3]. TLC of benzophenones is also mentioned in several more recent papers as being useful for the identification of pure benzodiazepines or for the identification of benzodiazepines and metabolites in biological fluids[4–7].

In this paper we describe the separation of the nine benzophenones obtained by acid treatment of 19 benzodiazepines on the TLC plate.

EXPERIMENTAL

Samples

The origins and structures of the benzodiazepine derivatives I to XIX have been given previously[1]. Their names are listed in Table I, except for clobazam (VIII), triazolam (XVII) and alprazolam (XVIII), which were not hydrolysed into benzophenones. Table I also lists the corresponding benzophenones. Samples XXIV and XXV were kindly provided by Wyeth (Brussels, Belgium). All other benzophenones were obtained by hydrolysis of the first-mentioned corresponding benzodiazepine (Table I). For this purpose 25 mg of the benzodiazepine were dissolved in 10 ml of 4 *N* hydrochloric acid. The solution was kept in a boiling water-bath for 1 h, was then brought to pH 10 with 10 *N* sodium hydroxide solution and was finally extracted twice with 15 ml of chloroform. The combined organic layers were washed with water, dried over anhydrous sodium sulphate and evaporated to dryness. The residues were purified when necessary by column chromatography over silica gel 60 (0.040–0.063 mm)

0021-9673/80/0000–0000/$02.25

(E. Merck, Darmstadt, G.F.R.) with methylene chloride as the mobile phase, except for XX and XXI, where 5% (v/v) of acetone had to be added. All of the structures were confirmed by infrared spectroscopy and mass spectrometry.

TABLE I

BENZOPHENONES AND RELATED BENZODIAZEPINES

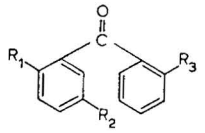

R_1	R_2	R_3	*Benzophenones*	*Benzodiazepines*
$NHCH_2CH_2N(C_2H_5)_2$	Cl	F	2-(Diethylaminoethylamino)-5-chloro-2′-fluorobenzophenone (XX)	Flurazepam (III)
NH_2	NO_2	H	2-Amino-5-nitrobenzophenone (XXII)	Nitrazepam (XIV)
NH_2	NO_2	Cl	2-Amino-5-nitro-2′-chlorobenzophenone (XXIII)	Clonazepam (XIII)
NH_2	Cl	H	2-Amino-5-chlorobenzophenone (XXIV)	Oxazepam (XVI) Chlordiazepoxide (XIX) Chlorazepate (X) Desmethyldiazepam (XI)
NH_2	Cl	Cl	2-Amino-2,5-dichlorobenzophenone (XXV)	Lorazepam (XV)
$NHCH_3$	NO_2	F	2-Methylamino-5-nitro-2′-fluorobenzophenone (XXVI)	Flunitrazepam (V)
$NHCH_3$	Cl	H	2-Methylamino-5-chlorobenzophenone (XXVII)	Camazepam (VI) Diazepam (IV) Temazepam (IX) Ketazolam (VII) Medazepam (II)
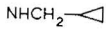	Cl	H	2-Cyclopropylmethylamino-5-chlorobenzophenone (XXVIII)	Prazepam (I)
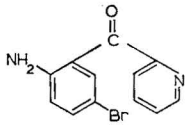			2-Amino-5-bromobenzoylpyridine (XXI)	Bromazepam (XII)

Stationary and mobile phases

Generally DC-Fertigplatten Kieselgel 60 F 254 (Merck) were used, but other brands of ready-made silica gel plates were also tried, *viz.*, Stratochrom Si F 254 (Carlo Erba, Milan, Italy) and DC-Fertigplatten Si F (Riedel-de Haën, Hannover, G.F.R.). The plates were used without prior activation. Methylene chloride–chloroform (1:1) was generally used as the mobile phase (A). Both solvents were of "reinst" quality (Merck). Other mobile phases were also used, *viz.*: B, chloroform; C, benzene; D, benzene–chloroform (3:1); E, benzene–nitromethane (30:1); F, toluene–diethyl-

amine (4:1); G, benzene–methanol (96:6); and H, cyclohexane–acetone (9:1). All ratios are expressed in volumes.

Chromatographic procedure

The benzophenones were dissolved in chloroform (0.4%, w/w) and 0.5-μl (2-μg) amounts were spotted on the TLC plate. The benzodiazepines were dissolved in methanol (0.4%, w/v), except for X, which was dissolved in water and then diluted with methanol to a final concentration of 80% (v/v) of methanol. Amounts of 2.5 μl (10 μg) were spotted. Then 5 μl of 15% (v/v) sulphuric acid was placed over each spot, whereafter the TLC plate was covered with a glass plate and kept for 20 min in an oven at 120 °C. The plate was cooled to room temperature and each spot was covered with 10 μl of ammonia solution (25%, w/v). The spots were dried, first in a stream of air and then by heating at 120 °C for 5 min. Paper-lined chromatographic chambers were equilibrated with the mobile phase for at least 1 h. The plates were developed over a distance of 15 cm, dried in a stream of warm air and examined under a UV lamp with a maximum output a about 254 nm (Sylvania G 15 T8 A lamp) or at about 366 nm (Philips HPW 125-W lamp). The detection limit for benzophenones was less than 0.5 μg at the shorter wavelength; the sensitivity was lower at the higher wavelength. All experiments were carried out at temperatures between 20 and 25 °C.

Photography

The technique and materials have been mentioned previously[1]. Two Philips HPW 125-W lamps were used as the 366-nm light source.

RESULTS AND DISCUSSION

Fig. 1 shows a chromatogram of the pure benzophenones obtained with mobile phase A on a Merck plate. Comparable results were obtained with the other brands of plates. Table II lists the R_F values obtained with the different mobile phases. All except A and B have been mentioned in the literature as suitable for the separation of benzophenones[6–13]. R_F values from the literature are also given where available. No literature values are mentioned for mobile phase D since Lafargue *et al.* used aluminium oxide plates[11].

Mobile phase A separates the nine benzophenones but has the disadvantage that XX does not migrate. It must be noted that for this mobile phase the quality of the solvents is important, as the amount of ethanol, present as a stabiliser, can influence the separation. Mobile phase C is widely used for the separation of benzophenones. With this mobile phase an even better separation is obtained when no paper lining is used. The values thus obtained correspond best to those in the literature. The markedly higher values obtained by Hermans and Kamp[8] may be due to the use of home-made plates, which generally give higher R_F values. With this mobile phase lower R_F values are recorded and therefore it is less suitable for chromatography after hydrolysis on the TLC plate because several benzophenones could disappear amongst the lower background spots. For mobile phases E, F and G a reasonable agreement with the literature values is observed. The higher values for G can again be explained by the use of home-made plates by Gräfe and Schmeling[6]. For mobile phase H totally different values were obtained, probably owing to the use of a particular brand of

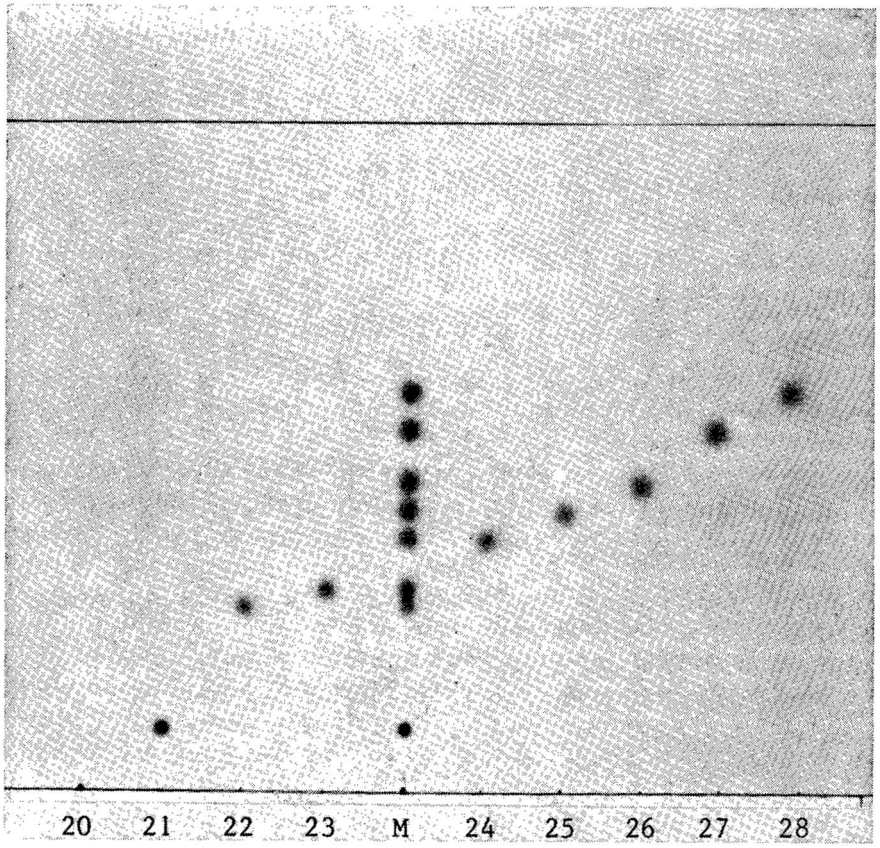

Fig. 1. Chromatogram of pure benzophenones obtained using methylene chloride–chloroform (1:1) (A) as the mobile phase. The arabic numbers of the spots correspond to the roman numbers listed in Table I.

TABLE II

R_F VALUES OF BENZOPHENONES ON MERCK PLATES

Benzophenone	*Mobile phase*																			
	A	*B*	*C (with paper lining)*	*C (without paper lining)*				*D*	*E*			*F*		*G*		*H*	
				This work	*Ref. 8*	*Ref. 9*	*Ref. 10*		*This work*	*Ref. 12*		*This work*	*Ref. 13*	*This work*	*Ref. 6*	*This work*	*Ref. 7*	
XX	0.00	0.01	0.00	0.00				0.00	0.00			0.64		0.10	0.17	0.03		
XXI	0.09	0.16	0.02	0.02				0.03	0.04			0.37		0.41		0.07		
XXII	0.29	0.31	0.10	0.15	0.20	0.17	0.20	0.14	0.15			0.27		0.43	0.47	0.05		
XXIII	0.32	0.32	0.11	0.19				0.15	0.17	0.13		0.25	0.27	0.42		0.04		
XXIV	0.38	0.43	0.18	0.30	0.39	0.34	0.32	0.24	0.26	0.20		0.44	0.47	0.54	0.61	0.15	0.43	
XXV	0.43	0.45	0.24	0.39		0.46	0.41	0.28	0.31			0.40	0.42	0.54	0.61	0.11		
XXVI	0.47	0.52	0.21	0.35				0.29	0.29			0.54		0.58		0.10		
XXVII	0.55	0.58	0.36	0.56	0.73	0.69	0.56	0.42	0.43	0.37		0.63	0.63	0.63	0.73	0.34	0.73	
XXVIII	0.61	0.62	0.45	0.69			0.70	0.50	0.52			0.66		0.66	0.75	0.42		

silica gel plates (Gelman ITLC Type SA) and possibly also to the use of an unsaturated chamber. The best separations are obtained with mobile phases A and C.

Figs. 2 and 3 show the same chromatogram obtained after *in situ* hydrolysis of the 19 benzodiazepine derivatives. The only difference is that 254- and 366-nm light sources were used, respectively. Observing the intensities of the spots in Fig. 3, one should not erroneously conclude that detection by black light is more sensitive: this effect is due only to a longer exposure time. The photographs clearly show that, in addition to the benzophenones, a considerable number of other hydrolysis products are formed. Most of these migrate very little and thus do not interfere. Their identities have not yet been investigated.

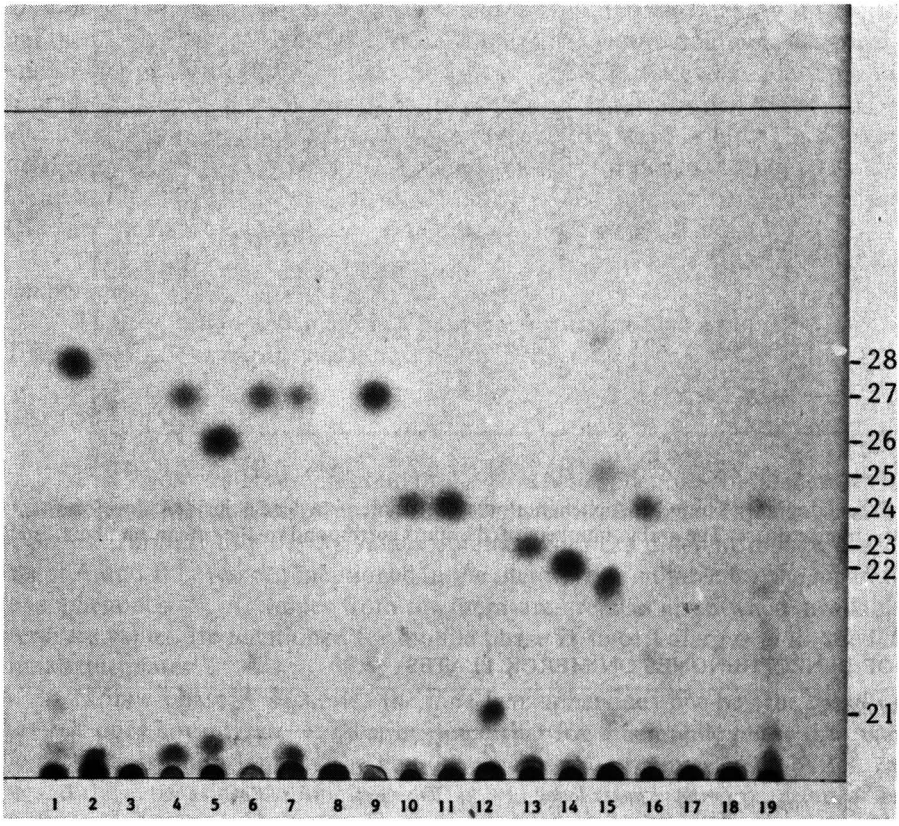

Fig. 2. Chromatogram obtained after hydrolysis of the benzodiazepines on the plate with methylene chloride–chloroform (1:1) (A) as the mobile phase. Detection with a 254-nm light source. The numbers of the spots correspond to those listed in Table I.

To obtain a good hydrolysis it is necessary to cover the spots, moistened with dilute sulphuric acid, with a glass plate; omitting this detail causes rapid evaporation of the water with partial or no hydrolysis as a consequence. This is probably the reason why Hermans and Kamp[8] did not succeed in hydrolysis on the plate. The importance of this detail was mentioned by Schillings *et al.*[14]. Schütz and Schütz[15]

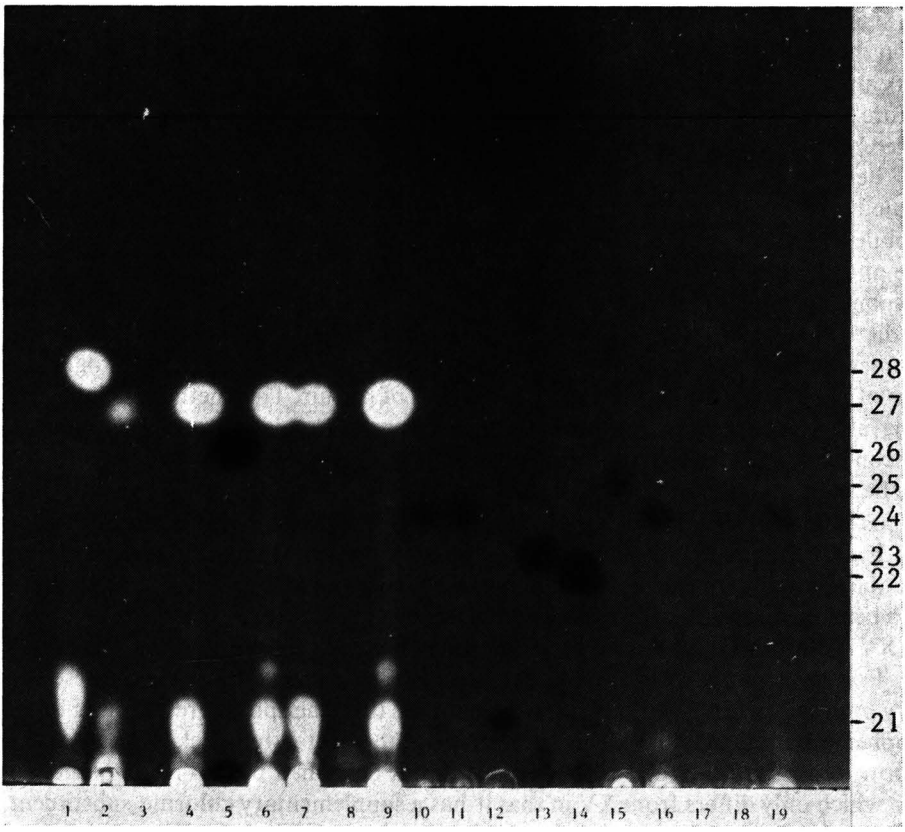

Fig. 3. Chromatogram obtained after hydrolysis of the benzodiazepines on the plate with methylene chloride–chloroform (1:1) (A) as the mobile phase. Detection with a 366-nm light source. The numbers of the spots correspond to those listed in Table I.

uses hydrochloric acid for the hydrolysis, but this acid is unsuitable when UV light is used for the detection: background effects prevent normal detection of the spots.

Medazepam (II) shows only a very weak spot of XXVII, which is best seen in Fig. 3. The acid hydrolysis of II is mentioned by some authors as being only very partial[16,17], others report it as not occurring[11,18], while some do not mention any problem in connection with this hydrolysis[9,10]. Although the hydrolysis on the plate of II into XXVII is only very partial, we obtained a better result when the hydrolysis was carried out as mentioned under *Samples*. The yield was about 10% of the theoretical value. One author even reports the formation of another benzophenone (XXIX) by hydrolysis of II[6].

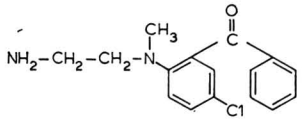

XXIX

When the hydrolysis was carried out as stipulated by Gräfe and Schmeling[6], the benzodiazepine remained unchanged. Medazepam behaves chromatographically

in the same way as described for XXIX. In acidic conditions II shows up as a reddish spot on the plate, and when the plate is sprayed with an alkaline solution this colour disappears. Gräfe and Schmeling[6] noticed the same behaviour for their substance. We therefore conclude that the structure XXIX was erroneously assigned to the unchanged benzodiazepine.

Benzophenone XX does not migrate in system A and therefore III cannot be identified together with the other benzodiazepines. A second development of the plate in mobile phase F can solve this problem. Benzophenone XX is a tertiary aliphatic amine and therefore needs a base, stronger than ammonia, to be liberated from the corresponding salts. With regard to this, TLC of XX in mobile phase F, which contains diethylamine, is no problem. However, if another system were to be used it is recommended that the spot be treated with diethylamine prior to chromatography. Excess of base can easily be removed by a stream of hot air. This method, using a second development, is valid only when no other benzodiazepines are present. Indeed, the secondary hydrolysis products of several benzodiazepines migrate together with XX. The same has been observed for unreacted II.

Triazolam (XVII) and alprazolam (XVIII) do not hydrolyse on the plate. These benzodiazepines are also stable in hot 4 *N* hydrochloric acid and therefore cannot be identified by the benzophenone method. Clobazam (VIII) is not expected to form a benzophenone on hydrolysis as it is a 1,5-benzodiazepine. The benzodiazepines VIII, XVII and XVIII do not migrate with mobile phase A.

For lorazepam (XV), it can be seen in Fig. 2 that the spot of one of these secondary products, with R_F 0,29, is even more intense than the spot corresponding to the benzophenone itself (R_F 0.43). This substance is not detected by black light. As far as we know, secondary hydrolysis products were not described for XV. For oxazepam (XVI), which only differs from XV in that it has a supplementary chlorine substituent, several secondary products are mentioned in the literature[19–21], with different proposed structures. The hydrolysis was also carried out under different conditions, so that comparison is difficult. A first attempt to compare the reaction products obtained by the different hydrolysis procedures was carried out by TLC. Insufficient separation of the complex mixtures complicated the interpretation of the results and it was decided to try to solve the problem by high-performance liquid chromatography. The results will be reported later. From Fig. 2 it is already obvious that XV and XVI do not behave in a completely analogous way.

We believe that the TLC method presented here can be an aid in the identification of benzodiazepines and their derivatives.

ACKNOWLEDGEMENT

The authors thank Dr. G. Janssen for mass spectrometric identifications.

REFERENCES

1 I. Wouters, E. Roets and J. Hoogmartens, *J. Chromatogr.*, 179 (1979) 381.
2 D. M. Hailey, *J. Chromatogr.*, 98 (1974) 527.
3 J. M. Clifford and W. F. Smyth, *Analyst (London)*, 99 (1974) 241.
4 R. W. T. Seitzinger, *Pharm. Weekbl.*, 110 (1975) 1073.
5 R. W. T. Seitzinger, *Pharm. Weekbl.*, 110 (1975) 1109.

6 G. Gräfe and W. Schmeling, *Deut. Apoth.-Ztg.*, 116 (1976) 163.
7 K. K. Kaistha and R. Tadrus, *J. Chromatogr.*, 154 (1978) 211.
8 R. B. Hermans and P. E. Kamp, *Pharm. Weekbl.*, 102 (1967) 1123.
9 C. Schütz and H. Schütz, *Arch. Toxikol.*, 30 (1973) 183.
10 R. D. Maier and K. H. Wehr, *Arch. Toxikol.*, 32 (1974) 341.
11 P. Lafargue, J. Meunier and Y. Lemontey, *J. Chromatogr.*, 62 (1971) 423.
12 H. D. Beckstead and S. J. S. Smith, *Arzneim.-Forsch.*, 18 (1968) 529.
13 P. G. L. C. Krugers Dagneaux, *Pharm. Weekbl.*, 108 (1973) 1025.
14 R. T. Schillings, S. R. Shrader and H. W. Ruelius, *Arzneim.-Forsch.*, 21 (1971) 1059.
15 C. Schütz and H. Schütz, *Z. Klin. Chem. Klin. Biochem.*, 10 (1972) 528.
16 J. A. F. de Silva and C. V. Puglisi, *Anal. Chem.*, 42 (1970) 1725.
17 H. Oelschläger and H. P. Oehr, *Pharm. Acta Helv.*, 45 (1970) 708.
18 K. Besserer, S. Henzler, E. Kohler and H. J. Mallach, *Arzneim.-Forsch.*, 21 (1971) 2003.
19 G. Caille, J. Braun, D. Gravel, R. Plourde, *Can. J. Pharm. Sci.*, 8 (1973) 42.
20 M. E. Esteve, S. Lamdan, C. H. Gaozza, *Rev. Farm. (Buenos Aires)*, 118 (1976) 118.
21 J. Gasparic, J. Zimak, P. Sedmera, Z. Breberova, J. Volke, *Collect. Czech. Chem. Commun.*, 44 (1979) 2243.

Journal of Chromatography, 194 (1980) 270–272
Elsevier Scientific Publishing Company, Amsterdam — Printed in The Netherlands

CHROM. 12,738

Note

Simple and fast separation of the iodotyrosines by thin-layer chromatography

M. LEDERER*
Laboratorio di Cromatografia del C.N.R., Rome (Italy)
(Received February 13th, 1980)

In recent years there have evolved highly efficient and fast separations, both in gas chromatography (GC) and high-performance liquid chromatography (HPLC). To obtain such separations, all factors involved had to be evaluated and optimised, and the effort necessary was often considerable.

Thin-layer chromatography (TLC), paper chromatography and paper electrophoresis have been re-examined only much later and it was realized that here also extremely efficient separations were possible, comparable to those in GC and HPLC, if optimization was aimed at. There are many publications dealing with high-performance TLC (HPTLC) and we have shown recently that paper electrophoresis can also yield excellent separations within 5 min by a very simple scale reduction of the arrangement[1].

In this paper we report another kind of simple separation, which requires no optimized support or elaborate equipment, and separates tyrosine (T), monoiodotyrosine (MIT) and diiodotyrosine (DIT) in 10 min.

While looking for a suitable separation of iodide, MIT, DIT, triiodotyrosine (T_3) and thyroxine (T_4) in relation to a clinical problem, we found that various books and reviews (for example, ref. 2) indicate that there are numerous paper chromatographic and TLC systems which can achieve this separation. However, our attention was held by a very simple technique in which these compounds are separated by paper chromatography with 3% sodium chloride solution[3].

Repeating this work, we found that development took over 30 min and yielded a good separation, but with elongated spots, as was also evident from the original paper[3].

Transferring this separation to cellulose thin layers, we obtained remarkably compact spots and development took only 10 min. In such a short period no problems of saturating the atmosphere, evaporation from the layer, etc., exist with an aqueous solution, so that the development could be carried out in microscope staining jars, simply covered with a glass plate.

EXPERIMENTAL AND RESULTS

Solutions of T, MIT, DIT, T_3 and T_4 were prepared in methanol with a small amount of ammonia and stored in a refrigerator.

* Present address: Postfach, Sils-Maria, 7514, Switzerland.

0021-9673/80/0000–0000/$02.25

The solutions were spotted on to Polygram Cel 300 layers (80 × 40 mm) with a glass capillary, so as to form spots about 3 mm in diameter.

The layers were developed immediately with the aqueous solvent in a microscope staining jar, covered with a flat piece of glass, for exactly 10 min, in which time the solvent rose 65 mm.

The thin layer was withdrawn, dried in an oven, dipped into the reagent (we used 0.5% ninhydrin in acetone + 1% acetic acid) and heated again in the oven at 110 °C until spots appeared. The average time taken from the spotting to obtaining the finished chromatogram was 15–17 min.

A typical separation is shown in Fig. 1. There is an excellent separation of T–MIT–DIT, while T_3 and T_4 remain at the point of application. Probably a longer development or other "optimization" could also separate T_3 and T_4.

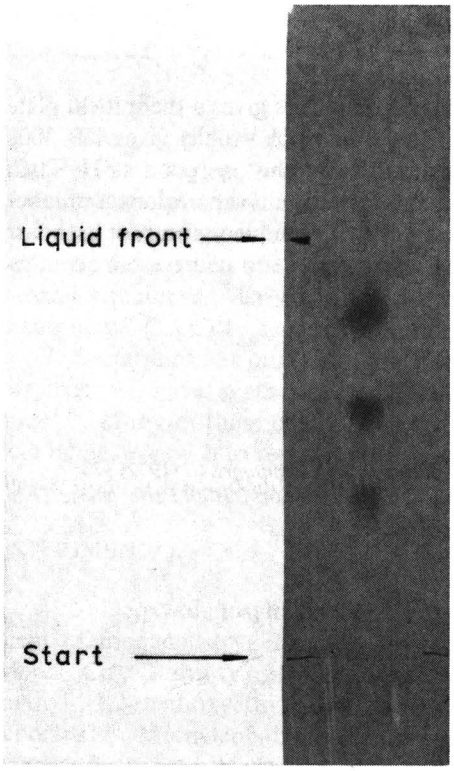

Fig. 1. TLC separation of tyrosine, monoiodotyrosine and diiodotyrosine on cellulose developed with 0.5 *N* NaCl. Length of thin layer, 80 mm.

The separation proved to be extremely reproducible. Changes in sodium chloride concentration or pH or the addition of small amounts of an organic solvent had only a small effect on the R_F values, as shown in Table I. We feel that in this respect it is a considerable improvement over the various separations involving partition systems.

Some comments can be made on the efficiency of the separation. The MIT spot

TABLE I

R_F VALUES OF IODOTYROSINES ON CELLULOSE THIN LAYERS WITH AQUEOUS SOLVENTS

Layer: Polygram Cel 300 (80 × 40 mm). Length of development: 10 min, in which time the solvent moved 55 mm.

Solvent	*R_F values*					
	T	*MIT*	*DIT*	T_3	T_4	*Iodide*
0.5 *N* NaCl	0.83	0.58	0.37	0	0	0.86
2 *N* NaCl	0.76	0.50	0.29		0	
0.5 *N* NaCl + *n*-propanol (9:1)	0.82	0.66	0.48			
10% Acetic acid	0.85	0.635	0.43	0.09 + tail	0	
0.1 *M* NaH_2PO_4 (pH ~ 3.2)	0.86	0.63	0.42			
0.1 *M* K_2HPO_4	0.86	0.72	0.66			

is 3 mm long and the distance of development is 55 mm. This gives a theoretical plate number of 5000, which compares favourably with TLC, which usually gives 400–3000 theoretical plates and is, according to Halpaap and Ripphahn[4], as good as HPTLC. Perhaps it could also be used as an illustration that for efficient separations a number of factors are important and if some are favourable (*e.g.*, an aqueous solvent with fast equilibrium and fast development) there is no need to resort to micro-scale arrangements and very fine particles of the adsorbent.

REFERENCES

1 M. Lederer, *J. Chromatogr.*, 171 (1979) 403.
2 L. G. Plaskett, *Chromatogr. Rev.*, 6 (1964) 91.
3 D. K. Jaiswal, J. Chander, B. Singh and K. P. Chakraborty, *J. Chromatogr.*, 67 (1972) 373.
4 H. Halpaap and J. Ripphahn, in A. Zlatkis and R. E. Kaiser (Editors), *High Performance Thin-Layer Chromatography*, Elsevier, Amsterdam, 1977, p. 95.

Journal of Chromatography, 194 (1980) 273–274
Elsevier Scientific Publishing Company, Amsterdam — Printed in The Netherlands

CHROM. 12,759

Note

Thin-layer chromatography of acid-labile cobalamins

RICHARD B. SILVERMAN*
Department of Chemistry, Harvard University, Cambridge, MA 02138 (U.S.A.)
and
D. DOLPHIN*
Department of Chemistry, The University of British Columbia, Vancouver, British Columbia V6T 1W5 (Canada)

(First received October 29th, 1979; revised manuscript received February 12th, 1980)

Because of the complex structure of corrinoids, the common methods of analysis, *viz.*, nuclear magnetic resonance spectroscopy, infrared spectroscopy, and elemental analysis, are not very informative with these compounds and much of corrinoid chemistry relies on optical absorption and chromatographic data. The relatively few reports concerning the separation of corrinoids have dealt mostly with natural vitamin B_{12} derivatives[1–7]. Firth *et al.*[8] have used cellulose thin-layer chromatography (TLC) to separate a variety of synthetic cobalamines.

Because of our interest in the mechanism of action of coenzyme B_{12}-dependent enzymes, we have synthesized and studied reactions of analogues of alkylcobalamins[9,10]. Many of these compounds are quite similar in structure and some are very acid labile. We wish to report the separation of these cobalamins by TLC on cellulose under slightly basic conditions.

EXPERIMENTAL

5′-Deoxyadenosylcobalamin was a gift of Professor Robert Abeles, Department of Biochemistry, Brandeis University, U.S.A., and cyanocobalamin a gift of Merck Co., Rahway, NJ, U.S.A. 2,3-Dihydroxypropyl-, 1,3-dioxa-2-cyclopentylmethyl-, 2,2-diethoxyethyl-, and formylmethylcobalamin were prepared as previously reported[9,10]. Methylcobalamin was prepared by the method of Dolphin[11]. Hydroxocobalamin was synthesized as previously reported[9]. The compounds were dissolved in 0.5% concentrated aqueous ammonia and applied to 20 cm long, 0.1 mm thick microcrystalline cellulose plates (E. Merck, distributed by Brinkmann, Westbury, NY, U.S.A., as Celplate-22 without indicator). Ascending TLC was performed at ambient temperature in the dark for a distance of at least 10 cm, eluting with *n*-butanol–ethanol–water, (10:3:7) containing 0.5% concentrated aqueous ammonia. Because of the intense red color of these compounds, visual detection was employed.

* Present address: Department of Chemistry, Northwestern University, Evanston, IL 60201, U.S.A.

0021-9673/80/0000–0000/$02.25

RESULTS

Table I summarizes the R_F values for the various axial ligand-substituted cobalamins. The two R_F values given for 2, 3 dihydroxypropylcobalamin are for the two compounds which result from the synthesis previously described[10]. These two compounds may be the two diastereomeric forms of 2,3-dihydroxypropylcobalamin.

As Firth *et al.*[8] found previously, small changes in the structure of the axial ligand dramatically effect the mobility of cobalamins on cellulose.

TABLE I

R_F VALUES FOR AXIAL LIGAND SUBSTITUTED COBALAMINS

Axial ligand-cobalamin	R_F
2,2-Diethoxyethyl-	0.62
Methyl-	0.60
1,3-Dioxa-2-cyclopentylmethyl-	0.56
Formylmethyl-	0.51
Cyano-	0.48
2,3-Dihydroxypropyl-	0.46
	0.38
5'-Deoxyadenosyl-	0.34
Hydroxo-	0.22

ACKNOWLEDGEMENTS

This work was supported by the U.S. National Institutes of Health (AM 14343) and the National Research Council of Canada.

REFERENCES

1 G. Tortolani and P. G. Ferry, *J. Chromatogr.*, 88 (1974) 430; and references therein.
2 L. Chima and R. Mantovan, *Farmaco, Ed. Prat.*, 17 (1962) 473.
3 T. Sasaki, *J. Chromatogr.*, 24 (1966) 452.
4 J. C. Linnel, H. A. A. Hussein and D. M. Matthews, *J. Clin. Pathol.*, 23 (1970) 820.
5 D. I. Bilkus and L. Mervyn, in H. R. V. Arnstein (Editor), *Cobalamins, Glaxo Symposium, 1970*, Churchill, London, 1971, p. 17; *C. A.*, 77 (1972) 98446n.
6 H. Vogelmann and F. Wagnet, *J. Chromatogr.*, 76 (1973) 359.
7 E. F. Walborg, D. B. Ray, and L. E. Öhrberg, *Anal. Biochem.*, 29 (1969) 433.
8 R. A. Firth, H. A. O. Hill, J. M. Pratt and R. G. Thorp, *Anal. Biochem.*, 23 (1968) 429; and references therein.
9 R. B. Silverman and D. Dolphin, *J. Amer. Chem. Soc.*, 98 (1976) 4626.
10 R. B. Silverman and D. Dolphin, *J. Amer. Chem. Soc.*, 98 (1976) 4633.
11 D. Dolphin, *Methods Enzymol.*, 18C (1971) 34.

Journal of Chromatography, 194 (1980) 275
Elsevier Scientific Publishing Company, Amsterdam — Printed in The Netherlands

CHROM 12,735

Book Review

Guide to gas chromatography literature, Vol. 4, by A. V. Signeur, IFI/Plenum, New York, Washington, London, 1979, VII + 1321 pp., price US$ 145.00, ISBN 0-306-68204-4.

This volume, containing 16,357 new entries, is the fourth in a series on gas chromatographic bibliographic data (the first volume, in 1964, contained 7577 entries, the second, in 1967, 7989 entries and the third, in 1974, 15,741 entries). Each paper cited is presented with bibliographic information [author(s), full title of the paper and source with full page numbers, but no address of the author(s)]. The volume has an author index and an extensive (159 pp.) subject index. It is printed by an inexpensive technique.

A brief statistical examination revealed the following about the collected material: approximately 85% of the material was published in 1971–1975, less than 5–7% in 1970 and 1976, and very little (less than 1.5%) in 1969 and 1977.

The entries include references to *Chemical Abstracts*, which is of considerable value for papers in foreign languages or coming from not readily available sources. However, as a result some information is out of date.

As with the earlier volumes in the series, this volume provides useful and fairly complete information for any search for GC data. However, owing to the ever increasing price of these volumes (the first one costs US$ 15.00), the current one is very expensive for individuals.

Brno (Czechoslovakia) J. JANÁK

0021-9673/80/0000–0000/$02.25

Journal of Chromatography, 194 (1980) 276
Elsevier Scientific Publishing Company, Amsterdam — Printed in The Netherlands

CHROM. 12,736

Book Review

Instrumental inorganic chemistry, by G. K. Wolf, R. W. Kiser and G. Schwedt, Springer, Berlin, Heidelberg, New York, 1979, IV + 220 pp., 64 figs., 23 tables, price DM 98.00, US$ 53.90, ISBN 3-540-09338-9

This book, No. 85 in the *Topics in Current Chemistry* series, contains three review articles. The first one, by G. K. Wolf, is entitled "Chemical effects of ion bombardment". The major sections deal with fundamentals of the interactions of heavy ions with matter, experimental (bombardment and implantation techniques, analysis of irradiation effects and products), chemistry of bombarded solids (radiation chemistry, reaction with various target sample types) and surface chemistry (corrosion, oxidation, catalytic and tribological properties). This well written and documented review (289 refs.) will interest everybody concerned with materials science and solid-state chemistry.

The second paper, by R. W. Kiser, is a review on "Doubly charged negative ions in the gas phase", with a discussion of the experimental work reported by different groups using different equipment. In spite of some controversial theoretical calculations and some negative experimental results, the opinion of the author, one of the discoverers of these species 14 years ago, is that, at present, nearly 20 doubly charged anions with lifetimes of $>10^{-5}$ sec have been effectively produced and detected. Suggestions for plausible formation mechanisms and electronic configurations are developed. There are 318 references.

The third part, by G. Schwedt, entitled "Chromatography in inorganic trace analysis", is a review of the possibilities of various chromatographic techniques (gas, liquid, thin-layer and paper) essentially in the field of metal analysis. Many tables provide rapid information on the chromatographic systems and detectors used and detection limits obtained in analysing a given element, either in test solutions or in different materials. Inclusion of titles of papers in the bibliography will be very useful for the reader interested in a particular problem. However, the field has grown rapidly in the last 10 years and the bibliography (345 refs.) is rather incomplete: apart from specific papers on trace analysis, several general books and reviews on chromatographic inorganic analysis have been omitted. A major interest of the review is the possible comparison between different chromatographic techniques and it will be very useful as a first approach to those looking for a highly sensitive and selective method for trace element analysis.

Villetaneuse (France) C. POMMIER

0021-9673/80/0000–0000/$02.25

PUBLICATION SCHEDULE FOR 1980

Journal of Chromatography (incorporating *Chromatographic Reviews*) and *Journal of Chromatography, Biomedical Applications*

MONTH	D 1979	J	F	M	A	M	J	J	A	S	O	N	D
Journal of Chromatography	185 186	187/1 187/2 188/1	188/2 189/1 189/2	189/3 190/1	190/2 191 192/1	192/2 193/1 193/2 193/3	194/1 194/2 194/3	195/1 195/2 195/3	196/1 196/2 196/3	The publication schedule for further issues will be published later.			
Chromatographic Reviews			184/1	184/2					184/3				
Biomedical Applications		181/1	181/2	181/ 3-4	182/1	182/2	182/ 3-4	183/1	183/2				

INFORMATION FOR AUTHORS

(Detailed *Instructions to Authors* were published in Vol. 193, No. 3, pp. 529–532. A free reprint can be obtained by application to the publisher)

Types of Contributions. The following types of papers are published in the *Journal of Chromatography* and the section on *Biomedical Applications:* Regular research papers (Full-length papers), Short communications and Notes. Short communications are preliminary announcements of important new developments and will, whenever possible, be published with maximum speed. Notes are usually descriptions of short investigations and reflect the same quality of research as Full-length papers, but should preferably not exceed four printed pages. For reviews, see page 2 of cover under Submission of Papers.

Manuscripts. Manuscripts should be typed in double spacing on consecutively numbered pages of uniform size. The manuscript should be preceded by a sheet of manuscript paper carrying the title of the paper and the name and full postal address of the person to whom the proofs are to be sent. Authors of papers in French or German are requested to supply an English translation of the title of the paper. As a rule, papers should be divided into sections, headed by a caption (e.g., Summary, Introduction, Experimental, Results, Discussion, etc.). All illustrations, photographs, tables, etc. should be on separate sheets.

Summary. Full-length papers and Review articles should have a summary of 50–100 words which clearly and briefly indicates what is new, different and significant. In the case of French or German articles an additional summary in English, headed by an English translation of the title, should also be provided. (Short communications and Notes are published without a summary.)

Illustrations. The figures should be submitted in a form suitable for reproduction, drawn in Indian ink on drawing or tracing paper. Each illustration should have a legend, all the *legends* being typed (with double spacing) together on a *separate sheet*. If structures are given in the text, the original drawings should be supplied. Coloured illustrations are reproduced at the author's expense, the cost being determined by the number of pages and by the number of colours needed. The written permission of the author and publisher must be obtained for the use of any figure already published. Its source must be indicated in the legend.

References. References should be numbered in the order in which they are cited in the text, and listed in numerical sequence on a separate sheet at the end of the article. Please check a recent issue for the lay-out of the reference list. Abbreviations for the titles of journals should follow the system used by *Chemical Abstracts*. Articles not yet published should be given as "in press", "submitted for publication", "in preparation" or "personal communication".

Proofs. One set of proofs will be sent to the author to be carefully checked for printer's errors. Corrections must be restricted to instances in which the proof is at variance with the manuscript. "Extra corrections" will be inserted at the author's expense.

Reprints. Fifty reprints of Full-length papers, Short communications and Notes will be supplied free of charge. Additional reprints can be ordered by the authors. An order form containing price quotations will be sent to the authors together with the proofs of their article.

News. News releases of new products and developments, and information leaflets of meetings should be addressed to: The Editor of the News Section, Journal of Chromatography/Journal of Chromatography, Biomedical Applications, Elsevier Scientific Publishing Company, P.O. Box 330, 1000 AH Amsterdam, The Netherlands.

Advertisements. Advertisement rates are available from the publisher on request. The Editors of the journal accept no responsibility for the contents of the advertisements.

The merits and scope of

modern thin-layer chromatography

can, of course, be fully exploited only with a complete system of compatible instruments for sample application, chromatogram development, and quantitative evaluation.

Whether you choose conventional TLC, high-performance TLC with linear chromatogram development or circular TLC,

CAMAG has the right system for you.

1. Sample application

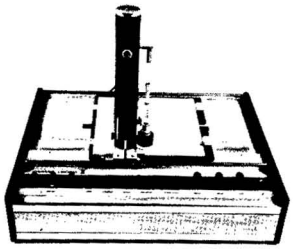

CAMAG LINOMAT III

narrow band sample application, 5–500 µl

conventional TLC · linear HPTLC

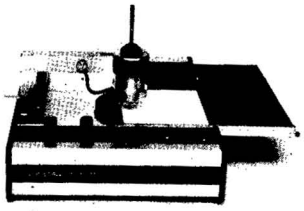

CAMAG NANOMAT

application with fixed-volume sample capillary, 100 nl, 200 nl or 0.5–5 µl

conventional TLC · linear HPTLC · circular HPTLC

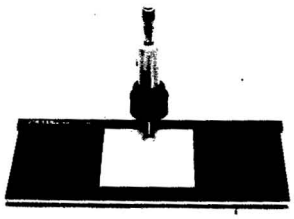

CAMAG Nano-Applicator Micro-Applicator

variable volume sample application with micrometer syringe, 50–230 nl, or 0.5–2.3 µl

conventional TLC · linear HPTLC · circular HPTLC

2. Chromatogram development

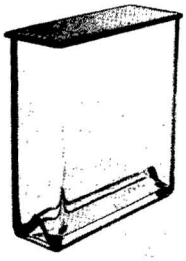

CAMAG Twin-Trough Chamber

versatile, economical and reliable

conventional TLC

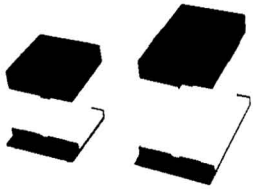

CAMAG HPTLC Linear Chamber

separation of 32 samples on a single 10 x 10 cm HPTLC plate, or 72 samples on a 20 x 10 cm plate

linear HPTLC

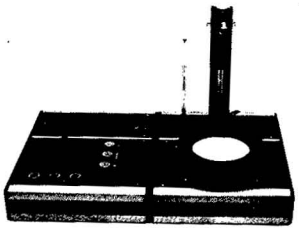

CAMAG U-Chamber Chromatograph acc. to R. E. Kaiser

Most efficient HPTLC method based on circular developing technique; also suitable for HPTLC/HPLC transfer

circular HPTLC

3. Quantitative evaluation

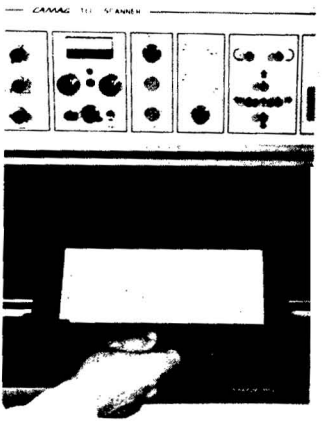

CAMAG TLC/HPTLC Scanner

for conventional and high-performance thin-layer chromatograms

Three scanning modes for circular chromatograms

Automatic evaluation of all scanning tracks of a complete chromatogram

conventional TLC · linear HPTLC · circular HPTLC

If you are planning to set up a new TLC laboratory, or to extend your existing TLC equipment

CAMAG specialists will help.

CAMAG

Homburgerstr. 24 · CH-4132 Muttenz (Switzerland) · Tel. 061-61 34 34 · Telex 62 64
Bismarckstr. 27–29 · D-1000 Berlin 41 · Tel. 030-795 10 91 · Telex 184 0